University Library



A gateway to Melbourne's research publications

Minerva Access is the Institutional Repository of The University of Melbourne

Author/s:
Woodford, Sarah Claire

Title:
Biomechanical function of the native and prosthetic temporomandibular joints

Date:
2023-08

Persistent Link:
https://hdl.handle.net/11343/340195

Terms and Conditions:
Terms and Conditions: Copyright in works deposited in Minerva Access is retained by the copyright owner. The work may not be altered without permission from the copyright owner. Readers may only download, print and save electronic copies of whole works for their own personal non-commercial use. Any use that exceeds these limits requires permission from the copyright owner. Attribution is essential when quoting or paraphrasing from these works.

# BIOMECHANICAL FUNCTION OF THE NATIVE AND PROSTHETIC TEMPOROMANDIBULAR JOINTS

**Sarah Claire Woodford**

ORCID: 0000-0003-4756-0198

Submitted in total fulfilment of the requirements for the degree of
Doctor of Philosophy

January 2024

Department of Biomedical Engineering
Faculty of Engineering and IT
The University of Melbourne

# Abstract

The temporomandibular joint (TMJ) is a coupled synovial joint connecting the skull and the mandible; and is essential for biting, swallowing and speech, and required for maintaining quality of life. Disorders of the TMJ are common, with 5% to 60% of the adult population showing clinical signs of a TMJ disorder, including muscle and joint pain and tenderness, and restricted mandibular movements. Total TMJ replacement (TMJR) surgery is the established treatment for end-stage TMJ disorders such as degenerative joint disease and ankylosis and is used in mandibular reconstruction following condylar fractures and tumor resection. This procedure has been shown to increase mouth opening capacity, reduce pain and improve quality of life; however, biomechanical TMJ function following total TMJR surgery is poorly understood. As a result, the ability for total TMJR surgery to restore jaw function remains limited.

The objective of this thesis was to evaluate the jaw and TMJ kinematics, maximum voluntary bite force, muscle functionality and TMJ loading for unilateral total TMJR patients and compare them to healthy control subjects. A systematic literature review was conducted to critically investigate published literature on measurement modalities used to quantify mandibular and TMJ kinematics in six degrees-of-freedom. Measurement techniques fell into four main categories, namely mechanical linkage systems, magnetic tracking systems, video motion analysis and radiographic tracking. Magnetic tracking was identified as a technique with high motion measurement accuracy which circumvents skin motion artefact by attaching sensors directly to the teeth. Following this, magnetic tracking was used to develop a modelling framework to evaluate subject-specific three-dimensional (3D), dynamic bite forces during biting and chewing. Measurement of jaw motion was captured on one healthy adult using a Dental Motion Decoder (DMD) system (Ignident, Ludwigshafen, Germany); this samples the position and orientation of two low-profile electromagnetic field sensors attached to the teeth. The subjects occlusal anatomy was quantified using an intra-oral scanner. Following this, the subject was instructed to chew and maximally compress a rubber sample between their teeth. The occlusal anatomy, rubber geometry and experimentally measured rubber material properties were combined in a finite element model. The measured mandibular motion was used to kinematically drive model simulations of chewing and biting on the rubber sample, and 3D dynamic bite forces were calculated. A validation study found excellent correlation between

experimentally measured force during tooth-rubber penetration and that predicted from the modelling framework.

Following this, an optoelectronic tracking system was used to measure jaw kinematics during mandibular border movements and biting of a rubber sample for 6 total unilateral TMJR patients and 10 age- and gender-matched healthy controls. Optoelectronic tracking was employed for its ease of use in a research setting, as the DMD system previously used is restricted to clinical environments. Finite element analysis (FEA) was employed to calculate the maximum voluntary bite force. Musculoskeletal models were used to investigate muscle and TMJ loading. Unilateral total TMJR patients had restricted anterior mobility of their prosthetic condyles, this resulted in limited opening, lateral and protrusive movement capacity. During chewing, unilateral total TMJR patient's prosthetic condyles were positioned significantly inferiorly to those of healthy controls, suggesting a weakness of the elevator muscles on the operated side. There was a non-significant trend that healthy controls had higher maximum voluntary bite force than unilateral total TMJR patients. Furthermore, total unilateral TMJR patents had higher maximum voluntary bite force when biting on their contralateral molars than their ipsilateral molars. Unilateral total TMJR patients had high medial pterygoid forces on the ipsilateral side and significantly lower temporalis forces on the ipsilateral side compared to the contralateral side. In addition, total unilateral TMJR patients had lower TMJ loading than control subjects, particularly on their native contralateral joint. This abnormal loading may be a mechanism associated with degenerative changes that have been observed in the contralateral joint following unilateral total TMJR surgery.

This thesis presents new data describing jaw kinematics and kinetics following TMJR surgery, and proposes new techniques to support rigorous biomechanical analysis of the mandible, dental structures and TMJ both in clinical and research settings. The results of this thesis may guide the design and evaluation of TMJ prosthetics, prosthodontic devices, dental restorations and maxillofacial orthopaedic implants; furthermore, these results may influence physiotherapy prescription following unilateral total TMJR surgery to enhance long-term patient outcomes.

# Table of Contents

Abstract ..... i
Table of Contents ..... iii
List of Figures ..... v
List of Tables ..... xi
List of Appendices ..... xiv
Third party copyright material ..... xv
Declaration ..... xviii
Preface ..... xix
Acknowledgements ..... xxiii
**Chapter 1: Introduction ..... 25**
1.1 Motivation ..... 25
1.2 Research aims ..... 25
1.3 Thesis outline ..... 26
**Chapter 2: Literature review ..... 28**
2.1 Anatomy and structure ..... 28
2.2 Functionality ..... 29
2.3 Pathologies of the temporomandibular joint ..... 32
2.4 Treatment of temporomandibular joint disorders ..... 36
2.5 Temporomandibular joint prosthesis design ..... 40
2.6 Post-surgical outcomes of total temporomandibular joint replacement ..... 47
**Chapter 3: Measurement of normal and pathological mandibular and temporomandibular joint kinematics: A systematic review ..... 55**
3.1 Significance ..... 55
3.2 Abstract ..... 55
3.3 Introduction ..... 56
3.4 Materials and methods ..... 57
3.5 Results ..... 59
3.6 Discussion ..... 75
3.7 Update ..... 78
**Chapter 4: Low-profile magnetic field sensors in the measurement and modelling of three-dimensional jaw kinematics and occlusal loading ..... 81**
4.1 Significance ..... 81
4.2 Abstract ..... 81
4.3 Introduction ..... 82

4.4 Materials and methods ..... 83
4.5 Results ..... 88
4.6 Discussion ..... 93
**Chapter 5: Kinematics of the jaw following total temporomandibular joint replacement surgery ..... 99**
5.1 Significance ..... 99
5.2 Abstract ..... 99
5.3 Introduction ..... 100
5.4 Materials and Methods ..... 101
5.5 Results ..... 106
5.6 Discussion ..... 113
**Chapter 6: Muscle and joint mechanics during maximum-force biting following total temporomandibular joint replacement surgery ..... 117**
6.1 Significance ..... 117
6.2 Abstract ..... 117
6.3 Introduction ..... 118
6.4 Materials and methods ..... 120
6.5 Results ..... 126
6.6 Discussion ..... 135
**Chapter 7: Conclusions and future work ..... 141**
7.1 Summary ..... 141
7.2 Limitations ..... 142
7.3 Future directions ..... 143
**Bibliography ..... 149**
**Appendices ..... 185**
Appendix A ..... 185
Appendix B ..... 188
Appendix C ..... 191
Appendix D ..... 196
Appendix E ..... 204

# List of Figures

Figure 1.1: Flow-chart of thesis structure. ..... 27

Figure 2.1: Primary masticatory muscles including the temporalis, masseter, lateral and medial pterygoid muscles (a). Suprahyoid muscles including the geniohyoid, mylohyoid, digastric and stylohyoid muscles (b). ..... 28

Figure 2.2: Temporomandibular joint anatomy (Litin 2009). ..... 29

Figure 2.3: CT scan of ankylosis patient. Red arrow indicates extensive bony ankylosis of the left TMJ. Figure adapted from Dimitroulis et al. (2013). ..... 34

Figure 2.4: Internal derangement of the TMJ. Normal refers to the normal anatomic position of the TMJ disc during maximal mouth opening. Anterior disc displacement with reduction shows the anteriorly displaced disc returning to a normal anatomical position upon maximal opening. Anterior disc displacement without reduction shows the anteriorly displaced disc during closed and maximal opening positions with disc thickening present. Figure adapted from Warbuton, G. (2021). ..... 35

Figure 2.5: CBCT scans showing a normal condylar head (a) and an osteoarthritic condylar head (b) from a sagittal (left) and coronal (right) view. Red arrows highlight regions of severely degenerated bone. Figure adapted from Brierly et al. (2022). ..... 36

Figure 2.6: Early condylar prosthesis. Rubber prosthesis fixated with dental clasps, for surgical management after hemimandibulectomy (a). Tin prosthesis fixed with a detachable plate to allow removal of the prosthesis for wound cleaning (b). Ivory prosthesis with a spike to allow anchorage into the trabecular bone of the residual mandible (c). Figures adapted from Driemel et al (2009). ..... 41

Figure 2.7: Evolution of total TMJ prosthesis designs. Shown is the Christiansen condyle prosthesis (a), the Vitek-Kent condyle prosthesis (b), the Sonneburg total TMJ prosthesis (c), the early Techmedica/TMJ concepts total TMJ prosthesis (d), the Hoffman and Pappas total TMJ prosthesis (e), the early Biomet condyle prosthesis (f), the Christiansen stock (g) and custom (h) total TMJ prosthesis and the Groningen total TMJ prosthesis (i). Further details of each system can be found in Table 2.2. Figures adapted from Driemel et al. (2009). ..... 43

Figure 2.8: TMJ concepts custom implant system (a), Zimmer Biomet stock TMJ system (b), and the Maxoniq ArthroJaw total joint replacement system (c). Figures a and b adapted from Goswami et al. (2009). ..... 47

Figure 2.9: Maximum interincisal opening distance and self-reported values for pain and interference with eating evaluated using a visual analogue scale for a group of 288 total TMJ replacement patients, measured preoperatively and up to 3 year post-operative (Giannakopoulos et al. 2012). ..... 48

Figure 2.10: Trajectories of the left and right condylar points and the central incisors during maximum mouth opening of a unilateral total TMJ replacement patient. Viewed from the coronal plane (a) and an oblique projection (b). Figure adapted from Leiggener et al. (2012). ..... 49

Figure 2.11: Condylar range of motion (CRoM) and Incisal range of motion (InRoM) kinematics during opening, lateral and protrusive movements. Figure adapted from Linsen et al. (2012)..... 50

Figure 2.12: Long-term bilateral muscle activity for the anterior temporalis and masseter muscles of unilateral total TMJR patients (Linsen et al. 2020). ..... 52

Figure 2.13: Cranial view of mandible showing bite locations numbered 1 to 13 (a). Maximum bite force and corresponding TMJ reaction force as a function of bite location for an intact mandible and for a unilateral TMJ prosthesis (b). Prosthetic and contralateral joint reaction forces normalised against the maximum bite force, as a function of bite location (c). Where $FB$ = maximum bite force, $FJL$ and $FJR$ = left amd right TMJ reaction force for an intact mandible, $FP$ and $FJC$ = prosthetic and contralateral joint reaction force of a unilateral TMJR patient, M = molar, P = premolar, C = canine, I = incisor. Figure adapted from Van Loon et al. (1998). ..... 54

Figure 3.1: Flow chart illustrating systematic review search results adopted in the present study. ..... 58

Figure 3.2: Quality assessment results for studies included in this systematic review including the average score for each question in the quality assessment tool (a), and the average total quality score for each measurement technique (b). Red bars indicate questions that were poorly addressed (i.e. an average score of < 1.4). The number of studies using each measurement technique in given in parenthesis and the range of total quality scores for each measurement technique is indicated by the whiskers..... 60

Figure 3.3: Technology used in the measurement of jaw and TMJ kinematics including the Case Gnathic Replicator, with two face-bows attached to the mandibular and maxillary teeth, and transducers mounted to the face-bows for recording displacement (Messerman 1967) (a). Electromechanical axiograph mounted to subject's mandible using an occlusal clutch, and attached to the forehead via a headband (Sadat-Khonsari et al. 2003a) (b). Ultrasonic tracking system, featuring three ultrasonic emitters mounted to the lower teeth via a metal clutch, and four ultrasonic receivers mounted on the head via a face-bow (Baqaien et al. 2007) (c). Magnetic tracking system used for quantifying condylar trajectories using custom plastic dental stents with magnetic sensors are attached to incisors and metal beads attached to molars to enable motion data registration using CT scans (Baltali et al. 2008b) (d). Optoelectronic tracking system which features lightweight frames containing three pairs of photocells are attached to the upper and lower incisors and canines, and two perpendicular cathode ray tubes which measures movements of these photocells to be reconstructed to evaluate 3D marker trajectories (Visscher et al. 2000) (e). 3D Scanning using adhesive targets attached to the teeth, and real-time CBCT scanning and digital reconstruction for the right lateral movement (Kwon et al. 2019) (f), and Cone beam CT system with custom-made video x-ray fluoroscopy function for radiographic evaluation of dynamic TMJ kinematics (Chen et al. 2013b) (g). ..... 74

Figure 3.4: Magnetic DMD system with magnetic sensors fixed to participant's premolars using dental cement (a). The motion of these sensors can be registered to subject-specific dental geometry reconstructed from an intra-oral scanner (b), resulting in three orthogonal translations and rotations of the

mandible with respect to the maxilla during habitual mastication (c). Data given are expressed about an anatomic coordinate system with the x-direction, y-direction and z-direction aligned with the lateral, anterior and superior directions, respectively. 76

Figure 3.5: Flow chart illustrating systematic review search results between 3rd April 2019 and 2nd January 2024. 78

Figure 3.6: Bar chart showing the frequency of studies published using the jaw and TMJ kinematic measurement techniques between 3rd April 2019 and 2nd January 2024. 79

Figure 3.7: Intraoral photograph of the electromagnetic tracking device developed by Morikawa et al (2022) (a). Photograph of the sensor module, attached to the mandibular teeth, including a magnetic and motion sensor (b). Images adapted from Morikawa et al. (2022). 80

Figure 3.8: The MODJAW optical scanning system. Figure adapted from Solaberrieta et al. (2018). 80

Figure 4.1: DMD experimental setup showing participant with electromagnetic field sensors attached to the teeth and the electromagnetic source located approximately 8 cm above the subject's head (a). 3D model of the participant's mandibular and maxillary teeth with rubber held between the premolars obtained through the intra-oral scan (b). Finite element model of the premolars (grey) and rubber (blue) constructed from the intra-oral scan data. Teeth that were not in contact with the rubber were removed during simulations, for computational efficiency (c). The red-dashed area indicates the region that was represented using the finite element model. 87

Figure 4.2: Validation experimental setup showing human tooth cemented into a custom-made fixture, the blue rubber sample lies between the tooth and the load cell (a) and experimental results compared against computational model output corresponding to this loading scenario (b). The RMS error between experiment and model was 1.39 N. 88

Figure 4.3: Vertical translation of the mandible measured during ten chewing cycles. Black curves represent mean cycle data, while the shaded region indicates one standard deviation about the mean. 89

Figure 4.4: Mandibular protrusive and laterotrusive movements during mean chewing of rubber sample, projected onto the occlusal plane. Data is given for the incisors, premolars, first molars and second molars. White, yellow and black markers refer to the points at 0%, 50% and 100% of the chewing cycle respectively. X, Y and Z represent the lateral (left), posterior and superior directions respectively. All trajectory images adhere to scale in lower left corner. 90

Figure 4.5: Tooth-specific mandibular bite forces for mean chewing and maximum-force bite tests. Data are given for the incisors, premolars, first molars and second molars. All forces are given in Newtons; X, Y and Z represent the lateral (left), posterior and superior directions, respectively. 90

Figure 4.6: Evolution of the contact pressure distribution along the maxillary (top row) and mandibular (bottom row) dental arches at 25%, 50%, 75% and 100% of the mean chewing cycle. Contact pressure values are given in MPa. 93

Figure 5.1: Design of the custom-made motion tracking plate fixed to its dental stone cast. Visible are three retroreflective markers (top of image), clear lingual base plate, metal clasps around the second premolars and molars and wire extending extraorally connecting the clasps to the retroreflective markers (a). Participant with maxillary and mandibular tracking plates in place (b). Marker coordinate system with the origin aligned with the centre of marker 1. Positive Y is aligned with the vector from markers 1 to 3. Positive X is perpendicular to the vectors from markers 1 to 2 and 1 to 3. Positive Z is perpendicular to the X and Y directions (c). Anatomical coordinate system with the occlusal (blue), sagittal (red), and frontal (grey) planes displayed. Positive X, Y and Z directions correspond to the left, posterior and superior directions respectively (d). ..... 105

Figure 5.2: Maximum mouth opening trajectory, viewed from the frontal and sagittal planes, for a representative control subject (a) and unilateral total TMJ replacement patient (b). Open circles represent landmarks at the maximum occlusion position, while closed circles represent landmarks at the maximum mouth open position. Black, red, and blue lines indicate incisal, left condyle and right condyle trajectories, respectively..... 106

Figure 5.3: Maximum lateral excursion to the right projected onto the transverse plane for a representative control subject (a), and unilateral total TMJ replacement patient (b). Dashed lines represent the mandible position at the maximum occlusal position, while the rendered mandible represents the mandible position at the maximum lateral excursion position. Open circles represent landmarks at the mouth closed position, while closed circles represent landmarks at the maximum lateral position. Black, red, and blue lines indicate incisal, left condyle and right condyle trajectories, respectively. ..... 107

Figure 5.4: Mean movements of the mandibular incisor point, non-working condyle and working condyle during one normalised cycle of molar chewing. Movements are shown for control subjects chewing on either side of the mouth (red), unilateral total TMJ replacement patients chewing on their contralateral molars (blue) and unilateral total TMJ replacement patients chewing on their ipsilateral molars (black). The start and end point of each cycle was from a partially closed jaw position, compressing the rubber sample between the molars. Dashed lines represent movement of a prosthetic condyle. Positive X, Y and Z represent lateral (left), posterior and superior directions, respectively. ..... 110

Figure 5.5: Mean movements of the mandibular incisor point, non-working condyle and working condyle during one normalised cycle of molar chewing. Movements are shown for control subjects chewing on either side of the mouth (red), unilateral total TMJ replacement patients chewing on their contralateral molars (blue) and unilateral total TMJ replacement patients chewing on their ipsilateral molars (black). Movement of the mandibular incisors and natural condyles are represented by an open circle, while movements of the prosthetic condyles are represented by an asterisk. Positive X, Y and Z represent lateral (left), posterior and superior directions, respectively. ..... 111

Figure 6.1: Anatomical coordinate system with X directed laterally (left), Y directed posteriorly and Z directed superiorly (a), and definitions of mandibular naming convention (b). The mandibular width is the distance between the right and left

condylar points, the mandibular length is the distance between the intercondylar point and the mandibular central incisors. The working TMJ is defined as the TMJ on the same side as the bite, the non-working TMJ is defined as the TMJ on the opposite side to the bite. ..... 122

Figure 6.2: Three-dimensional model of the participants mandibular and maxillary teeth with rubber held between the first molars (a), finite element model of the first molars (grey) and rubber (blue) constructed from the laser scan data (b), and the finite element model of the first molars compressing the rubber sample in a maximum force bite (c). The finite element model includes only the teeth that will contact the rubber for computational efficiency, indicated by the red dashed lines. ..... 124

Figure 6.3: Rigid-body musculoskeletal model illustrating the pterygoid sub-regions in the frontal plane (a) and temporalis and masseter sub-regions in the sagittal plane of healthy controls (b). The superior and inferior sub-regions of the operated lateral pterygoid muscles are removed in the models of unilateral total TMJR patients. ..... 125

Figure 6.4: Net maximum voluntary bite force and direction for control subjects (blue) and unilateral total TMJR patients biting on their contralateral (yellow) or ipsilateral (pink) first molars. Bite force is reported as the reaction force on the mandibular teeth with respect to the mandibular anatomic coordinate system. The lateral component of bite force directed buccally is defined as positive, and that directed lingually is defined as negative. Statistically significant differences ($p < 0.05$) are identified by an asterisk. ..... 128

Figure 6.5: Net maximum muscle force and asymmetry index of the medial pterygoid, inferior lateral pterygoid, posterior temporalis, anterior temporalis, and superficial masseter muscles for control subjects (blue) and unilateral total TMJR patients biting on their contralateral (yellow) or ipsilateral (pink) first molars. Muscle forces are given for the working (W) and non-working (NW) sides of the jaw. Statistically significant differences ($p < 0.05$) are identified by an asterisk. TMJR-C and TMJR-I indicate unilateral total TMJR patients biting on their contralateral and ipsilateral molars, respectively. ..... 130

Figure 6.6: Maximum net joint force and direction for the working (W) and non-working (NW) joints of control subjects (blue) and unilateral total TMJR patients biting on their contralateral (yellow) or ipsilateral (pink) first molars. To aid comparison of the muscle and TMJ reaction loads between biting sides, the lateral component of joint force directed laterally is defined as positive, and that directed medially is defined as negative. Statistically significant differences ($p < 0.05$) are identified by an asterisk. TMJR-C and TMJR-I indicate unilateral total TMJR patients biting on their contralateral and ipsilateral molars, respectively. ..... 131

Figure 6.7: Contribution of joint force and dominant muscle forces to the superior-inferior component of bite force during a maximum force bite for control subjects (a) and unilateral total TMJR patients when biting on their contralateral and ipsilateral molars (b). Anterior temporalis (blue), superficial masseter (pink) and medial pterygoid (yellow) forces are indicated separately, contribution from remaining muscles is summed and represented as “other” (black). ..... 134

Figure 7.1: OsseoFrame (Maxoniq) subperiosteal implant design (a) and panoramic x-ray showing patient 12 months post-operatively. Figure adapted from Dimitroulis et al (2023). ..... 147

# List of Tables

Table 2.1: Interpositional devices, fossa- eminence and condylar prosthesis..... 44

Table 2.2: Total TMJ replacement systems ..... 45

Table 3.1: Quality assessment tool employed in this systematic review. The scoring system was derived from the STROBE statement (Elm et al. 2007), the Downs and Black checklist (Downs and Black 1998), and previously reported reliability and feasibility appraisal tools (Crowe and Sheppard 2011)..... 59

Table 3.2: Details of studies identified in this systematic literature review that employ mechanical linkage systems. Study details provided include, where available, author details, participant characteristics, TMJ/mandible condition, medical imaging modality, kinematic parameters measured, reported tracking accuracy and methodological quality rating..... 63

Table 3.3: Details of studies identified in this systematic review that employ magnetic tracking systems. Study details provided include, where available, author details, participant characteristics, TMJ/mandible condition, medical imaging modality, kinematic parameters measured, reported tracking accuracy and methodological quality rating. ..... 65

Table 3.4: Details of studies identified in this systematic review that employ video motion analysis combined with 3D morphology data derived from X-ray, CT or MRI. Study details provided include, where available, author details, participant characteristics, TMJ/mandible condition, medical imaging modality, kinematic parameters measured, reported tracking accuracy and methodological quality rating. ..... 68

Table 3.5: Details of studies identified in this systematic review that employ video motion analysis without use of medical imaging. Study details provided include, where available, author details, participant characteristics, TMJ/mandible condition, kinematic parameters measured, reported tracking accuracy and methodological quality rating. ..... 70

Table 3.6: Details of studies identified in this systematic review that employ radiographic tracking using single-plane video x-ray fluoroscopy and CT data. Study details provided include, where available, author details, participant characteristics, TMJ/mandible condition, kinematic parameters measured, reported tracking accuracy and methodological quality rating. ..... 72

Table 4.1: Magnitude and direction of the mean chewing force for each mandibular tooth. ..... 92

Table 4.2: Magnitude and direction of the peak maximum-force bite value for each mandibular tooth. ..... 93

Table 4.3: Published maximum bite force data for adult males with healthy dentition. Given are gender, age and sample size of subjects, and the reported bite forces for the second molars, first molars, premolars and incisors, where available. Bite forces given are mean ± one standard deviation. ..... 95

Table 5.1: Participant details including age, joint replacement side, post operative measurement time and mandibular size. ..... 102

Table 5.2: Kinematics data at maximum mouth opening, maximum lateral excursion, and maximum protrusion positions in unilateral total TMJ replacement subjects and healthy controls. Displacements were measured as the position of each landmark with respect to its position with the mandible in the maximum occlusion position and reported as mean (SD). Measurements of lateral incisal deflection for unilateral total TMJ replacement patients are expressed as ± to represent deflection to the ipsilateral side, regardless of joint replacement side. Statistical comparisons in kinematics were made between unilateral total TMJ replacement patients and healthy controls using a Mann-Whitney U-test. Positive X, Y and Z represent lateral (left), posterior and superior directions, respectively. Level of significance was defined by * $p < 0.05$, ** $p < 0.01$, *** $p < 0.001$. ..... 108

Table 5.3: Kinematics data at the start point and turning point of molar chewing cycles. Displacements were measured as the position of each landmark with respect to its position with the mandible at maximum occlusion and reported as mean (SD). Statistical comparisons in kinematics were made between unilateral total TMJ replacement patients and healthy controls using a Mann-Whitney U-test. Positive X, Y and Z represent lateral (left), posterior and superior directions, respectively. Level of significance was defined by * $p < 0.05$, ** $p < 0.01$, *** $p < 0.001$. ..... 112

Table 6.1: Participant details, including age at time of data collection, joint replacement side, post operative measurement time and mandible size as defined in fig. 6.1b. ..... 121

Table 6.2: Maximum voluntary bite force magnitude and direction for control subjects and unilateral total TMJR patients when biting on their first molars. Values are given as mean (SD). Bite force is reported as the reaction force on the mandibular teeth with respect to the anatomic coordinate system. To aid comparison between biting sides, the lateral component of bite force directed buccally is defined as positive, and that directed lingually is defined as negative. P values are given for comparisons between healthy controls and unilateral total TMJR patients, determined through Mann-Whitney U-tests ($Pa$), and for comparisons between unilateral total TMJR patients biting on their contralateral and ipsilateral molars, determined through Wicoxon signed-rank tests ($Pb$). * represents significant differences. ..... 127

Table 6.3: Maximum muscle force magnitude for each muscle on the working and non-working side of the mandible and the asymmetry index of each muscle for each participant group. Values are given as mean (SD). P values are given for comparisons between healthy controls and unilateral total TMJR patients, determined through Mann-Whitney U-tests ($Pa$), and for comparisons between unilateral total TMJR patients biting on their contralateral and ipsilateral molars, determined through Wilcoxon signed-rank tests ($Pb$). * represents significant differences. ..... 129

Table 6.4: TMJ reaction force magnitude, direction and ratio of TMJ force to bite force for the working and non-working condyles of control subjects and unilateral total TMJR patients at the time of maximum voluntary bite force. Values are given as mean (SD). To aid comparison of the muscle and TMJ reaction loads

between biting sides, the lateral component of joint force directed laterally is defined as positive, and that directed medially is defined as negative. Values are given as mean (SD). P values are given for comparisons between healthy controls and unilateral total TMJR patients, determined through Mann-Whitney U-tests ($Pa$), and for comparisons between unilateral total TMJR patients biting on their contralateral and ipsilateral molars, determined through Wilcoxon signed-rank tests ($Pb$). * represents significant differences..... 132

Table A.D.1:Musculotendon properties of the generic, unscaled rigid body musculoskeletal model. ..... 200

# List of Appendices

| | |
|---|---|
| 2D | Two-dimensional |
| 3D | Three-dimensional |
| 4D | Four-dimensional |
| CAD | Computer aided design |
| CAM | Computer aided manufacture |
| CBCT | Cone-beam computerised tomography |
| CT | Computerised tomography |
| DMD | Dental motion decoder |
| EMG | Electromyography |
| FDA | United States food and drug administration |
| FEA | Finite element analysis |
| ID | Internal derangement |
| MeSH | Medical subject headings |
| MIO | Maximum interincisal opening |
| MRI | Magnetic resonance imaging |
| PMMA | Polymethyl methacrylate |
| PRISMA | Preferred reporting items for systematic reviews and meta-analysis |
| RMS | Root-mean-square |
| sEMG | Surface electromyography |
| TGA | Therapeutic goods administration |
| TMJ | Temporomandibular joint |
| TMJR | Temporomandibular joint replacement |
| TMD | Temporomandibular disorder |
| USNRC | United States nuclear regulatory commission |

# Third party copyright material

| Citation information for Third party copyright material | Location of item in thesis | Permission granted Y/N |
|---|---|---|
| *Temporomandibular joint* by the Mayo foundation for medical education and research, 2009 https://www.mayoclinic.org/diseases-conditions/tmj/symptoms-causes/syc-20350941 | p. 29 | Y |
| *Figure 5: Catastrophic TMJ changes. Category 5 joint on coronal CT scan showing catastrophic changes to the TMJ resulting in extensive bony ankylosis. TMJ surgical resection with total joint replacement is normally indicated although some may argue the medially displaced condyle may be salvageable in some cases.* Dimitroulis, G. (2013). "A new surgical classification for temporomandibular joint disorders". *International journal of oral and maxillofacial surgery*, 42(2), 218-222. | p. 34 | Y |
| *Figure 63.1: Normal and displaced disc positions, with and without reduction.* Warbuton, G. (2021). "Internal derangements of the temporomandibular joint". *Oral and maxillofacial Surgery for the Clinician*, 1361-1380. | p. 35 | Y |
| *Figure 2: Conebeam CT scans showing a normal condylar head from a sagittal and coronal perspective on the LEFT, and a category 5 destructive osteoarthritic condylar head from the sagittal and coronal aspects on the RIGHT.* Brierly, G., Thomas, A., & Dimitroulis, G. (2023). "A five-year review of the OMX temporomandibular prosthetic total joint replacement system". *Oral and Maxillofacial Surgery*, 27(1), 131-139. | p. 36 | Y |
| *Figure 2b: Immediate hard rubber prosthesis, after Schröder, for surgical management after hemimandibulectomy.* *Figure 2d: Tin splinting, after Fritzsche, with splint support allowing the removal of the immediate prosthesis for wound cleansing.* *Figure 2e: Ivory implant prosthesis, after König and Roloff, with a spike to allow the prosthesis to be anchored in the spongy bone of the residual mandible.* Driemel, O., Ach, T., Müller-Richter, U.D.A., Behr, M., Reichert, T.E., Kunkel, M., & Reich, R. (2009). "Historical development of alloplastic temporomandibular joint replacement before 1945". *International journal of oral and maxillofacial surgery*, 38(4), 301-307. | p. 41 | Y |
| *Figure 2a: Prosthesis for the singular replacement of the condyle. Christiansen Type I, Christiansen Type II.* *Figure 2b: Condylar prosthesis after Vitek-Kent.* *Figure 2c: AO/ASIF TMJ prosthesis (Synthes GmbH, Umkirch, Germany.* *Figure 4a: Total, stock TMJ prosthesis after Christiansen (TMJ Inc, Golden, CO, USA).* *Figure 4b: Total, custom-made TMJ prosthesis after Christiansen (TMJ Inc, Golden, CO, USA).* *Figure 4d: Total TMJ prosthesis after Hoffman-Pappas (Endotec, South Orange, NJ, USA).* *Figure 4e: Total TMJ Concepts prosthesis (TMJ Concepts, Ventura, CA, USA).* *Figure 4f: Total Grongingen prosthesis.* *Figure 4g: Total TMJ prosthesis after Sonnenburg.* Driemel, O., Braun, S., Müller-Richtar, U.D.A., Berh, M., Reichert, T.E., Kunkel, M., & Reich, R. (2009). "Historical development of alloplastic temporomandibular joint | p. 43 | Y |

| | | |
|---|---|---|
| replacement after 1945 and state of the art". *International journal of oral and maxillofacial surgery*, 38(9), 909-920. | | |
| *Figure 8: The Techmedica/TMJ Concepts prosthesis.*<br>*Figure 9b: The W. Lorenz/Biomet TMJ total prosthesis.*<br>Ingawale, S., & Goswami, T. (2009). "Temporomandibular joint: disorders, treatments, and biomechanics". *Annals of biomedical engineering*, 37, 976-996. | p. 47 | Y |
| *ArthroJaw total joint replacement system* by Maxoniq<br>https://maxoniq.com/products/arthrojaw | p. 47 | Y |
| *Figure 3: Trajectories of specific mandibular points (the mandible is shown as semi-transparent). (A) Frontal view of the trajectories of the right lateral condylar pole, an interincisal mandibular point and the left lateral condylar pole during one opening/closing cycle. (B) Oblique view of the same mandibular points during opening/closing cycles.*<br>Leiggener, C.S., Erni, S., & Gallo, L.M. (2012). "Novel approach to the study of jaw kinematics in an alloplastic TMJ reconstruction". *International journal of oral and maxillofacial surgery*, 41(9), 1041-1045. | p. 49 | Y |
| *Figure 2: Condylar range of motion (CRoM) and incisal range of motion (InRoM) kinematics during opening, lateral, and protrusive movements, measured as curvilinear path (CP) and/or linear distance (LD), in patients with condylar hypermobility. T0, preoperatively; T1, 2 months postoperatively; T2, 6 months postoperatively; T3, at least 12 months postoperatively.*<br>Linsen, S.S., Reich, R.H., & Teschke, M. (2012). "Mandibular kinematics in patients with alloplastic total temporomandibular joint replacement – a prospective study". *Journal of oral and maxillofacial surgery*, 70(9), 2057-2064. | p. 50 | Y |
| *Figure 1c: Cranial view of a mandible with unilateral TMJ prosthesis showing the bite locations numbered 1 to 13. M = Molar, P = premolar, C = Canine, I = Incisor.*<br>*Figure 3: Maximum bite force ($F_B$) and corresponding TMJ reaction forces as a function of bite location for an intact mandible ($F_{JL}$, $F_{JR}$) and for a unilateral TMJ prosthesis ($F_P$, $F_{JC}$) with CR = 15.*<br>*Figure 8: Maximum prosthesis reaction force ($F_P$) and the corresponding CTMJ reaction force ($F_{JC}$) normalised against the corresponding maximum bite force, as a function of bite location. The location of the CR = 15.*<br>Van Loon, J.P., Otten, E., Falkenström, C.H., De Bont, L.G.M., & Verkerke, G.J. (1998). "Loading of a unilateral temporomandibular joint prosthesis: a three-dimensional mathematical study". *Journal of dental research*, 77(11),1939-1947. | p. 54 | Y |
| *Figure 6: Photograph of the sensor module, including a magnetic and a motion sensor.*<br>*Figure 9e: Intraoral photographs during simultaneous measurement with the present sensor and the WinJMA system.*<br>Morikawa, K., Isogai, R., Nonaka, J., Yoshida, Y., Haga, S., & Maki, K. (2022). "A new intraoral six-degrees-of-freedom jaw movement tracking method using magnetic fingerprints". *Sensors*, 22(22), 8923. | p. 80 | Y |
| *Figure 1a: MODJAW*<br>Solaberrieta, E., Barrenetxea, L., Minguez, R., Iturrate, M., & De Prado, I. (2018). "Registration of mandibular movement for dental diagnosis, planning and treatment". *International Journal on Interactive Design and Manufacturing (IJIDeM)*, 12, 1027-1038. | p. 80 | Y |
| *OsseoFrame Subperiosteal Dental Implant* by Maxoniq<br>https://maxoniq.com/products/osseoframe | p. 147 | Y |

| | | |
|---|---|---|
| *Figure 4: The panoramic x-ray of the patient at 12 months post-surgery shows the subperiosteal frame seated neatly against the severely atrophic maxilla.* Dimitroulis, G., Gupta, B., Wilson, I., & Hart, C. (2023). "The atrophic edentulous alveolus. A preliminary study on a new generation of subperiosteal implants". *Oral and Maxillofacial Surgery*, 27(1), 69-78. | p. 147 | Y |

# Declaration

This is to certify that:

i. This thesis comprises only my original work towards the PhD

ii. Due acknowledgment has been made in text to all other materials used

iii. This thesis is fewer than 100,000 words in length, exclusive of tables, figures, bibliographies, and appendices.

Signature: _____

Date: _____04/01/2024_____

# Preface

This thesis research has been carried out at the Department of Biomedical Engineering, University of Melbourne with industry collaboration from Maxoniq, Melbourne (formerly OMX solutions). The data presented in the main body of this thesis was collected at a private clinic in East Melbourne or at The University of Melbourne. Ethical approvals were obtained from the University of Melbourne Human Research Ethics Committee (HREC ID: 1853328.1) and have been included in Appendix E.

The studies reported in this thesis were supported by the ARC Training Centre for Medical Implant Technologies (ARC CMIT).

## PUBLICATIONS FORMING PART OF THIS THESIS

This is a thesis with publications. Chapters 3 to 6 are author-accepted versions of manuscripts according to the University of Melbourne guidelines. The contributions towards these publications are as follows:

### Chapter 3:

Woodford, S. C., Robinson, D. L., Mehl, A., Lee, P. V. S & Ackland, D. C. (2020). *Measurement of normal and pathological mandibular and temporomandibular joint kinematics: A systematic review*. Journal of Biomechanics, 111, 109994.

| Author | Proportion | Contributions |
|---|---|---|
| Sarah Woodford | 75% | Study conception and design, study execution, data analysis and interpretation, draft and review of manuscript |
| Dale Robinson | 5% | Study design, review of manuscript |
| Albert Mehl | 5% | Study design, review of manuscript |
| Peter V.S. Lee | 5% | Study design, review of manuscript |
| David Ackland | 10% | Study conception and design, study execution, data interpretation, review of manuscript |

**Chapter 4:**

Woodford, S. C., Robinson, D. L., Edelmann, C., Mehl, A., Röhrle, O., Lee, P. V. S & Ackland, D. C. (2021). *Low-profile electromagnetic field sensors in the measurement and modelling of three-dimensional jaw kinematics and occlusal loading*. Annals of Biomedical Engineering, 49 (6), 1561-1571.

| Author | Proportion | Contributions |
|---|---|---|
| Sarah Woodford | 65% | Study conception and design, study execution, computational analysis, data analysis and interpretation, draft and review of manuscript |
| Dale Robinson | 7.5% | Study design, computational analysis, data analysis and interpretation, review of manuscript |
| Cornelia Edelmann | 5% | Study design, review of manuscript |
| Albert Mehl | 5% | Study design, review of manuscript |
| Oliver Röhrle | 5% | Study design, review of manuscript |
| Peter V.S. Lee | 5% | Study design, review of manuscript |
| David Ackland | 7.5% | Study conception and design, study execution, data interpretation, review of manuscript |

**Chapter 5:**

Woodford, S. C., Robinson, D. L., Abduo, J., Lee, P. V. S. & Ackland, D. C. (2023). *Kinematics of the jaw following total temporomandibular joint replacement surgery*. Journal of Biomechanics, 159, 111741.

| Author | Proportion | Contributions |
|---|---|---|
| Sarah Woodford | 70% | Study conception and design, study execution, data analysis and interpretation, draft and review of manuscript |
| Dale Robinson | 10% | Study design, data interpretation, review of manuscript |
| Jaafar Abduo | 5% | Study design, review of manuscript |
| Peter V.S. Lee | 5% | Study design, review of manuscript |
| David Ackland | 10% | Study conception and design, study execution, data interpretation, review of manuscript |

**Chapter 6:**

Woodford, S. C., Robinson, D. L., Abduo, J., Lee, P. V. S. & Ackland, D. C. (2023). *Muscle and joint mechanics during maximum-force biting following total temporomandibular joint replacement surgery*. Biomechanics and Modelling in Mechanobiology. Accepted for publication on the 20th December 2023.

| Author | Proportion | Contributions |
|---|---|---|
| Sarah Woodford | 70% | Study conception and design, study execution, computational analysis, data analysis and interpretation, draft and review of manuscript |
| Dale Robinson | 10% | Study design, data interpretation, review of manuscript |
| Jaafar Abduo | 5% | Study design, review of manuscript |
| Peter V.S. Lee | 5% | Study design, review of manuscript |
| David Ackland | 10% | Study conception and design, study execution, data interpretation, review of manuscript |

For the purpose of structural homogeneity in this thesis, each publication that has been included as a stand-alone chapter has been modified in layout and reference style for consistency in this thesis. In some circumstances further details have been added to the original publications to create connections between each chapter and aid the flow of the thesis. All publication references have been collated into a unified bibliography at the end of this thesis. The figure and table identifiers have been changed from the research articles from which they have been taken to match the order of the thesis. Each figure/table are defined by the number of the chapter followed by the number of the figure/table within the chapter. Supplementary material that appeared as supplementary online information for each publication has been included in an appendix to this thesis.

## CONFERENCE PROCEEDINGS ARISING FROM WORK IN THIS THESIS

- Woodford, S. C., Robinson, D. L., Edelmann, C., Mehl, A., Röhrle, O., Lee, P. V. S & Ackland, D. C. (2021). *A new measurement and modelling approach to quantify occlusal loading across the dental arch*. The 12th Australasian Biomechanics Conference (ABC12). Held virtually. **Winner of 2021 New Investigator Award**

- Woodford, S. C., Robinson, D. L., Lee, P. V. S., Abduo, J., Dimitroulis, G & Ackland, D. C. (2022). *Three-dimensional kinematics of the jaw following unilateral and bilateral prosthetic TMJ surgery*. Australian and New Zealand Orthopaedic Research Society. Gold Coast, Australia.
- Woodford, S. C., Robinson, D. L., Mehl, A., Röhrle, O., Lee. P. V. S & Ackland, D. C. (2022). *The contribution of the masticatory muscles to production of three-dimensional occlusal loads across the dental arch*. The International Combined Orthopaedic Research Societies (ICORS) World Congress of Orthopaedic Research. Edinburgh, UK.
- Woodford, S. C., Robinson, D. L., Lee, P. V. S., Abduo, J., Dimitroulis, G & Ackland, D. C. (2022). *Three-dimensional kinematics of the jaw following unilateral and bilateral prosthetic TMJ surgery*. The International Combined Orthopaedic Research Societies (ICORS) World Congress of Orthopaedic Research. Edinburgh, UK.
- Woodford, S. C., Robinson, D. L., Dimitroulis, G., Abduo, J., Lee, P. V. S & Ackland, D. C. (2022). *3D kinematics of the prosthetic temporomandibular joint during jaw activities of daily living*. The 13th Australasian Biomechanics Conference (ABC13). Brisbane, Australia. **Winner of 2022 New Investigator Award.**

# Acknowledgements

I would like to express my profound gratitude to my supervisors for the guidance and support they offered me during the course of my PhD candidature, their support was consistent and dependable during a very challenging time. I would like to thank my principal supervisor, A/Prof. David Ackland for enthusiastically and patiently guiding me through this project, while allowing me the autonomy and flexibility to make it my own. I am grateful to my co-supervisors, Dr Dale Robinson for his patience and technical brilliance and Prof. Peter Lee for his wisdom and feedback. I am also grateful to my committee chair, Prof. Andrea O'Connor for generously supporting and guiding me through this project.

I would like to extend my sincere thanks to the teams at Maxoniq and Dimitroulis & Associates for their assistance and encouragement, particularly Dr George Dimitroulis for generously sharing his clinical wisdom and enthusiasm for this field.

I am deeply grateful to all of the wonderful women who chose to be involved in these experiments. Participation in this study was quite involved and the experiment was rather unconventional. Not only did each participant generously give their time, but they were genuinely enthusiastic and supportive of this research and a pleasure to spend time with.

I'm grateful to have undertaken this research as part of the ARC Centre for Medical Implant Technologies, who have provided an extremely supportive environment and a plethora of development opportunities for all their students. Furthermore, I want to thank my colleagues in the biomechanics research group and the broader Department of Biomedical Engineering at Melbourne University; particularly Sarah Safavi, Ryan Tiew, Yihang Yu, Yichen Huang, Dr Hans Grey, Dr Fatemeh Malekipour and Meg Belmonte for their stimulating discussions, continuous friendship and incredible support through this PhD journey.

Finally, I would like to thank my family for their unwavering support and belief in me; particularly my wonderful husband Eddie and our beautiful children Leah and Jude, who have made me stronger, better and more fulfilled than I could have ever imagined.

.

# Chapter 1: Introduction

## 1.1 MOTIVATION

The temporomandibular joint (TMJ) is a six degree-of-freedom bilateral synovial joint connecting the mandible to skull. The TMJ is essential for normal mandibular function, and facilitates execution of biting, swallowing and speech. Temporomandibular joint disorders (TMD) are common, with epidemiological studies indicating that between 5% to 60% of the adult population suffer from at least one TMD symptom at any given time (Ryan et al. 2019). Common symptoms include headaches, bruxism, joint pain, muscle pain, joint clicking and hearing loss (Manfredini et al. 2003; Cooper and Kleinberg 2007; Matheson et al. 2023). Females are disproportionately affected by TMD, with female-to-male ratios ranging from 2:1 to 7:1 (Wilkes 1989; Godoi et al. 2010). Unlike most joint disorders, TMDs typically affect younger adults. The age distribution at onset on TMD has bimodal peaks at 32.7 years and 54.2 years (Manfredini et al. 2010). Total TMJ replacement (TMJR) surgery is the established treatment for end-stage TMD such as ankylosis, degenerative joint disease and nonreducing internal derangements (ID), when conservative treatments are unsuccessful. TMJR surgery is also used in mandibular reconstruction following condylar fracture, tumor resection and to treat birth defects. During total TMJR surgery, the native condyle and articular disk are resected and replaced with a two-part prosthesis. This surgery has been shown to reduce pain, increase range of motion, minimise dietary restrictions and improve quality of life for patients (Mercuri et al. 2007; Zou et al. 2018). Despite these positive clinical outcomes, post-surgical joint kinematics, maximum voluntary bite force, muscle functionality and joint loading remains poorly understood, this limits the ability for total TMJR surgery to restore normal jaw function.

## 1.2 RESEARCH AIMS

This thesis investigates the mandibular and TMJ kinematics, maximum voluntary bite force, muscle functionality and joint loading of native mandibles and those reconstructed with a unilateral total TMJR.

The specific research aims are:

1. To critically evaluate and compare techniques available for measurement of jaw and TMJ kinematics.

2. To develop an experimental and computational pipeline for the measurement of three-dimensional (3D), dynamic and physiologically relevant bite forces.
3. To evaluate jaw and TMJ kinematics for total unilateral TMJR patients and compare these data to those in age matched healthy controls.
4. To evaluate maximum voluntary bite force, muscle functionality and joint loading for total unilateral TMJR patients and compare these data that those in age matched healthy controls.

## 1.3 THESIS OUTLINE

Chapter 2 provides a brief background on the anatomy, functionality, pathology and treatments of TMJ disorders, TMJ prosthesis design and post-surgical outcomes following total TMJR as a basis for the remainder of this thesis. Subsequently, chapter 3 identifies and compares techniques available for the measurement of six-degree-of-freedom mandibular and TMJ kinematics. Based on the advantages and disadvantages of current mandibular kinematics measurement techniques identified in chapter 3, chapter 4 investigates the use of new low-profile magnetic field sensors, combined with intra-oral laser scanning in the measurement of mandibular kinematics. Furthermore, this study presents a modelling pipeline, using the three-dimensional mandibular kinematics as input, to evaluate dynamic, three-dimensional bite forces during habitual chewing and maximum force clenching into a rubber sample. Following this, chapter 5 investigates the effect of total TMJR surgery on jaw and TMJ kinematics. Maximum border movements and habitual chewing are investigated to determine the maximum mobility limits and mobility of the normal and prosthetic TMJ. Subsequently, chapter 6 builds on our understanding of jaw functionality in the healthy and TMJR populations. Using the mandibular kinematics reported in chapter 5 to drive computational simulations outlined in chapter 4, the effect of total TMJR on maximum voluntary bite force is investigated. This study extends upon the computational modelling pipeline outlined in chapter 4 to evaluate and contrast the masticatory muscle performance and joint loading of the healthy and TMJR populations. Finally, chapter 7 summarises this thesis, discusses the limitations of these studies and suggests future research. This thesis structure is visually represented in Figure 1.1.

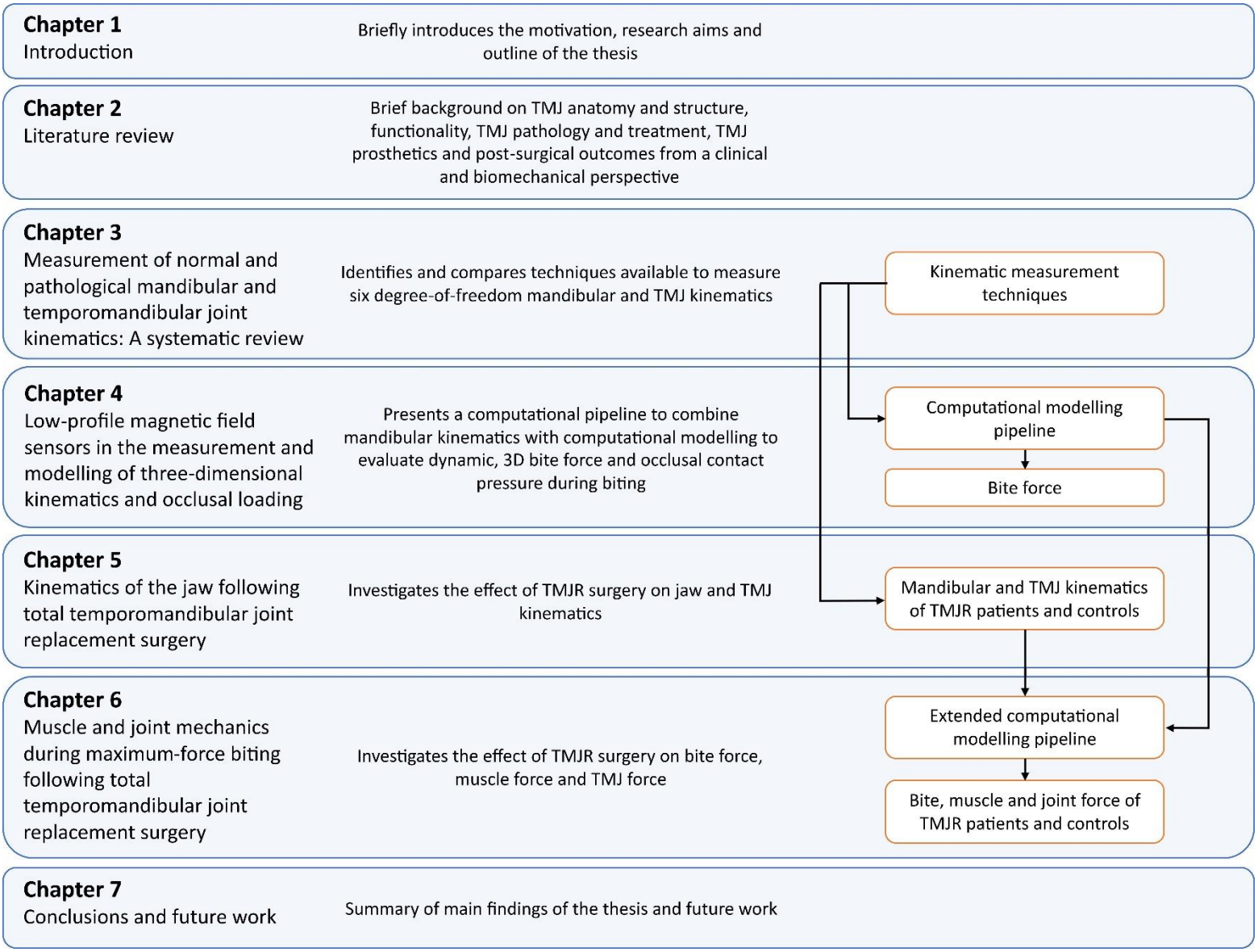



Figure 1.1: Flow-chart of thesis structure.

# Chapter 2: Literature review

## 2.1 ANATOMY AND STRUCTURE

The masticatory system is a group of craniofacial structures that controls the process of chewing, swallowing and speaking. The three major bones of the masticatory system are the maxilla, the mandible and the temporal bone. A minor bone, the hyoid bone, is an attachment structure for the tongue and the suprahyoid muscles, this sits beneath the mandible (Figure 2.1b) (National Academies of Sciences Engineering and Medicine 2020). Four primary muscles of mastication connect the mandible to the skull and are responsible for mastication and mandibular movements. The masseter and temporalis muscles are responsible for elevating the mandible, the medial pterygoid muscle acts to elevate the mandible and move it laterally, and the lateral pterygoid muscle is responsible for anterior translations of the mandibular condyle (Figure 2.1a). Conversely, the suprahyoid muscles (digastric, stylohyoid, mylohyoid and geniohyoid) attach the hyoid bone to the mandible, tongue and skull (Figure 2.1b). The suprahyoid muscles are active during mouth opening, however they do not contribute to the production of bite forces (Auvenshine and Pettit 2020; National Academies of Sciences Engineering and Medicine 2020).

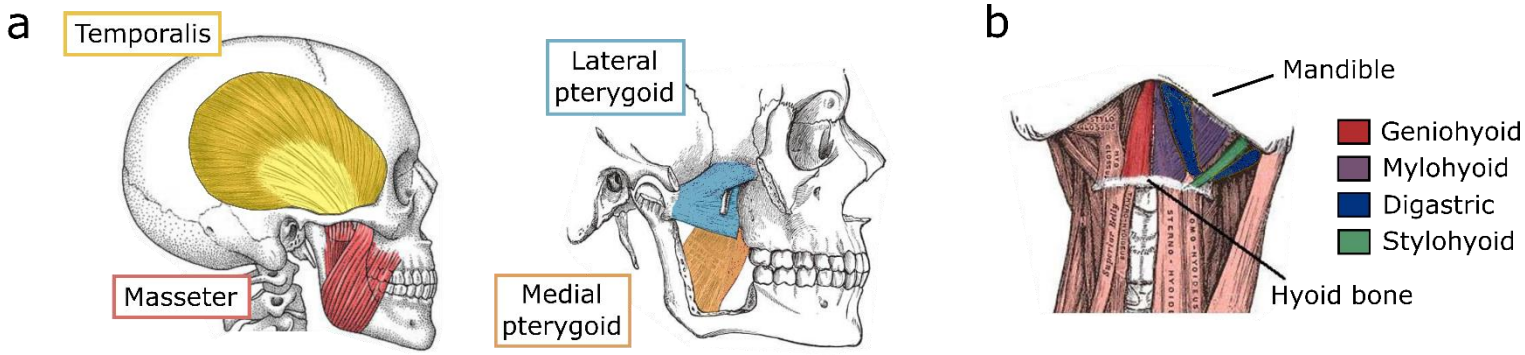



Figure 2.1: Primary masticatory muscles including the temporalis, masseter, lateral and medial pterygoid muscles (a). Suprahyoid muscles including the geniohyoid, mylohyoid, digastric and stylohyoid muscles (b).

The TMJ is a bilateral synovial joint connecting the condylar head of the mandible to the glenoid fossa of the temporal bone. The articulating surfaces of the bones are separated by a fibrocartilage disc (Figure 2.2). The TMJ disc divides the TMJ into two anatomically and functionally separate components. The superior component, located between the disc and the mandibular fossa is responsible for the translational movement of the joint. The inferior

component, located between the disc and the mandibular condyle allows rotational movement of the joint (Ferrario et al. 2005).

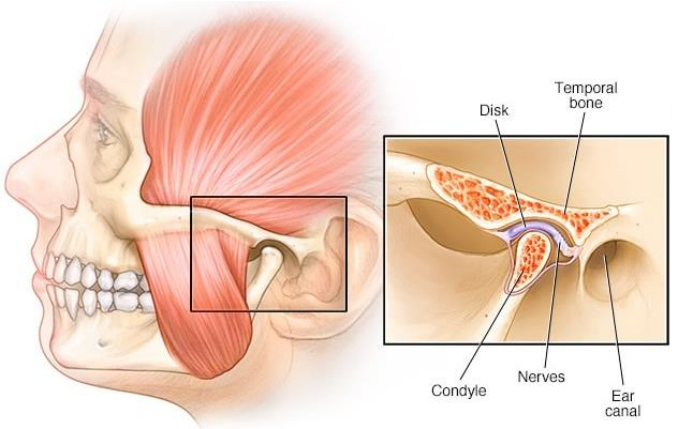



Figure 2.2: Temporomandibular joint anatomy (Litin 2009).

## 2.2 FUNCTIONALITY

The TMJ is a six degree-of-freedom joint that is capable of rotating about three perpendicular axis and translating in three directions. This mobility facilitates mandibular movements such as opening, lateral excursions and protrusion of the jaw. Complex jaw movements such as chewing are achieved through a combination of these primary mandibular movements.

Temporomandibular joint and jaw functionality varies with age (Mioche et al. 2004; M.A. and F.M. 2007; Palinkas et al. 2010), gender (Palinkas et al. 2010; Tamura and Shiga 2014; Iwasaki et al. 2017) and mandibular size (Sella-Tunis et al. 2018; Laird et al. 2020). Unless stated otherwise, reference values pertaining to jaw or TMJ functionality throughout this thesis are given for adult subjects of mixed gender, ethnicity and mandibular dimensions. The following sub-sections describe known TMJ and jaw functionality in the healthy population. A review of previously published literature regarding TMJ kinematics in the total TMJR population may be found in section 2.6.

### 2.2.1 Maximum border movements

Mandibular border movements include maximum mouth opening, maximum lateral excursions to the left and right and maximum protrusive movements. These non-functional movements are restricted by anatomical structures such as the TMJ, muscles and ligaments. As damage to these structures results in restricted mandibular border movements, they are often

used as clinical markers of jaw and TMJ health, and have therefore been extensively studied in the healthy adult population (Yu et al. 2017).

Maximum mouth opening is achieved through a rotation of the mandible about the intercondylar axis combined with an anterior translation. Anterior mandibular translations are achieved through simultaneous anterior translations of both mandibular condyles, in which the condyle and TMJ disc glide forwards along the temporal bone. This movement is primarily driven by the lateral pterygoid muscle, and the mandible is pulled backwards on closing by the posterior fibres of the temporalis muscles (Ombregt 2013). Maximum interincisal opening distances in healthy individuals range from 45.6 mm to 55.7mm (Ferrario et al. 2005), with condylar translations of 11.9 mm to 12.3 mm (Travers et al. 2000). The percentage of mandibular movement explained by rotation in the inferior TMJ compartment at maximum mouth opening is 77%, with 23% of mandibular movement attributed to translation in the superior TMJ compartment (Ferrario et al. 2005).

During lateral excursions of the jaw, the mandible is designated into working and non-working sides. Specifically, the side that the mandible is moving towards is the working side, while the side that the mandible is moving away from is the non-working side. During maximum lateral excursions, the working condyle rotates in the transverse plane and moves posteriorly 0.5 mm to 1 mm (Atwood 1968; Gibbs et al. 1971; McKay et al. 1992). The non-working condyle moves anteriorly between 7.1 mm and 8.3 mm (Buschang et al. 2001; Mapelli et al. 2016) to allow lateral movement of the incisors of 7.9 mm to 9.7 mm (C. et al. 2011; Mapelli et al. 2016). The angle in the sagittal plane between the intercondylar axis at the maximum occlusion and lateral excursive positions is referred to as the Bennett angle, this is often used to describe lateral jaw movements. In the healthy adult population the average Bennett angle is 7.5° (Cordeiro et al. 2018).

Mandibular protrusion is achieved via anterior translation of both condyles by 7.1 mm to 8.1 mm (Buschang et al. 2001; Mapelli et al. 2016). Unlike mouth opening, protrusion involves negligible rotation of the mandible in the sagittal plane; the only mandibular rotation is that necessary to move the mandibular incisors below the maxillary incisors. Healthy adults are capable of 6.6 mm to 7.7 mm (C. et al. 2011; Mapelli et al. 2016) of protrusive incisal motion.

### 2.2.2 Chewing

Chewing, also referred to as mastication, is a sophisticated combination of opening, lateral and protrusive jaw movements essential for bolus processing prior to digestion. Similar

to lateral excursions, the mandible is designated into working and non-working sides during chewing. The side of the mandible that the bolus is being chewed on is referred to as the working side, and the non-chewing side is referred to as the non-working side. The non-working condyle is observed to move further in the inferior and posterior directions during each chewing cycle than the working condyle (Miyowaki et al. 2001). As a result, the incisors move in a tear-drop shape when viewed in the frontal plane, with the mouth opening phase medial to a more lateral mouth closing phase. Dynamic mandibular movements during chewing are affected by the bolus size (Shiga et al. 2001; Bhatka et al. 2004), bolus hardness (Anderson et al. 2002), and chewing frequency (Throckmorton et al. 2001a).

The bite force magnitudes required for food breakdown have been estimated to be between 118 N and 124 N for cooked meat and raw carrot (Eerikainen and Kononen 1987; Poli et al. 2021). Human bite force capacity varies across the dental arch with the highest bite forces generated at the first molars. Technological limitations restrict the measurement of bite force in the healthy population to static, unidirectional measurements (Roehrle et al. 2018) (see section 4.3 for further discussion on bite force measurement). Healthy adults have unidirectional first molar bite force capacity of between 264 N (Palinkas et al. 2010) and 965 N (Pruim et al. 1980). This large range in measured bite force capacity reflects the variations in cranio-facial morphology and occlusal status throughout the adult population (Koc et al. 2010). Bite force is generated primarily by activation of the masseter and temporalis muscles. Activation of the medial pterygoid muscles contributes to lateral shear bite force production, which provides a grinding action to facilitate food breakdown.

Chewing is the functional activity with the highest muscle activations in the masticatory system (Farella et al. 2008), potentially leading to the highest loading at the TMJ's. Loading at the TMJ has been linked to the development of TMJ disorders. Specifically, animal models have shown that acute mechanical overloading can cause severe damage to articular cartilage within the joint (Radin et al. 1984), this often proceeds the development of degenerative disorders such as osteoarthritis (Thompson et al. 1991). As TMJ loading cannot be measured in humans *in vivo* non-invasively, mathematical models and computational methods such as finite element analysis (FEA) remain the standard for study of TMJ loading during chewing. Mathematical models suggest that for unilateral chewing at the first molar the non-working joint experiences loading of 45% to 90% of the applied bite force, while the working joint is loaded at 45% to -20% of the bite force (Ferrario and Sforza 1994), where positive and negative values indicate compressive and tensile loading of the joint, respectively. Furthermore, TMJ

loading varies with the direction of the applied bite force, with the lowest TMJ loads coinciding with vertically directed bite force and higher TMJ loading resulting from off-axial bite forces (Smith et al. 1986; Schindler et al. 2007; Iwasaki et al. 2009). Similarly, the chewing position across the dental arch affects the loads at the TMJ. Chewing on the anterior teeth such as the incisors leads to higher ratio of TMJ force to bite force than chewing with the posterior teeth (Ferrario and Sforza 1994). Based on these trends, the clinical treatment of TMJ disorders often involve the prescription of altered diet to reduce bite forces and therefore TMJ loads. Patients with pain in one TMJ are also recommended to chew on the painful side in an effort to reduce loading to the pathological joint (Sagl et al. 2021).

## 2.3 PATHOLOGIES OF THE TEMPOROMANDIBULAR JOINT

TMD is a group of musculoskeletal conditions involving pain and/or dysfunction of the masticatory muscles, TMJ's and associated structures (List and Jensen 2017). Epidemiological studies in multiple countries show that approximately 5% to 60% of the population suffers from at least one TMD symptom at any time (Ryan et al. 2019); however, only 3% to 7% of the adult population actually seeks out care for the pain and dysfunction associated with TMD (Carlsson 1999). Females are disproportionately affected by TMD, with female-to-male ratios ranging from 2:1 to 7:1 (Wilkes 1989; Godoi et al. 2010). The age distribution at onset on TMD has bimodal peaks corresponding to two distinct groups of TMD patients. The first group is characterised by disc displacement with an absence of degenerative disorders, with a mean age of 32.7 years. The second group features signs and symptoms of inflammatory-degenerative joint disorders, with a mean age of 54.2 years (Manfredini et al. 2010). The economic burden of TMD is high, with estimates of about $4 billion per annum in the United States (Gatchel et al. 2006). The economic burden is inflated by the long and costly journey that patients experience to receive diagnosis and care for TMD, caused by notoriously disorganised care pathways for TMD (Breckons et al. 2017). Furthermore, while TMD patients have a low rate of absenteeism from work, it is estimated that the quality and quantity of work that they can provide for their employer is reduced by 12%, due to their persistent state of pain, resulting in considerable "hidden costs" to their employers and the economy (Slade and Durham 2020).

The exact pathophysiology of TMD is unclear, however it is shown to be a multifactorial disorder where biological, psychological and social factors combine to predispose, perpetuate or initiate TMD (Slade et al. 2013; Kapos et al. 2020). A large retrospective study (n = 4,528) of a single clinician over 25 years quantified the incidence of common TMD symptoms including headaches (79%), bruxism (58%), TMJ pain (54%), ear pain (52%), jaw clicking or

popping sounds (51%), neck pain (51%), tinnitus (37%), dizziness (37%), hearing loss (36%) and hyperacuity to sound (23%) (Manfredini et al. 2003; Cooper and Kleinberg 2007; Matheson et al. 2023). Additionally, TMD patients often present with comorbid psychopathology, such as post-traumatic stress disorder, depression and anxiety (Gallo et al. 2008), and other comorbid conditions such as fibromyalgia, irritable bowel syndrome, chronic fatigue syndrome and sleep disturbances (Aaron et al. 2000; Hoffmann et al. 2011; Maixner et al. 2016).

The classification of TMD can be seperated into disorders of the masticatory muscles (extra-articular TMD) and disorders of the joint (intra-articular TMD). Details of the most common types of extra-articular and intra-articular TMD's can be found in sections 2.3.1 and 2.3.2, respectively.

### 2.3.1 Extra-articular temporomandibular disorder

Extra-articular TMD are disorders of the masticatory muscles that may result in pain, tenderness and reduced movement capacity. These muscle-related disorders represent the largest sub-group of TMD diagnoses and include local myalgia, myofascial pain and myofibrotic contracture (Stohler 1999). Local myalgia and myofascial pain are both characterised by pain in the masticatory muscles, this is broadly believed to result from muscle fatigue and tension, although their exact pathogenesis is poorly understood (Winocur-Arias et al. 2022). The two conditions differ in the locale of the experienced pain, with local and referred muscle pain being associated with local myalgia and myofascial pain, respectively (Schiffman et al. 2015). Myofibrotic contracture results from excessive tissue adhesions within the muscle sheaths, this prevents the muscle fibres from sliding over themselves thus inhibiting full lengthening of the muscle. Myofibrotic contracture often results from trauma to the muscles, and while it is not a painful condition, it does result in limited mandibular range of motion (Rossi et al. 2023).

### 2.3.2 Intra-articular temporomandibular disorder

Intra-articular TMD are disorders of the TMJ which often result in joint pain and reduced range of motion. These include TMJ hypermobility and hypomobility, internal derangements and degenerative joint diseases. Temporomandibular joint hypermobility is a state where wide mouth opening movements leads to subluxation or luxation of the joint, often accompanied by pain and clicking within the TMJ (Grochala et al. 2021). TMJ hypermobility is accompanied by the correct positioning of the articular disc during movements, which distinguishes it from internal derangements. Hypermobility of the TMJ can result from excessive mouth opening and

injury or damage to the joint capsule. The repeated subluxation may result in lengthening of the ligaments, potentially leading to disorders of the articular disc (Okeson 2019).

Temporomandibular joint hypomobility is a state where jaw movements are restricted. The most common intra-articular form of TMJ hypomobility is TMJ ankylosis, which is characterised by a fibrous or bony fusion of the condylar head to the glenoid fossa, resulting in restricted jaw movements (Figure 2.3). Trauma and infection are the leading causes of TMJ ankylosis (Ayn et al. 2022); however, ankylosis can also occur following TMJ surgery and as a result of systemic diseases such as rheumatoid arthritis (Maimaiti et al. 2017).

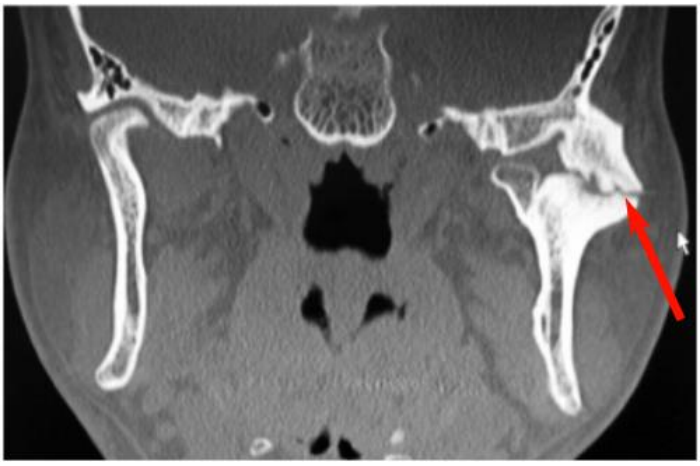


Figure 2.3: CT scan of ankylosis patient. Red arrow indicates extensive bony ankylosis of the left TMJ. Figure adapted from Dimitroulis et al. (2013).

Disc displacement (also referred to as disc derrangements or internal derangement) is the most common type of intra-articular TMD, and includes 41.1% of all TMD patients (Manfredini et al. 2011). Disc displacement is defined as a joint dysfunction associated with an abnormal disc position and damage to the internal structures of the joint (Tatli and Machon 2017). Disc displacement result from trauma or parafunctional habits which cause degenerative changes in the articular structures, increased friction and gradual disc displacement (Israel 2016). Internal derangements can be classified as either reducing or nonreducing (Figure 2.4) (Warbuton 2021). In reducing disc displacements the TMJ disc sits anteriorly to its native position in the closed mouth position, but reduces to the normal position upon maximal mouth opening; this is accompanied by painless clicking early in the opening and late in the closing movements, with unrestricted mandibular motion. In nonreducing disc displacements the displaced disc is thickened and does not reduce upon maximal openng, clinical symtoms include chronic pain and restricted mandibular movements (Murphy et al. 2013). Reducing disc displacements will typically progress to nonreducing disc displacements if not treated.

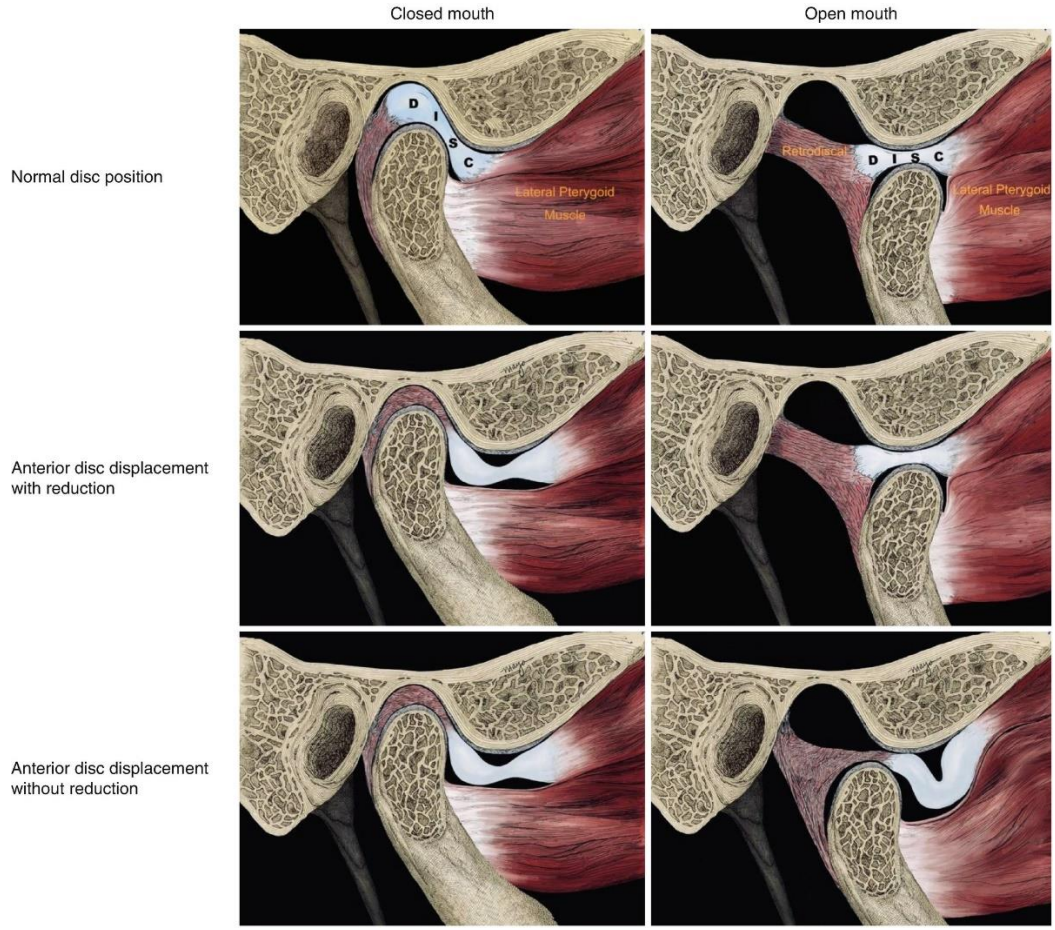



Figure 2.4: Internal derangement of the TMJ. Normal refers to the normal anatomic position of the TMJ disc during maximal mouth opening. Anterior disc displacement with reduction shows the anteriorly displaced disc returning to a normal anatomical position upon maximal opening. Anterior disc displacement without reduction shows the anteriorly displaced disc during closed and maximal opening positions with disc thickening present. Figure adapted from Warbuton, G. (2021).

The TMJ can also be affected by degenerative joint diseases such as osteoarthritis or osteoarthrosis, depending on whether inflammatory or non-inflammatory states exist, respectively (Murphy et al. 2013). Degenerative joint disease affects the cartilage, subchondral bone, synovial membrane, and other structures, leading to degradation of the articular cartilage and joint remodelling (Kalladka et al. 2014) (Figure 2.5). This can result in pain, restriction of jaw movements and reduced quality of life (Trize et al. 2018; Al-ani 2021). The prevalence of degenerative joint disease among TMD patients ranges from 18% (Kim et al. 2016) to 85% (Rudisch 2003), depending on diagnostic criteria and type of imaging used during diagnosis (Pantoja et al. 2019).

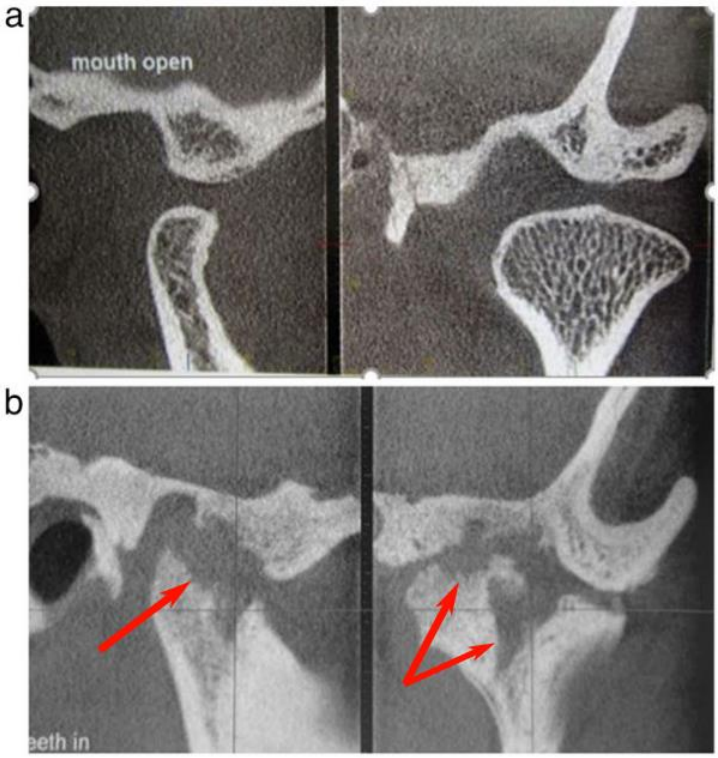



Figure 2.5: CBCT scans showing a normal condylar head (a) and an osteoarthritic condylar head (b) from a sagittal (left) and coronal (right) view. Red arrows highlight regions of severely degenerated bone. Figure adapted from Brierly et al. (2022).

## 2.4 TREATMENT OF TEMPOROMANDIBULAR JOINT DISORDERS

The main goal of any treatment for a TMJ disorder is to restore normal mandibular function and reduce pain (Dimitroulis 2011). As TMD is a multifactorial disorder, the best results are achieved through the careful consideration of contributing factors such as stress, depression, and oral parafunctional habits such as bruxism (Auerbach et al. 2001; Dimitroulis 2018). Reversible conservative therapies are strongly suggested as the first line of treatment based on the evidence of treatment risks and benefits (Greene 2010), with invasive surgical treatments often considered a last resort (Dimitroulis 2011). Between 3% to 7% of all TMD patients seek out treatment (Carlsson 1999), of those about 95% of treatment strategies begin with non-invasive or minimally-invasive treatments (Dimitroulis 2018). For those who seek professional treatment, less than 5% harbour a functional or pathological problem in their TMJ which may be amenable to surgery (Dimitroulis 2011).

Treatments for TMD can be categorised as non-invasive, minimally invasive or invasive. The following subsections describe the main treatment strategies applied to combat pain and restricted movements in TMD patients.

### 2.4.1 Non-invasive treatments

Non-invasive TMD treatments include patient education, self-management strategies, physical therapy, pharmacotherapy, psychotherapy and occlusal splints and/or adjustments. These are the first line of treatment for TMD. Patient education in the treatment of TMD can bring real bio-clinical, cognitive and psychological benefits to patients by allowing them to better understand their illness and treatment, and therefore to improve their health behaviour and self-management strategies (Albano et al. 2019). Self-management strategies for TMD may include optimal head posture, sleep hygiene, soft diet, thermal therapy, breathing exercises and avoidance of oral parafunctions such as daytime clenching, nail biting and gum chewing (Durham et al. 2013; Durham and Breckons 2016; Kapos et al. 2020; Matheson et al. 2023). These techniques all help reduce pain and dysfunction, but critically they provide patients with some autonomy to control their symptoms in recurrent TMD episodes (Kapos et al. 2020).

Physical therapy may involve electrotherapy, postural awareness, therapeutic exercises and manual therapy (Gray et al. 1994; Matheson et al. 2023). Electrotherapy interventions include transcutaneous electric nerve stimulation, ultrasound and laser techniques. These are implemented to reduce inflammation, increase local blood flow and promote muscle relaxation, however their ability to reduce TMD pain and improve range of motion is disputed (Treacy 1999; Murphy et al. 2013). Manual therapy involves physical therapists using their hands to apply direct pressure to muscles and joints (Matheson et al. 2023), this is often used in conjunction with exercises designed to strengthen and improve mobility in the masticatory and cervical spine muscles (Murphy et al. 2013).

Pharmacotherapeutic interventions include the use of muscle relaxants and nonsteroidal anti-inflammatory drugs (NSAIDs) to reduce TMD muscle and joint pain, respectively (Alstergren and Davidson 2017). As TMD's often occur with psychological symptoms such as anxiety and depression, multimodal non-invasive treatment often includes psychological therapies such as individual counselling and cognitive behavioural therapy, both of which are correlated with long-term (>3 months) improvements in TMD pain, depression and interference with daily activities (Aggarwal and Main 2019; Melo et al. 2020).

Occlusal splints and occlusal adjustments work to establish balance in the masticatory system. They do this by modifying the biomechanics to achieve the most stable bite position, which is correlated to conservative TMJ loads, thus protecting the joint (Murphy et al. 2013). Furthermore, occlusal splints which provide full coverage of occlusal surfaces worn at night may be used to control bruxism (Ingawale and Goswami 2009). Whilst occlusal splints and

adjustments decrease pain and improve mandibular movements in the short to medium term, their long-term effectiveness remains debated (Ingawale and Goswami 2009; Zhang et al. 2020).

### 2.4.2 Minimally invasive treatments

Minimally invasive TMD treatments include intra-muscular and intra-articular injections, acupuncture, arthrocentesis and arthroscopic surgery. Pain in the masticatory muscles can be reduced with intra-muscular injections of botulinum toxin, platelet-rich plasma, collagen and morphine (Nowak et al. 2021). Intra-articular Injections of corticosteroids and high-molecular-weight sodium hyaluronate are intended to treat the chronic pain and associated movement restrictions arising from osteoarthritis. However, studies indicate both regenerative and degenerative responses to such injections and therefore their use remains controversial (Dionne 1997; Mountziaris et al. 2009). Acupuncture for TMD involves inserting needles around the ear, face, jaw and into the masticatory muscles. Randomised clinical trials have provided evidence of the effectiveness of acupuncture to reduce TMD muscle pain in comparison to sham acupuncture (Yuan et al. 2016; Carla et al. 2017).

Arthrocentesis and arthroscopic surgery require access to the joint capsule to lubricate articulating surfaces and reduce inflammation, referred to as closed TMJ surgical procedures. During arthrocentesis a sterile needle is used to drain fluid from the joint, the joint is then flushed of debris and inflammatory cytokines using a sterile solution (Murphy et al. 2013). Following arthrocentesis patients experience a significant reduction in pain, increase in range of motion and increased self-assessed general improvement, often circumventing or postponing the need for invasive surgical treatment (Nitzan and Price 2001). Arthroscopic surgery is a more invasive procedure in which the surgeon may break intra-articular adhesions that may be preventing TMJ disc movement, it can also involve disc repositioning and repair (Murphy et al. 2013; Dimitroulis 2018). This procedure is often applied to cases of nonreducing internal derangements; however, one randomised clinical trial found no advantages for arthroscopy compared to conservative non-surgical management when considering short and medium term pain, range of motion and chewing impairments (Schiffman et al. 2014).

### 2.4.3 Invasive treatments

While most TMD patients are treated with non-invasive or minimally invasive treatments, patients with fracture of the mandibular condyle due to trauma, and those with severe pain or joint dysfunction lasting more than 6 months, are typically considered for surgical intervention

(Gauer and Semidey 2015; Matheson et al. 2023). Invasive treatments include discectomy, disc replacement and joint reconstruction. This group of treatments are also referred to as open TMJ surgical procedures.

Discectomy is the surgical procedure of choice for disc perforation and is also applied in cases of nonreducing internal derangements (Werkman et al. 2022). This involves surgically removing the damaged articular disc from the TMJ with or without subsequent disc replacement. Following discectomy, disc replacement can be performed with a range of autologous or alloplastic materials. The majority of surgeons use autogenous fat to replace the articular disc, although dermal-fat, temporalis muscle, temporalis fascia and cryopreserved umbilical membrane or cartilage are also used (Connelly et al. 2019; Werkman et al. 2022). Alloplastic disk replacements are seldom performed after the notable Vitek Teflon prosthesis failures of the 1970's, where degradation of the prosthesis material led to particulate debris that simulated an osteolytic local foreign-body reaction (Murphy et al. 2013). This response caused resorption of the condyle and fossa, producing perforations in the middle cranial fossa (Murphy et al. 2013). Following discectomy without disc replacement there is evidence of osteophytes and flattening of the articular surfaces within the joint, these changes radiologically appears as osteoarthritis (Dimitroulis 2011). Disc replacements intend to cushion the condyle and fossa to prevent these adaptions; however, some authors conclude that these changes are indicators of adaptive change rather than degenerative disorders and do not need to prevented (Eriksson and Westesson 2001). There is no consensus in the literature regarding the necessity of disc replacement after discectomy, with positive long-term functional outcomes achieved both with and without replacement (Miloro et al. 2017; Machoň et al. 2020).

Following the exhaustion of conservative non-surgical and surgical treatment options a joint replacement may be appropriate. If either the condyle or the fossa is replaced, the treatment is a partial temporomandibular joint replacement, if the condyle and fossa are both replaced the treatment is known as a total TMJR. Partial or total TMJR surgery may be required for cases of bony ankylosis, recurrent fibrous ankylosis, degenerative joint disease, aseptic necrosis of the condyle, advanced rheumatoid arthritis, tumours involving the condyle or mandibular ramus and loss of condyle from trauma or pathology (Ingawale and Goswami 2009). Joint replacement materials include autologous grafts and alloplastic materials. Costochondral rib grafts are a comprehensive reconstruction option, they are easily harvested and can be fashioned into a new condyle and secured to the mandibular ramus with wires or screws (Dimitroulis 2011). As a

native tissue, the adaptability and lack of immunogenetic potential offer advantages over alloplastic options (Murphy et al. 2013).

Costochondral grafts give excellent functional results when used to treat defects caused by pathology or trauma. However, the results can be poor when used to reconstruct the joints of TMD patients, as the loss of vertical height produced by graft resorption can lead to recurrence of both joint and muscle pain (Murphy et al. 2013). Furthermore, costochondral grafts are not appropriate for use in older patients because of the brittle nature of the aged bone which increases the likelihood of fracture and ankylosis (Dimitroulis 2011). Alloplastic total joint replacements are well suited to TMD patients and the older population, these consist of a metal condyle attached to the mandibular ramus, which articulates within a polymer fossa prosthesis (more information on TMJ prosthesis design can be found in section 2.5). These systems are shown to provide long-term improvements in pain, range of motion and quality of life (Mercuri et al. 2007; Zou et al. 2018) (more information on TMJ replacement outcomes can be found in section 2.6). Similar to other orthopaedic implants, the lifetime of total alloplastic TMJ reconstructions are in the range of 10 to 15 years (Ingawale and Goswami 2009). Considering the relative youth of the patient population, secondary TMJR surgeries are often necessary (Murphy et al. 2013).

## 2.5 TEMPOROMANDIBULAR JOINT PROSTHESIS DESIGN

### 2.5.1 Historical development

The first documented attempt at alloplastic reconstruction of a TMJ component was performed by neurosurgeon John Carnochan, who in 1840 carved a piece of wood to be used as an interpositional device inserted between the glenoid fossa and the condyle as treatment for a severely ankylosed TMJ (Mercuri 2016, 2019; De Meurechy and Mommaerts 2018). Over the next 120 years, there have been sporadic reports of surgeons developing one-off interpositional devices constructed from gold (Driemel et al. 2009a), ivory (Partsch et al. 1932), aluminium (Orlow 1903), tantalum foil (Eggers 1946) and stainless steel (Smith et al. 1957; Mercuri 1998) in an attempt to treat ankylosis. Early interpositional devices had a tendency to be displaced. This prompted Robinson's design, in 1960, of a stainless steel plate that covered the glenoid fossa and articular eminence, this was fixed to the zygomatic arch using 2 screws in an attempt to mitigate displacement (Smith et al. 1957). This marked the first of many iterations of fossa-eminence prosthesis designs (Table 2.1). The first condylar prosthesis was developed by Martin in 1878. Made from natural rubber, this and other early condylar prosthesis

were not intended as functional replacements, instead their main purpose was to prevent postoperative scar contraction and provide sufficient tissue support (Driemel et al. 2009a; De Meurechy and Mommaerts 2018). Early designs of condylar prosthesis often failed due to poor fixation to the mandible, this was initially achieved via a spike on the prosthesis which was placed into the mandibular trabecular bone or through clips that attached to the molars (Figure 2.6) (Driemel et al. 2009a). Intermediate iterations in condylar prosthesis design utilised metal mesh for the ramal component to encourage osseointegration (Hahn 1964) and intermedullary stems (Flot et al. 1984); however, current designs typically achieve stable long term fixation using screws (Table 2.1) (Driemel et al. 2009b; De Meurechy and Mommaerts 2018).

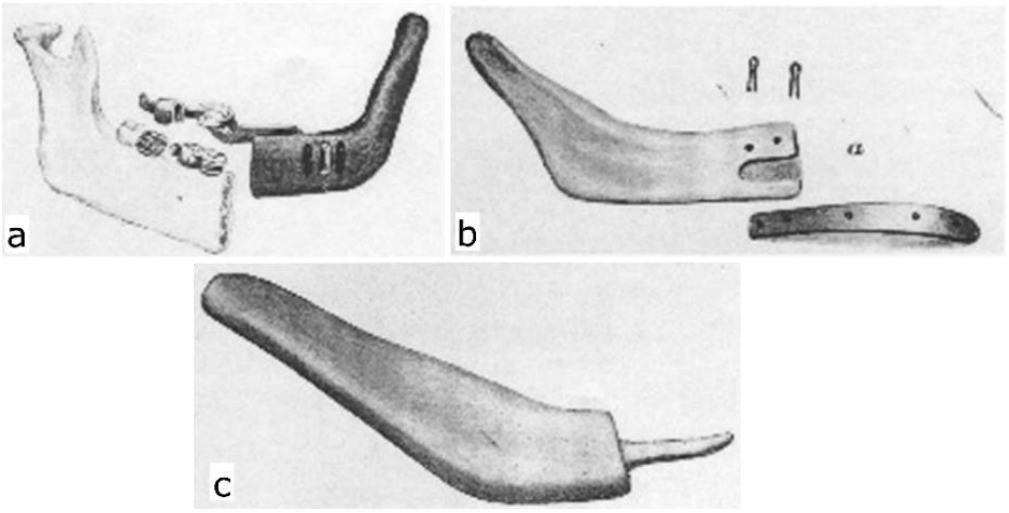



Figure 2.6: Early condylar prosthesis. Rubber prosthesis fixated with dental clasps, for surgical management after hemimandibulectomy (a). Tin prosthesis fixed with a detachable plate to allow removal of the prosthesis for wound cleaning (b). Ivory prosthesis with a spike to allow anchorage into the trabecular bone of the residual mandible (c). Figures adapted from Driemel et al (2009).

Initial devices consisted of either a fossa or condylar prosthesis, however it soon became clear that the isolated use of a condylar prosthesis led to resorption of the glenoid fossa (De Meurechy and Mommaerts 2018). This motivated the first use of a total TMJ prosthesis in 1965 by Christiansen, who combined a Vitallium fossa-eminence prosthesis with a cast Vitallium ramus component fixed to a polymethyl methacrylate (PMMA) head (Figure 2.7a) (Mercuri 1998; Driemel et al. 2009b; De Meurechy and Mommaerts 2018). Following Christiansen's inaugural use of a total TMJ system, several surgeons, researchers and companies proposed different total TMJ prosthetic iterations (Figure 2.7 & Table 2.2). Early iterations had metal-to-metal interfaces of the condyle and fossa (Kummoona 1978; van Loon et al. 1995; Driemel et al. 2009b), which lead to negative patient outcomes due to poor wear performance at the

articulating surface (Kummoona 1978; van Loon et al. 1995; Driemel et al. 2009b). To mitigate this, recent designs apply surface treatment to the articulating surfaces to harden the material and improve wear performance, or employ acrylic or polymer material for either the condylar head or the fossa (van Loon et al. 1995; Giannakopoulos et al. 2012). At present, the TMJ Concepts and the Zimmer Biomet systems have United States Food & Drug Administration (FDA) approval (see Section 2.5.3), and until recently, these two systems have maintained the dominant share of the prosthetic TMJ market worldwide. However, tariffs, healthcare restrictions and the cost of business with foreign countries have made these two devices prohibitively expensive and unavailable in many countries. This has prompted the development of several emerging systems globally (Elledge et al. 2019). In 2019, Elledge et al. (Elledge et al. 2019) identified 27 emerging TMJ replacement systems worldwide, of which 21 are custom designed, 4 have been given regulatory approval and 11 are manufactured using selective laser melting or direct metal laser sintering 3D printing technology (Elledge et al. 2019).

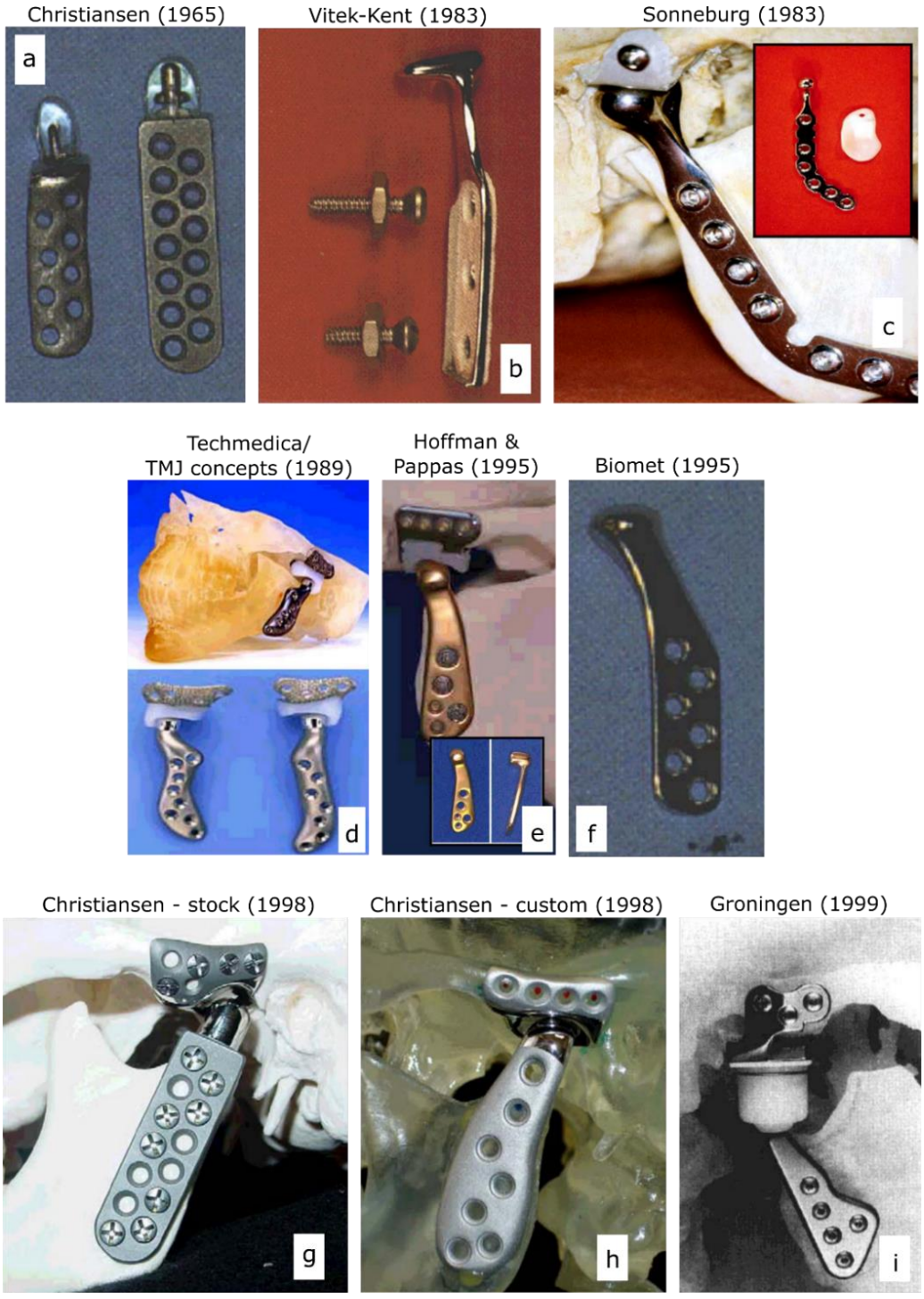



Figure 2.7: Evolution of total TMJ prosthesis designs. Shown is the Christiansen condyle prosthesis (a), the Vitek-Kent condyle prosthesis (b), the Sonneburg total TMJ prosthesis (c), the early Techmedica/TMJ concepts total TMJ prosthesis (d), the Hoffman and Pappas total TMJ prosthesis (e), the early Biomet condyle prosthesis (f), the Christiansen stock (g) and custom (h) total TMJ prosthesis and the Groningen total TMJ prosthesis (i). Further details of each system can be found in Table 2.2. Figures adapted from Driemel et al. (2009).

Table 2.1: Interpositional devices, fossa- eminence and condylar prosthesis

| Surgeon/Designer/Company (Co) | Year | Type | Material | Fixation | Regulatory | Custom /Stock | Figure |
|---|---|---|---|---|---|---|---|
| Carnochan | 1840 | Interpositional | Wood | | | | |
| Martin | 1878 | Condyle | Rubber | | | | |
| Rosner | 1889 | Interpositional | Gold | | | | |
| Gluck | 1890 | Condyle | Ivory | Spike in ramal component inserted into trabecular bone | | | Figure 2.7c |
| Schroder | 1901 | Condyle | Rubber | Screws or clipped to teeth | | | Figure 2.7a |
| Fritzsche | 1901 | Condyle | Tin | Screws or clipped to teeth | | | Figure 2.7b |
| Orlow | 1903 | Interpositional | Gold-coated aluminium plates | | | | |
| Partsch | 1917 | Condyle | Glass | Screws or clipped to teeth | | | |
| Partsch | 1932 | Interpositional | Ivory | | | | |
| Risdon | 1934 | Interpositional | Gold foil | | | | |
| Risdon | 1934 | Interpositional | Metallic plate | | | | |
| Eggers | 1946 | Interpositional | Tantulum foil | | | | |
| Goodsell | 1947 | Interpositional | Tantulum foil | | | | |
| Smith and Robinson | 1957 | Interpositional | Stainless steel plates | | | Custom | |
| Robinson | 1960 | Fossa-eminence prosthesis | Stainless steel | Screws | | | |
| Christensen | 1963 | Fossa-eminence prosthesis | Cobalt-Chromium | Screws | | Stock | |
| Hahn | 1964 | Condyle | Vitalium mesh with an acrylic condyle | Osseointegration | | | |
| Morgan | 1965 | Fossa-eminence prosthesis | Cobalt-Chromium | | | Stock | |
| Robinson | 1968 | Interpositional | Silastic sponge | | | | |
| Kent | 1972 | Condyle | Teflon | | | | |
| Kriens | 1973 | Fossa-eminence prosthesis | Silastic | | | | |
| Vitek | 1976 | Interpositional | Teflon | | FDA approved, later retracted | | |
| Spiessel | 1976 | Condyle | Titanium | Intramedullary placement | | | |
| Raveh | 1982 | Condyle | Titanium | Screws | | Stock | |
| Flot | 1984 | Condyle | Titanium with polyethylene domed "cap" over the condylar head | Intermedullary stem | | Stock | |

Table 2.2: Total TMJ replacement systems

| Surgeon/Designer /Company (Co) | Year | Type | Material | Fixation | Regulatory | Custom/ Stock | Figure |
|---|---|---|---|---|---|---|---|
| Christiansen | 1965 | Total TMJ replacement | Fossa: Vitalium<br>Condyle: Viatalium ramus with PMMA condylar head | | | | Figure 2.8a |
| Kiehn | 1974 | Total TMJ replacement | Fossa: Vitalium<br>Condyle: Vitalium | PMMA cement | | | |
| Momma | 1977 | Total TMJ replacement | Fossa: Vitalium<br>Condyle: Vitalium | Fossa: Screws<br>Condyle: Screws | | | |
| Kummoona | 1977 | Total TMJ replacement | Fossa: Cobalt-Chromium<br>Condyle: Cobalt-Chromium | Fossa: Screws<br>Condyle: Intramedullary stem and PMMA | | Stock | |
| Vitek, Kent | 1983 | Total TMJ replacement | Fossa: Teflon and Proplast<br>Condyle: Cobalt-Chromium | Fossa: Screws<br>Condyle: Screws | FDA approved, later retracted | Stock | Figure 2.8b |
| Sonnenburg and Fethke | 1983 | Total TMJ replacement | Fossa: High-pressure polymerised polyethylene<br>Condyle: Titanium/Palladium alloy | Fossa: Screw and PMMA cement<br>Condyle: Screws | | Custom | Figure 2.8c |
| Vitek, Kent | 1986 | Total TMJ replacement | Fossa: UHMWPE and proplast<br>Condyle: Cobalt-Chromium | Fossa: Screws<br>Condyle: Screws | FDA approved, later retracted | Stock | |
| Techmedica (Co)/TMJ concepts (Co) | 1989 | Total TMJ replacement | Fossa: Titanium mesh coated with UHMWPE<br>Condyle: Titanium alloy shaft with Cobalt-Chromium-Molybdenum head | Fossa: Screws and osseointegration<br>Condyle: Screws | Recieved FDA approval in 1999 | Custom | Figure 2.8d |
| Butow | 1992 | Total TMJ replacement | Fossa: Titanium with Nitride surface treatment<br>Condyle: Titanium with Nitride surface treatment | | | Stock | |
| Hoffman and Pappas | 1995 | Total TMJ replacement | Fossa: Titanium mesh with UHMWPE articulating surface<br>Condyle: Titanium | Fossa: Screws and osseointegration<br>Condyle: Micro-locking screws | | Stock | Figure 2.8e |
| Lorenz/Biomet (Co) | 1995 | Total TMJ replacement | Fossa: UHMWPE<br>Condyle: Cobalt-Chromium with titanium plasma spray on ramal surface | Fossa: Screws<br>Condyle: Screws | Received FDA approval in 2005 | Stock | Figure 2.8f |
| Chase/Nexus (Co) | 1996 | Total TMJ replacement | Fossa: Vitalium<br>Condyle: Vitalium ramus with Cobalt-Chromium condylar head | Fossa: Screws<br>Condyle: Screws | | stock | |
| Christiansen | 1998 | Total TMJ replacement | Fossa: Cobalt-Chromium<br>Condyle: Cobalt-Chromium | Fossa: Screws<br>Condyle: Screws | FDA approved, later retracted | both | Figure 2.8g & h |
| Goningen (Co) | 1999 | Total TMJ replacement | Fossa: Titanium with Zirconia plate on articulating side<br>Condyle:Titanium ramus with the condyle composed of a zirconia ball<br>Disc: UHMWPE | Fossa: Screws<br>Condyle: Screws | | Stock and Custom | Figure 2.8i |

### 2.5.2 Prosthetic temporomandibular joint customisation

Total TMJ prostheses are available as either stock or custom devices. Stock devices consist of mandibular and fossa attachments available in different sizes and styles; however, the articulating surfaces of the condylar head and fossa remain the same, regardless of the component size (Gerbino et al. 2017). Stock devices are time and cost efficient to use intraoperatively; however, these solutions are not always appropriate for patients with complex anatomical requirements. This gap motivated the development of customised TMJ prostheses designed to interface with patient-specific bony anatomy. This concept eliminates the need for host bone removal, or for adaption of stock components, such as bending or shimming with bone or alloplastic cement, to achieve a close fit (Johnson et al. 2017). Furthermore, computer aided design (CAD)/computer aided manufacture (CAM) custom prostheses allow the generation of custom cutting guides and surgical planning, reducing the operating time, operating cost and risk of infection (Mercuri 2013; Gerbino et al. 2017). There is debate about whether stock and custom TMJ prosthesis deliver equivalent functional outcomes and quality of life for patients. Some studies report significantly larger postsurgical jaw opening, lower pain and fewer complications for custom prosthesis compared to stock (Wolford et al. 2003; Kanatsios et al. 2022); while other studies report no significant differences (Zou et al. 2018). However, custom devices are typically applied to the "worst case" anatomical situations, or patients who have had multiple invasive and unsuccessful procedures; therefore, making direct comparisons of their outcomes to stock devices, which are typically used for simple cases with good bone stock, is difficult (Johnson et al. 2017).

### 2.5.3 Regulation of prosthetic temporomandibular joints

At present, there are two TMJ replacement systems with approval from the FDA, namely the TMJ concepts system (formerly Techmedica; Ventura, CA, USA) and the Zimmer Biomet system (Jacksonville, FL, USA) (Figure 2.8a & b). The TMJ concepts system comprises custom prosthetics, and while Zimmer Biomet produce both custom and stock devices, only the latter currently has FDA approval. In the Australian market, the supply and use of TMJ prosthetics is regulated by the Therapeutic Goods Administration (TGA). At present, the Australian Register of Therapeutic Goods (ARTG) includes the Lyka Smith Combined TMJ System, the Zimmer Biomet stock TMJ system, the Signature Orthopaedics prosthesis and the Maxoniq ArthroJaw total joint replacement system (Figure 2.8c).

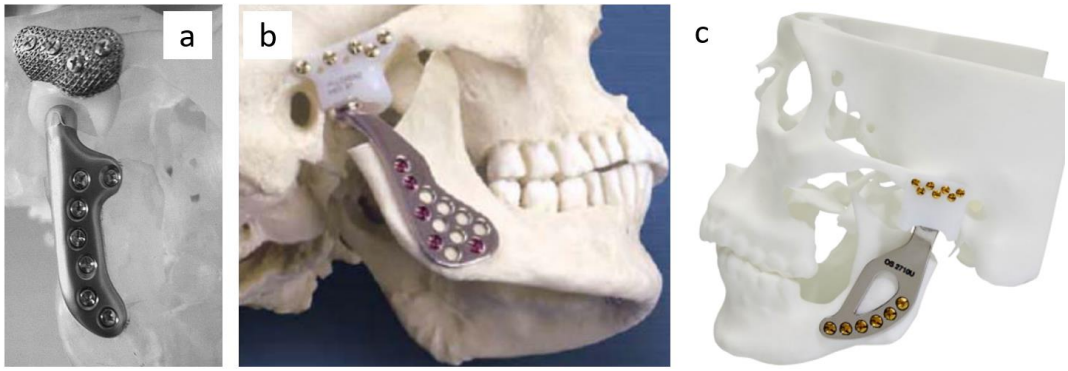


Figure 2.8: TMJ concepts custom implant system (a), Zimmer Biomet stock TMJ system (b), and the Maxoniq ArthroJaw total joint replacement system (c). Figures a and b adapted from Goswami et al. (2009).

## 2.6 POST-SURGICAL OUTCOMES OF TOTAL TEMPOROMANDIBULAR JOINT REPLACEMENT

### 2.6.1 Clinical outcomes

Clinical evaluation of the TMJ includes measuring jaw motion, and evaluating pain, dietary restrictions and quality of life. Pre-operative and post-operative evaluation of jaw motion is limited to the measure of maximum interincisal opening distance (MIO), which is the linear distance between the mandibular and maxillary central incisors at the maximum mouth open position. Healthy individuals have MIO distances of between 46.6 mm and 51.3 mm (Naeije 2002; Voiner et al. 2011). Preoperative patients have mean MIO of 20.4 mm, and following total TMJ replacement with the Biomet Microfixation device this increases steadily to 30.9 mm twelve months after the surgery (Figure 2.9) (Giannakopoulos and Sinn 2012). While these results are specifically for the Biomet device, systematic reviews of postsurgical outcomes have found no statistically significant differences between the postsurgical MIO of patients implanted with Biomet, TMJ concepts or Nexus systems (Zou et al. 2018). Evaluation of MIO is valuable as a rapid and easily accessible measure of jaw range of motion; however, it correlates poorly with the functionality of the TMJ, particularly in the case of unilateral total TMJR patients, and its results should be interpreted with caution (Travers et al. 2000).

Preoperative and postoperative pain and interference with eating can be evaluated using a visual analogue scale, where patients are asked to rate their pain from 0 to 10, where 0 is “no pain” and 10 is “the worst pain imaginable”, and interference with eating from 0 to 10, where 0 is “no interference” and 10 is “liquids only”. Mean preoperative scores are 8.4 and 8.2 for pain and interference with eating, respectively. These values decrease steadily until 3 years

post-operative where mean scores are 2.6 and 2.5 for pain and interference with eating respectively (Figure 2.9) (Giannakopoulos and Sinn 2012).

In the clinical literature, post operative results are typically grouped for both unilateral and bilateral total TMJR patients. However, these patient groups are fundamentally different. The presence of a native condyle improves the range of motion of unilateral total TMJR patients compared to bilateral total TMJR patients (Wojczynska et al. 2016; Wojczyńska et al. 2021). Furthermore, unilateral total TMJR patients report higher levels of pain than bilateral total TMJR patients (Wojczynska et al. 2016). This patient grouping in the clinical literature presents a limitation in our current understanding and should be considered when interpreting these results.

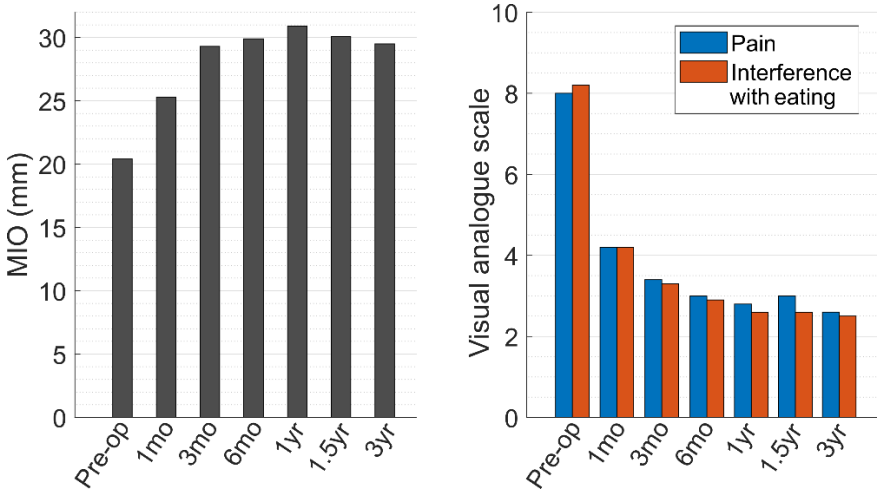



Figure 2.9: Maximum interincisal opening distance and self-reported values for pain and interference with eating evaluated using a visual analogue scale for a group of 288 total TMJ replacement patients, measured preoperatively and up to 3 year post-operative (Giannakopoulos et al. 2012).

### 2.6.2 Biomechanical outcomes

Despite a considerable body of literature on the long-term clinical results of total TMJ replacement, TMJ kinematics, maximum voluntary bite force, muscle function and TMJ loading following TMJR surgery remains poorly understood. The following subsections describe the current literature regarding these biomechanical outcomes.

#### 2.6.2.1 Kinematics

Kinematics of the TMJ refers to the movement of the mandible relative to the skull, it is vital for daily activities such as chewing and production of speech. Understanding the

kinematics of the TMJ is essential for diagnosis and treatment of TMD disorders and improving the outcomes of TMJ prosthetics. Measuring kinematics throughout the body with skin mounted sensors and markers introduces errors from the motion of the skin relative to the underlying bone, referred to as skin motion artefact. Due to these errors, accurate three-dimensional mandibular kinematics are difficult to measure. In the healthy population jaw kinematics have been quantified using axiography, ultrasonic tracking, magnetic and optoelectronic tracking (see Chapter 3 for a review of jaw tracking technologies). In the total TMJR population, jaw kinematics have been quantified using optoelectronic tracking. Leiggener et al. (2012) performed a case study tracking a unilateral total TMJR patient's three-dimensional jaw kinematics during maximum opening and protrusive movements. During mouth opening, the mean translations of the prosthetic condyle was constrained to only 5.4 mm compared to 24.8 mm for the native contralateral condyle. This resulted in an asymmetrical mouth opening trajectory, although the large anterior movements of the contralateral condyle facilitated an acceptable MIO distance of 43.3 mm (Figure 2.10) (Leiggener et al. 2012).

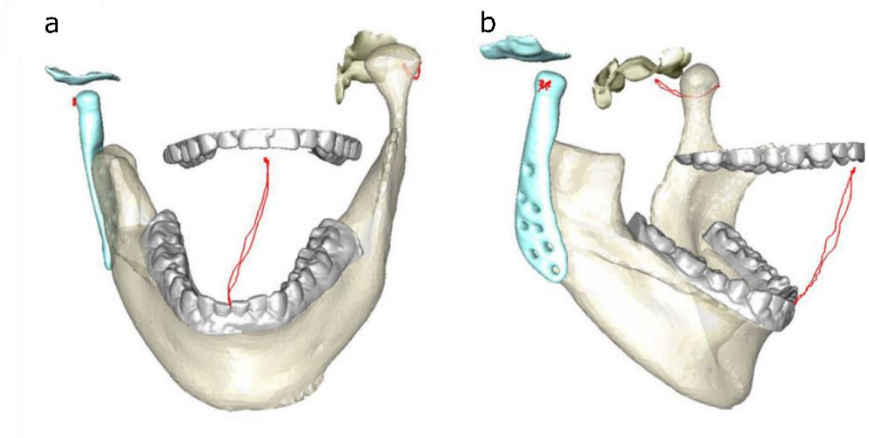



Figure 2.10: Trajectories of the left and right condylar points and the central incisors during maximum mouth opening of a unilateral total TMJ replacement patient. Viewed from the coronal plane (a) and an oblique projection (b). Figure adapted from Leiggener et al. (2012).

Wojczńska et al. (2016) used optoelectronic tracking to study a cohort of 7 unilateral and 8 bilateral total TMJR patients, with the mean time from operation to examination of 4.4 years, and compared them to a selection of 15 control subjects who were not age or gender matched. This larger study found similar prosthetic condyle mobility for unilateral TMJR patients as Leiggener's case study. Furthermore, the qualitative assessment revealed that the prosthetic condyles of bilateral total TMJR patients showed similar movement patterns to those of unilateral TMJR patients. Interestingly, during maximum mouth opening, the native contralateral condyle of unilateral TMJR patients translated anteriorly significantly further than

those of healthy controls (unilateral contralateral: 14.4 ± 9.5 mm, unilateral ipsilateral: 5.2 ± 3.4 mm, bilateral: 3.8 ± 1.9 mm, Controls: 6.1 ± 3.3 mm), suggesting hypermobility of the native condyle post-operatively (Wojczynska et al. 2016).

Linsen et al. (2012) evaluated the return of condylar mobility following total TMJR surgery using ultrasonic jaw tracking, finding that condylar range of motion during mouth opening steadily increased from 7.2 mm at 2 months post-operatively to 14.1 mm at 12 months post-operatively. This improvement translated to improvements in MIO from 21.8 mm at 2 months post-operatively to 25.7 mm at 12 months post-operatively. However, the increase in condylar mobility had little impact on the return of lateral and protrusive range of motion (Figure 2.11) (Linsen et al. 2012).

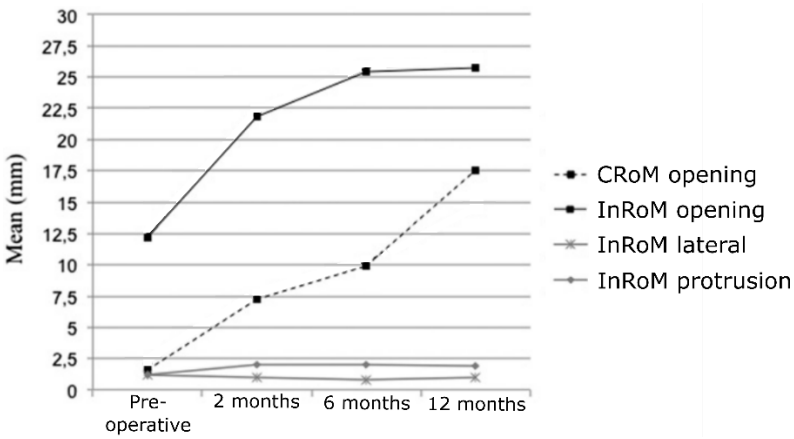



Figure 2.11: Condylar range of motion (CRoM) and Incisal range of motion (InRoM) kinematics during opening, lateral and protrusive movements. Figure adapted from Linsen et al. (2012).

### 2.6.2.2 Bite force

Bite force refers to the load that an individual exerts on their teeth through activation of their masticatory muscles, and is often used a measure of the function and integrity of the masticatory system. However, it is notoriously difficult to measure, and at present, technological limitations have restricted bite force evaluation to static, one-dimensional measurements of maximum voluntary bite force. This has limited our understanding of critical shear forces at the tooths surface and physiologically relevant sub-maximal bite forces (see Chapter 4: for a discussion on bite force measurement).

Linsen et al. (2018) measured bite force on 13 patients reconstructed with total unilateral TMJR following segmental resection of the mandible. A mean maximum voluntary bite force of 222.2 ± 93.1 N was measured on the contralateral first molars at a mean follow up of 2.2

years post-operatively (Linsen et al. 2018). Similarly, Speksnijder et al. (2022) evaluated 12 unilateral TMJR patients an average of 2.5 years post-operatively and found a mean maximum voluntary bite force of 201.0 ± 159.7 N, significantly lower than age and gender matched healthy controls of 463.9 ± 301.2 N. The bite force recordings taken on each patient's ipsilateral and contralateral first molars were averaged in this study (Speksnijder et al. 2022). Linsen et al. (2021) also evaluated the long-term recovery of maximal voluntary bite force following total unilateral TMJR surgery. Measurements were taken on the contralateral first molars, showing significantly higher bite forces 2 to 3 years post-operatively (225.1 ± 118.2 N) compared to preoperative measurements (129.5 ± 124.6 N) (Linsen et al. 2021).

#### 2.6.2.3 Masticatory muscle function

Masticatory muscle function refers to the activation and forces of the masticatory muscles, including the symmetry of muscle forces between the working and non-working side of the jaw. Masticatory muscle function is critical for effective chewing and speech, and can be compromised in patients experiencing disorders of the TMJ. Total TMJR surgery requires the severing of the lateral pterygoid muscle, the detachment of the masseter muscle at its insertion to the lateral ramus, and may involve resection of the coronoid process, thus sacrificing the temporalis insertion point (Linsen et al. 2020). There is limited literature on how these adaptions affects the function of the masticatory muscles. Surface electromyography (sEMG) has been used to measure the myoelectric output of superficial muscles including the temporalis and masseter muscles. Linsen et al. (2021) employed sEMG to measure the activity of the contralateral anterior temporalis and masseter muscles during biting, both before and after total unilateral TMJR surgery, finding that muscle activity increased steadily for 4 years after surgery (Linsen et al. 2021). The same research group also extended this analysis to study the long-term bilateral muscle activity for a set of 14 unilateral total TMJR patients. This study found that the anterior temporalis tended to have higher activity on the ipsilateral side, whereas the average activity of the masseter muscle was higher on the contralateral side (Figure 2.12) suggesting long-term atrophic changes to the operated masseter (Linsen et al. 2020). Interestingly, when comparing results for patients with custom vs stock prosthesis, this study found higher activity from the operated masseter muscle when custom prosthesis were used (Linsen et al. 2020).

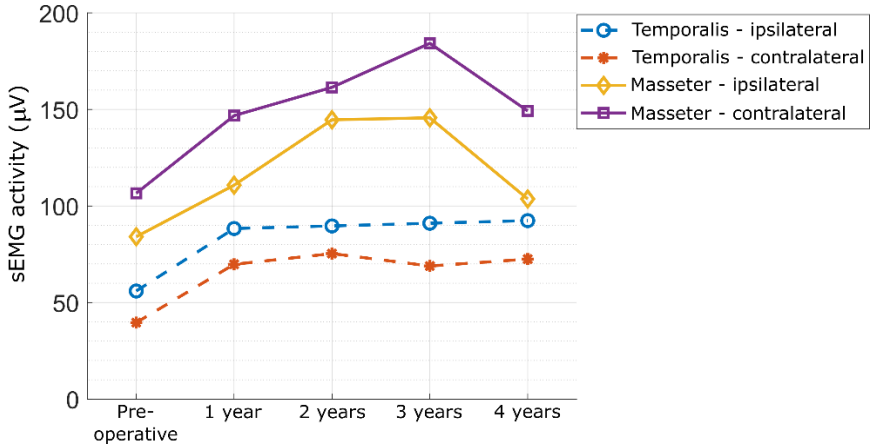



Figure 2.12: Long-term bilateral muscle activity for the anterior temporalis and masseter muscles of unilateral total TMJR patients (Linsen et al. 2020).

sEMG has a relatively large pick-up volume, therefore the recorded signal includes the activity from all muscles in this volume. The error introduced from the signal recorded by electrodes placed on the skin above a muscle of interest, but produced by another muscle, is known as crosstalk (Mesin 2020). There are unavoidably large crosstalk errors when using sEMG to measure the function of the deeper masticatory muscles, such as the medial or lateral pterygoid muscles, therefore sEMG can not be used to assess the muscle function of the whole masticatory system. Conversely, while in-dwelling fine-wire EMG has been used to record electrical activity of the deep masticatory muscles (Vitti and Basmajian 1977; Widmalm et al. 1981; Iwasaki et al. 2003), its invasive nature limits its use and it has not yet been applied to investigate the muscle function following TMJR surgery. As a conseuqence, the function of these deeper muscles is typically investigated using musculoskeletal modelling. Musculoskeletal modelling has been used in two case studies to evaluate muscle function following total unilateral TMJR surgery (Ackland et al. 2017, 2018). Both studies use isotropically scaled generic models to evaluate muscle forces during worst-case bilateral biting on the first molars, finding high muscle forces in the temporalis, masseter and medial pterygoid muscles. However they failed to model the surgical damage to the lateral pterygoid, temporalis or masseter muscle and therefore can not be used to investigate the compensatory muscle recruitment presumed to result from this. Similarly, as both studies applied bite and muscle forces derived from stomatognathically healthy test patients, the results are only somewhat transferrable to the TMJR population.

#### 2.6.2.4 Joint loading

Joint loading represents the forces experienced by the TMJ's during daily activities such as biting and during mandibular movements. It is critical in understanding the functional performance of the TMJ and to design and evaluate TMJ prosthesis. The performance and longevity of TMJ prostheses are limited by the cyclic loading, the internal stress distributions within the prosthesis, and material wear at the articulating surfaces. These factors can lead to complications such as prosthesis fracture, screw loosening and the release of particles and ions to the surrounding tissues (Pinto-Borges et al. 2023). These adverse effects are either directly or indirectly related to the magnitude and direction of TMJ loading. Loading of the human TMJ cannot be quantified *in vivo;* therefore, at present it has only been estimated by mathematical analysis and musculoskeletal modelling.

Van Loon et al. (1998) performed the first comprehensive mathematical study to evaluate prosthetic and contralateral joint loading of a unilateral TMJR patient during unilateral biting along the dental arch (Figure 2.13a). The prosthetic joint experienced 50% higher loading than an intact mandible, whilst the contralateral joint loads remained within the normal limits of an intact mandible (Figure 2.13b). The highest bite forces and joint loads occurred during biting on the molars, however the ratio of joint loading to bite force was typically higher for the prosthetic joint than the contralateral joint (Figure 2.13c), indicating that the prosthetic side was less efficient in transferring muscle forces into a bite force than the native contralateral side (van Loon et al. 1998).

FEA of unilateral TMJR patients during a 200N bilateral molar biting have quantified prosthetic and contralateral joint loads to be 69.6 N and 55.0 N, respectively. This study found that the simulated removal of the operated lateral pterygoid muscle lead to higher lateral shear forces at the prosthetic joint compared the contralateral joint (Ackland et al. 2017). This finding had been supported by finite element studies reporting higher loading (Ackland et al. 2018) and stresses (Bekcioglu et al. 2017) in the prosthetic joint compared to the contralateral joint. However, these studies applied muscle forces calculated for intact mandibles and then removed the lateral pterygoid muscle on the operated side. By failing to use pathological bite and muscle forces, or to consider the compensatory muscle recruitment presumed to result from the removal of the lateral pterygoid muscle, these studies have limited capacity to investigate the distribution of loads across the prosthetic and contralateral condyles.

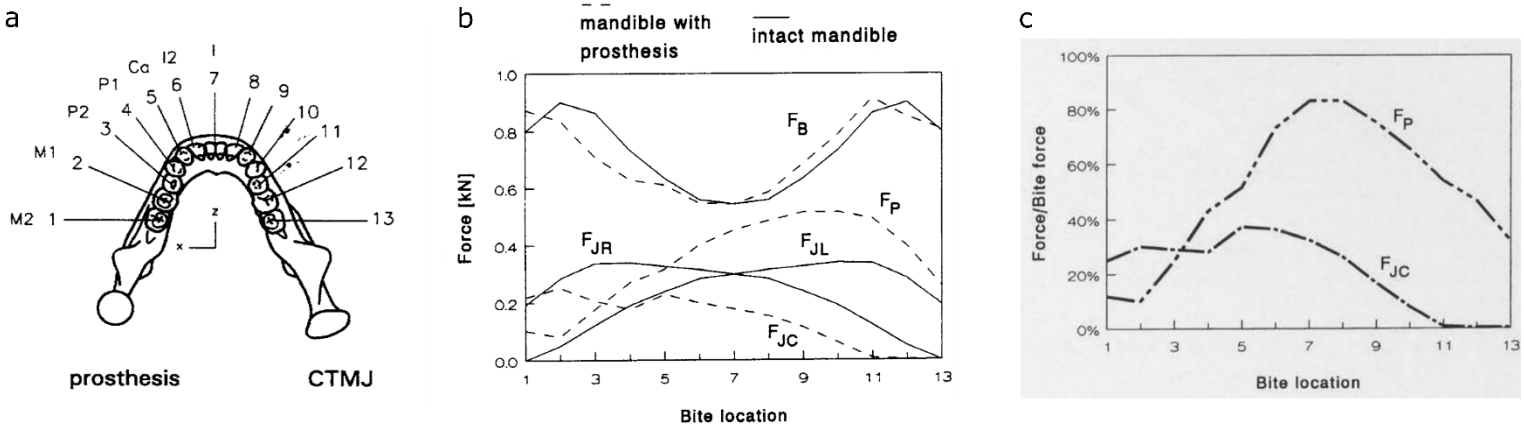



Figure 2.13: Cranial view of mandible showing bite locations numbered 1 to 13 (a). Maximum bite force and corresponding TMJ reaction force as a function of bite location for an intact mandible and for a unilateral TMJ prosthesis (b). Prosthetic and contralateral joint reaction forces normalised against the maximum bite force, as a function of bite location (c). Where $F_B$ = maximum bite force, $F_{JL}$ and $F_{JR}$ = left amd right TMJ reaction force for an intact mandible, $F_P$ and $F_{JC}$ = prosthetic and contralateral joint reaction force of a unilateral TMJR patient, M = molar, P = premolar, C = canine, I = incisor. Figure adapted from Van Loon et al. (1998).

# Chapter 3: Measurement of normal and pathological mandibular and temporomandibular joint kinematics: A systematic review

This chapter is presented as the author-accepted manuscript of a peer-reviewed article published in the *Journal of Biomechanics* (2020, 111, 109994)

## 3.1 SIGNIFICANCE

This study identified and compared techniques available for the measurement of six-degree-of-freedom mandibular and temporomandibular joint kinematics. The findings of this study will guide selection of mandibular and TMJ kinematic measurement in clinical and research applications.

## 3.2 ABSTRACT

TMJ and mandibular motion plays a pivotal role in the function of the dentition and associated hard and soft tissue structures, and facilitates mastication, oral communication, and access to respiratory and digestive systems. Quantification of mandibular kinematics facilitates the evaluation of TMJ function, and is clinically relevant in cases of prosthetic rehabilitations, TMJ disorders, osteoarthritis, trauma, tumour resection and congenital abnormalities which are known to directly influence mandibular motion and loading. The objective of this systematic review was to critically investigate published literature on historic and contemporary measurement modalities used to quantify mandibular and TMJ kinematics with six degrees of freedom in vivo. The electronic databases of Scopus, Web of Science, Medline, Embase and Central were searched and one hundred and nine relevant articles identified. Publication quality was documented using a modified Downs and Black checklist. Axiography and ultrasonic tracking are commonly employed in the clinical setting due to their simplicity and capacity to rapidly produce low-fidelity mandible motion data. Magnetic and optoelectronic tracking have been used in combination with dental splints to produce higher measurement accuracy while minimising skin motion artefact, but at the expense of setup time and cost. Four-dimensional (4D) Computed Tomography provides direct 3D measurements of mandible and TMJ motion while circumventing skin motion artefact entirely but employs ionising radiation, is restricted

to low sampling frequencies and requires time-consuming image processing. Recent advances in magnetic tracking using miniature sensors adhered to the teeth in combination with intraoral scanning may facilitate rapid and high precision mandibular kinematics measurement in the clinical setting. The findings of this review will guide selection and application of mandibular and TMJ kinematic measurement for both clinical and research applications.

## 3.3 INTRODUCTION

The TMJ is a bilateral synovial joint between the skull and the mandible comprising the glenoid fossa of the temporal bone, the condylar head of the mandible, and the articular cartilage and disc. Motion of the TMJ is essential for normal mandibular function and maintaining quality of life, providing the mechanism for biting, chewing, swallowing and speech. The American Academy of Orofacial Pain estimates that 75% of the U.S. population experiences temporomandibular disorders that directly impact mandibular motion at some point in their life, with 5 to 10% of those requiring surgical or non-surgical treatment (Gatchel et al. 2006). Loss of TMJ function and mandibular pain is associated with reduced diet and social dysfunction (Reisine and Weber 1989), and has been directly attributed to annual costs to the US healthcare system of over $2 billion (Gatchel et al. 2006).

TMJ motion measurements are used clinically to provide an objective basis for diagnosing musculoskeletal disorders of the jaw (Soboļeva et al. 2005), monitoring the progression and outcome of treatments, including the comparison of pre- and post-surgical joint function in orthognathic surgery patients (Landes and Sterz 2003) and have been applied during surgery allowing an intra-operative functional investigation of the temporomandibular joint to guide the surgical procedure (Ewers et al. 2005). These measurements are finding increasing clinical use through the uptake of digital dentistry, they provide a measure of dynamic occlusion (Bando et al. 2009) and are used to drive CAD/CAM packages (Röhrle et al. 2009; Gutman and Keller 2018) and dental articulators (Ratzmann et al., 2007), these facilitate the fabrication of dentures and fixed prosthodontic restorations. Additionally, these measurements play an important role in medical research by facilitating development of tests to screen for temporomandibular dysfunction (Sadat-Khonsari et al. 2003a), for evaluating mandibular function, outcomes of TMJ reconstructive and total joint replacement surgery (Alsawaf et al. 1993; C. et al. 2011; Ugolini et al. 2017), therapeutic measures such as occlusal splints (Ettlin et al. 2008; Vilanova et al. 2014), and for assessing the functional performance of dental implants and prosthetics (Baltali et al. 2008a; Leiggener et al. 2012; Wojczynska et al. 2019). Mandibular kinematics has also been used to quantify the effects of gender on mandibular

function and disease progression (Buschang et al. 2000; Lewis et al. 2001; Ferrario et al. 2005; Mapelli et al. 2009), as well as age-related changes in mandibular behaviour (Gibbs et al. 1982; Martin et al. 2000; Baqaien et al. 2007).

Mandibular motion measurement techniques can be broadly classified into four categories: (i) mechanical linkage systems, (ii) magnetic tracking systems, (iii) video motion analysis, and (iv) radiographic tracking. Mechanical linkage systems include axiography, the Case Gnathic Replicator and ultrasonic tracking, and involve rigidly fixing instrumented face-bows to the teeth from which mandibular motion can be directly measured. Magnetic tracking systems have been adopted to acquire kinematics data from electromagnetic sensors mounted to anatomical landmarks such as dental structures. Similarly, video motion analysis methods such as cinematography and optoelectronic tracking employ stereophotogrammetry to directly measure mandibular motion from the position of markers located on the face, or attached to the mandibular or maxillary teeth. In contrast, radiographic tracking can directly measure bone motion and include video x-ray fluoroscopy and 4D computed tomography (CT).

The aim of this systematic review was to investigate published literature on historic and contemporary measurement modalities used to evaluate normal and pathological mandibular and TMJ kinematics with six degrees of freedom in vivo. The outcomes of this study may be useful in guiding motion measurement experiments for the clinic and research setting.

## 3.4 MATERIALS AND METHODS

### 3.4.1 Database Search Strategy

A literature search was conducted to identify previously published articles that describe the measurement of mandibular or TMJ kinematics with six degrees of freedom. The study was compliant with the recommended Preferred Reporting Items for Systematic reviews and Meta-Analyses (PRISMA) statement (Moher et al. 2009). Articles were identified through a systematic search of the following databases: (1) Scopus, (2) Web of Science, (3) MEDLINE, via Ovid, (4) EMBASE, via Ovid and (5) CENTRAL database. These databases were searched for entries published in English prior to 2nd April 2019. To maximise the possibility of capturing all relevant articles, a broad search strategy was used with the following terms:

“temporomandibular joint” OR “jaw” OR “mandib*”, AND

“kinematic*” OR “biomechanic*” OR “dynamic*” OR “jaw motion” OR “motion analysis”

Key search terms were matched with medical subject headings (MeSH) and truncations were used to enable the search to retrieve all possible variations of a specific word.

### 3.4.2 Selection Criteria

After removing duplicates from the search results, all titles and abstracts were assessed to determine whether they fulfil the inclusion criterion. To be included in this review, studies were required to meet the following criteria: (i) focused on the healthy, symptomatic or surgically altered TMJ, or mandible (jaw) and (ii) measured dynamic kinematics of the hard tissue of the mandible or TMJ with six degrees of freedom. Exclusion criteria included (i) animal studies, and (ii) studies of robotic mouth actuators. The references of all full text articles were manually checked for relevant titles to be included in the review. There was no restriction based on study type.

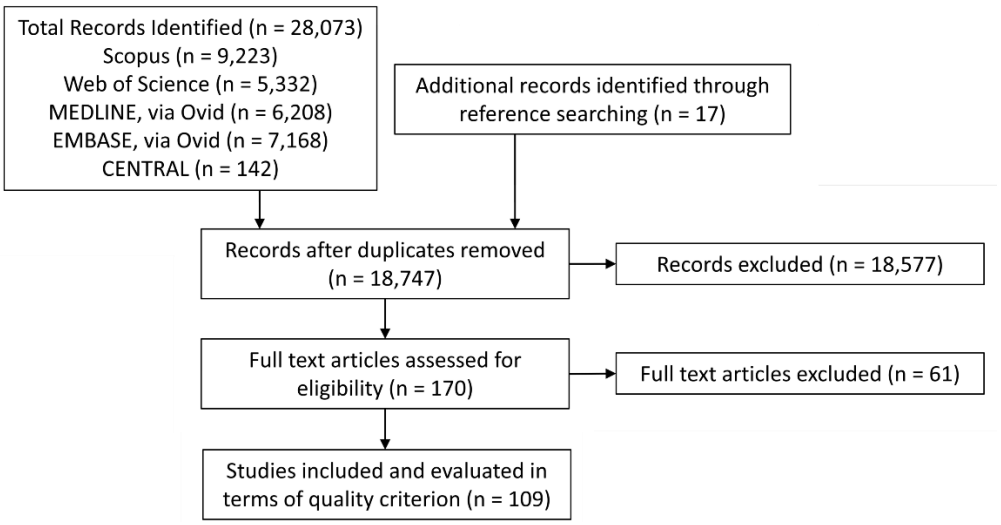



Figure 3.1: Flow chart illustrating systematic review search results adopted in the present study.

### 3.4.3 Article Quality Assessment

The quality of all included studies was evaluated using a customised quality assessment tool which included principles from the STROBE statement (Elm et al. 2007), the Downs and Black checklist (Downs and Black 1998), and established reliability and feasibility appraisal tools (Crowe and Sheppard 2011). Quality evaluation guidelines for systematic reviews covering broadly similar themes were also consulted (Peters et al. 2010; Hart et al. 2016; Pourahmadi et al. 2019).

The assessment tool was developed using a scored checklist of quality assessment questions (Table 3.1). Each question was attributed a score of 2, 1 or 0 based on whether the

question in a given paper was clearly addressed, partially addressed or not addressed, respectively. Quality scores were collated and their mean and range calculated. High methodological quality was defined as a score of ≥ 20 (with a maximum 22), moderate quality was defined as a score of > 14 and < 20, and low quality was defined as a score of ≤ 14. Scores were cross-checked by two independent reviewers (SCW and DCA), and discussion between reviewers used to resolve any discrepancies in score.

Table 3.1: Quality assessment tool employed in this systematic review. The scoring system was derived from the STROBE statement (Elm et al. 2007), the Downs and Black checklist (Downs and Black 1998), and previously reported reliability and feasibility appraisal tools (Crowe and Sheppard 2011)

| | |
|---|---|
| 1 | Is the scientific background and rationale for the study clearly described? |
| 2 | Are the research objectives or aims clearly stated? |
| 3 | Are the precise details of the measurement system design and setup described? |
| 4 | Are the parameters to be measured clearly stated? |
| 5 | Is the selection of participants and controls clearly described? |
| 6 | Is participant inclusion and exclusion criteria clearly stated? |
| 7 | Is the equipment to participant attachment method clearly described? |
| 8 | Where relevant, is the registration system between anatomy and motion measurements clearly described? |
| 9 | Are participant movement tasks clearly defined? |
| 10 | Was there a discussion of the errors introduced in the preparation/measurement system/data handling? |
| 11 | Are the main outcomes of the study clearly stated? |

### 3.4.4 Data Extraction

In addition to methodological quality, four categories of data were extracted from each identified study. The extracted data covers details regarding the study population including participant details and the health of their TMJ and jaw, the inclusion of subject-specific anatomic data, the measurement technique and its reported accuracy and the reported kinematic parameters (Tables 3.2 – 3.6).

## 3.5 RESULTS

### 3.5.1 Search Strategy and Methodological Quality

The initial literature search identified 28,073 titles, 18,747 of which remained after the removal of duplicates. After screening titles and abstracts, 170 studies were found to be potentially eligible, with 109 titles subsequently selected for consideration after verification of inclusion and exclusion criteria (Figure 3.1, Tables 3.2 – 3.6). An additional 17 studies were identified and included in the review by searching the references of included articles. The

methodological quality scores ranged from 11 to 22, with an average score of 17.39. There were 22 studies of high quality, 73 studies of moderate quality and 14 studies of low quality. In order to highlight all measurement techniques all studies were included in the review regardless of their methodological quality.

The areas where most studies performed poorly were the description of participant selection, the description of the equipment to participant attachment method and the discussion of measurement errors (Figure 3.2A) (see appendix tables A.A.1 and A.A.2). Studies involving the Case Gnathic Replicator, magnetic tracking and optoelectronic tracking were associated with the highest average methodological quality scores, a reflection of the capacity of these techniques to generate high quality research outputs. Studies using modern measurement techniques such as 3D scanning and video x-ray fluoroscopy often had low participant numbers and failed to include details of participant selection, reflected by relatively low average study quality scores. More user-friendly techniques, particularly those that leveraged commercially available equipment such as axiography and ultrasonic tracking, were often employed in multidisciplinary studies. These tended to include only limited discussion of the measurement technique, how the measurement device interfaced with study participants, and measurement accuracy, which brought down their average quality score (Figure 3.2B).

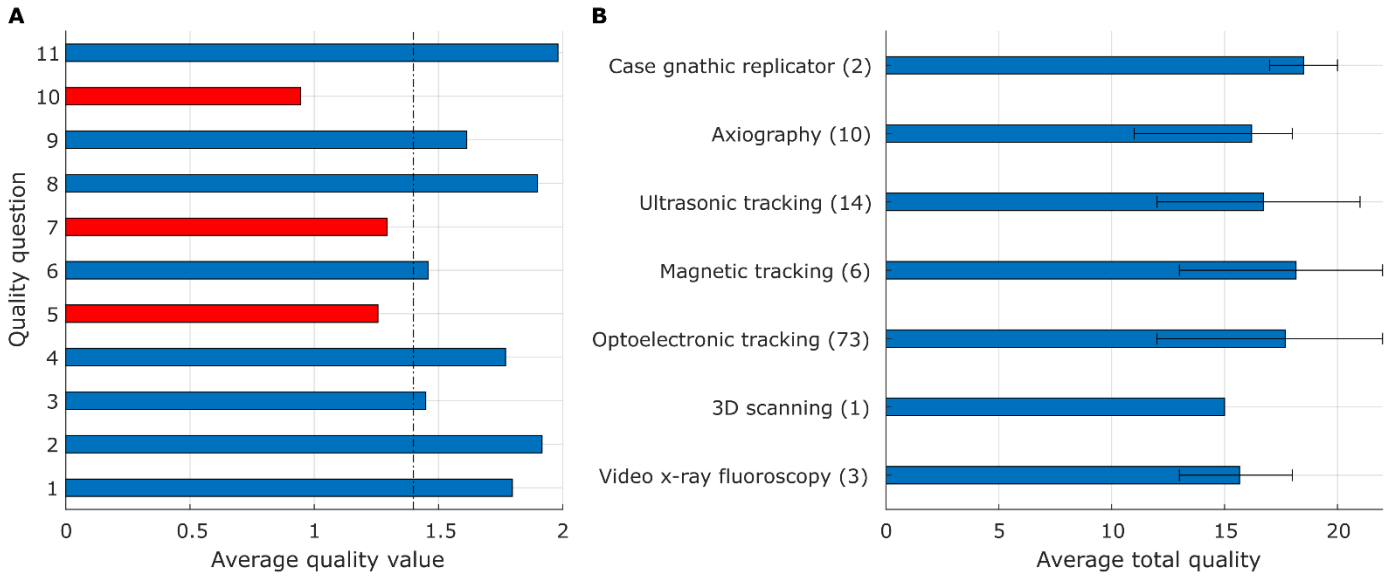



Figure 3.2: Quality assessment results for studies included in this systematic review including the average score for each question in the quality assessment tool (a), and the average total quality score for each measurement technique (b). Red bars indicate questions that were poorly addressed (i.e. an average score of < 1.4). The number of studies using each measurement technique in given in parenthesis and the range of total quality scores for each measurement technique is indicated by the whiskers.

### 3.5.2 MECHANICAL LINKAGE SYSTEMS

#### 3.5.2.1 Case Gnathic Replicator

The Case Gnathic Replicator, which was first developed in 1969, was one of the earliest strategies for calculating 3D mandible kinematics. It comprises six incremental linear displacement transducers mounted between a maxillary face-bow and a mandibular face-bow (Figure 3.3A). The face-bows are attached to the mandible and maxilla via occlusal clutches, which are typically cemented to the surfaces of the teeth. The transducers are used to record relative motion between the face-bows onto magnetic tapes, which can then be played back using a computer, or used to operate casts which replicate the movements of the mandible at reduced speeds (Gibbs et al. 1973; Alexander et al. 1984). The mandibular face-bow is specifically designed to be lightweight, at approximately 60 g (Alexander et al. 1984) to avoid interfering with normal mandibular motion, however the device is still considered unwieldy, and measurement is time-consuming with extensive calibration required (Piancino and Kyrkanides 2016). Two studies, one of moderate and one of high methodological quality, employed the Case Gnathic Replicator to measure condylar and incisor trajectories. These data were used to drive dental articulators and assess the effect of tooth contact on TMJ pain (Gibbs et al. 1971; Coffey et al. 1989). One study of moderate quality reported the measurement error to be less than 0.13 mm (Gibbs et al. 1971) (Table 3.2).

#### 3.5.2.2 Axiography

Contemporary axiographs can be either mechanical or electromechanical and consist of a double face-bow attached to the participant via occlusal clutches or to the head. The mandibular face-bow is equipped with two styli which trace mandibular movement onto two flaps positioned over the condylar region of the maxillary face-bow (Figure 3.3B). Axiography is commonly used to measure condylar and incisal trajectories, condylar inclination angles and Bennett angles (Alsawaf et al. 1993; Theusner et al. 1993; Bernhardt et al. 2003; Sadat-Khonsari et al. 2003b; Kucukkeles et al. 2005; Hirai et al. 2009; Hüe 2011; Wieckiewicz et al. 2014; Ghodsi and Rasaeipour 2018), and has been employed clinically for diagnostic purposes (Wagner et al. 2003) for evaluating both intra- and post-operative mandibular function (Landes and Sterz 2003; Ewers et al. 2005), and for driving dental articulators (Tamaki et al. 1997). It is considered a relatively rudimentary measurement system that is inexpensive and can be rapidly setup. One study of moderate quality assessed the measurement error of electromechanical axiographs, by mounting the lower face-bow to an X/Y measuring table equipped with micrometre screws to control movement, the recorded displacement was

compared to the actual movement of the face-bow, the study reported errors of 0.07 mm per 5 mm travelled in the sagittal plane, and 0.57 mm per 5 mm travelled in the transversal plane (Sadat-Khonsari et al. 2003a) (Table 3.2), these are primarily a result of vibration of the face-bow and errors in styli placement. Additionally, the weight of the face-bows, which has been measured at 96 g (Schierz et al. 2014), loads the mandible inferiorly which may ultimately restrict normal dynamic mandibular motion and result in premature fatigue (Kenworthy et al. 1997).

#### 3.5.2.3 Ultrasonic tracking

Ultrasonic technology has been adapted to measure motion of the mandible by embedding ultrasonic emitters in a face-bow rigidly attached to a subject's mandibular teeth, with ultrasonic receivers positioned in a carrier attached to their head. In this manner, the real-time latency periods of sequentially transmitted ultrasonic pulses between these carriers can be recorded, and the relative motion of the mandible calculated (Figure 3.3C). Ultrasonic tracking has been used to quantify dynamic condylar and incisal trajectories (Morneburg and Pröschel 1998; Schwestka-Polly et al. 1999; Wang et al. 2009; Ko et al. 2012, 2015; Teng et al. 2015; Linsen et al. 2016; Yen et al. 2017; Kiseri et al. 2018) and TMJ anatomy (Stiesch-Scholz et al. 2006; Baqaien et al. 2007; Ratzmann et al. 2007) (Table 3.2). The face-bows, which each weigh 25 g (Baqaien et al. 2007), are quick and easy to mount, giving this technology the advantage of rapid measurement with application in large cohorts (Baqaien et al. 2007; Reicheneder et al. 2013; Kordaß et al. 2014). Ultrasonic tracking provides an extraoral measure of condylar inclination angles and is often considered the 'gold standard' data input to drive dental articulators (Ratzmann et al. 2007). The measurement accuracy of an ultrasonic tracking system was evaluated by mounting the lower face-bow on a micrometre table to control its movement (Hugger et al. 2001). This study reported that for movement paths of up to 20 mm, the mean errors were found to be 0.10 mm in the transversal direction, 0.13 mm in the sagittal direction and 0.17 mm in the vertical direction, however studies report a range of measurement accuracies from 0.1 mm to 0.2 mm (Table 3.2). Since condylar movement involves both rotation and translation, implementation of a singular condylar reference point is not sufficient to fully define the motion of the condyle in six degrees-of-freedom (Peck et al. 1997, 1999).

Table 3.2: Details of studies identified in this systematic literature review that employ mechanical linkage systems. Study details provided include, where available, author details, participant characteristics, TMJ/mandible condition, medical imaging modality, kinematic parameters measured, reported tracking accuracy and methodological quality rating.

| | Authors | Participant characteristics (n,gender) | TMJ/jaw condition | Imaging | Kinematic parameters | Reported measurement accuracy | Quality rating |
|---|---|---|---|---|---|---|---|
| Case Gnathic Replicator | Coffey et al., 1989 | n = 8, 4M:4F | Asymptomatic | - | Condylar trajectories | 0.13mm for translation | 20 |
| | Gibbs et al., 1971 | n=12, NS | Malocclusions | - | Condylar and incisal trajectories | 0.13 mm for translations | 17 |
| Axiography | Alsawaf et al., 1993 | n=22, 12M:10F | Post cranial base tumor resection surgery | - | Condylar trajectories | - | 17 |
| | Bernhardt et al., 2003 | n=30, 19M:11F | Asymptomatic | - | Mandibular trajectories and condylar inclination angle | 0.20 mm | 18 |
| | Ghodsi & Rasaeipour, 2008 | n=50, 33M:17F | Asymptomatic | - | Bennett angle and condylar inclination angle | - | 17 |
| | Hirari et al., 2009 | n=22, NS | Square mandible | CT/MRI | Incisal trajectories | - | 11 |
| | Hüe et al., 2011 | n=60, 26M:34F | Asymptomatic | - | Condylar trajectories | - | 18 |
| | Sadat-Khonsari et al., 2003a | n=30, 11M:19F | TMJ dysfunction | - | Kinematic hinge axis | 0.57 ± 0.09 mm per 5 mm of condylar translation | 16 |
| | Sadat-Khonsari et al., 2003b | n=8, 4M:4F | Asymptomatic | - | Helical axis trajectory | 0.57 ± 0.09 mm per 5 mm of condylar translation | 15 |
| | Tamaki et al., 1997 | n=45, 10M:35F | Asymptomatic | - | Bennet angle, horizontal condylar inclination and hinge axis trajectory | - | 17 |
| | Theusner et al., 1993 | n=49, 24M:25F | Joint noise, tenderness or muscle tenderness | - | Condylar trajectories | - | 15 |
| | Wieckiewicz et al., 2014 | n=3, 0M:35F | Asymptomatic | - | Condylar path inclination | - | 18 |
| Ultrasonic Tracking | Baqaien et al., 2007 | n=213, 103M:110F | Asymptomatic | - | Condylar inclination angle | - | 18 |
| | Kiseri et al., 2018 | n=35, 13M:22F | Asymptomatic | CT | Condylar trajectories | - | 18 |
| | Ko et al., 2012 | n=50, 16M:34F | Orthognathic surgery | - | Condylar and incisal trajectories | - | 21 |
| | Ko et al., 2015 | n=21, 7M:14F | Class III malocclusion/Mandibular deviation | - | Condylar and incisal trajectories | - | 14 |
| | Kordaß et al., 2014 | n=259, 100M:159F | Asymptomatic | - | Condylar trajectories | - | 14 |
| | Linsen et al., 2016 | n=36, 8M:28F | Class I and Class II malocclusion | - | Condylar, incisal and helical axis trajectories | 0.10 mm | 19 |
| | Morneburg et al., 1998 | n=60, 34M:26F | Asymptomatic | - | Condylar trajectories and kinematic hinge axis | 0.20 mm for translations, 3.00° for rotations | 16 |
| | Ratzmann et al., 2007 | n=23, 11M:12F | Asymptomatic | - | Kinematic hinge axis and condylar inclination angles | - | 12 |
| | Reicheneder et al., 2013 | n=132, 68M:64F | Asymptomatic | - | Incisal trajectories and condylar path inclination | - | 19 |
| | Schwestka-Polly et al., 1999 | n=40, NS | Dysgnathia | - | Mandibular rotations | - | 16 |
| | Stiesch-Scholz et al., 2006 | n=60, NS | Craniomandibular disorder | - | Bennet angle, horizontal condylar inclination and incisal inclination | 3.00-4.00° for rotations | 19 |
| | Teng et al., 2015 | n=63, 17M:46F | Orthognathic surgery | - | Condylar and incisal trajectories | - | 18 |
| | Wang et al., 2009 | n=44, 23M:21F | Mandibular protrusion | - | Condylar trajectories | - | 14 |
| | Yen et al., 2017 | n=20, 18M:2F | Zygomatic fracture | - | Condylar and incisal trajectories | - | 16 |

### 3.5.3 MAGNETIC TRACKING SYSTEMS

#### 3.5.3.1 Magnetic tracking

Magnetic tracking systems calculate the position and orientation of a point in space using a calibrated sensor that records change in current within a magnetic field. This technique has been well established in biomechanical studies of the spine, shoulder, knee and foot (Johnson and Anderson 1990; Russell et al. 1993; Woodburn et al. 1999; Hill et al. 2007) and has gained popularity due to the portability and low cost of the hardware. In the research setting, magnetic sensors 22.6 × 12.7 × 11.4 mm in size have been either adhered directly to the teeth using dental adhesive or attached to custom dental splints worn by the participant (Baltali et al. 2008b) (Figure 3.3D). To evaluate TMJ kinematics, the motion tracking data may be registered to bony anatomy using CT scans and custom dental splints with captive radio-opaque beads. However, this application exposes participants to ionising radiation, and dental splints are known to interfere with occlusion, limiting the complete intercuspation by approximately 1 to 2 mm (Baltali et al. 2008b). Magnetic tracking is sensitive to the presence of nearby ferromagnetic materials, and test subjects must sit on a non-ferrous chair away from metal objects to avoid measurement distortion and errors. Magnetic tracking has been used to measure condylar and incisal trajectories, define the location of the mandibular helical axis, and quantify the effects of partial TMJ reconstruction surgery on mandibular kinematics (Baltali et al. 2008b, a; Yamamoto et al. 2009; Keller et al. 2012; Minami et al. 2018). One study of high methodological quality used a high precision calibration device to show magnetic tracking sensor measurement errors to be 0.03 ± 0.13 mm (mean ± SD) for linear distances and 0.36 ± 0.44 mm for curvilinear pathways (Baltali et al. 2008b), however studies have reported the measurement error to range from 0.03 mm to 0.80 mm (Table 3.3).

Magnetic tracking has advanced in recent years through the development of miniaturized magnetic sensors, 10 × 5 × 5 mm in size attached directly to the teeth with dental cement. These sensors can be quickly attached and removed, do not interfere with dental occlusion during biting, and have sampling frequencies of up to 120 Hz (Baeyens et al. 2013). Sensor data can be registered to bone embedded coordinate systems by digitising bony or dental landmarks using a stylus sensor (Baeyens et al. 2013), or to 3D scans of the dental arch using intra-oral scanners, thus providing dynamic measurements of kinematics for the maxillary and mandibular teeth and the associated TMJ's, without the need for CT scanning.

Table 3.3: Details of studies identified in this systematic review that employ magnetic tracking systems. Study details provided include, where available, author details, participant characteristics, TMJ/mandible condition, medical imaging modality, kinematic parameters measured, reported tracking accuracy and methodological quality rating.

| Authors | Participant characteristics (n,gender) | TMJ/jaw condition | Imaging | Kinematic parameters | Reported measurement accuracy | Quality rating |
|---|---|---|---|---|---|---|
| Baeyens et al., 2013 | n=12, 5M:7F | Asymptomatic | - | Condylar and helical axis trajectories | Static resolution of 0.50 mm. Additional error of 2-4%, from interference to magnetic field. | 15 |
| Baltali et al., 2008 | n=5, 0M:5F | Degenerative TMJ disorders | CT | Condylar and incisal trajectories | 0.03 ± 0.13 mm for linear distance, 0.36 ± 0.44 mm for curvilinear pathways. | 20 |
| Baltali et al., 2008 | n=14, NS | Pre- and post- partial fossa replacement surgery | CT | Condylar, incisal and helical axis trajectories | 0.03 ± 0.13 mm for linear distance, 0.36 ± 0.44 mm for curvilinear pathways. | 19 |
| Keller et al., 2012 | n=36, 2M:34F | Pre- and post- partial fossa replacement surgery | CT | Condylar, incisal and helical axis trajectories | 0.05 mm for translations and 0.20° for rotations | 13 |
| Minami et al., 2018 | n=14, 6M:8F | Asymptomatic | - | Incisal trajectories and mandibular rotations | Static resolution of 0.80 mm for position and 0.15° for orientation | 20 |
| Yamamoto et al., 2009 | n=20, 15M:5F | Asymptomatic | - | Incisal trajectories | 0.05 mm for translations and 0.03° for rotations | 22 |

### 3.5.4 VIDEO MOTION ANALYSIS

#### 3.5.4.1 Optoelectronic tracking

Optoelectronic tracking involves measurement of the 3D positions of markers rigidly attached to the mandible and the maxilla. Optoelectronic markers emit infrared or near-infrared light (active markers) or reflect it (passive retro-reflective markers), while marker positions recorded by two or more cameras are used to calculate 3D marker trajectories (Figure 3.3E). To measure mandibular motion, markers are typically attached to a lightweight frame which is rigidly attached to the teeth via subject-specific dental splints, or via adhesion directly to the teeth. In addition to these methods, fixation to the head has been performed using eyeglasses (Gallo et al. 1997; Travers et al. 2000; Crane et al. 2010, 2013), headbands (Ostry et al. 1997; Kim et al. 2013; Calixtre et al. 2017) and reference caps (Leader et al. 1997, 2003). The key advantages of this approach are that markers can be positioned on mandibular and skull landmarks in order to define anatomical coordinate systems used for evaluating kinematics, and motion data can be recorded at high speeds. This technology has been used extensively in biomechanics laboratories to study human gait (Caldas et al. 2017) and joint kinematics (Small et al. 1996; Murphy et al. 2006; Hanley and Tucker 2018), but can be costly and time consuming to setup and calibrate, and require a dedicated laboratory space to accommodate the cameras, which would be impractical in most clinical settings.

TMJ kinematics has been quantified using optoelectronic systems by registering mandibular motion recordings from marker trajectories to the 3D geometry of the mandible, obtained by digitally reconstructing magnetic resonance imaging (MRI) or CT scans. This technique, first described in 1994 and often referred to as Dynamic Stereometry (Krebs et al. 1994), involves registering optoelectronic kinematic data to bone-fixed coordinate systems defined from the location of non-collinear spheres measured using CT or MRI. Imaging is typically performed with the patient biting on a custom made occlusal splint attached to a frame carrying the active or passive markers and spheres, facilitating subsequent coordinate system transformation between the optoelectronic system and the bone-fixed coordinate system.

Optoelectronic tracking systems have been used to evaluate gender-specific mandibular kinematics (Lewis et al. 2001), study the effects of pain on jaw movements (Zhao et al. 2012; Bhaskaracharya et al. 2015; Amhamed et al. 2016), investigate muscle activation during jaw motion (Lobbezoo et al. 2000; Goto et al. 2001; Sforza et al. 2009; De Felicio et al. 2013), assess outcomes of orthognathic surgery (Sforza et al. 2010; Ugolini et al. 2017), and quantify the effects of occlusal splint therapy on mandibular kinematics (Ettlin et al., 2008). Optoelectronic tracking systems have been employed in 17 high quality studies, 49 moderate quality studies and 7 low quality studies (Tables 3.4 and 3.5) to measure condylar trajectories and mandibular motion during mandibular border movements (Siegler et al. 1991; Yatabe et al. 1995, 1997; Zhang et al. 1995; Gallo et al. 1997; Abbink et al. 1999; Ćatić and Naeije 1999; Slater et al. 1999; Visscher et al. 2000; Buschang et al. 2001; Lewis et al. 2001; Naeije 2002; Leader et al. 2003; Lemoine et al. 2005; Johnson et al. 2007; Hosogai et al. 2008; Coutant et al. 2008, 2011; Fang and Kuo 2008; Hayasaki et al. 2008; Mapelli et al. 2009, 2016; Hayashi et al. 2009; Kim et al. 2010; Sforza et al. 2010; C. et al. 2011; Ugolini et al. 2018), mastication (Siegler et al. 1991; Ogawa et al. 1998, 2001; Gallo et al. 2000, 2006; Saitoh et al. 2002; Naeije and Hofman 2003; Gerstner et al. 2005; Röhrle et al. 2009; Kubota et al. 2010; Kalaykova et al. 2011; Minami et al. 2011; Hayashi et al. 2012; Remijn et al. 2017; Tomonari et al. 2017) and speech (Ostry et al. 1997; Shiller et al. 1999, 2001). Additionally, dynamic stereometry has been used to study intra-articular joint space (Krebs et al. 1995; Fushima et al. 2003; Ettlin et al. 2008; Gallo et al. 2008; Terajima et al. 2008; Chang et al. 2015; Yashiro et al. 2015b, a) and intra-articular stress fields during mandibular opening and closing movements (Zaugg et al. 2012).

One study of high methodological quality reported a measurement error of 0.11 ± 0.08 mm in calculation of linear distances using optoelectronic tracking (Fushima et al. 2003),

however the measurement errors for translations range from 0.10 mm to 1.00 mm (Tables 3.4 and 3.5). These errors are primarily a result of warping within the rigid marker frames, poor fixation between the marker frames and the mandible (Otake et al. 2006), and identification of the centre of active LED markers (Airoldi et al. 1994). The major limitation of most optoelectronic kinematic measurement systems is that markers, which are attached directly to the skin, move relative to the underlying bone resulting in errors known as skin motion artefact. This can result in mandible position measurement errors of up to 3.27 mm during mandibular opening and closing movements (Chen et al. 2011). Skin-motion artefact can be overcome by attaching tracking markers directly to dental splints; however, splint manufacture can be time consuming, and requires specialist expertise and equipment for fabrication on a subject-specific basis. Markers may also be directly attached to the teeth, but it can be challenging to accurately register marker positions to jaw morphological data, and this approach is rarely performed.

Table 3.4: Details of studies identified in this systematic review that employ video motion analysis combined with 3D morphology data derived from X-ray, CT or MRI. Study details provided include, where available, author details, participant characteristics, TMJ/mandible condition, medical imaging modality, kinematic parameters measured, reported tracking accuracy and methodological quality rating.

| | Authors | Participant characteristics (n,gender) | TMJ/jaw condition | Imaging | Kinematic parameters | Reported measurement accuracy | Quality rating |
|---|---|---|---|---|---|---|---|
| Optoelectronic Tracking | Chang et al., 2015 | n=26, 10M:16F | Dentoskeletal malocclusion | CT | Intra-articular joint space | 0.30 mm for translations | 18 |
| | Coutant et al., 2011 | n=32, NS | Asymptomatic | X-ray | Condylar rotations and translations | NS | 14 |
| | Ettlin et al., 2008 | n=10, 5M:5F | Asymptomatic | MRI | Condylar trajectories and intra-articular joint space | NS | 16 |
| | Fang & Kuo, 2008 | n=1, NS | Asymptomatic | CT | Incisal trajectories | 0.19 mm for translations | 15 |
| | Fushima et al., 2003 | n=10, 3M:7F | Asymptomatic | MRI | Intra-articular joint space | 0.11 ± 0.08 mm for translations | 21 |
| | Gallo et al., 2008 | n=11, 4M:7F | Asymptomatic | MRI | Condylar trajectories and intra-articular joint space | NS | 16 |
| | Goto et al., 2001 | n=4, 4M:0F | Asymptomatic | MRI | Mandibular translations and rotations | Static resolution of 0.10 mm | 18 |
| | Hayasaki et al., 2008 | n=20, 0M:20F | Asymptomatic | X-ray | Condylar, incisal and molar trajectories | 0.19 mm | 17 |
| | Hosogai et al., 2008 | n=2, 0M:2F | Condylar errosion | CT | Condylar trajectories | 0.50 mm for translations | 16 |
| | Kim et al., 2010 | n=15, 4M:11F | Mandibular deviation | CT | Condylar trajectories | NS | 14 |
| | Kim et al., 2013 | n=14, 6M:8F | Class I and Class III molar relationship | CT | Condylar trajectories | NS | 15 |
| | Krebs et al., 1994 | n=5, 3M:2F | Asymptomatic | MRI | Condylar trajectories and intra-articular joint space | 0.11% to 1.33% of motion path for translations, 0.70° for rotations | 22 |
| | Krebs et al., 1995 | n=1, 0M:1F | Asymptomatic | MRI | Intra-articular joint space | Static resolution of 0.20 mm | 20 |
| | Kubota et al., 2010 | n=48, 11M:37F | Asymptomatic | X-ray | Condylar, incisal and molar trajectories and mastication cycle data | NS | 17 |
| | Leader et al., 2003 | n=6, 3M:3F | TMD | MRI | Condylar trajectories | 0.89 mm for translations | 18 |
| | Leiggener et al., 2012 | n=1, 0M:1F | TMJ reconstruction | MRI | Condylar and incisal trajectories | 0.01 mm for translations. Not including errors from MRI segmentation and registration | 15 |
| | Otake et al., 2006 | n=1, 0M:1F | Asymptomatic | CT | Kinematic hinge axis and intra-articular joint space | 0.34 ± 0.25 mm for translations, 0.40 ± 0.30° for rotations | 15 |
| | Saitoh et al., 2002 | n=1, 0M:1F | Crossbite | X-ray | Condylar and incisal trajectories | NS | 16 |
| | Terajima et al., 2008 | n=1, 0M:1F | Jaw deformities | CT | Intra-articular joint space and occlusal contact area | 0.19 mm, not including errors from CT image segmentation and registration | 17 |
| | Wojczynska et al., 2019 | n=5, 1M:4F | Total TMJ replacement | MRI | Condylar trajectories | Static resolution of 5.0 µm, MRI reconstruction error of 1.00 mm | 12 |
| | Yashiro et al., 2015 | n=10, 0M:10F | Asymptomatic | MRI | Condylar trajectories and intra-articular joint space | NS | 14 |
| | Yashiro et al., 2015 | n=20, 0M:20F | Facial asymettry | CT/MRI | Condylar trajectories and intra-articular joint space | NS | 16 |
| | Zaugg et al., 2012 | n=6, 4M:2F | Asymptomatic | MRI | Condylar trajectories and intra-articular stress-fields | Static resolution of 0.01 mm, MRI reconstruction error of up to 1.00 mm | 21 |
| 3D scanning | Kwon et al., 2019 | n=1, 1M:0F | Asymptomatic | CT | Kinematic hinge axis | Static resolution of 4.1-6.9 µm, marker noise of 4.4-37.7 µm. | 15 |

#### 3.5.4.2 3D scanning

3D scanning is a non-invasive technology that digitises the shape, texture and colour of an object, ultimately producing a 3D point cloud of the surface topology. By attaching adhesive markers to the surfaces of the mandibular and maxillary incisors, and inserting a lip and cheek retractor to ensure consistent visibility of the markers, their positions may be tracked during mandibular movement using a structured light 3D scanner at a framerate of 50 frames per second (Figure 3.3F). This motion data has been registered to 3D CBCT scans to evaluate condylar trajectories during mandibular border movements (Kwon et al. 2019). Alignment of kinematic data from the 3D scan to the CBCT models is achieved via image registration software. This method is reported to have potential in the study of mandibular kinematics in the clinic, since it requires only the placement of a retractor and small adhesive markers, and is fast and low cost (Kwon et al. 2019). By attaching small markers directly to the teeth, skin motion artefact and unintended loading of the mandible can be mitigated; however, it may restrict natural mandibular motion, while CBCT registration greatly increases data processing time and exposes participants to ionising radiation. One study of moderate quality showed that 3D scanning can quantify the position of a circular marker with a precision of 4.1 - 6.9 µm (Kwon et al. 2019) (Table 3.4).

Table 3.5: Details of studies identified in this systematic review that employ video motion analysis without use of medical imaging. Study details provided include, where available, author details, participant characteristics, TMJ/mandible condition, kinematic parameters measured, reported tracking accuracy and methodological quality rating.

| Authors | Participant characteristics (n,gender) | TMJ/jaw condition | Kinematic parameters | Reported measurement accuracy | Quality rating |
|---|---|---|---|---|---|
| Abbink et al., 1999 | n=8, 4M:4F | Asymptomatic | Mandibular translations | - | 17 |
| Amhamed et al., 2016 | n=14, 9M:5F | Asymptomatic | Mandibular translations and mastication cycle data | - | 18 |
| Bhaskaracharya et al., 2015 | n=31, 8M:23F | History of pain | Incisal trajectories and velocity | - | 18 |
| Buschang et al., 2000 | n=26, 15M:11F | Asymptomatic | Incisal trajectories and mastication cycle data | - | 21 |
| Buschang et al., 2001 | n=27, 0M:27F | Asymptomatic | Condylar and incisal trajectories | - | 20 |
| Calixtre et al., 2017 | n=36, 19M:17F | Asymptomatic | Condylar and incisal trajectories | - | 17 |
| Ćatić & Naeije, 1999 | n=40, 13M:27F | Anterior disc displacement | Hinge axis and kinematic centre trajectories | - | 14 |
| Coutant et al., 2008 | n=32, NS | Asymptomatic | Condylar rotations and translations | ± 1.00 mm for 22 mm of translation | 14 |
| Crane et al., 2010 | n=22, 2M:20F | Asymptomatic | Mandibular translations and velocity | - | 18 |
| Crane et al., 2013 | n=22, 2M:20F | Asymptomatic | Mandibular translations and mastication cycle data | - | 18 |
| De Felicio et al., 2013 | n=20, 8M:12F | TMD | Condylar and incisal trajectories and mastication cycle data | 0.15 mm for translations | 21 |
| Ferrario et al., 2005 | n=27, 12M:15F | Asymptomatic | Incisal trajectories | Static resolution of 0.09 mm | 21 |
| Gallo et al., 1997 | n=30, 17M:13F | Asymptomatic | Helical axis trajectory | 0.70 mm for translations and 2.00° for rotations | 21 |
| Gallo et al., 2000 | n=7, 2M:5F | Asymptomatic | Helical axis trajectory | - | 19 |
| Gallo et al., 2006 | n=50, 12M:38F | Anterior disc displacement with reduction | Helical axis trajectory | 1.00 mm for translations, 1.90° for rotations | 21 |
| Gerstner et al., 2005 | n=46, 13M:33F | Asymptomatic | Mandibular trajectories | Static resolution of 0.30 mm | 19 |
| Hayashi et al., 2009 | n=10, 5M:5F | Anterior cross bite | Finite helical axis | - | 16 |
| Hayashi et al., 2012 | n=10, 7M:3F | Anterior cross bite | Incisal trajectories and finite helical axis | 0.19 mm for translations | 18 |
| Johnson et al., 2007 | n=1, 0M:1F | TMD | Mandibular translations and rotations | Static resolution of 0.43 mm, dynamic error of 0.06 mm for translations and 0.12° for rotations | 15 |
| Kalaykova et al., 2011 | n=15, 2M:13F | Anterior disc displacement with reduction | Condylar trajectories | - | 16 |
| Leader et al., 1997 | n=20, 3M:17F | TMD | Incisal trajectories | - | 18 |
| Lemoine et al., 2005 | n=10, 5M:5F | Asymptomatic | Mandibular centre of rotation | Static resolution of 0.10 mm, error of 0.62° for rotations | 17 |
| Lewis et al., 2001 | n=56, 29M:27F | Asymptomatic | Kinematic hinge axis and incisal trajectories | Static resolution of 0.15 mm | 19 |
| Lobbezoo et al., 2000 | n=5, 5M:0F | Asymptomatic | Condylar translations and rotations | - | 15 |
| Mapelli et al., 2009 | n=26, 12M:14F | Asymptomatic | Condylar trajectories | - | 19 |
| Mapelli et al., 2016 | n=40, 5M:35F | TMD | Condylar and incisal trajectories | - | 18 |
| Minami et al., 2011 | n=10, 3M:7F | Asymptomatic | Smoothness of mandibular movements | - | 18 |
| Naeije and Hofman, 2003 | n=10, 5M:5F | Asymptomatic | Condylar trajectories | - | 14 |
| Naeije, 2002 | n=35, 17M:18F | Asymptomatic | Condylar rotations and translations | - | 16 |
| Ogawa et al., 1998 | n=41, 16M:25F | Asymptomatic | Incisal trajectories | 0.10 mm for translations | 21 |
| Ogawa et al., 2001 | n=20, 9M:11F | Asymptomatic | Mandibular translations | 0.10 mm for translations | 21 |
| Ostry et al., 1997 | n=5, 5M:0F | Asymptomatic | Kinematic hinge axis | - | 15 |
| Remijn et al., 2017 | n=22, 9M:13F | Cerebral Palsy | Mandibular translations and mastication cycle data | Measurement error <15.1% | 17 |
| Röhrle et al., 2009 | n=1, 1M:0F | Asymptomatic | Incisal and molar trajectories | - | 19 |
| Sforza et al., 2009 | n=36, 20M:16F | Mandibular condyle fracture | Mandibular translations and rotations | - | 19 |
| Sforza et al., 2010 | n=58, 28M:30F | Class II and III malocclusions | Kinematic hinge axis | - | 15 |
| Sforza et al., 2011 | n=46, 23M:23F | Condylar fracture | Incisal trajectories | - | 20 |

Table 3.5 (continued)

| Authors | Participant characteristics (n,gender) | TMJ/jaw condition | Kinematic parameters | Reported measurement accuracy | Quality rating |
|---|---|---|---|---|---|
| Shiller et al., 1999 | n=7, NS | Asymptomatic | Mandibular translations and rotations | - | 18 |
| Shiller et al., 2001 | n=8, NS | Asymptomatic | Mandibular rotations | ±1.00° | 18 |
| Siegler et al., 1991 | n=3, NS | Asymptomatic | Condylar trajectories | - | 17 |
| Slater et al., 1999 | n=10, 4M:6F | Asymptomatic | Condylar trajectories | - | 19 |
| Tomonari et al., 2017 | n=32, 22M:10F | Asymptomatic | Condylar, incisal and molar trajectories | 0.12 mm for translations | 18 |
| Travers et al., 2000 | n=27, 0M:27F | Asymptomatic | Condylar and incisal trajectories | - | 21 |
| Ugolini et al., 2017 | n=18, 6M:12F | Pre- and post-orthognathic surgery | Condylar and incisal trajectories | - | 19 |
| Ugolini et al., 2018 | n=31, 12M:19F | Pre- orthognathic surgery | Condylar translations and rotations | - | 20 |
| Visscher et al., 2000 | n=10, 4M:6F | Asymptomatic | Condylar and incisal trajectories | Static resolution of 0.27 mm | 18 |
| Yatabe et al., 1995 | n=20, 10M:10F | Asymptomatic | Condylar trajectories | Static resolution of 0.27 mm | 19 |
| Yatabe et al., 1997 | n=20, 10M:10F | Asymptomatic | Condylar trajectories | Static resolution of 0.27 mm | 19 |
| Zhang et al., 1995 | n=1, 0M:1F | Asymptomatic | Condylar trajectories and mandibular rotations | 0.24 mm for translations and 0.40° for rotations | 20 |
| Zhao et al., 2012 | n=26, 12M:14F | Asymptomatic | Incisal trajectories and mastication cycle data | - | 18 |

## 3.5.5 RADIOGRAPHIC TRACKING

### 3.5.5.1 Video x-ray fluoroscopy

Single plane video x-ray fluoroscopy employs radiography to calculate bone and joint motion, achieved by registering the position of the 3D geometry of the skull and the mandible reconstructed from CT scans to two-dimensional (2D) dynamic motion from video x-ray fluoroscopy recordings (Figure 3.3G). Two studies of moderate quality (Chen et al. 2013a, b) and one study of low quality (Yamazaki et al. 2014) employed single-plane video x-ray fluoroscopy to evaluate rigid body motion, including condylar rotations and translations of the normal functioning mandible during mouth opening and mastication. Pose-estimation has been achieved by minimising a weighted edge-matching score calculated when aligning the reconstructed 3D mandible derived from CT scans to the fluoroscopic images (Chen et al. 2013b, a), or by tracking the position of radio-opaque tantalum beads in customized mouthpieces worn by the participants (Yamazaki et al. 2014).

Video x-ray fluoroscopy is known to overcome skin-motion artefact by producing direct measures of mandible motion relative to the maxilla. One study of moderate quality found video x-ray fluoroscopy to have motion measurement errors of 0.20 ± 0.20 mm for in-plane translations, 1.00 ± 1.40 mm for out of plane translations and 0.2 ± 0.7° for rotations during mouth opening and mastication using single-plane fluoroscopy (Chen et al. 2013a) (Table 3.6). Out-of-plane errors can be reduced by a factor of 10 using bi-plane fluoroscopy; however, this comes at the expense of greater radiation dosage, additional image processing time, and a more

significant initial expense of equipment (Tersi et al. 2013). At present, bi-plane fluoroscopy is yet to be employed in studies of mandibular kinematics.

The use of video x-ray fluoroscopy in measurement of mandibular and TMJ kinematics has been adopted primarily in the research setting due to high computation time required for image processing. The total radiation dose for a 10 second single-plane fluoroscopy recording is approximately 135 μSv, about 15% of the acceptable annual dose suggested by the United States Nuclear Regulatory Commission (USNRC) (Chen et al. 2013a). The image acquisition rate limit can be as low as 7.5 frames per second, which may limit the fidelity of dynamic mandibular motion measurements, particularly during mastication.

Table 3.6: Details of studies identified in this systematic review that employ radiographic tracking using single-plane video x-ray fluoroscopy and CT data. Study details provided include, where available, author details, participant characteristics, TMJ/mandible condition, kinematic parameters measured, reported tracking accuracy and methodological quality rating.

| Authors | Participant characteristics (n,gender) | TMJ/jaw condition | Kinematic parameters | Reported measurement accuracy | Quality rating |
|---|---|---|---|---|---|
| Chen et al., 2013a | n=1, 0M:1F | Asymptomatic | Condylar rotations and translations | 1.00 ± 1.40 mm for translations, 0.20 ± 0.70° for rotations | 16 |
| Chen et al., 2013b | n=1, 0M:1F | Asymptomatic | Kinematic hinge axis | 1.00 ± 1.40 mm for translations, 0.20 ± 0.70° for rotations | 18 |
| Yamazaki et al., 2014 | n=1, NS | Asymptomatic | Condylar rotations and translations | 0.73 mm for translations, 0.23° for rotations | 13 |

### 3.5.5.2 Four-dimensional computed tomography (CT)

Four-dimensional computed tomography (4D CT) can be used to directly measure mandibular kinematics by digitally reconstructing geometric data obtained from 4D CT image sequences. Originally used for surgical planning, 4D CT was first employed in the measurement of wrist kinematics in 2011 (Leng et al. 2011), and has since been used to assess mandibular kinematics during mastication after mandibular reconstruction surgery (Akashi et al. 2016) and in TMJ osteoarthritis patients (Akashi et al. 2018). While 4D CT has been minimally applied to mandibular or TMJ kinematics measurement, it has the potential to become the 'gold standard' for these measurements as it avoids errors associated with skin-motion artefact, transoral device motion and bone coordinate registration errors. While the accuracy of 4D CT has not been reported for mandibular kinematics, a study of wrist motion reported errors in the range 0.02-0.30 mm for translation and 0.00-0.68° for rotation (Zhao et al. 2015). The

application of 4D CT in the clinical setting has been limited by radiation dosage. For a 10-15 second scan with a field of view of 220 mm and a frame rate of 7.5 frames per second, the effective radiation dose has been reported at 3.58 ± 0.88 mSv (Akashi et al. 2016), about 350% of the acceptable annual dose suggested by the USNRC. Restricted frame rate, limited field of view, and significant image processing time for kinematics measurement are other drawbacks of this technique.

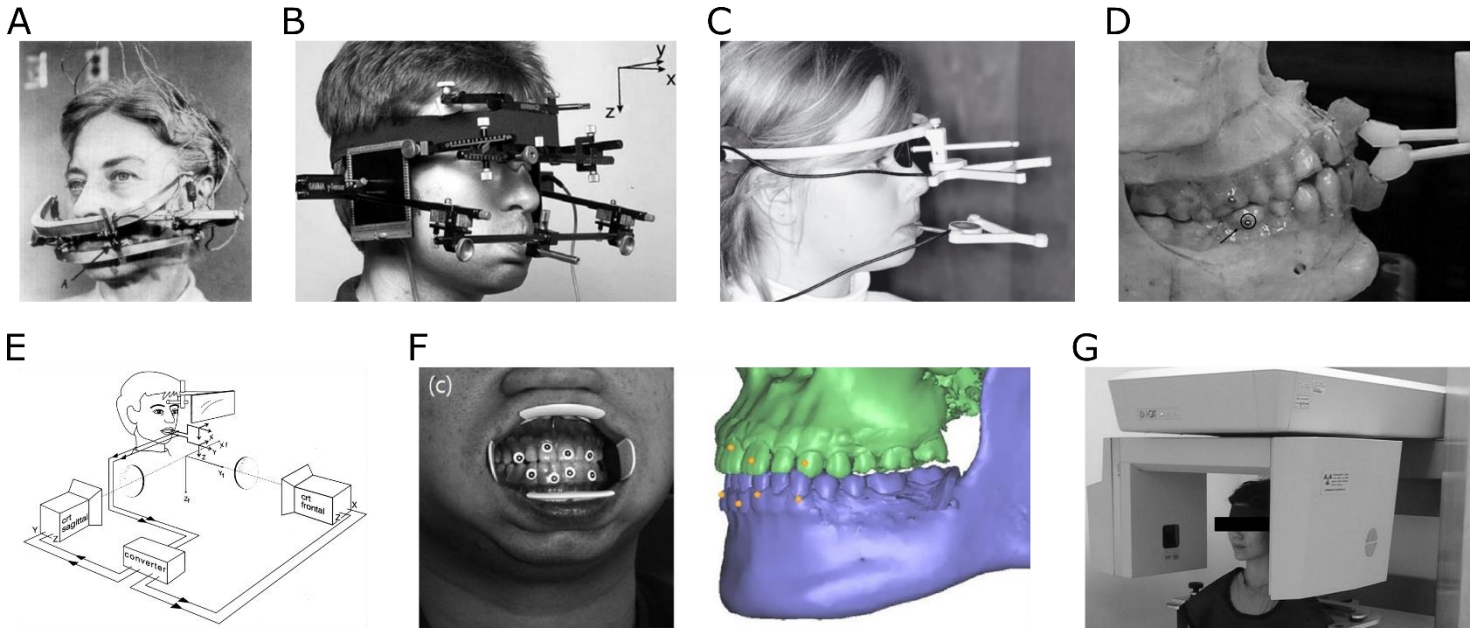



Figure 3.3: Technology used in the measurement of jaw and TMJ kinematics including the Case Gnathic Replicator, with two face-bows attached to the mandibular and maxillary teeth, and transducers mounted to the face-bows for recording displacement (Messerman 1967) (a). Electromechanical axiograph mounted to subject's mandible using an occlusal clutch, and attached to the forehead via a headband (Sadat-Khonsari et al. 2003a) (b). Ultrasonic tracking system, featuring three ultrasonic emitters mounted to the lower teeth via a metal clutch, and four ultrasonic receivers mounted on the head via a face-bow (Baqaien et al. 2007) (c). Magnetic tracking system used for quantifying condylar trajectories using custom plastic dental stents with magnetic sensors are attached to incisors and metal beads attached to molars to enable motion data registration using CT scans (Baltali et al. 2008b) (d). Optoelectronic tracking system which features lightweight frames containing three pairs of photocells are attached to the upper and lower incisors and canines, and two perpendicular cathode ray tubes which measures movements of these photocells to be reconstructed to evaluate 3D marker trajectories (Visscher et al. 2000) (e). 3D Scanning using adhesive targets attached to the teeth, and real-time CBCT scanning and digital reconstruction for the right lateral movement (Kwon et al. 2019) (f), and Cone beam CT system with custom-made video x-ray fluoroscopy function for radiographic evaluation of dynamic TMJ kinematics (Chen et al. 2013b) (g).

## 3.6 DISCUSSION

Mandibular kinematics have played an important role in evaluating internal muscle and joint forces (Rohrle and Pullan 2007), improving TMJ prosthesis design (Ackland et al. 2017) and assessing occlusal loading (Röhrle et al. 2018b). The quantification of mandibular border movements and condylar rotations and translations are clinically relevant for evaluating the presence and severity of TMJD's and for performing pre- and post-treatment comparisons respectively. In general, sub-millimetre accuracies and palpated approximations of condyle locations are sufficient for these clinical measures; however, for practicality clinical measurements typically require rapid data collection, ease of use and minimal invasiveness, and is most commonly performed using mechanical linkage systems such as axiography and ultrasonic position monitoring. Commercial ultrasonic tracking equipment is gaining popularity over axiography, as it is faster and simpler to deploy, requires less calibration, and employs lightweight face-bows that do not impede natural mandibular motion. Research applications, which tend to favour accuracy over measurement and data processing time, have traditionally favoured electromagnetic and optoelectronic tracking systems; however, recent advances in miniature magnetic sensor design have facilitated both rapid and accurate acquisition of mandibular kinematics and may be suitable as a tool in the clinical settings.

Quantification of TMJ kinematics cannot ordinarily be performed using mandibular motion data alone, and condyle positions must be determined relative to those of the skull. Axiography, the Case Gnathic Replicator, ultrasonic, electromagnetic and optoelectronic tracking all rely on either kinematically determined approximations of condyle location (a fixed joint centre-of-rotation), or approximations of condyle position based on the digitisation of palpated landmarks. This is typically achieved by identifying a landmark on the anatomic condyle; however, this point may differ from the actual joint centre of rotation by between 4.5mm and 10 mm (Gallo et al. 1997, 2008). For accurate approximations of condyle location using these systems, motion tracking data must be registered to 3D mandibular anatomy, which can be achieved using medical imaging such as MRI or CT. While radiographic tracking such as video x-ray fluoroscopy or 4D CT provide direct measures of mandible or TMJ motion, the associated exposure to ionising radiation may present an ethical dilemma.

Sophisticated magnetic tracking systems such as the Dental Motion Decoder (DMD) (Ignident, Ludwigshafen) overcome the size and cost constraints of optoelectronic systems through the use of small magnetic sensors directly to the teeth (Figure 3.4A), eliminating the requirement for custom dental splints. A handheld intraoral scanner can be employed to digitise

both the sensor and dental topology simultaneously (Figure 3.4B), which enables registration of motion data to 3D geometry of the dental arches. Following registration, mandibular motion can then be recorded in six degrees-of-freedom during dynamic activities including chewing (Figure 3.4C). While in their infancy, these systems show future promise as a clinical tool for mandibular motion analysis due to the potential for fast and accurate non-invasive data collection in a confined space; however, TMJ motion analysis may still be challenging due to the limited capacity of this system to accurately locate the mandibular condyle, or quantify TMJ centre of rotation.

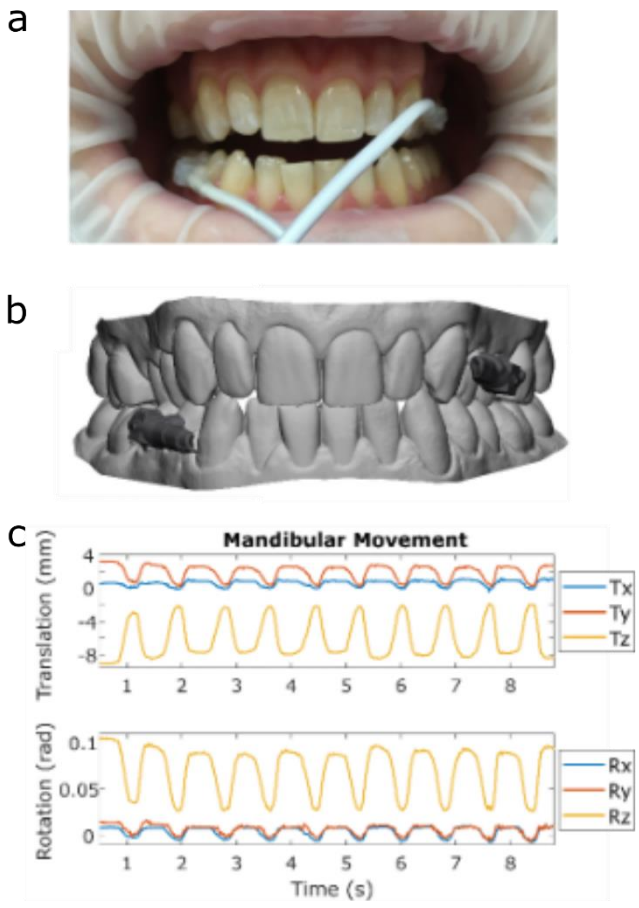



Figure 3.4: Magnetic DMD system with magnetic sensors fixed to participant's premolars using dental cement (a). The motion of these sensors can be registered to subject-specific dental geometry reconstructed from an intra-oral scanner (b), resulting in three orthogonal translations and rotations of the mandible with respect to the maxilla during habitual mastication (c). Data given are expressed about an anatomic coordinate system with the x-direction, y-direction and z-direction aligned with the lateral, anterior and superior directions, respectively.

Measurement of accurate mandibular kinematics has directly facilitated estimation of occlusal and mandibular loading during static and dynamic tasks. For example, 3D subject-specific bite force and occlusal pressure distributions have been estimated by driving finite element model simulations of dynamic chewing on a rubber sample with mandibular motion data acquired from optoelectronic tracking (Röhrle et al. 2018b). This modelling approach overcomes the practical limitations of employing conventional uniaxial bite force transducers i.e. biting down on a metal sensor, which may be difficult and uncomfortable for a subject, and provides 3D bite force data, including shear loading at the occlusal surface; however, such an approach requires highly accurate mandibular kinematics. Our calculations have shown that a jaw kinematics error of just 0.21 mm may lead to a discrepancy in bite force of approximately 40 N. Combining high precision motion data with computational simulations also has broad application in evaluating muscle and joint function. Muscle forces during activities of daily living can be calculated using musculoskeletal models and motion data by solving the static indeterminacy problem i.e. that there are more muscle-tendon actuators than degrees of freedom of TMJ motion, prohibiting calculation of a unique muscle force solution. This has been achieved using optimisation-based methods and electromyography (EMG) driven modelling approaches (Rohrle and Pullan 2007; Sagl et al. 2019). Finite element models of the entire jaw complex that combine kinematics and muscle-tendon loading have subsequently been used to evaluate bone stress and strain (Koolstra and Van Eijden 2005), and have had application in design and evaluation of TMJ prostheses (Ackland et al. 2015, 2017).

In conclusion, axiography and ultrasonic tracking provide fast and cost-effective mandibular motion measurements for use in the clinical setting; however, these methods are associated with greater measurement errors and the required hardware may have potential to hinder natural mandibular movement. Optoelectronic tracking generates accurate and robust motion analysis data but is expensive, requires a large, dedicated laboratory space, and necessitates fabrication of person-specific dental splints to overcome skin motion artefact. Radiographic methods such as video x-ray fluoroscopy and 4D CT provide direct measures of mandibular motion but are associated with significant radiation exposure and data processing time. Miniature magnetic tracking sensors that can be quickly adhered to teeth, combined with intra-oral scanning, shows promise in providing unobtrusive, rapid and accurate measurements of mandibular motion in both the clinic and research setting.

## 3.7 UPDATE

The systematic review was updated in 2024 to identify any new work and advancements in the field of jaw tracking since the original publication of the review. The database search strategy outlined in section 3.4.1 was repeated for studies published between 3rd April 2019 and 2nd January 2024 yielding 2,084 studies. All titles and abstracts were screened to determine whether they fulfill the inclusion criterion outlined in section 3.4.2. Following this, 33 studies were identified to be included in this review update (Figure 3.5).

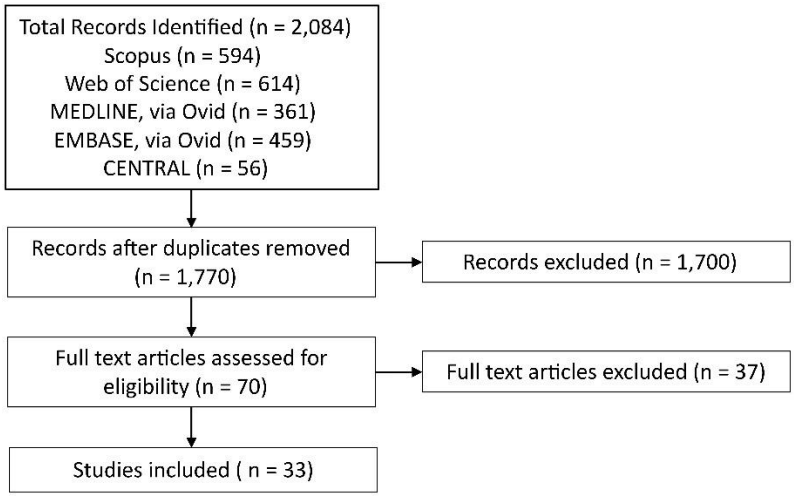



Figure 3.5: Flow chart illustrating systematic review search results between 3rd April 2019 and 2nd January 2024.

Similar to the initial review, the majority of studies employed ultrasonic or optoelectronic tracking for their usability and accuracy, respectively. Four studies used axiography (Allison et al. 2022; Ahlers et al. 2023; Ermolin et al. 2023; Lepidi et al. 2023), seven used ultrasonic tracking (Choi et al. 2019; Melchior et al. 2019; Sugihara et al. 2020; Guo et al. 2022; Siu et al. 2022; Lin et al. 2023; Wang et al. 2023). Three studies employed magnetic tracking systems, two of those used the commercial DMD system (Goob et al. 2020; Woodford et al. 2021) and one developed new magnetic tracking technology (Morikawa et al. 2022). Optoelectronic tracking was the most commonly used method and was employed in 17 studies. Optoelectronic tracking was combined with CT scans (Feng et al. 2021, 2023; Shu et al. 2021b, a, 2022b, a, 2023; Wojczyńska et al. 2021; Zhang et al. 2022; Ma et al. 2022; Woodford et al. 2023), MRI scans (Jurt et al. 2020; Shu et al. 2022b; Bescond et al. 2023) or used independently (Iwase et al. 2019; Farronato et al. 2021; Allison et al. 2022). Three new studies were identified that used radiographic tracking. Previously only used in case studies, one study used video X-ray

fluoroscopy on a larger sample size (n=10) (Chen et al. 2021), and two new studies used four dimensional CT (Huang et al. 2020; Kimoto et al. 2023). Two studies utilised multiple techniques. Lepidi et al (2023) used optoelectronic tracking as a gold standard to evaluate the accuracy of axiography in the assessment of sagittal condylar inclination (Lepidi et al. 2023). Allison et al (2022) used both optoelectronic tracking and axiographs at two different measurement sites out of practical convenience in their study of children with cerebral palsy (Allison et al. 2022). No studies were identified in this time period employing the case gnathic replicator or 3D scanning to measure jaw or TMJ kinematics (Figure 3.6).

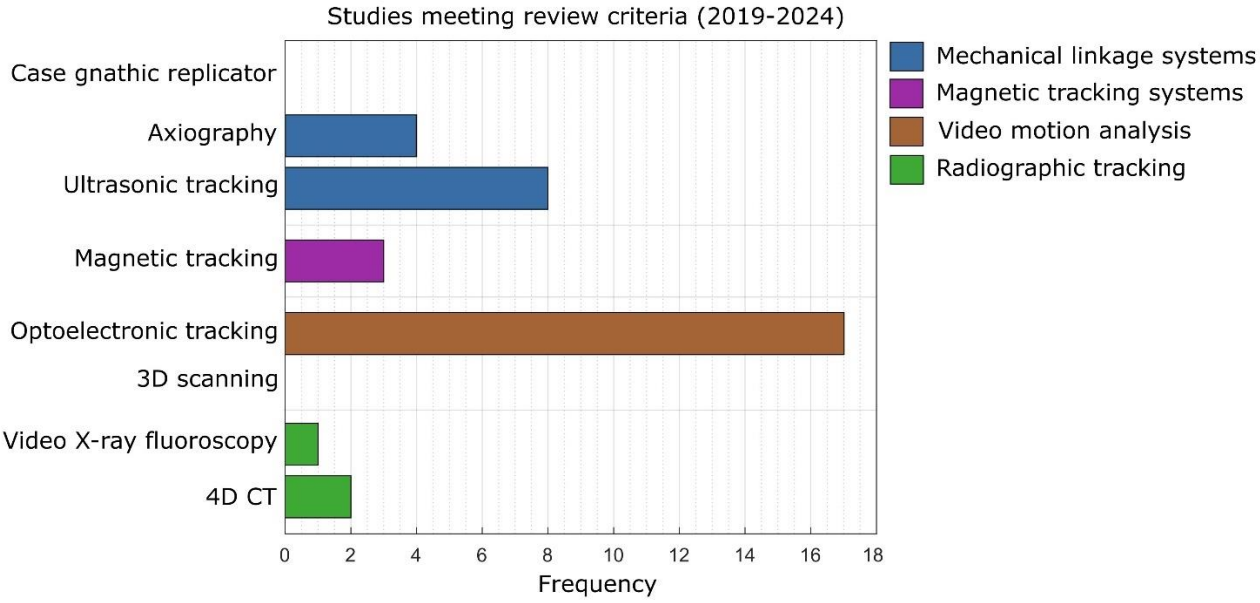



Figure 3.6: Bar chart showing the frequency of studies published using the jaw and TMJ kinematic measurement techniques between 3rd April 2019 and 2nd January 2024.

Two studies have made notable improvements to the usability of magnetic and optoelectronic tracking. Morikawa et al (2022) developed an electromagnetic tracking system where the permanent magnet, a miniature magnetic sensor and a motion sensor are all built in to a set of mouthpieces contained within the oral cavity (Figure 3.7). At present the system accuracy is low (3 mm); however, by removing the need for large scale devices or extra-oral appliances this system may increase the accessibility of routine kinematic measurements clinically (Morikawa et al. 2022). Feng et al (2023) employed the commercially available MODJAW optoelectronic tracking system (MODJAW, Sainte-Helene-du-Lac, France) to measure jaw kinematics during restricted mouth opening and closing movements (Figure 3.8) (Feng et al. 2023). While its kinematic accuracy has not yet been determined, the devices

simplicity makes it clinically viable and may lend the technology to research applications on large sample sizes.

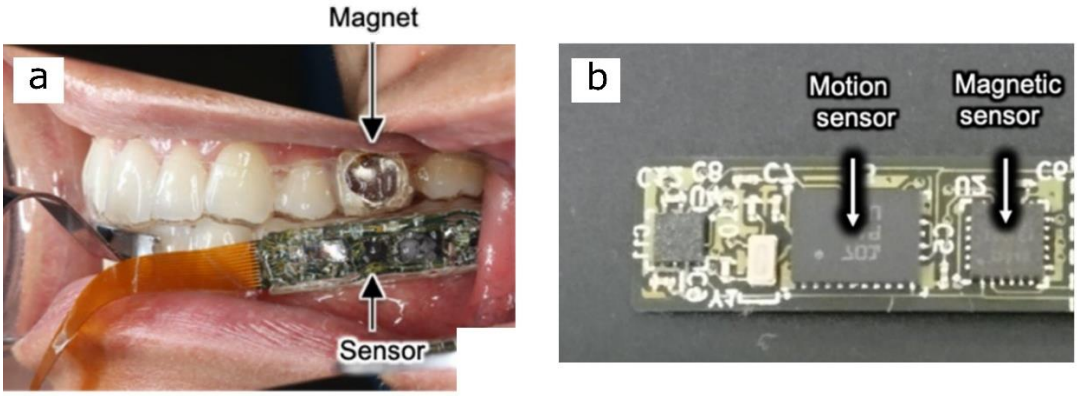



Figure 3.7: Intraoral photograph of the electromagnetic tracking device developed by Morikawa et al (2022) (a). Photograph of the sensor module, attached to the mandibular teeth, including a magnetic and motion sensor (b). Images adapted from Morikawa et al. (2022).

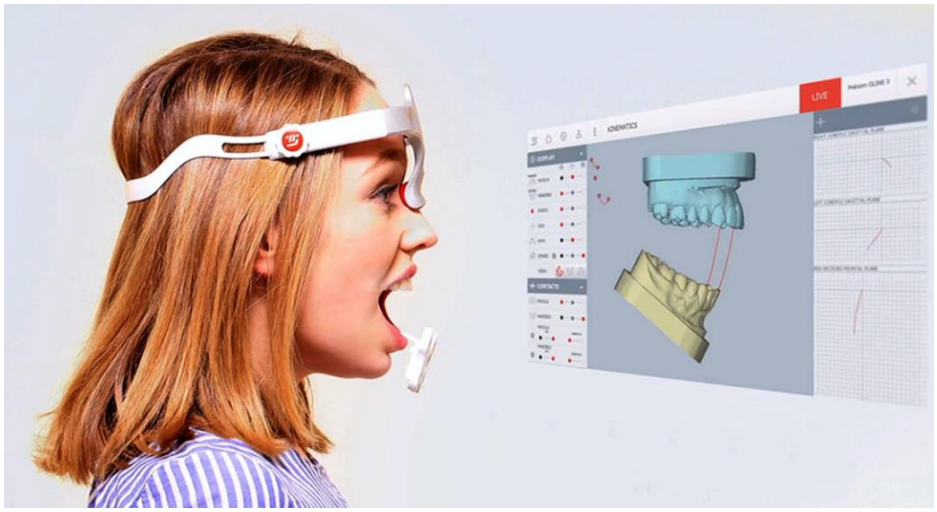


Figure 3.8: The MODJAW optical scanning system. Figure adapted from Solaberrieta et al. (2018).

# Chapter 4: Low-profile magnetic field sensors in the measurement and modelling of three-dimensional jaw kinematics and occlusal loading

This chapter is presented as the author-accepted manuscript of a peer-reviewed article published in *Annals of Biomedical Engineering* (2021, 49(6), pp. 1561-1571)

## 4.1 SIGNIFICANCE

Given major limitations in quantifying occlusal loading using traditional transducers, this chapter addresses this challenge by combining mandibular kinematics, obtained using low-profile magnetic field sensors, with intra-oral laser scanning and computational modelling to calculate occlusal loading. This study presents the first dynamic, 3D occlusal load estimates during habitual chewing and maximum force clenching of a rubber sample.

## 4.2 ABSTRACT

Dynamic occlusal loading during mastication is clinically relevant in the design and functional assessment of dental restorations and removable dentures, and in evaluating temporomandibular joint dysfunction. The aim of this study was to develop a modelling framework to evaluate subject-specific dynamic occlusal loading during chewing and biting over the entire dental arch. Measurements of jaw motion were performed on one healthy male adult using low-profile magnetic field sensors attached to the teeth, and occlusal anatomy quantified using an intra-oral scanner. During testing, the subject chewed and maximally compressed a piece of rubber between both second molars, first molars, premolars and their central incisors. The occlusal anatomy, rubber geometry and experimentally determined rubber material properties were combined to construct a finite element model, where the recorded mandibular motion was used to drive the virtual mandibular teeth into the rubber sample to simulate the experimentally observed chewing and biting. These simulations were used to predict three-dimensional dynamic bite forces and the dynamic contact pressure across the occlusal surfaces. Both chewing and biting on the first molars produced the highest bite forces across the dental arch, and a large amount of anterior shear force was produced at the incisors and the second molars. During chewing, the initial tooth-rubber contact evolved from the buccal

sides of the molars to the lingual sides at full mouth closure. Low-profile magnetic field sensors provide a clinically relevant measure of jaw kinematics with sufficient accuracy to drive finite element models of occlusal loading during chewing and biting. The presented modelling framework provides a basis for calculation of physiological, dynamic occlusal loading across the dental arch.

## 4.3 INTRODUCTION

Mastication is an essential function required for food breakdown and is achieved by the action of the masticatory muscles in generating dynamic bite force and occlusal loading. The magnitude and direction of bite force, which gives rise to occlusal loading, varies along the dental arch (Ferrario et al. 2004a; Bakke 2006) and is influenced by sex (Waltimo and Kononen 1993), age (Varga et al. 2011), facial morphology (Proffit et al. 1983) and ethnicity (Shinogaya et al. 2001). It is considered an important determinant of jaw function (Bakke 2006; Umesh et al. 2016), required for maintaining diet and quality of life (Lepley et al. 2011). Measurements of both bite force and occlusal loading have played a role in diagnosing disorders of the TMJ (Bonjardim et al. 2005; Kogawa et al. 2006), assessing mandibular fracture treatment (Kshirsagar et al. 2011), and the effects of malocclusions (Sonnesen et al. 2001; Bakke 2006), and are also critical for the design and functional assessment for dental restorations, dental implants and total TMJ prosthetics (Rismanchian et al. 2009; Hasan et al. 2016; Winter et al. 2020).

Maximum voluntary bite force has been experimentally measured using strain gauges (Ferrario et al. 2004a; Rismanchian et al. 2009), force transducers (Tortopidis et al. 1998), pressure-sensitive film (Kumagai et al. 1999) and piezoelectric transducers (Flanagan et al. 2012). While these devices may have high force measurement accuracy, they typically provide a static uni-directional force quantity as a subject compresses the device between their teeth, and are inadequate for capturing realistic dynamic occlusal loads such as those occurring during biting, chewing or grinding in situ. Three-component force transducers have also been employed to measure bite force and occlusal shear loading; however, these devices record biting under non-physiological conditions, such as tooth compression onto a metal plate, and may underestimate true bite force magnitude due to the subject's fear of tooth damage during testing (van Eijden 1991). Since dynamic force magnitude and direction at the occlusal surface cannot currently be directly measured during normal mastication, the three-dimensional loads incurred by the dental structures and transmitted to the underlying bone remain poorly understood (Röhrle et al. 2018a).

Computational modelling has been used to estimate TMJ loading (Sagl et al. 2019), prosthetic TMJ stresses (Ackland et al. 2015), dental implant loading (Robinson et al. 2019), and the mechanical and thermal loads involved in dental restorations (Mackerle 2004). Recent modelling studies have estimated dynamic occlusal loading during a maximum force bite (clench) and chewing (Röhrle et al. 2018b, a) by employing jaw kinematics data measured experimentally together with detailed models of the occlusal anatomy derived from medical imaging. While this approach produces dynamic compressive and shear force distributions at the occlusal surfaces using finite element model simulations, it requires development of customised dental splints for optical motion analysis as well as micro-computed tomography (μCT) of dental impressions to digitise occlusal anatomy, which may not be practical in the clinical setting. Furthermore, this approach has only been applied to the first molar to date, and at present, the loading incurred by the second molar and premolars during biting and chewing, and the incisors during dynamic biting, has not been quantified to date.

The aim of this proof-of-concept study was twofold. Firstly, to employ a new low-profile magnetic-field-sensor that can be quickly affixed to dental enamel, together with intra-oral scanning, to produce accurate measurements of occlusal kinematics during biting and chewing; and secondly, to use these measurements to estimate subject-specific occlusal loading over the entire dental arch using computational modelling. The technique reported in the present study provides a strong foundation for practical dynamic kinematics analysis and bite force estimation in both the clinic and research settings.

## 4.4 MATERIALS AND METHODS

### 4.4.1 Subject recruitment

One male participant (age: 39 yrs, weight: 82 kg) with healthy dentition and no history of mandibular disorders or dental pain was recruited and provided informed consent to participate in this study.

### 4.4.2 Jaw motion experiments

Motion analysis experiments were performed using the DMD system (Ignident, Ludwigshafen, Germany), which samples at 66 Hz the position and orientation of two low-profile magnetic field sensors of dimensions 1 × 4 × 2 mm (4 × 9 × 3 mm including coating) within a pre-defined magnetic field volume of approximately 220 $cm^3$ in size. The measurement error or the sensor position tracking in the capture volume was 0.01 ± 0.20 mm, which was calculated as the error in the distance computed between two adjacent sensors set at a fixed

distance of 50.0 mm as they were randomly moved through the entire capture volume (see Appendix B). Two low-profile magnetic sensors were fixed to the participant's teeth on the buccal surface using dental adhesive (Optibond FL, Kerr Dental, USA) and cured using ultraviolet light (Demi Plus, Kerr Dental, USA). One sensor was attached to the left maxillary premolar, and another on the right mandibular premolar approximately 3 mm away from the occlusal surface to limit interference during chewing. The participant wore a disposable lip retractor to aid in passage of wires from the mouth, and was seated upright immediately below the magnetic source (Figures 3.4a and 4.1a). The surfaces of all teeth on the mandible and maxilla and the magnetic sensors were digitised using an intra-oral scanner (Trios 3 Pod v. 1.18.2.6, 3Shape, Denmark).

The participant then held a soft polyurethane rubber sample of dimensions 20 mm × 20 mm × 5 mm between the second molars on the left (dominant) side, and the rubber sample and second molars were then scanned with the intra-oral scanner to register the position of the rubber relative to the teeth (Figure 4.1b). Ten continuous chewing cycles at the subjects preferred bite force were undertaken. The participant then performed maximal compression of the rubber sample between the second molars for three seconds. The chewing and maximum-force bite protocols were repeated at the first molars and premolars of both left and right sides, as well as the central incisors. During each task, jaw motion was simultaneously recorded from the two magnetic sensors using the DMD system. To register the positions of the sensors to the occlusal anatomy, a triangular surface mesh of the teeth and sensors was generated from the intra-oral scan with an average maximum edge length of 0.15 mm, and the local coordinate system of the mandibular and maxillary sensors expressed in an arbitrary coordinate system associated with the mandibular and maxillary occlusal surface geometries, respectively. Mean inter-occlusal distances were reported for all movements and mean mandibular protrusion and laterotrusion motion projected onto the occlusal plane and reported for the chewing cycles.

### 4.4.3 Material testing

The material properties of the rubber sample were derived experimentally using a materials test system. The rubber sample was assumed to be a visco-hyperelastic material with a near-incompressible material response, and was represented using a three-element Weichert model: one non-linear spring element to describe the hyperelastic material behaviour and two parallel Maxwell elements to represent the material's viscoelasticity. The hyperelastic material response was measured using an Instron 5848 Microtester with a 2 kN load cell (Instron, Norwood, MA, USA). Five rubber samples of dimensions 10 mm × 10 mm × 5 mm were

compressed at a rate of 0.5 mm per second to a maximum compressive load of 1.5 kN. This load cycle was repeated 3 times and the mean stress-strain curve was used to mathematically derive the hyperelastic material response (see Appendix B). This material behaviour was modelled using the phenomenological Ogden model, which was chosen due to its stability at high compressive strains. For isotropic materials, the strain energy density function is defined as:

$$W(\lambda_1, \lambda_2, \lambda_3) = \sum_{i=1}^{N} \frac{\mu_i}{\alpha_i} (\lambda_1^{\alpha_i} + \lambda_2^{\alpha_i} + \lambda_3^{\alpha_i} - 3) \quad (1)$$

where N = 1, $\lambda_i$ are the principal stretch ratios, and $\mu_i$ and $\alpha_i$ are the phenomenological material constants ($3.75 \times 10^5\ Pa$ and $8.35 \times 10^4\ Pa$, respectively) obtained using least-squares optimisation on the experimentally measured stress-strain curves ($R^2 = 0.9996$). The viscoelastic stress-relaxation response of the five rubber samples was subsequently measured on the Instron 5848 Microtester by performing a compression at a rate of 1 mm per second to a compressive load of 100 N and holding this position for 90 seconds. This stress-relaxation protocol was then repeated for a compressive load of 200 N. The mean relaxation modulus curve was derived from the relaxation modulus of all five specimens, for both the 100 N and 200 N compressions to mathematically model the viscoelastic material response (see Appendix B). This viscoelastic model was represented as a second-order Prony series, with a relaxation modulus given by:

$$g_R(t) = 1 - \sum_{i=1}^{N} g_i \left(1 - \exp\left(\frac{-t}{\tau_i}\right)\right) \quad (2)$$

where N = 2, t is time and $g_i$ and $\tau_i$ are the phenomenological material constants (first order: $2.88 \times 10^{-2}$ and 0.15 s, second order: $1.71 \times 10^{-2}$ and 1.78 s respectively), which were obtained by using least-squares optimisation with the experimentally measured stress-relaxation curves ($R^2 = 0.9997$).

### 4.4.4 Computational modelling

A 3D surface model of the subject's dental geometry was reconstructed from the intra-oral scans using 3-matic 13.0 (Materialise, Leuven, Belgium). The model, which included all maxillary and mandibular teeth, was meshed with triangular shell elements of edge lengths ranging from 0.26 mm to 0.35 mm, and imported into a commercially available finite element modelling package (Abaqus 2017, Dassault Systems, Paris, France).

The three-dimensional geometry of the rubber sample used during the experiment was reconstructed in the finite element model, and intra-oral scans of the participant holding the rubber between their teeth were used to register the position of the virtual rubber sample

between the teeth (Figure 4.1c). The virtual rubber sample was meshed using hexahedral elements with an element length of 0.35 mm, and assigned the visco-hyperelastic material properties derived from the mechanical testing. Since tooth enamel has a much greater stiffness compared to that of the rubber, the teeth were assumed rigid bodies.

The mandibular kinematics data obtained from the jaw motion experiments was used to kinematically drive the finite element model simulations of chewing and biting. The measured movement of the mandible corresponded to the movement of the virtual mandibular teeth and was applied as six boundary conditions in the model i.e., three rotations and three translations. The virtual maxillary teeth were assumed fixed, and during simulations, the virtual rubber sample was compressed between the mandibular and maxillary teeth. Tooth-rubber contact was modelled using the penalty method, minimising the penetration of the tooths surfaces into the rubber surfaces with an infinite coefficient of friction to avoid sliding of the teeth over the rubber, which was representative of the experimental test conditions. Mass scaling was applied to select elements of the rubber sample to reduce computational time (see Appendix B).

Quasi-static simulations using an explicit dynamics analysis were performed with parallelization over 6 cores on a desktop PC with an Intel Core i7 3.4 GHz processor and 16 GB memory. Contact pressure was reported over the occlusal surfaces, and bite forces were reported for the mandibular and maxillary teeth with respect to an anatomic co-ordinate system aligned with the occlusal plane. Specifically, the x-, y- and z-directions corresponded to the lateral (left), posterior and superior directions, respectively. Chewing cycles were defined as commencing just after initial contact between the teeth and the rubber (0%) and finishing at the time of maximum bite force (100%).

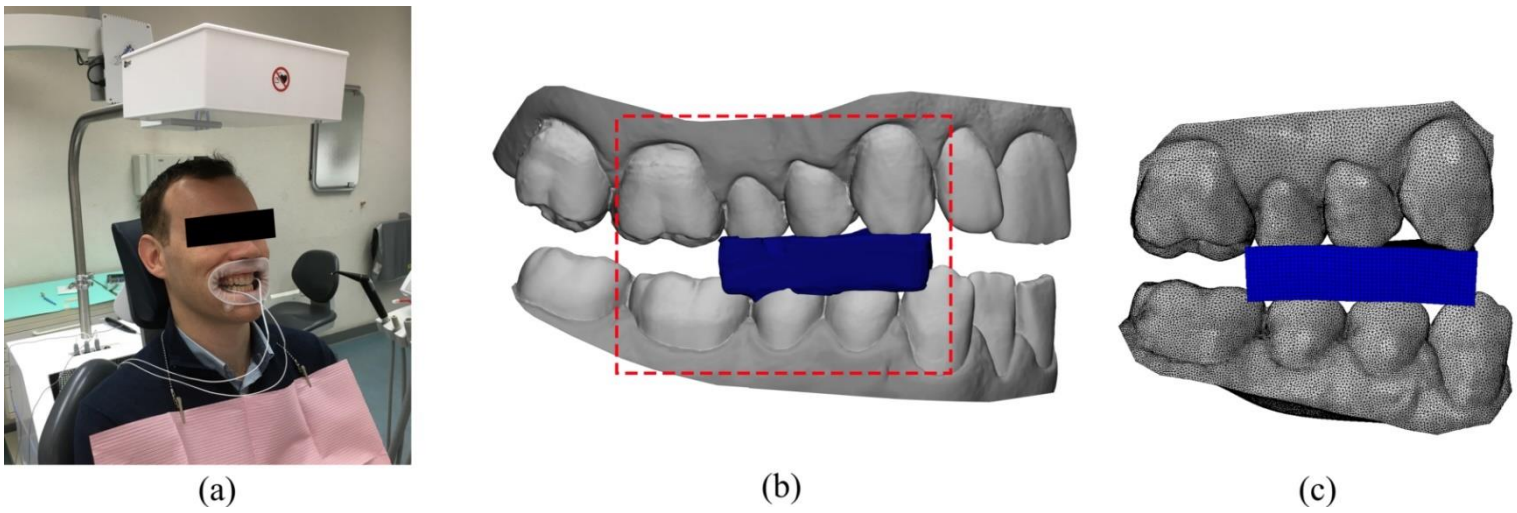



Figure 4.1: DMD experimental setup showing participant with electromagnetic field sensors attached to the teeth and the electromagnetic source located approximately 8 cm above the subject's head (a). 3D model of the participant's mandibular and maxillary teeth with rubber held between the premolars obtained through the intra-oral scan (b). Finite element model of the premolars (grey) and rubber (blue) constructed from the intra-oral scan data. Teeth that were not in contact with the rubber were removed during simulations, for computational efficiency (c). The red-dashed area indicates the region that was represented using the finite element model.

### 4.4.5 Model validation

To validate the finite element model, an independent compression experiment was performed on a single tooth against the rubber using the Instron 5848 microtester (Figure 4.2(a)). One intact, adult second molar was sourced from the Melbourne Dental School and fixed to a custom-designed potting fixture with dental plaster. This tooth was aligned to a thin cylinder of the rubber material (diameter: 30 mm, height: 5.5 mm), and compressed at a rate of 0.5 mm per second to a displacement of 4 mm, while uniaxial reaction force was measured by the load cell. The tooth-potting fixture assembly was imaged using µCT (µCT 50; Scanco Medical, Brüttisellen, Switzerland) with a voxel size of 0.02 mm, and the resultant images were segmented to obtain a surface mesh of the combined fixture and tooth. The tooth geometry was imported into a finite element model and meshed with triangular shell elements of length ranging from 0.23 mm to 0.35 mm. The rubber was simulated as a cylinder matching the dimensions of the rubber and meshed using hexahedral elements of element size 0.35 mm, following a mesh convergence analysis (see Appendix B). The tooth was modelled as a rigid body and the rubber as a deformable visco-hyperelastic material with material properties and contact conditions as described above. The virtual tooth was compressed against the rubber following the compressive displacement measurements, and the calculated uniaxial reaction force was compared to that measured experimentally.

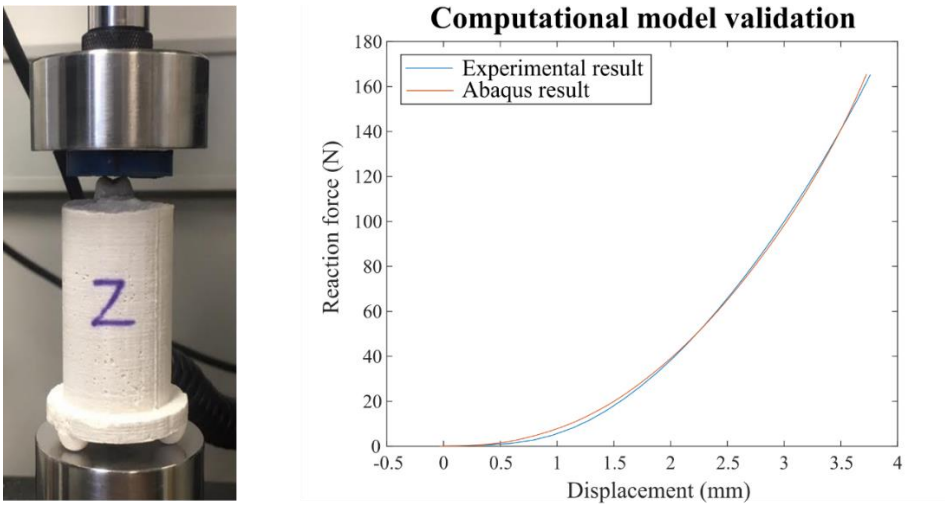



Figure 4.2: Validation experimental setup showing human tooth cemented into a custom-made fixture, the blue rubber sample lies between the tooth and the load cell (a) and experimental results compared against computational model output corresponding to this loading scenario (b). The RMS error between experiment and model was 1.39 N.

## 4.5 RESULTS

The model validation simulations demonstrated a root-mean-square (RMS) error of 1.39 N between the simulated and experimentally measured uniaxial reaction forces on the Instron load cell (Figure 4.2(b)).

During chewing, the inter-occlusal gap was smallest for the left second molar (1.28 mm) followed by the premolars (left: 1.55 mm, right: 1.51 mm), incisors (1.66 mm), first molars (left: 2.50 mm, right: 2.22 mm) and the right second molar (2.61 mm) (Figure 4.3). Throughout the mean chewing cycles, the mandible protruded forwards during mouth closure, with the position of maximum mandibular protrusion occurring at 100% mouth closure for both second molars (left: 1.63 mm, right: 2.76 mm), the right first molar (2.13 mm) and the incisors (0.97 mm). Maximum mandibular protrusion during chewing also occurred in the vicinity of 100% mouth closure for the right (2.24 mm) and left (1.75 mm) premolars respectively, while a small amount of mandibular retrusion occurred for the mean chewing cycle on the left first molar (0.3 mm) (Figure 4.4). Limited mandibular laterotrusion was recorded for all teeth during chewing (Figure 4.4).

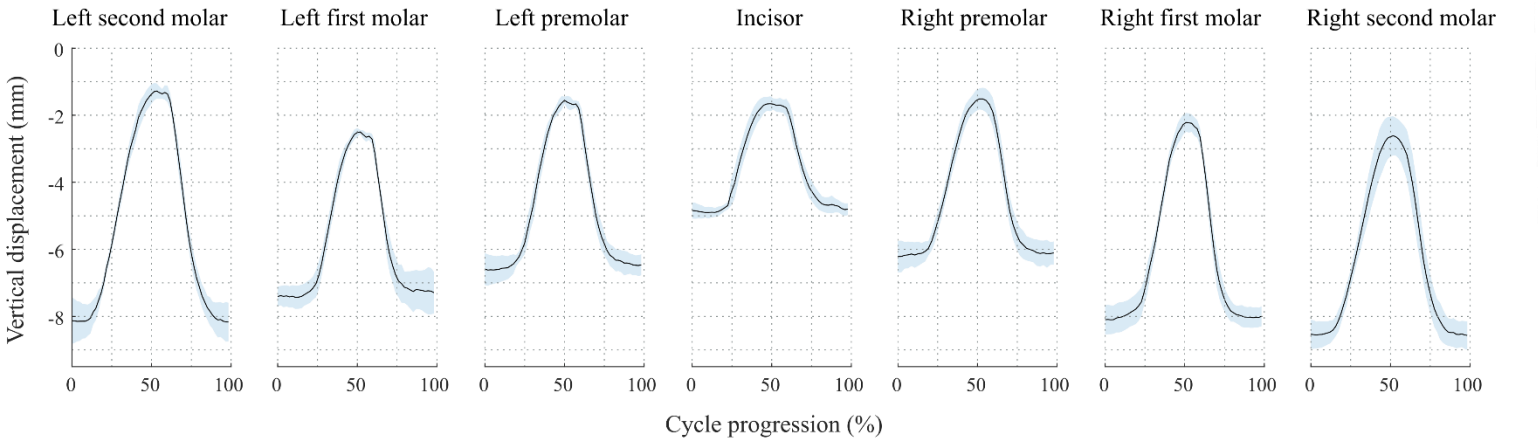



Figure 4.3: Vertical translation of the mandible measured during ten chewing cycles. Black curves represent mean cycle data, while the shaded region indicates one standard deviation about the mean.

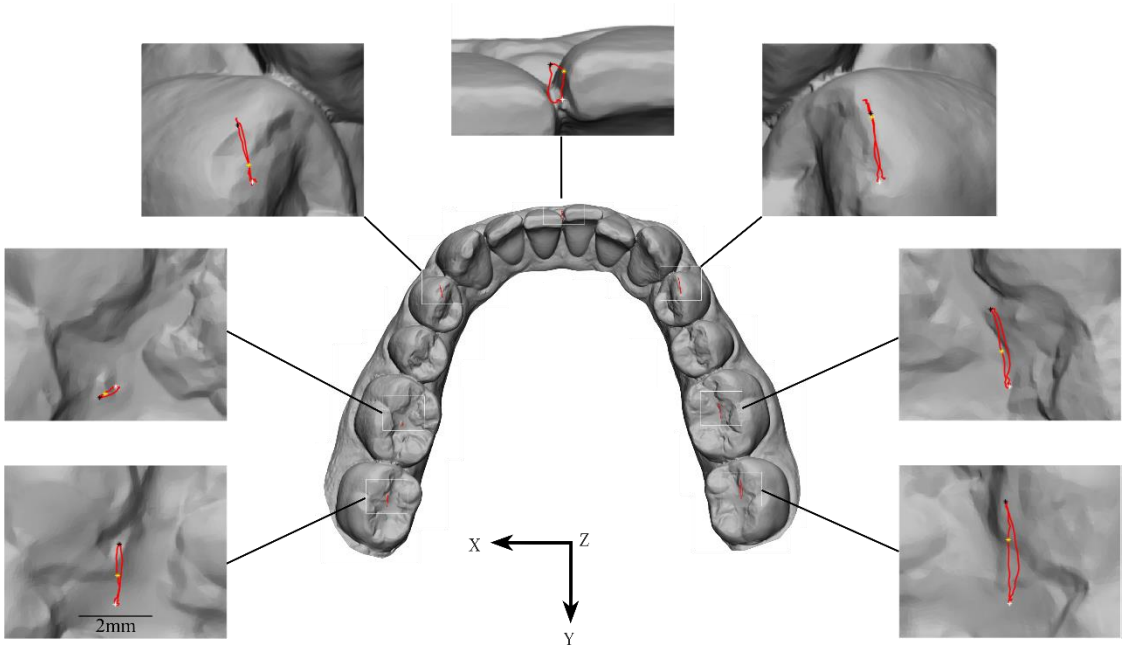



Figure 4.4: Mandibular protrusive and laterotrusive movements during mean chewing of rubber sample, projected onto the occlusal plane. Data is given for the incisors, premolars, first molars and second molars. White, yellow and black markers refer to the points at 0%, 50% and 100% of the chewing cycle respectively. X, Y and Z represent the lateral (left), posterior and superior directions respectively. All trajectory images adhere to scale in lower left corner.

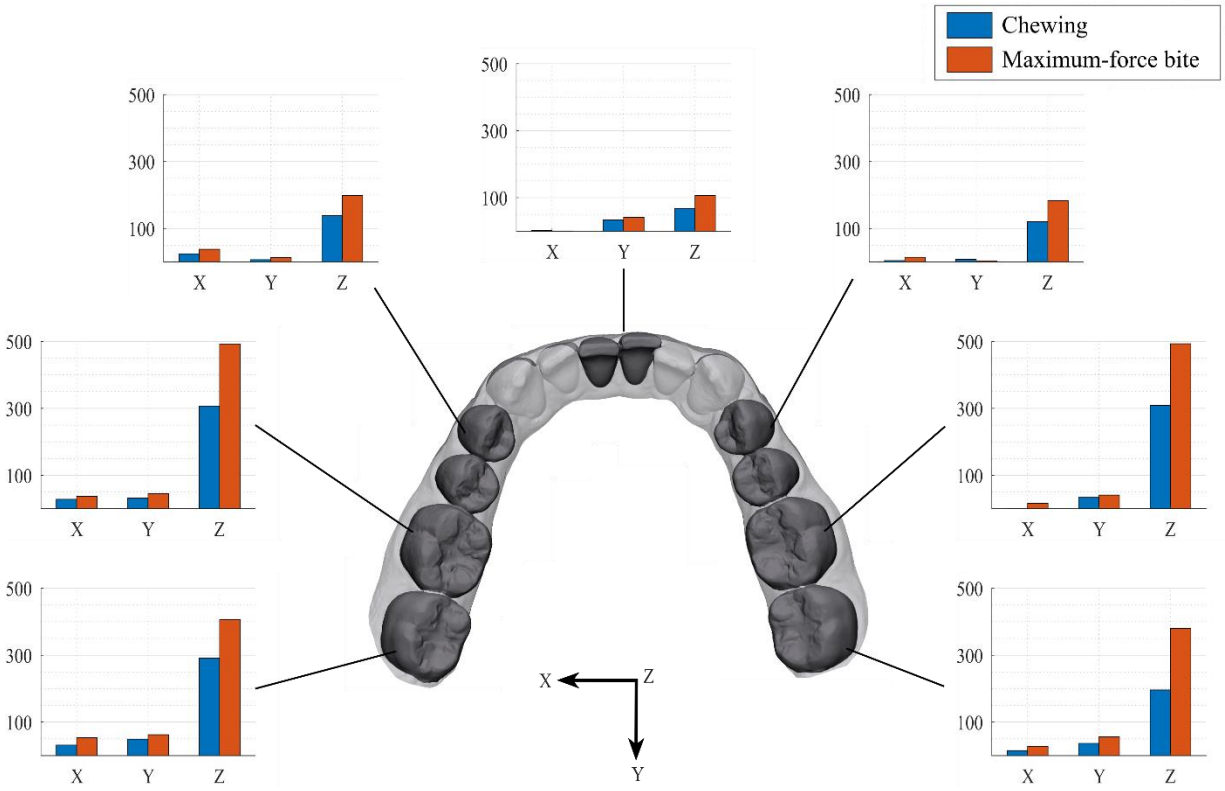



Figure 4.5: Tooth-specific mandibular bite forces for mean chewing and maximum-force bite tests. Data are given for the incisors, premolars, first molars and second molars. All forces are given in Newtons; X, Y and Z represent the lateral (left), posterior and superior directions, respectively.

The first molars generated the largest bite forces of all teeth, a finding consistent for both chewing (left: 309 N, right: 311 N) and maximum-force biting (left: 496 N, right: 495 N). The incisors generated the smallest bite forces during chewing (75 N) and maximum-force biting (114 N) (Figure 4.5). The average bite forces on the first molars, premolars and incisors were 124%, 50% and 33% of that on the second molars (Figure 4.5, Tables 4.1 and 4.2). During chewing, the highest bite forces on the mandibular teeth were directed anteriorly, this was particularly prominent on the incisors, with the maximum force directed 26.7° anteriorly, and the second molars, with the maximum force directed 9.6° and 10.6° anteriorly (Table 4.1). This trend was also seen for maximum-force biting, with the maximum force directed 21.4° anteriorly for the incisors and 8.7° and 8.6° anteriorly for the second molars (Table 4.2). The mandibular bite forces were higher for the maximum-force bite than during chewing across the entire dental arch (Figure 4.5, Tables 4.1 and 4.2).

For the first molar, the tooth-rubber contact evolution during chewing was shown to progress from the buccal sides of both maxillary and mandibular first molars towards the lingual side during jaw closure. At 100% jaw closure during chewing, maximum stress regions occurred over the distobuccal and distolingual cusps of the first molars, while the highest stresses in the rubber occurred between the disto-lingual cusps of the maxillary and mandibular. During chewing with the second molars, the tooth-rubber contact was initiated on the buccal side of the mandibular tooth, and the buccal side of the mesial maxillary cusp and the lingual side of the posterior maxillary cusp, this progressed towards the lingual side of both second molars during jaw closure (Figure 4.6). By 100% jaw closure, the highest stress in the rubber was between the maxillary mesiobuccal cusp and its opposing mandibular ridge of the second molars.

Table 4.1: Magnitude and direction of the mean chewing force for each mandibular tooth.

| Tooth | Cycle Progression | Bite Force (N) | | | | Bite Force Direction (degrees) | |
|---|---|---|---|---|---|---|---|
| | | X | Y | Z | Magnitude | X | Y |
| Second Molar (left) | 25% | -1.0 | -11.0 | 43.8 | 45.2 | -1.3 | -14.1 |
| | 50% | -3.6 | -20.3 | 83.5 | 86.0 | -2.4 | -13.7 |
| | 75% | -8.1 | -31.4 | 152.8 | 156.2 | -3.1 | -11.6 |
| | 100% | -31.4 | -49.2 | 291.8 | 297.6 | -6.1 | -9.6 |
| First Molar (left) | 25% | -2.8 | -5.9 | 41.4 | 41.9 | -3.8 | -8.1 |
| | 50% | -6.4 | -12.2 | 86.6 | 87.6 | -4.2 | -8.0 |
| | 75% | -14.0 | -20.7 | 170.3 | 172.1 | -4.7 | -6.9 |
| | 100% | -28.2 | -31.4 | 305.8 | 308.7 | -5.3 | -5.9 |
| Premolar (left) | 25% | -3.7 | -1.7 | 20.6 | 21.0 | -10.2 | -4.8 |
| | 50% | -7.1 | -3.1 | 41.7 | 42.4 | -9.7 | -4.3 |
| | 75% | -13.6 | -4.8 | 77.0 | 78.3 | -10.0 | -3.5 |
| | 100% | -23.9 | -7.3 | 131.6 | 134.0 | -10.3 | -3.2 |
| Incisors | 25% | 0.1 | -4.7 | 11.5 | 12.4 | 0.5 | -22.4 |
| | 50% | -0.6 | -11.6 | 26.6 | 29.0 | -1.4 | -23.5 |
| | 75% | -1.4 | -20.9 | 44.7 | 49.4 | -1.8 | -25.1 |
| | 100% | -2.2 | -33.8 | 67.4 | 75.4 | -1.9 | -26.6 |
| Premolar (right) | 25% | 0.5 | -1.9 | 24.9 | 24.9 | 1.1 | -4.3 |
| | 50% | 0.2 | -3.6 | 45.6 | 45.8 | 0.3 | -4.5 |
| | 75% | 1.2 | -5.7 | 78.1 | 78.3 | 0.9 | -4.1 |
| | 100% | 3.4 | -8.2 | 120.3 | 120.6 | 1.6 | -3.9 |
| First Molar (right) | 25% | -2.0 | -7.6 | 50.0 | 50.6 | -2.3 | -8.6 |
| | 50% | -3.8 | -14.2 | 101.2 | 102.2 | -2.1 | -8.2 |
| | 75% | -3.3 | -23.2 | 176.7 | 178.2 | -1.1 | -7.3 |
| | 100% | -0.2 | -34.1 | 308.9 | 310.7 | 0.0 | -6.3 |
| Second molar (right) | 25% | 1.8 | -8.0 | 40.6 | 41.5 | 2.5 | -11.2 |
| | 50% | 4.2 | -15.6 | 75.2 | 76.9 | 3.2 | -11.7 |
| | 75% | 8.9 | -25.6 | 124.0 | 127.0 | 4.1 | -11.7 |
| | 100% | 15.0 | -36.5 | 196.0 | 199.9 | 4.4 | -10.6 |

Table 4.2: Magnitude and direction of the peak maximum-force bite value for each mandibular tooth.

| Tooth | Bite Force (N) | | | | Bite Force Direction (degrees) | |
|---|---|---|---|---|---|---|
| | X | Y | Z | Magnitude | X | Y |
| Second molar (left) | -53.8 | -62.5 | 406.7 | 415.0 | -7.6 | 8.7 |
| First molar (left) | -37.4 | -45.5 | 492.7 | 496.2 | -4.6 | 5.2 |
| Premolar (left) | -37.9 | -13.5 | 198.4 | 202.4 | -11.0 | 4.1 |
| Incisors | -0.2 | -41.6 | 106.5 | 114.3 | -0.1 | 21.4 |
| Premolar (right) | 14.1 | -3.5 | 183.6 | 184.2 | 4.6 | 1.2 |
| First molar (right) | 15.9 | -40.9 | 493.0 | 495.0 | 1.7 | 4.6 |
| Second molar (right) | 28.2 | -56.2 | 380.2 | 385.4 | 4.0 | 8.6 |

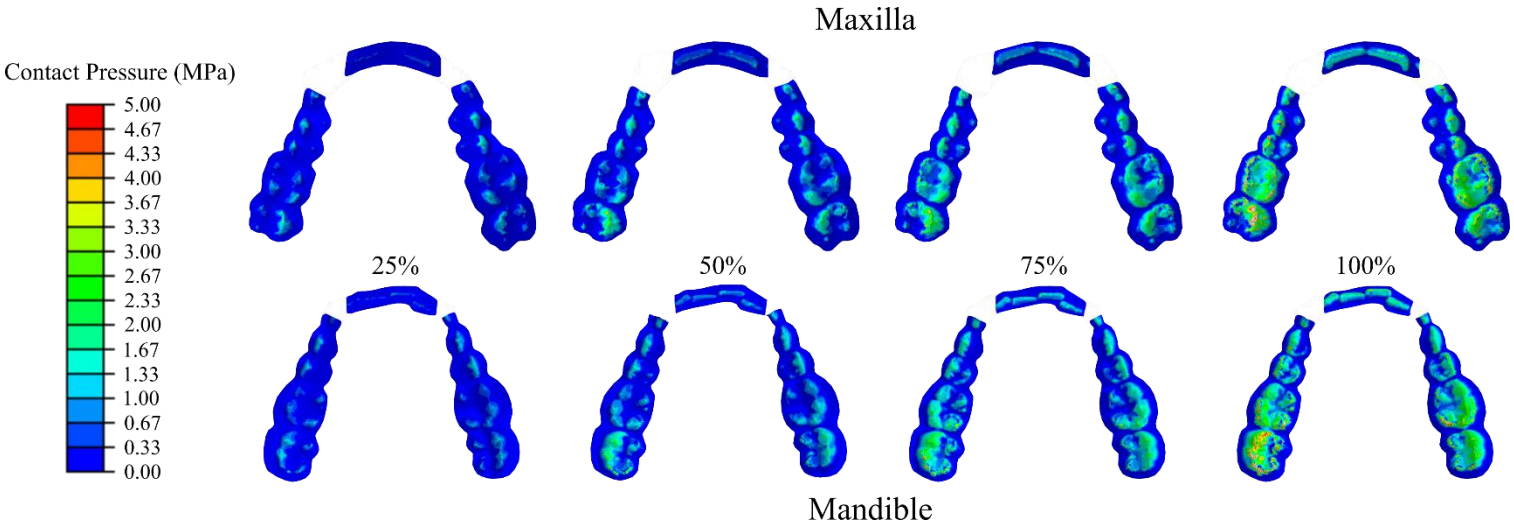



Figure 4.6: Evolution of the contact pressure distribution along the maxillary (top row) and mandibular (bottom row) dental arches at 25%, 50%, 75% and 100% of the mean chewing cycle. Contact pressure values are given in MPa.

## 4.6 DISCUSSION

This study presented a subject-specific computational modelling framework for evaluating jaw kinematics, bite forces and the occlusal loading distribution during chewing and maximum-force biting using a new magnetic-field-based kinematics measurement system. In conventional approaches, jaw kinematics are measured using mechanical devices such as axiography (Sadat-Khonsari et al. 2003b), point tracking methods such as optoelectronic tracking (Buschang et al. 2000) or radiographic techniques such as x-ray fluoroscopy (Chen et al. 2013b). Mechanical devices and point tracking techniques often involve attachment of bulky

equipment such as face-bows to the mandibular teeth, which may load the jaw inferiorly and interfere with natural jaw motion and occlusion. Additionally, techniques such as optoelectronic tracking typically use skin mounted markers, which are prone to significant skin motion artefact (Chen et al. 2011). Radiographic methods such as 4D Computed Tomography, which provide direct kinematic measurement without skin motion artefact, expose the subject to ionising radiation, and have therefore had limited application. For a full review of mandibular motion tracking techniques see Woodford et al. (2020) (Woodford et al. 2020). In contrast, the DMD system employed in the present study provides accurate non-invasive jaw kinematics measurement that can be rapidly performed chairside with little setup time. The low-profile electromagnetic trackers that are adhered to the teeth do not interfere with natural motion of the jaw during chewing, they provide dynamic measurement of kinematics without skin motion artefact, and bypass the requirement to fabricate subject-specific splints. These features lend the system well to jaw motion measurement in both the research laboratory and clinic.

Traditional bite force measurements are limited to quantifying static, unidirectional, maximal occlusal loads obtained through non physiological conditions such as clenching on a hard metal surface (Koc et al. 2010; Röhrle et al. 2018a). Whilst previous efforts have been made to measure the three-dimensional components of occlusal loads, this technology relies on implanting sensors within restored teeth and therefore cannot be applied to participants with healthy dentition (Mericske-stern 1998; Kawaguchi et al. 2007). Similarly, dynamic occlusal loading has been measured using a novel application of strain gauges, however these recordings are also limited to quantification of unidirectional loads (Shimada et al. 2012). The presented measurement and modelling methodology provides a novel alternative to existing measurement techniques, it does not require the participant to bite down on a hard surface, which has been shown to prevent maximum bite force capacity (Koc et al. 2010). To the authors knowledge this is the first technique capable of measuring dynamic three-dimensional loading and thus allows the analysis of sub-maximal loading of the teeth, like that observed in functionally relevant activities such as mastication, and permits quantification of shear loading at the tooth surface, which negatively affects the stress distribution within dental structures (Röhrle et al. 2018a). This modelling methodology overcomes practical limitations associated with bite-force measurements, and shows great promise for research in the fields of biomechanics and dental restorations.

The results of this study are in reasonable agreement with data reported sporadically in the literature. For example, the superior, protrusive and lateral mandibular movements during chewing with the first molar (5.9 mm, 2.2 mm and 0.54 mm respectively) reported in the present

study were similar to those of Röhrle et al. (2018) who also studied chewing of rubber samples with similar material properties and dimensions (approximately 5.0 mm, 2.0 mm and 0.50 mm respectively) (Röhrle et al. 2018b). This study found maximum-force bite loads of approximately 400 N, 495 N, 195 N and 115 N for the second molars, first molars, premolars and central incisors respectively. These results are consistent with bite force data previously measured for the first molars (546 N) (Raadsheer et al. 1999), premolars (254 N) and central incisors (146 N) (Ferrario et al. 2004a), but are lower than some average bite forces reported elsewhere for healthy adult males (Hellsing 1980; van Eijden 1991; Waltimo and Kononen 1993; Ferrario et al. 2004b; Varga et al. 2011; Al-Omiri et al. 2014; Umesh et al. 2016) (Table 4.3). This study found chewing loads of approximately 249 N, 310 N, 127 N and 75 N for the second molars, first molars, premolars and central incisors respectively. These values are lower than those reported for cyclic chewing of rubber on the first molar and premolars (617.8 N) (Röhrle et al. 2018b), which may be due to differences in the models used to represent the rubber material properties. However, we surmise that the calculated bite forces fall within the expected range given the large variability in bite force measurements between subjects and across different measurement modalities (Tortopidis et al. 1998).

Table 4.3: Published maximum bite force data for adult males with healthy dentition. Given are gender, age and sample size of subjects, and the reported bite forces for the second molars, first molars, premolars and incisors, where available. Bite forces given are mean ± one standard deviation.

| Authors | Gender | Age (years) | Sample Size | Bite Force (N) | | | |
|---|---|---|---|---|---|---|---|
| | | | | Second Molar | First Molar | Premolar | Incisors |
| Hellsing, 1980[18] | M | N/A | 8 | - | - | - | 161 ± 29.6 |
| van Eijden, 1991[10] | M | 31.1 (mean) | na | 723 ± 138 | - | 583.0 ± 99.0 | - |
| Waltimo and Kononen, 1993[48] | M | 22-35 | 15 | - | 847.0 ± 131.0 | - | 287.0 ± 75.0 |
| Raadsheer et al., 1999[32] | M | 18-36 | 58 | - | 545.7 ± 115.1 | - | - |
| Ferrario et al., 2004[12] | M | 20-29 | 8 | - | 785.0 ± 203.1 | - | - |
| Ferrario et al., 2004[11] | M | 19-29 | 36 | 294.3 ± 55.92 | 306.1 ± 42 | 254.1 ± 72.2 | 146.17 ± 44.4 |
| Varga et al., 2011[47] | M | 18 | 14 | - | 777.7 ± 78.7 | - | - |
| Al-Omiri et al., 2014[2] | M | 28-57 | 20 | - | 651.5 ± 59.9 | - | - |
| Umesh et al., 2016[46] | M | 24-35 | 20 | | 629.5 ± 64.5 | 365.0 ± 36.0 | 262.5 ± 32.0 |

The highest occlusal forces were consistently located at the first molars, both for chewing and maximum-force biting. This finding contradicts the mechanical lever theory (Gosen 1974), a popular belief that the jaw functions as a third-class lever; where the condyle acts as a hinge, the tooth produces a bite force, and the muscle produces a force located between these points. Based on this theory, for a constant maximum muscle force, the magnitude of the maximum occlusal load applied by a tooth depends only on the distance between the tooth and the muscle attachment point. Therefore, the posterior teeth closer to the muscle attachment point are capable of higher occlusal loads than anterior teeth located further from the muscle attachment point. The mechanical lever theory predicts that the bite forces on the first molar, premolars and central incisors will be 90%, 83% and 69% of that on the second molar respectively (Gosen 1974), however, the results of this study found the bite forces on the first molar, premolars and central incisors to be 124%, 50% and 33% of that on the second molars, respectively, while several other empirical studies reported similar inconsistencies with the mechanical lever theory (Hattori et al. 2003, 2009; Ferrario et al. 2004a). Our finding supports the alternative principle stated by Hattori et. al. that the critical limit of maximum jaw loading may be the load-bearing capacity of the periodontal tissues (Hattori et al. 2003) – since the first molar generally has the largest root surface area of all teeth (Hujoel 1994), less load is transmitted to the periodontal tissue and larger bite forces may be permissible without pain. The findings of this study also suggest that the periodontally borne load, expressed as tooth-specific bite force divided by the total tooth root surface area, is constant across the dental arch (Hattori et al. 2003).

This study demonstrated that a large amount of anterior shear loading is present during chewing and maximal-force biting, particularly on the incisors and second molars, a finding consistent with other studies of three-dimensional occlusal loading (Rues et al. 2008; Hattori et al. 2009; Röhrle et al. 2018b). During chewing and maximum-force biting the subject's mandible moved anteriorly with little lateral motion, resulting in more anterior shear loading than lateral shear loading. Shear loading at the tooth surface greatly increases the magnitude of the maximum stress within the tooth (Romeed et al. 2012) and introduces a bending moment at the bone near the base of the tooth due to the shear loading at the occlusal surface producing a tooth cantilever effect (Röhrle et al. 2018b). For implant supported prostheses, this could increase the transfer of occlusal loads to the underlying cortical bone and may lead to negative outcomes such as early implant loosening or failure of the implant-bone interface (Barbier et al. 1998). Additionally, the higher stresses at either an implanted or restored tooths surface may lead to implant failure due to fractures or fatigue failure (Drummond 2008). Furthermore, the

production of non-axial occlusal loads requires higher activation forces from the masticatory muscles and results in higher TMJ loads in comparison to axial occlusal loads (Schindler et al. 2007; Rues et al. 2008). The results of this study indicate that musculoskeletal model predictions of TMJ loading that use bite force measures with no shear loading considerations may ultimately under-estimate joint force predictions.

The present study showed that the evolution of occlusal contact during chewing is consistent with studies of the first molar and premolars that found that the bolus is compressed between opposing cusps of the maxillary and mandibular teeth (Röhrle et al. 2018b). This interaction between opposing cusps may be necessary to achieve the force and stress concentrations necessary to grind and breakdown food during mastication, which is supported by evidence that subjects with greater occlusal contact area are better equipped to mechanically breakdown foods (Wilding 1993; Owens et al. 2002).

This study showed that the mean inter-occlusal gap during chewing on the left second molar (1.28 mm) was much smaller than that of its neighbouring first molar (2.50 mm) or the right second molar (2.61 mm) (Figure 4.3). We note that variability between the repeated occlusal movements may be present in these results, potentially arising from subject familiarisation with the experimental protocol. This variability has been found for both within- and between-cycle recordings, and is largest for the vertical displacement measures (Keeling et al. 1991; Lassauzay et al. 2000). In this experiment, the left second molar was the first loading trial to be conducted – the unexpectedly low inter-occlusal gap may be due to subject adaption to the experimental protocol, which should be considered in future studies.

Some limitations of this study ought to be noted. First, errors in kinematics measurement translate directly to variability in occlusal loading, but the extent of this is not well understood. We ran four finite element simulations of habitual mastication for the right first molar with the mandibular jaw closure offset by the mean measurement error of ±0.01 mm, as well as mean plus standard deviation of ±0.21 mm, which produced force calculation errors of ± 2 N and ± 42 N, respectively (see Appendix B). This demonstrates that calculation of bite force using finite element model simulations in the present study depend on highly accurate measurements of jaw kinematics, as well as high quality registration of magnetic sensors to occlusal anatomy. Second, errors in the calculated occlusal load may also be introduced through the material model, contact formulation, mesh discretisation and the solver used in the FEA, however the mesh convergence and validation studies were performed to keep these errors to a minimum whilst retaining a viable computational expense. Third, while the validation experiment found high accuracy of the bite force results, it should be highlighted that only

uniaxial compression was studied. This is a simplified approximation of the complex and dynamic jaw movements of mastication and should be considered when interpreting the results. Finally, this study was limited to a sample size of one, and future studies ought to employ this technique on a larger participant cohort to enable generalisation of results and a thorough statistical analysis.

In conclusion, this study reports a new high accuracy method of measuring jaw kinematics using low-profile magnetic field sensors that are suitable for both the clinic and research settings. By combining these measurements with occlusal anatomy derived from intra-oral scans and finite element model simulations, we derived calculations of dynamic, three-dimensional occlusal loading during biting and chewing. This measurement and modelling framework, which we validated with independent testing, produces physiologically relevant occlusal load estimates which are otherwise impossible to achieve using conventional bite force transducers. This study showed that unilateral chewing and biting using the first molars produced more bite force than that of the second molar, pre-molar and incisors, supporting the theory that the critical limit of maximum jaw loading may be the load-bearing capacity of the periodontal tissues. Future studies ought to employ this technique on a larger participant cohort to enable generalisation of results. The motion measurement system and modelling framework presented may be useful for design and evaluation of patient-specific prosthodontic devices and dental restorations, diagnosis of TMJ disorders, and in surgical planning of dental, oral and maxillofacial surgical procedures.

# Chapter 5: Kinematics of the jaw following total temporomandibular joint replacement surgery

This chapter is presented as the author-accepted manuscript of a peer-reviewed article published in the *Journal of Biomechanics* (2023, 159, 111741).

## 5.1 SIGNIFICANCE

This study investigated the effect of total temporomandibular joint replacement surgery on jaw and temporomandibular joint kinematics. The functional activities of maximum border movements and habitual chewing were investigated to determine the maximum mobility limits and the routine mobility of the joint respectively. This study is the first to report chewing kinematics following total TMJ replacement surgery, highlighting the physiologically relevant post-operative functionality compared to border movements alone.

## 5.2 ABSTRACT

Total TMJ replacement surgery aims to improve mandibular function, reduce pain and improve quality of life in patients suffering from end-stage TMJ disorders. Traditional post-operative jaw evaluation is carried out using maximum interincisal opening distance measurement; however, this can correlate poorly to joint function. The present study aimed to evaluate 3D jaw motion during border movements and chewing in unilateral total TMJ replacement patients and healthy controls. Motion analysis experiments were performed on six total TMJ replacement patients and ten age-matched healthy controls. Subject-specific motion tracking plates worn by each participant were registered to CT scans of each participant's skull and mandible to enable anatomical mandibular kinematics measurement using an optoelectronic system. Participants performed 15 repetitions of maximal opening, protrusion, lateral excursions, and chewing cycles. Total TMJ replacement patients had significantly smaller incisal displacements at maximum mouth opening relative to the controls (median difference: 7.1 mm, p=0.002) and a decrease in anterior translation of the prosthetic condyle (median difference: 10.5 mm, p=0.002). When TMJ replacement subjects chewed using their contralateral molars, there was a significant increase in inferior condylar translation of the non-working condyle (median difference: 9.7 mm, p = 0.016). This study found that unilateral total

TMJ replacement surgery was associated with mouth opening capacity within the range of healthy individuals, but reduced anterior movement of the prosthetic condyle and restricted protrusion and lateral excursions. The results provide future direction for prosthetic TMJ design to enhance postsurgical implant functionality and improve long-term clinical outcomes for prosthesis recipients.

## 5.3 INTRODUCTION

The TMJ is a coupled synovial joint connecting the mandible with the temporal bone of the skull, and is essential for speech, chewing, and swallowing. Osteoarthritis of the TMJ affects between 8% and 16% of the population (Kalladka et al. 2014) and can result in muscle and joint pain, abnormal TMJ clicking and restriction of mouth opening (Manfredini et al. 2011), which can result in poor diet (Kawashima Bori et al. 2020), and reduced general health status and quality of life (Miura et al. 1997, 2000). Total TMJ replacement surgery is the established treatment for end-stage TMJ disorders such as osteoarthritis, tumor resection and trauma, and involves resection of the pathological joint and implantation of a prosthetic condyle and fossa (Lobo Leandro et al. 2013). While TMJ replacement surgery has been shown to reduce pain and improve quality of life in end-stage TMJ disorder patients, post-operative evaluation of jaw function remains almost exclusively limited to measures of MIO distance (Johnson et al. 2017; Ackland et al. 2018; Zou et al. 2018).

Past studies have reported MIO distance, defined as the linear distance between mandibular and maxillary central incisors in the maximum mouth open position, to be between 46.6 mm and 51.3 mm in the healthy population (Naeije 2002; Voiner et al. 2011), and between 27.8 mm and 39.0 mm for unilateral total TMJ replacement patients (Voiner et al. 2011; Wojczynska et al. 2016). While limited MIO capacity (<35 mm) is associated with poor diet, increased incidence of depression and reduced quality of life (Scott et al. 2008; Johnson et al. 2015), the correlation between this linear measure and TMJ function remains poorly understood (Dijkstra et al. 1995; Naeije 2002). This has led to recommendations against use of MIO distance as a diagnostic indicator of TMJ function (Travers et al. 2000). Reproducible 3D measurement of jaw motion has been obtained using axiography, ultrasonic tracking, optoelectronic methods and 4D CT (Woodford et al. 2020); however, to date, these approaches have been limited to measurement of mandibular border movements, and 3D jaw motion analysis has not been performed for functional movements such as chewing.

Optoelectronic measurement of mouth opening movements in unilateral total TMJ replacement patients shows an asymmetrical jaw opening trajectory resulting from limited

translation of the ipsilateral TMJ, combined with hypermobility of the contralateral TMJ (Leiggener et al. 2012; Wojczynska et al. 2016; Wojczyńska et al. 2021). Wojczyńska et al. (2016) demonstrated that unilateral and bilateral total TMJ replacement surgery results in significantly shorter condylar excursions for prosthetic joints than for native joints during functional movements (Wojczynska et al. 2016). However, there is limited data available describing 3D TMJ motion in total TMJ replacement patients for functional movements, such as mouth opening, protrusion and lateral excursions, and functional activities such as chewing have not been examined to date. As a result, the ability for total TMJ replacement surgery to restore dynamic jaw function remains poorly understood.

The aim of this study was to employ a patient-specific motion tracking approach to evaluate 3D mandibular kinematics during mandibular border movements and chewing in unilateral total TMJ replacement patients and healthy age-matched controls. We hypothesized that there are significant differences in mandibular kinematics between groups, including reduced MIO capacity of unilateral total TMJ replacement patients, and lower mobility of prosthetic condyles compared to native condyles. This study presents the first evaluation of 3D jaw motion during activities of daily living in unilateral total TMJ replacement patients.

## 5.4 MATERIALS AND METHODS

### 5.4.1 Participant recruitment and imaging

Six female unilateral total TMJ replacement patients (mean age: 55.5 ± 5.9 yrs) and 10 female healthy control subjects were recruited for testing (mean age: 46.8 ± 4.9 yrs). This was a sample size of convenience, which has previously been used to detect significant differences in condylar movements between participant groups with a study power of p=0.97 (Wojczynska et al. 2016). Total TMJ replacement patients received the ArthroJaw TMJ replacement (Maxoniq, Melbourne), and were tested between 12- and 15-months post-surgery (Table 5.1). All participants had functional dentition at the time of testing, and were excluded if they had existing health conditions, experienced dental pain, were pregnant or breastfeeding, or had a history of orthodontic treatment. Control subjects with a history of mandibular or TMJ disorders or pain were excluded from the study. Ethical approval was obtained from the institutional Human Ethics Advisory Group (HREC 1853328.1) (Appendix E), and all participants provided written informed consent.

A CBCT scan with an isotropic voxel size of 0.4 mm was taken of each participant's mandible, maxilla and both TMJs. Imaging was performed with the participant lying on their back with their mandible in the maximum occlusion position. Images were digitally segmented

using threshold-based segmentation (Mimics, Materialise, Belgium) and 3D models of each participants mandible and skull, including dental anatomy, were reconstructed using commercial software (3-matic 13.0, Materialise, Belgium).

Table 5.1: Participant details including age, joint replacement side, post operative measurement time and mandibular size.

| Subject group | Age (years) | Joint replacement side | Measurement time post op (years) |
|---|---|---|---|
| Control | 55.7 | | |
| | 48.5 | | |
| | 44.5 | | |
| | 42.9 | | |
| | 55.5 | | |
| | 42.2 | | |
| | 45.0 | | |
| | 44.1 | | |
| | 45.3 | | |
| | 43.6 | | |
| TMJR | 59.1 | Right | 1.1 |
| | 49.6 | Right | 1.0 |
| | 55.7 | Right | 1.1 |
| | 64.9 | Left | 1.3 |
| | 51.4 | Right | 1.0 |
| | 48.6 | Right | 1.1 |

### 5.4.2 Motion analysis experiments

Both optoelectronic and electromagnetic tracking can accurately measure jaw and TMJ kinematics as found in Chapter 3. Electromagnetic tracking was used in the pilot study of Chapter 4, which was conducted in Zürich, Switzerland. However, the dental motion decoder (DMD) device employed in the pilot study was unavailable in Australia at the time of these experiments (2021 & 2022), therefore a custom optoelectronic tracking system was developed.

Pairs of lightweight subject-specific motion tracking plates that attach to each participant's mandibular and maxillary dental arches were developed to rigidly support triads of retro-reflective markers for dynamic optical motion analysis of the mandible(Röhrle et al. 2009). The jaw motion measurement precision of the tracking plates was 0.13 mm (see Appendix C). The plates were manufactured using dental stone casts after taking impressions of the mandibular and maxillary dental arches (Fig. 5.1a). They comprised self-curing polymethylmethacrylate lingual and palatal base plates to which stainless-steel wire clasps were attached for retention to the second premolars and molars. The wire clasps on each plate were positioned posteriorly to allow complete occlusion of the teeth and closure of the lips without obstruction. The dental clasps also provided stable mounting points for laser welded wire

extending extraorally to support the retroreflective markers (Fig. 5.1b). Plates were mounted onto dental stone casts of each participant and digitised using a handheld laser scanner with an accuracy of 0.05 mm (Artec Spider, Artec 3D, Luxembourg). A 3D stereolithography surface model was generated for each motion tracking plate using 3-matic software in order to register the retroreflective marker positions to the occlusal anatomy.

Each participant was seated with custom motion tracking plates fitted to their maxillary and mandibular dental arches (Fig. 5.1b). Participants were instructed to perform in random order, five cycles of maximum mouth opening, maximum protrusion, and maximum lateral excursions towards the left and right side. Each participant then supported a soft silicone rubber sample of dimensions 20 mm × 20 mm × 6 mm between their molars, which was derived from a visco-hyperelastic material with material properties defined previously (Woodford et al. 2021). Participants then chewed on the sample for several minutes or until they felt comfortable to proceed with testing. The rubber sample was centred and aligned in the buccal-lingual and mesial-distal directions of each participant's mandibular first and second molars. Participants were then asked to perform 10 continuous chewing cycles at their preferred speed and bite force. This process was repeated twice on each side of the mouth in a randomised order, with rest breaks given between each chewing cycle. During tasks, the trajectories of the six retroreflective markers were simultaneously recorded using a 4-camera video motion analysis system (Vero, Vicon, Oxfordmetrics, UK) sampling at a frequency of 100 Hz. All motion data were filtered using a low-pass filter with a cut-off frequency of 10 Hz.

### 5.4.3 Kinematics calculations

To quantify the position and orientation of the jaw with respect to the skull during testing, 3D mandible and skull models of each participant were registered to the motion analysis data. To achieve this, laser scans of each participant's motion tracking plates and dental impressions were registered to the dental geometry of the 3D model created from the CT scans using a global registration procedure. A marker coordinate system was defined for each marker triad from the motion tracking data (Fig. 5.1c), and rigid-body transformations were used to map the 3D models to the marker triad motion analysis data. All mandibular motion data were then expressed in an anatomical coordinate system. Specifically, the occlusal plane was defined by the maxillary incisal edges and the tips of the posterior maxillary molars, the sagittal plane defined perpendicular to the occlusal plane passing through the maxillary interincisal point and the midpoint between the left and right zygomaticofrontal sutures, and the frontal plane perpendicular to the occlusal and sagittal planes (Fig. 5.1d). The lateral and medial condylar

poles were identified on each side of the mandible and used to calculate the mid-point of the main condylar axis, which will be subsequently used as the right and left condylar reference points. The mandibular angle was defined as the angle between the lines connecting the midpoint between the left and right condylar points and incisal point for the maximum occlusal position and the measured frame.

Individual chewing cycles were identified by calculating the linear distance between the mandibular incisor positions for each frame and at maximum occlusion. The start and turning points of each cycle were defined by the frame with the minimum and maximum inferior distance between the mandibular incisors and their occlusal position, respectively. All chewing cycles were expressed relative to the right side of the jaw for comparison purposes (Throckmorton et al. 2003). Each chewing movement was normalised to 0-100% of the chewing cycle and incisal and condylar displacements at the start point and turning point were calculated. 3D coordinates of the incisors and condylar points were averaged across cycles to derive one normative chewing cycle trajectory for each participant.

### 5.4.4 Data analysis

Incisal and condylar displacements and mandibular angles were collated and statistically analysed for each movement. Data normality was assessed using Shapiro-Wilk testing. As the data followed a non-normal distribution, median differences were calculated between unilateral total TMJ replacement patients and control subjects using Mann-Whitney U-tests. Ninety-five percent confidence intervals and standard deviation were used as a measure of the data dispersion. A significance level of 5% was set for all comparisons ($p < 0.05$).

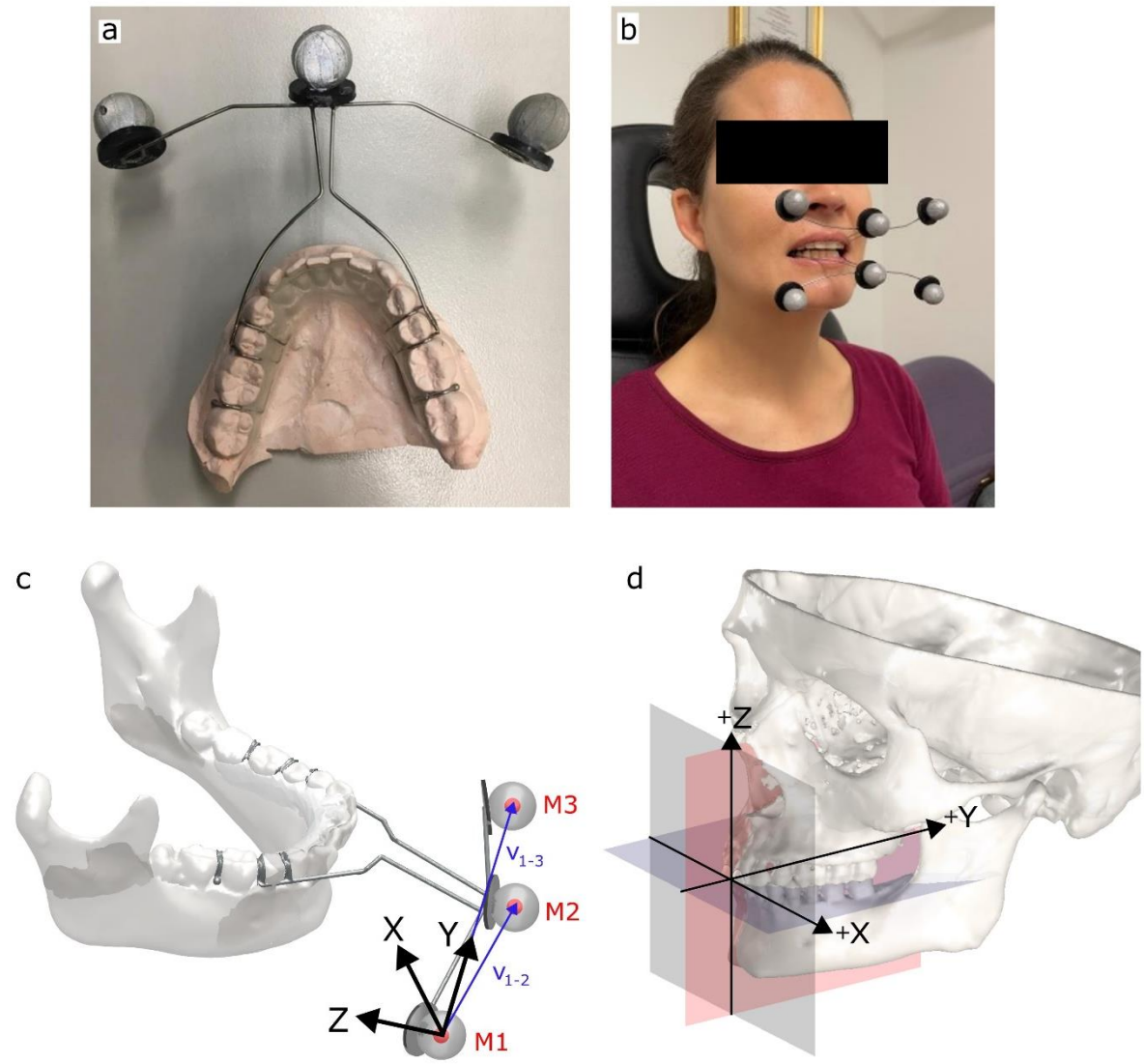



Figure 5.1: Design of the custom-made motion tracking plate fixed to its dental stone cast. Visible are three retroreflective markers (top of image), clear lingual base plate, metal clasps around the second premolars and molars and wire extending extraorally connecting the clasps to the retroreflective markers (a). Participant with maxillary and mandibular tracking plates in place (b). Marker coordinate system with the origin aligned with the centre of marker 1. Positive Y is aligned with the vector from markers 1 to 3. Positive X is perpendicular to the vectors from markers 1 to 2 and 1 to 3. Positive Z is perpendicular to the X and Y directions (c). Anatomical coordinate system with the occlusal (blue), sagittal (red), and frontal (grey) planes displayed. Positive X, Y and Z directions correspond to the left, posterior and superior directions respectively (d).

## 5.5 RESULTS

### 5.5.1 Maximum mouth opening

Unilateral total TMJ replacement patients had significantly smaller inferior incisal displacements at maximum mouth opening relative to the controls (median difference: 7.1 mm, 95% CI: [5.2 to 8.4], p = 0.002). There was a significant decrease in anterior translation of the prosthetic condyle during maximum mouth opening relative to controls (median difference: 10.5 mm, 95% CI: [8.1 to 11.6], p = 0.002), which led to an asymmetrical interincisal opening trajectory in unilateral total TMJ replacement patients (Fig. 5.2). A significant increase in lateral displacement of the incisors at maximum mouth opening was observed in the unilateral total TMJ replacement patients relative to control subjects (median difference: 3.9 mm, 95% CI: [3.4 to 4.7], p = 0.002) (Table 5.2).

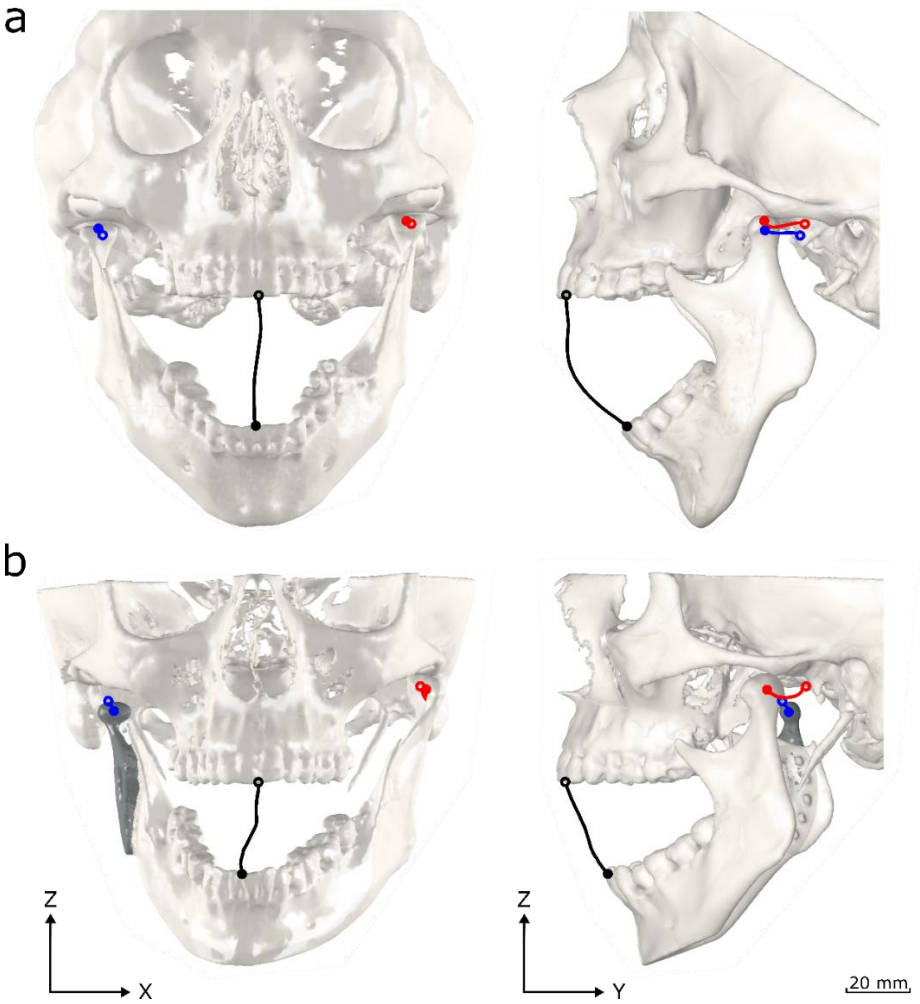



Figure 5.2: Maximum mouth opening trajectory, viewed from the frontal and sagittal planes, for a representative control subject (a) and unilateral total TMJ replacement patient (b). Open circles represent landmarks at the maximum occlusion position, while closed circles represent landmarks at the maximum mouth open position. Black, red, and blue lines indicate incisal, left condyle and right condyle trajectories, respectively.

### 5.5.2 Maximum laterotrusion

Lateral mandibular excursions were primarily achieved in healthy control subjects by a rotation of the mandible in the transverse plane (Fig. 5.3). A significant decrease in lateral movements of the incisors was observed in unilateral total TMJ replacement patients during lateral excursions relative to controls, both for incisal translation towards the contralateral side (median difference: 8.7 mm, 95% CI: [8.2 to 9.3], p = 0.002), and towards the ipsilateral side (median difference: 3.6 mm, 95% CI: [2.9 to 4.3], p = 0.002). Compared to controls, unilateral total TMJ replacement patients also exhibited significant decreases in the anterior translations of the non-working condyles at maximum lateral excursion, both for the ipsilateral (median difference: 9.7 mm, 95% CI: [8.4 to 11.3], p = 0.002) and the contralateral condyles (median difference: 2.9 mm, 95% CI: [1.8 to 5.0], p = 0.008) (Table 5.2).

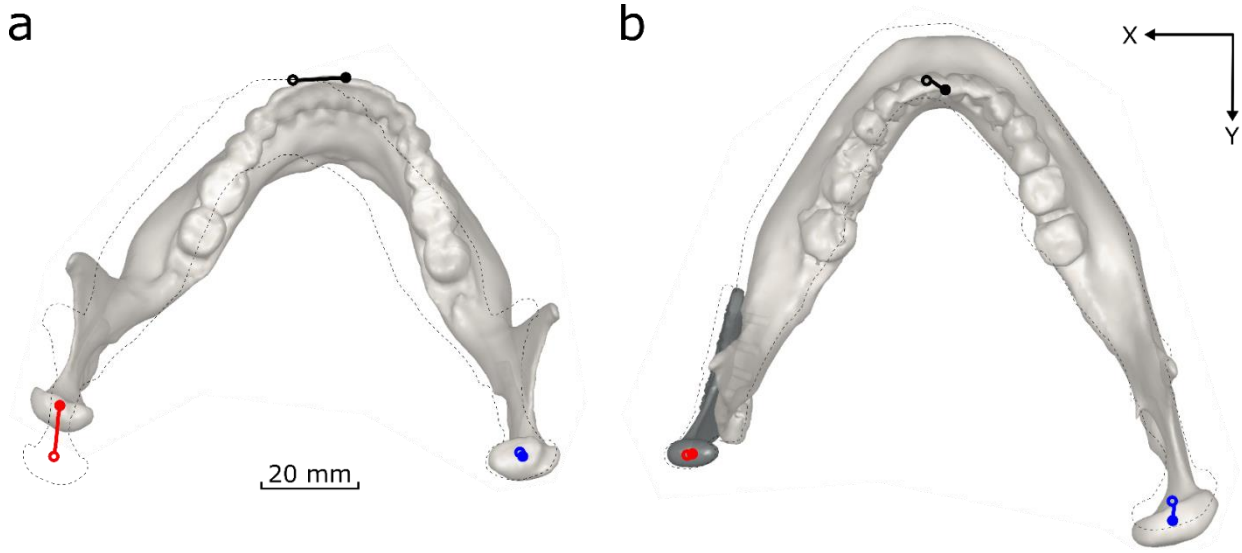



Figure 5.3: Maximum lateral excursion to the right projected onto the transverse plane for a representative control subject (a), and unilateral total TMJ replacement patient (b). Dashed lines represent the mandible position at the maximum occlusal position, while the rendered mandible represents the mandible position at the maximum lateral excursion position. Open circles represent landmarks at the mouth closed position, while closed circles represent landmarks at the maximum lateral position. Black, red, and blue lines indicate incisal, left condyle and right condyle trajectories, respectively.

### 5.5.3 Maximum protrusion

Significantly reduced anterior translations of the incisors at maximum protrusion was observed in unilateral total TMJ replacement patients relative to control subjects (median difference: 4.0 mm, 95% CI: [3.3 to 5.0], p = 0.002), as well as a significant decrease in anterior translations of both the ipsilateral (median difference: 9.0 mm, 95% CI: [7.6 to 10.7], p = 0.002) and contralateral condyles in these patients (median difference: 2.8 mm, 95% CI: [1.2 to 4.9], p = 0.003) (Table 5.2).

Table 5.2: Kinematics data at maximum mouth opening, maximum lateral excursion, and maximum protrusion positions in unilateral total TMJ replacement subjects and healthy controls. Displacements were measured as the position of each landmark with respect to its position with the mandible in the maximum occlusion position and reported as mean (SD). Measurements of lateral incisal deflection for unilateral total TMJ replacement patients are expressed as ± to represent deflection to the ipsilateral side, regardless of joint replacement side. Statistical comparisons in kinematics were made between unilateral total TMJ replacement patients and healthy controls using a Mann-Whitney U-test. Positive X, Y and Z represent lateral (left), posterior and superior directions, respectively. Level of significance was defined by * $p < 0.05$, ** $p < 0.01$, *** $p < 0.001$.

| **Maximum mouth opening** | | **Incisor displacement (mm)** | | | | **Condyle displacement (mm)** | | | | **Mandibular angle (degrees)** | | |
|---|---|---|---|---|---|---|---|---|---|---|---|---|
| **Subject** | **Condyle** | **X** | **Y** | **Z** | **Linear distance** | **X** | **Y** | **Z** | **Linear distance** | **Sagittal (X=0)** | **Coronal (Y=0)** | **Transverse (Z=0)** |
| Control (n=10) | Both | -0.1 (0.3) | 12.6 (1.1) | -41.8 (1.2) | 43.9 (1.0) | -3.0 (0.9) | -13.8 (0.7) | -5.0 (2.3) | 16.1 (0.3) | 30.6 (5.7) | 2.0 (1.6) | 1.9 (1.6) |
| TMJR (n=6) | Contralateral | ±4.5 (1.6)*** | 9.1 (1.9)*** | -34.9 (1.4)*** | 36.6 (1.4)*** | 0.3 (0.3)*** | -11.9 (2.2)* | -7.7 (1.4) | 15.0 (1.9)* | 24.1 (3.2)* | 7.2 (4.7)* | 4.4 (3.1) |
| | Ipsilateral | | | | | 0.3 (0.3)*** | -3.8 (1.7)*** | -6.5 (0.7) | 8.2 (1.0)*** | | | |

| **Maximum lateral excursion** | | **Incisor displacement (mm)** | | | | **Condyle displacement (mm)** | | | | **Mandibular angle (degrees)** | | |
|---|---|---|---|---|---|---|---|---|---|---|---|---|
| **Subject** | **Condyle** | **X** | **Y** | **Z** | **Linear distance** | **X** | **Y** | **Z** | **Linear distance** | **Sagittal** | **Coronal** | **Transverse** |
| Control | Non-working | 11.7 (0.5) | -1.5 (0.6) | -7.7 (1.3) | 14.6 (1.0) | -1.0 (0.5) | -11.4 (1.4) | -2.5 (0.7) | 12.5 (1.4) | 4.0 (3.2) | 15.9 (5.7) | 6.9 (1.1) |
| | Working | | | | | -1.3 (0.7) | 0.9 (0.9) | 0.0 (0.6) | 4.3 (0.3) | | | |
| TMJR | Ipsilateral Non-working | 3.0 (0.4)*** | 0.6 (0.7)*** | -6.8 (2.0) | 7.9 (1.4)*** | 0.3 (0.4)*** | -1.6 (0.6)*** | -6.6 (2.3)** | 7.5 (1.9)** | 2.6 (1.9) | 5.8 (4.8)* | 1.9 (0.9)*** |
| | Contralateral Working | | | | | 0.2 (0.5)*** | 1.8 (0.9) | -5.9 (2.3)*** | 7.2 (1.6)*** | | | |
| | Contralateral Non-working | 8.4 (0.2)*** | -4.1 (1.2)*** | -5.8 (0.9)* | 11.4 (1.5)* | -1.8 (0.7)* | -8.4 (1.3)** | -6.9 (2.0)*** | 11.3 (2.2)* | 2.0 (1.1) | 14.5 (5.7) | 5.1 (1.8) |
| | Ipsilateral Working | | | | | -1.9 (0.7)* | -0.3 (0.1) | -4.9 (2.0)*** | 5.8 (1.8)** | | | |

| **Maximum protrusion** | | **Incisor displacement (mm)** | | | | **Condyle displacement (mm)** | | | | **Mandibular angle (degrees)** | | |
|---|---|---|---|---|---|---|---|---|---|---|---|---|
| **Subject** | **Condyle** | **X** | **Y** | **Z** | **Linear distance** | **X** | **Y** | **Z** | **Linear distance** | **Sagittal** | **Coronal** | **Transverse** |
| Control | Both | -0.1 (0.4) | -9.0 (0.7) | -5.1 (2.4) | 11.2 (1.9) | -0.4 (0.4) | -11.0 (1.7) | -1.0 (0.5) | 11.4 (1.6) | 2.1 (1.4) | 2.6 (1.6) | 1.0 (0.6) |
| TMJR | Contralateral | ±4.2 (0.8)*** | -2.7 (2.6)*** | -7.5 (2.2) | 11.3 (1.9) | 0.2 (0.3)* | -8.0 (0.9)** | -5.7 (3.1)*** | 10.6 (1.9) | 2.0 (2.2) | 9.8 (4.3)*** | 3.5 (1.3)** |
| | Ipsilateral | | | | | 0.1 (0.3)* | -1.8 (0.4)*** | -4.1 (2.8)** | 5.6 (1.9)*** | | | |

### 5.5.4 Chewing

Unilateral total TMJ replacement patients exhibited significantly increased inferior translation of the condyles at the start of the chewing cycle relative to controls when chewing using the ipsilateral molars, which was observed for both the ipsilateral working condyle (median difference: 11.9 mm, 95% CI: [4.1 to 21.6], p = 0.011) and the contralateral non-working condyle (median difference: 10.4 mm, 95% CI: [1.4 to 18.9], p = 0.046) (Table 5.3). When the total unilateral TMJ replacement subjects chewed using their contralateral molars, there was a significant increase in inferior condylar translation of the non-working condyle (median difference: 9.7 mm, 95% CI: [0.7 to 17.6], p = 0.016). This was associated with a significantly larger mandibular angle in the sagittal plane at the start point of the chewing cycle when chewing on the contralateral molars than controls (median difference: 3.8°, 95% CI: [0.0 to 7.0], p = 0.039) (Table 5.3).

No statistically significant differences were observed in the normalised chewing trajectories ($p>0.05$); however, several non-significant trends provide valuable insight. Unilateral total TMJ replacement patients, when chewing on their ipsilateral molars, exhibited wider lateral chewing motions than control subjects (mean lateral range of motions 1.2 ± 1.2 mm and 0.3 ± 0.4 mm for TMJ replacement patients and controls, respectively). This was achieved through large anterior-posterior translations of the contralateral non-working condyle (Fig. 5.4). In contrast, when chewing on the contralateral molars, unilateral total TMJ replacement patients had higher mean inferior translations of the incisors (5.6 ± 1.3 mm) than control subjects (4.2 ± 1.1 mm) (Fig. 5.5).

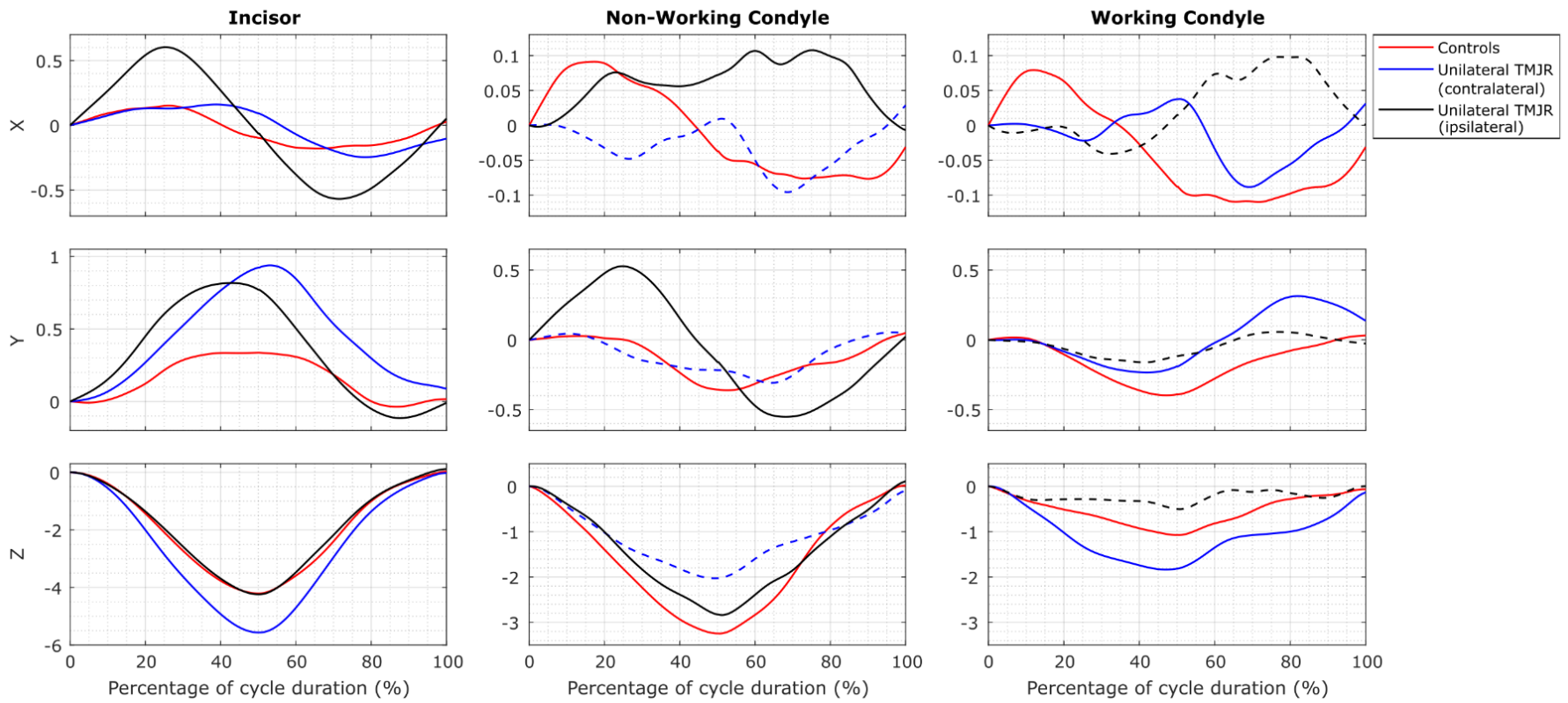



Figure 5.4: Mean movements of the mandibular incisor point, non-working condyle and working condyle during one normalised cycle of molar chewing. Movements are shown for control subjects chewing on either side of the mouth (red), unilateral total TMJ replacement patients chewing on their contralateral molars (blue) and unilateral total TMJ replacement patients chewing on their ipsilateral molars (black). The start and end point of each cycle was from a partially closed jaw position, compressing the rubber sample between the molars. Dashed lines represent movement of a prosthetic condyle. Positive X, Y and Z represent lateral (left), posterior and superior directions, respectively.

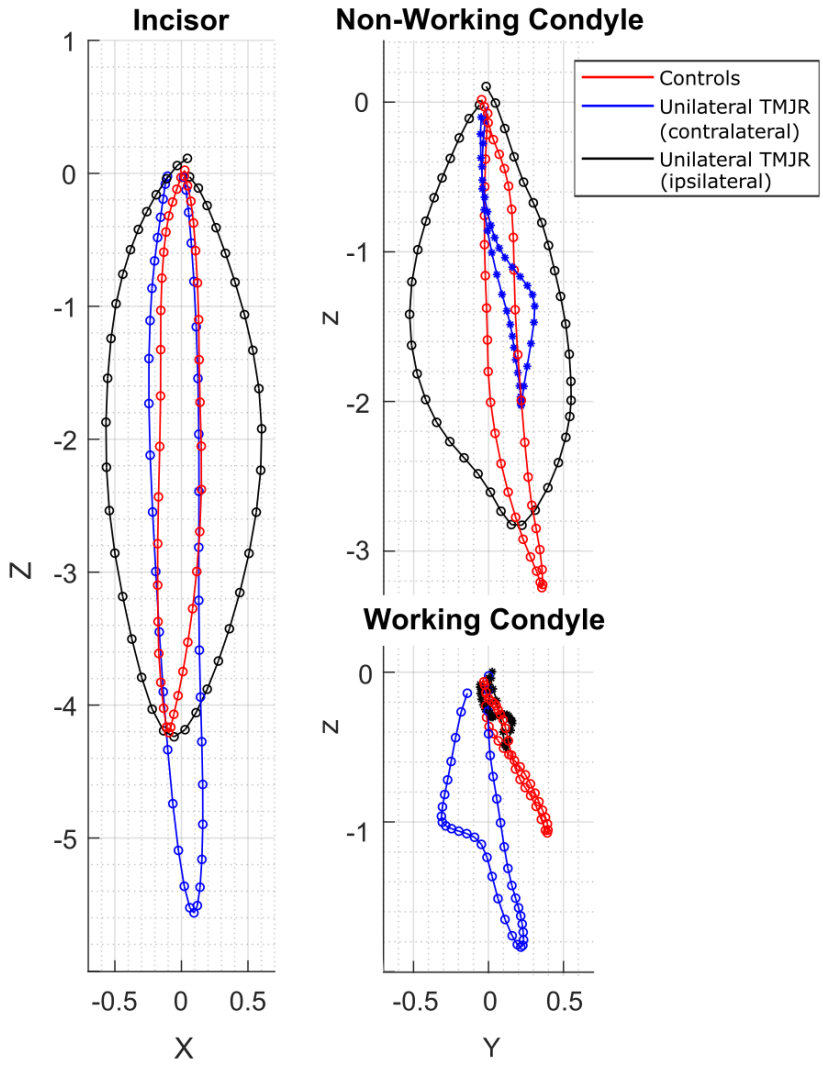



Figure 5.5: Mean movements of the mandibular incisor point, non-working condyle and working condyle during one normalised cycle of molar chewing. Movements are shown for control subjects chewing on either side of the mouth (red), unilateral total TMJ replacement patients chewing on their contralateral molars (blue) and unilateral total TMJ replacement patients chewing on their ipsilateral molars (black). Movement of the mandibular incisors and natural condyles are represented by an open circle, while movements of the prosthetic condyles are represented by an asterisk. Positive X, Y and Z represent lateral (left), posterior and superior directions, respectively.

Table 5.3: Kinematics data at the start point and turning point of molar chewing cycles. Displacements were measured as the position of each landmark with respect to its position with the mandible at maximum occlusion and reported as mean (SD). Statistical comparisons in kinematics were made between unilateral total TMJ replacement patients and healthy controls using a Mann-Whitney U-test. Positive X, Y and Z represent lateral (left), posterior and superior directions, respectively. Level of significance was defined by * $p < 0.05$, ** $p < 0.01$, *** $p < 0.001$.

| **Start point** | | **Incisor displacement (mm)** | | | | **Condylar displacement (mm)** | | | | | | | | **Mandibular angle (degrees)** | | |
|---|---|---|---|---|---|---|---|---|---|---|---|---|---|---|---|---|
| | | | | | | Non-working side | | | | Working side | | | | | | |
| **Subject** | **Chewing side** | X | Y | Z | Linear distance | X | Y | Z | Linear distance | X | Y | Z | Linear distance | Sagittal (X=0) | Coronal (Y=0) | Transverse (Z=0) |
| Control (n=10) | | 1.1 (1.4) | -6.2 (5.1) | -3.4 (2.8) | 8.9 (3.3) | 0.0 (3.8) | -2.8 (6.2) | -3.3 (6.1) | 9.3 (4.5) | -0.1 (4.2) | -0.1 (3.7) | -5.8 (6.5) | 9.8 (2.9) | 3.6 (1.0) | 6.1 (3.9) | 2.2 (2.1) |
| TMJR (n=6) | Ipsilateral | -1.7 (1.6)** | -4.1 (3.5) | -5.2 (4.4) | 7.5 (4.9) | 1.0 (1.9) | 0.7 (5.2) | -13.4 (8.7)* | 14.5 (8.8) | 1.0 (1.7) | 2.1 (2.5) | -13.4 (9.4)* | 13.9 (9.5)* | 7.5 (4.2) | 9.2 (7.2) | 2.3 (1.8) |
| | Contralateral | -0.2 (1.6) | -5.2 (3.3) | -4.3 (3.9) | 8.1 (2.3) | 1.3 (2.1) | 0.6 (3.8) | -9.6 (7.6)* | 11.8 (6.8)* | 1.2 (2.5) | 1.2 (4.4) | -15.7 (6.1) | 16.7 (5.7) | 7.2 (3.4)* | 8.4 (4.4) | 1.8 (1.4) |

| **Turning point** | | **Incisor displacement (mm)** | | | | **Condylar displacement (mm)** | | | | | | | | **Mandibular angle (degrees)** | | |
|---|---|---|---|---|---|---|---|---|---|---|---|---|---|---|---|---|
| | | | | | | Non-working side | | | | Working side | | | | | | |
| **Subject** | **Chewing side** | X | Y | Z | Linear distance | X | Y | Z | Linear distance | X | Y | Z | Linear distance | Sagittal (X=0) | Coronal (Y=0) | Transverse (Z=0) |
| Control (n=10) | | 1.4 (1.4) | -6.0 (5.4) | -7.3 (3.6) | 11.6 (2.5) | 0.0 (4.2) | -3.3 (6.4) | -6.3 (5.9) | 11.1 (4.6) | -0.1 (4.6) | -0.6 (3.6) | -6.8 (6.1) | 10.3 (3.2) | 2.9 (1.5) | 6.6 (4.0) | 2.6 (2.3) |
| TMJR (n=6) | Ipsilateral | -0.8 (1.4)* | -3.7 (3.7) | -10.7 (5.7) | 12.4 (4.8) | 1.2 (2.1) | 1.1 (6.2) | -19.4 (6.3)** | 20.5 (5.8)* | 1.1 (2.0) | 2.3 (2.3) | -16.9 (6.7)* | 17.3 (6.7)* | 4.8 (3.3) | 10.7 (7.0) | 2.6 (1.8) |
| | Contralateral | -0.7 (1.5) | -4.5 (3.8) | -9.9 (5.4) | 12.1 (4.3) | 1.0 (2.2) | 0.6(4.1) | -12.7 (7.1) | 14.0 (6.2) | 1.0 (2.6) | 1.4 (5.4) | -18.1 (6.6)* | 19.1 (6.4)* | 5.0 (4.2) | 9.0 (8.8) | 1.8 (1.3) |

## 5.6 DISCUSSION

The aim of the present study was to evaluate 3D kinematics of the jaw following unilateral total TMJ replacement surgery and compare the findings to those of healthy controls. Substantial differences were observed in incisal and condylar movements and mandibular angles between control subjects and unilateral total TMJ replacement patients during mandibular border movements and chewing. This included decreased mouth opening capacity and an asymmetrical incisal opening trajectory resulting from the limited anterior translations of the ipsilateral condyle in unilateral total TMJ replacement patients. Unilateral total TMJ replacement surgery was associated with limited lateral excursion capacity towards the contralateral side, although this did not significantly alter incisal trajectories during cyclic chewing. These findings were observed in joints reconstructed with the patient-specific ArthroJaw TMJ replacement system, a device that has Australian TGA approval and has been implanted in over 270 patients to date (Brierly et al. 2022). The results of this study illustrate motion following implantation of a semi-constrained ball-and-socket-type prosthetic articulation of the TMJ, and therefore the findings may be generalised to implants with similar joint geometry, including the Zimmer-Biomet (Jacksonville, Florida), TMJ concepts (Ventura, California) and Nexus TMJ systems (Salt Lake City, Utah).

This study found that prosthetic condyles have limited capacity to translate anteriorly within the fossa component after total TMJ replacement surgery. During maximum mouth opening the anterior translation of the contralateral condyle was three times that of the ipsilateral condyle. This imbalance resulted in asymmetrical mouth opening trajectories with lateral incisal deviations consistently larger than the 2 mm threshold normally accepted, a finding consistent with previous studies (Leiggener et al. 2012; Wojczynska et al. 2016; Wojczyńska et al. 2021). This functional deficiency is primarily due to the hemispherical design of the fossa prosthesis component, which does not represent the native fossa anatomy and prevents anterior condylar movements (Celebi et al. 2011; Genovesi et al. 2022). Severing the lateral pterygoid muscle, which occurs during condylectomy, also contributes to less anterior condylar movement capacity (Voiner et al. 2011; Linsen et al. 2012); however, cadaver studies simulating masticatory muscle contractions using weighted cables attached at the centre of each insertion point have found that reattachment of the lateral pterygoid muscle results in only small improvements in mandibular movement when the remaining muscle forces are kept constant (Celebi et al. 2011). Other theories for this functional limitation are loss of muscle tone in the masseter and medial pterygoid muscles (Mercuri and Anspatch 2003) and excessive scar tissue

(Linsen et al. 2012). These factors may explain the lack of prosthetic condylar mobility observed in this study.

The consequence of unilateral total TMJ replacement surgery on the native contralateral joint is poorly understood despite this joint being commonly affected by pathology post-operatively (Perez et al. 2016; Kim et al. 2021). Past studies have found that wide interincisal opening is achieved in unilateral total TMJ replacement patients via an anterior hypermobility of the native contralateral condyle (Van Loon et al. 1999; Leiggener et al. 2012; Wojczynska et al. 2016). These condylar movements are believed to alter the loads acting on the contralateral condyle. This may lead to remodelling of the native contralateral condylar structures (Kim et al. 2021), and increased likelihood of patients with a history of contralateral TMJ surgery to require bilateral total TMJ replacement surgery (Franco et al. 1997; Perez et al. 2016). The present study did not observe significantly larger anterior movements in the native contralateral condyles of unilateral total TMJ replacement patients relative to those of healthy controls; however, native contralateral condyles in unilateral total TMJ replacement patients had significantly larger inferior translations than those of healthy controls for lateral, protrusion and chewing movements (Table 5.2). Large superior-inferior condylar translations during functional activities may be associated with loading and unloading of the joint which may contribute to degeneration of the native contralateral joint in unilateral total TMJ replacement patients; however, further research is required to demonstrate this.

Adults perform approximately 7,000 chewing cycles per day (Hamrick et al. 2011; Sánchez-Ayala et al. 2013), and thus, kinematics of physiologically relevant load-bearing tasks such as chewing play an important role in implant functional performance (Woodford et al. 2021). When chewing with the ipsilateral molars, unilateral total TMJ replacement patients have wide lateral excursions of the incisors, suggesting a higher dependency on grinding chewing strokes relative to controls (Takada et al. 1994). These wider lateral incisal excursions were caused by increased anterior-posterior movements of the native contralateral non-working condyle, whilst the prosthetic condyle remained relatively stationary. When chewing on either side of the mouth, both condyles of unilateral total TMJ replacement patients were positioned significantly further inferiorly than those of controls, leading to larger sagittal mandibular angles. This may be due to a weakness of the elevator muscles in total TMJ replacement patients (Linsen et al. 2020) and may ultimately lead to impaired chewing efficiency. However, this may not necessarily negatively impact clinical outcomes, since patients with the ArthroJaw TMJ replacement have reported high satisfaction and improved diet (Dimitroulis et al. 2018).

While limited literature exists on the 3D kinematics of unilateral total TMJ replacement patients during border movements, 3D kinematics for bilateral total TMJ replacement patients have not been well documented previously. We obtained pilot kinematics data on one bilateral total TMJ replacement patient (see Appendix C) and showed that both prosthetic condyles have limited mean anterior translations of 0.2 mm during maximum mouth opening, with inferior incisal displacement to 33.1 mm, consistent with clinical MIO measurements (Voiner et al. 2011; Gerbino et al. 2016; Wojczynska et al. 2016). Maximum incisal protrusion and lateral excursions were limited in the bilateral total TMJ replacement patient (2.3 mm and 0.7 mm, respectively). However, the condylar displacements and mandibular angle during chewing were similar to those of the healthy control subjects indicating that healthy chewing kinematics may be aided by symmetry in the mandibular morphology. While findings of this participant cannot be generalised to the population, these results suggest that bilateral total TMJ replacement surgery yields acceptable mouth opening capacity and is likely to restore chewing movements to a functional level.

There are limitations of this study that ought to be considered. First, this study had a constrained sample size and may have been under-powered in some measures; however, the sample was sufficient to detect significant differences in the incisal and condylar displacements and mandibular angles during the movements evaluated. Second, only women were included in this study. This inclusion criteria was chosen because females represent the majority (86.1%) of all total TMJ replacement patients (Granquist et al. 2020), which is thought to be related to behavioural, psychosocial, hormonal and constitutional differences (Roda et al. 2007). Nonetheless, further research is required to assess functional jaw movements in males to generalise the study findings more broadly. Third, subject-specific motion tracking plates were designed to rigidly attach to each participant's teeth via wire clasps. While an assessment of one subject showed the motion tracking plates closely reproduced kinematics of the underlying teeth (see Appendix C), there may have been instances where the plates moved or vibrated during chewing tasks, which would introduce motion tracking errors. Finally, only patient-specific implants were considered. Approximately 41% of total TMJ replacement procedures currently use patient-specific implants, with those numbers expected to grow (Zou et al. 2018). The results of this study indicate that while patient-specific implants show favourable results, post-surgical functionality remains limited.

This study found that unilateral total TMJ replacement surgery was associated with mouth opening capacity within the range of healthy individuals, although reduced anterior movement of prosthetic condyles and restricted protrusion and lateral excursions were observed

relative to controls. When chewing on ipsilateral molars, unilateral total TMJ replacement patients exhibit wide lateral incisal excursions and larger anterior-posterior translations of the native contralateral condyle to compensate for the lower mobility of the prosthetic condyle. The methods documented in this study may be useful for assessing outcomes of dental and maxillofacial treatments. These results have implications for the development of improved prosthetic TMJ implant design to achieve healthy functionality and improve long-term outcomes.

# Chapter 6: Muscle and joint mechanics during maximum-force biting following total temporomandibular joint replacement surgery

This chapter is presented as the author-accepted manuscript of a peer-reviewed article published in *Biomechanics and Modelling in Mechanobiology* (2023).

## 6.1 SIGNIFICANCE

This study uses computational modelling to investigate the maximum voluntary bite force, muscle forces and TMJ loading following TMJR surgery. This is the first study to use measured pathological bite forces in models of the TMJR masticatory system and therefore provides the first evaluation of subject specific TMJ loading for unilateral total TMJR patients. This study's findings suggest that postoperative contralateral joint damage may be due to underloading of the joint induced by postoperative muscular asymmetries. This insight may be used to tailor surgical and therapeutic treatment for enhanced long-term patient outcomes.

## 6.2 ABSTRACT

Total temporomandibular joint replacement (TMJR) surgery is the established treatment for severe temporomandibular joint disorders. While TMJR surgery is known to increase mouth opening capacity, reduce pain and improve quality of life, little is known about post-surgical jaw function during activities of daily living such as biting and chewing. The aim of this study was to use subject-specific 3D bite force measurements to evaluate the magnitude and direction of joint loading in unilateral total TMJR patients and compare them to healthy control subjects. An optoelectronic tracking system was used to measure jaw kinematics while biting a rubber sample for 5 unilateral total TMJR patients and 8 controls. Finite element simulations driven by the measured kinematics were employed to calculate the resultant bite force generated when compressing the rubber between teeth during biting tasks. Subject-specific musculoskeletal models were subsequently used to calculate muscle and TMJ loading. Unilateral total TMJR patients generated a bite force of 249.6 ± 24.4 N and 164.2 ± 62.3 N when biting on the contralateral and ipsilateral molars, respectively. In contrast, controls generated a bite force of 317.1 ± 206.6 N. Unilateral total TMJR patients biting on the contralateral molars had a

significantly higher lateral TMJ force direction (median difference: 63.6°, $p = 0.028$), and a significantly lower ratio of working TMJ force to bite force (median difference: 0.17, $p = 0.049$) than controls. Results of this study may guide future TMJ prosthesis design, and provide insight into the loading of dental structures, which may influence the design and evaluation of dental implants.

## 6.3 INTRODUCTION

The temporomandibular joint (TMJ) is a bilateral synovial joint connecting the mandible to the skull which comprises the mandibular condyle, glenoid fossa of the temporal bone, and the articular cartilage and disc. Its function, which is to facilitate biting, chewing, swallowing and speech, is considered essential for maintaining quality of life. Painful disorders of the TMJ are common, with 36% of the population showing clinical signs of a TMJ disorder, including TMJ muscle and joint pain and tenderness, and limitations in mandibular function (Progiante et al. 2015). Total temporomandibular joint replacement (TMJR) surgery is the accepted approach for TMJ disorders such as degenerative joint disease, ankylosis and internal disc derangement when the condition cannot be managed by conservative treatment. There are clinical studies demonstrating that TMJR surgery reduces pain, increases mouth opening capacity, reduces dietary restrictions and improves patient quality of life (Dimitroulis et al. 2018; Zou et al. 2018; Woodford et al. 2023); however, unilateral TMJR patients often experience post-surgical degradation of their native contralateral joint, with up to 40% of patients requiring bilateral TMJR surgery within two years (Franco et al. 1997). While thought to be broadly related to joint loading (Perez et al. 2016; Linsen et al. 2021b), there is currently no consensus on mechanical factors associated with contralateral joint disease post-TMJR.

Bite force and TMJ muscle and joint forces are important determinates of implant and joint functional performance following TMJR, however they remain poorly understood post-operatively. Bite force has been measured using uniaxial transducers (Röhrle et al. 2018), with maximum voluntary bite force measurements for total TMJR patients ranging from 177 N to 201 N (Linsen et al. 2021b; Speksnijder et al. 2022), substantially lower than that of healthy individuals. This functional decrease has been attributed to muscle atrophy and degeneration, lower occlusal contact area and psychological factors (Linsen et al. 2013). A limitation in these measurements is that data were recorded using a uniaxial transducer, which does not record lateral shear forces at the occlusal surface. Shear forces at the tooth surface may be substantial following unilateral TMJR due to the muscle force imbalance resulting from intraoperative severing of the lateral pterygoid muscle, or functional asymmetries such as reverse-sequence

chewing patterns (Lewin & Ramadori 1985. A study of dynamic bite force in healthy subjects using a novel kinematics-driven simulation of mastication showed that shear forces can be as large as 42 N and 63 N on the central incisors and second molars, respectively (Woodford et al. 2021). These shear forces generate high stresses around the supporting bone of dental restorations (Pellizzer et al. 2011) and can be detrimental to the long-term integrity of prosthetic devices and dental restorations, as well as TMJ loading (Forero et al. 2019). At present, however, 3D bite forces in TMJR patients has not been measured to date.

Resultant TMJ force is generated by contraction of the masticatory muscles, including the masseter and temporalis; however, no technology is available to quantify joint force in vivo. As a consequence, bite force is typically decomposed into both muscle and joint forces using computational modelling (Ackland et al. 2015, 2017, 2018; Abdi et al. 2020; Guo et al. 2022). In the native jaw, a subject-specific musculoskeletal model of the masticatory system was used to show that the maximum joint force is approximately 76% of the maximum voluntary bite force measured at the premolars (de Zee et al. 2007). This ratio is likely to be considerably more variable in TMJR patients, since the lateral pterygoid muscle is severed intraoperatively, and the masseter detached to accommodate the ramal component of the prosthesis (Linsen et al. 2020). Mathematical modelling of unilateral total TMJR subjects has demonstrated large prosthetic TMJ loading (van Loon et al. 1998), increased lateral joint loads (Ackland et al. 2017) and higher native contralateral joint stresses compared to healthy controls (Bekcioglu et al. 2017). However, these mathematical models employ bite and muscle forces derived from stomatognathically healthy control subjects, and these results are not applicable to the TMJR population.

The aim of this study was to use subject-specific 3D measurements of bite force to evaluate the magnitude and direction of joint reaction forces, and the ratio of TMJ force to bite force in unilateral total TMJR patients and healthy controls. We hypothesised that joint reaction forces would have a significantly higher lateral component in unilateral total TMJR patients than healthy controls, and that unilateral TMJR patients would have a significantly lower ratio of TMJ force to bite force than healthy controls. The data produced in this study could help guide the design and evaluation of TMJ prosthesis and may influence the prescription of physiotherapy following unilateral total TMJR surgery.

## 6.4 MATERIALS AND METHODS

### 6.4.1 Subject recruitment and imaging

Five unilateral total TMJR patients (mean age: 55.9 ± 6.4 yrs) and eight healthy control subjects (mean age: 46.0 ± 4.3 yrs) were recruited for testing. Total TMJR patients were fitted with the ArthroJaw TMJR system (Maxoniq, Melbourne); testing took place 12 to 15 months post-operatively (Table 6.1). Participants recruited were women who were aged forty years or over at the time of testing and had functional dentition. Participants were excluded if they experienced ongoing dental pain, were undergoing orthodontic treatment or were pregnant or breastfeeding. Control subjects with any prior occurrences of TMJ disorders were not included in the study. Ethics approval for this study was provided by the institutional Human Ethics Advisory Group (HREC 1853328.1) (Appendix E), and subjects provided written consent.

Each participant had a cone-beam computed tomography (CBCT) scan taken of their mandible, maxilla and bilateral TMJ's, with a voxel size of 0.42 mm and a resolution of 0.5 mm (Aquilion One, Canon Medical Systems, USA). Participants were instructed to lie in a supine position with the mandible in the maximum occlusion position for the duration of the scan. Threshold-based segmentation was used to segment the mandible and maxilla of each participant, and 3D models were reconstructed using commercial software (mimics 21.0 and 3-matic 13.0, Materialise, Belgium). For each participant, mandibular width was calculated as the distance between the left and right condylar points, and mandibular length as the distance between the intercondylar point and the mandibular central incisor point (Fig. 6.1b).

Table 6.1: Participant details, including age at time of data collection, joint replacement side, post operative measurement time and mandible size as defined in fig. 6.1b.

| | Age (years) | Joint replacement side | Measurement time post op (years) | Mandible size | |
|---|---|---|---|---|---|
| | | | | Mandibular length (mm) | Mandibular width (mm) |
| Control | 48.5 | | | 85.3 | 92.3 |
| | 44.5 | | | 83.4 | 99.5 |
| | 42.9 | | | 76.2 | 96.9 |
| | 55.5 | | | 89.3 | 103.0 |
| | 42.2 | | | 89.8 | 105.9 |
| | 45.0 | | | 87.0 | 94.9 |
| | 44.1 | | | 95.5 | 108.3 |
| | 45.3 | | | 84.5 | 96.1 |
| TMJR | 59.1 | Right | 1.1 | 78.6 | 106.0 |
| | 55.7 | Right | 1.1 | 76.6 | 98.2 |
| | 64.9 | Left | 1.3 | 82.4 | 100.7 |
| | 51.4 | Right | 1.0 | 84.6 | 99.1 |
| | 48.6 | Right | 1.1 | 85.6 | 98.4 |

### 6.4.2 Jaw motion experiments

Jaw motion experiments have been explained in detail in (Woodford et al. 2023). Briefly, pairs of custom lightweight motion tracking plates were constructed to rigidly connect a triad of spherical retroreflective markers to each participant's dental arches. Dental stone casts were manufactured from impressions taken of the mandibular and maxillary teeth, upon which the plates were constructed (Fig. 5.1a). The plates consist of a polymethylmethacrylate base plate fixed to the second premolars and molars with stainless-steel wire clasps. A laser-welded wire attached to the base plate extended extraorally and was used to support three retroreflective markers (Fig. 5.1b). The plates were designed to facilitate complete occlusion of the teeth and unobstructed closure of the lips. Each motion tracking plate was scanned using a handheld laser scanner and a 3D surface model of the retroreflective markers and dental anatomy produced.

Pairs of custom motion tracking plates were fitted to the dental arches of each participant (Fig. 5.1b). Following this, participants supported a 20 mm × 20 mm × 6 mm soft silicone rubber sample between their teeth and were instructed to bite and chew on the sample until they felt familiar with the testing procedure. Rubber samples were centered between either the left or right first molars and aligned parallel to the mesiodistal axis. Each sample was in contact with 2-3 teeth per side, depending on the subject dentition. A photograph was taken of the rubber sample and surrounding teeth to record the rubbers position in relation to the dental arch (iPhone 12, Apple, California, US). The participant was then instructed to maximally compress the rubber between the selected teeth for three seconds while the trajectories of the six

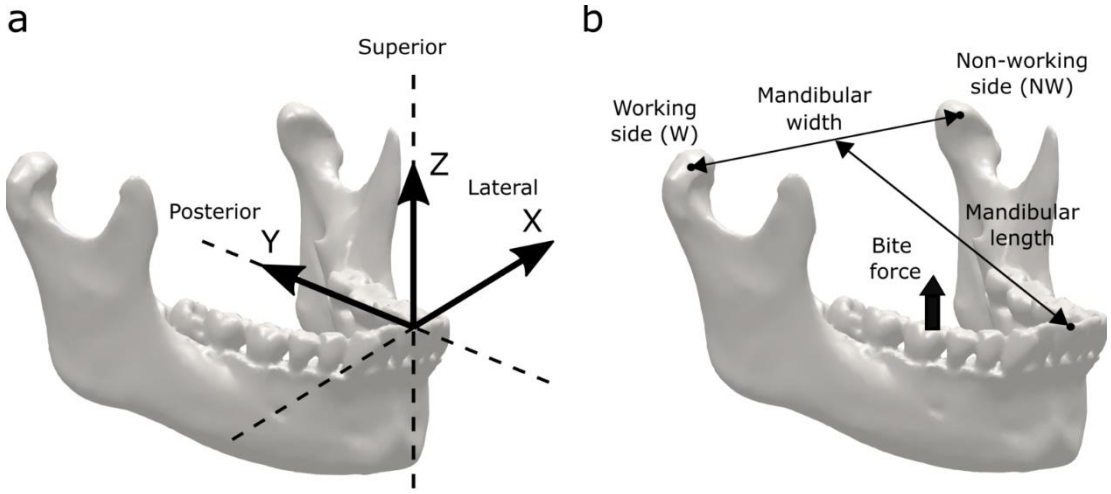



Figure 6.1: Anatomical coordinate system with X directed laterally (left), Y directed posteriorly and Z directed superiorly (a), and definitions of mandibular naming convention (b). The mandibular width is the distance between the right and left condylar points, the mandibular length is the distance between the intercondylar point and the mandibular central incisors. The working TMJ is defined as the TMJ on the same side as the bite, the non-working TMJ is defined as the TMJ on the opposite side to the bite.

retroreflective markers were captured using a 4-camera optoelectronic tracking system with a sampling frequency of 100 Hz and static resolution of 0.06 mm (Vero, Vicon, Oxfordmetrics, UK). All motion capture data were filtered using a low-pass filter with a cut-off frequency of 10 Hz. This motion tracking system has a precision of 0.13 mm (see Appendix D). This protocol was repeated twice on the left and right molars in random order with rest breaks offered between each movement.

To evaluate the position and orientation of the mandibular and maxillary dental arches, 3D models of the mandible and maxilla of each participant were aligned with the optoelectronic tracking data. To accomplish this, the 3D models of each participant's dental stone casts and motion tracking plates were mapped to the dental geometry from the CT scan with a global registration procedure. For each motion tracking frame, a coordinate system was created for each marker triad. Rigid body transformations were then applied to align the 3D models with the recorded motion of the marker triad. To allow comparison between participants the mandibular motion data was converted to an anatomical coordinate system, with origin at the maxillary interincisal point and aligned to the occlusal, sagittal and frontal planes, as has been done previously (Fig. 6.1a) (Woodford et al. 2023).

### 6.4.3 Bite force calculations

Finite element analysis was used to calculate bite force during the maximum compression biting task, following the authors previously published protocol (Woodford et al. 2021). The 3D model of each participant's dental arches were meshed using triangular shell elements with an average edge length of 0.25 mm and imported into a commercial finite element analysis package (Abaqus 2017, Dassault Systems, Paris, France). Rubber sample geometry was created in the finite element model and aligned with the molars to match the experimental sample placement (Fig. 6.2a). Following a mesh convergence analysis, its volume was meshed with hexahedral elements with edge lengths of 0.40 mm in the compressed region and 1.00 mm elsewhere (Fig. 6.2b) (Appendix D). The rubber elements were assigned visco-hyperelastic material properties computed through stress relaxation and compression testing (see Appendix D). Given the high stiffness of tooth enamel relative to rubber, the teeth were modelled as rigid bodies.

The recorded mandibular motion was used to drive finite element simulation of the mandibular and maxillary teeth compressing the rubber sample during maximum force biting (Fig. 6.2c). Kinematics were applied to the mandible at each timepoint by applying the resultant rotation and displacement, while the maxillary teeth were fixed in space. Tooth-rubber interaction was modelled using the penalty method. To avoid tangential sliding of the rubber surface over the teeth an infinite coefficient of friction was applied, and the penetration of the tooth surfaces into the rubber surfaces were minimised, this was representative of the experimental conditions. To improve computational efficiency while maintaining model accuracy, mass scaling was conservatively applied to the rubber model (see Appendix D). Bite forces were expressed as the reaction force on the mandibular teeth with respect to the anatomic coordinate system. This finite element model was validated, demonstrating an RMS error of 1.4 N for bite forces of 160 N (Woodford et al. 2021). Each bite was normalised to 0-100% of the bite cycle, which was defined at the time net bite force gradient first exceeded 0.3 N/s (0%) and the time at maximum net bite force (100%). The 3D bite force for each participant was averaged across the cycles. To aid comparison between biting on the left and right molars, lateral force components directed buccally and lingually were represented as positive and negative, respectively. Using high performance computing with an Intel Xion Gold 3.10 GHz processor and 400 GB memory, quasi-static simulations using an explicit dynamic analysis were executed with parallelisation over 20 cores, taking an average of 16.4 ± 10.3 hrs to solve.

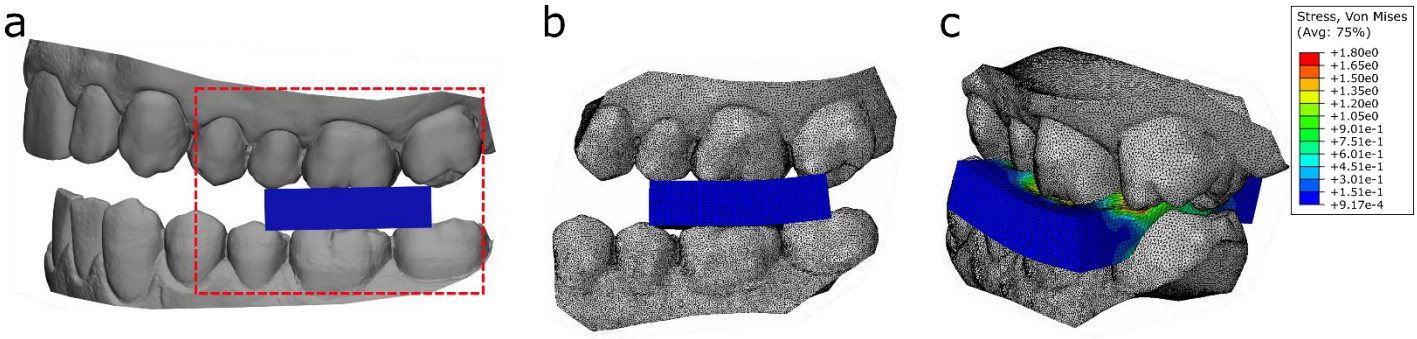



Figure 6.2: Three-dimensional model of the participants mandibular and maxillary teeth with rubber held between the first molars (a), finite element model of the first molars (grey) and rubber (blue) constructed from the laser scan data (b), and the finite element model of the first molars compressing the rubber sample in a maximum force bite (c). The finite element model includes only the teeth that will contact the rubber for computational efficiency, indicated by the red dashed lines.

### 6.4.4 Musculoskeletal modelling

A musculoskeletal model of each participant's jaw was constructed to estimate subject-specific muscle and joint forces at the TMJ. Open-source modelling software (Delp et al. 2007) was employed to create a generic rigid-body jaw model, with bony geometries and muscle architecture based on a previously published model (see Appendix D) (Ackland et al. 2017). The mandible articulated within the skull through two six degree-of-freedom TMJs. The anterior and posterior temporalis muscles, along with the superficial, deep anterior and deep posterior masseter muscles, and the medial, inferior lateral and superior lateral pterygoid muscles were modelled as Hill-type muscle-tendon actuators with muscle-tendon parameters derived from cadaveric studies (Fig. 6.3) (Koolstra et al. 2006). The generic mandible and skull anatomy, and the muscle paths were anisotropically scaled using the intercondylar distance and the distance between the mid-condyle point and the mandibular incisors of each participant. During scaling, a constant ratio of optimum fibre length and tendon slack length was maintained for each muscle.

Each participant's time varying bite force, calculated through finite element analysis, was applied to the mandibular first molars in the musculoskeletal model with the mandible in the maximum occlusion position. Bite force was decomposed into muscle and joint forces using an objective function that minimised the sum of squares of the muscle forces while adhering to force and moment equilibrium constraints. This objective function successfully recruits the masticatory muscles while allowing for asymmetric muscle function (May et al. 2001; Ackland et al. 2015). The superior and inferior sub-regions of the lateral pterygoid muscle were removed

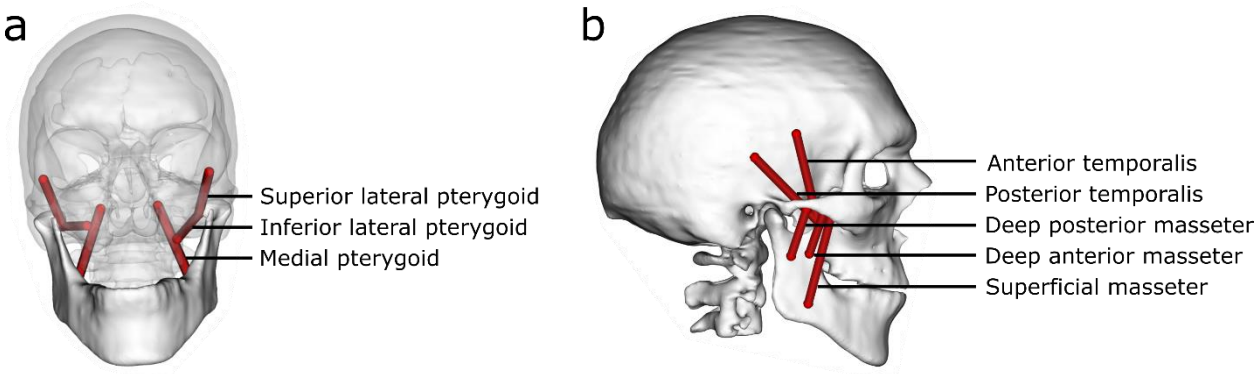



Figure 6.3: Rigid-body musculoskeletal model illustrating the pterygoid sub-regions in the frontal plane (a) and temporalis and masseter sub-regions in the sagittal plane of healthy controls (b). The superior and inferior sub-regions of the operated lateral pterygoid muscles are removed in the models of unilateral total TMJR patients.

on the ipsilateral side for unilateral total TMJR patients, which reflected the loss of muscle function resulting from intraoperative severing of the lateral pterygoid muscle during condylectomy. All remaining muscles were modelled as intact and fully functional (see Appendix D). To aid comparison between the left and right TMJ's, lateral force components directed laterally and medially were represented as positive and negative, respectively.

To quantify the relative contribution of each participants working side versus non-working side muscles (Fig. 6.1d) an asymmetry index was computed for each muscle, defined as

$$AI = \frac{F_{working} - F_{non-working}}{F_{working} + F_{non-working}} \quad (3)$$

Where $F_{working}$ is the muscle force on the working side and $F_{non-working}$ is the muscle force on the non-working side. Positive asymmetry index values up to 1 signify that the muscles on the working side exert greater force than those on the non-working side; similarly, negative asymmetry index values up to -1 suggest higher muscle forces on the non-working side (Ferrario and Sforza 1994).

### 6.4.5 Data analysis

Mann-Whitney U-tests were used to compare maximum bite force magnitude and direction, maximum muscle force, muscle asymmetry index, maximum joint force and direction and the ratio of TMJ force to bite force between unilateral total TMJR patients and controls. Wilcoxon signed-rank tests were used to compare these variables between unilateral total TMJR patients during biting on the contralateral and ipsilateral molars. Data normality was assessed using Shapiro-Wilk tests. Due to the non-normal data distribution, comparisons were made

using median differences, while data dispersion was indicated by standard deviation. The criterion for statistical significance was set at $p < 0.05$. The statistical analysis was performed in Minitab version 19 (Minitab LLC, Pennsylvania, USA).

## 6.5 RESULTS

There was a non-significant trend that control subjects had higher net maximum voluntary bite force (317.1 ± 206.6 N) than unilateral total TMJR patients, both when biting on their contralateral molars (249.6 ± 24.4 N) and their ipsilateral molars (164.2 ± 62.3 N) (Table 6.2). When biting on the contralateral molars, unilateral total TMJR patients had significantly higher bite force angle directed lingually than when biting on their ipsilateral molars (median difference: 7.3°, $p = 0.048$) (Fig. 6.4), which resulted in significantly higher lateral shear force directed lingually (median difference: 41.2 N, $p = 0.048$) (Table 6.2).

Table 6.2: Maximum voluntary bite force magnitude and direction for control subjects and unilateral total TMJR patients when biting on their first molars. Values are given as mean (SD). Bite force is reported as the reaction force on the mandibular teeth with respect to the anatomic coordinate system. To aid comparison between biting sides, the lateral component of bite force directed buccally is defined as positive, and that directed lingually is defined as negative. P values are given for comparisons between healthy controls and unilateral total TMJR patients, determined through Mann-Whitney U-tests ($P_a$), and for comparisons between unilateral total TMJR patients biting on their contralateral and ipsilateral molars, determined through Wicoxon signed-rank tests ($P_b$). * represents significant differences.

| | | Maximum bite force (N) | | | | | | | | | | | | Bite force direction (°) | | | | | |
|---|---|---|---|---|---|---|---|---|---|---|---|---|---|---|---|---|---|---|---|
| | Biting side | X | | | Y | | | Z | | | Total | | | X | | | Y | | |
| | | Force | $P_a$ | $P_b$ | Force | $P_a$ | $P_b$ | Force | $P_a$ | $P_b$ | Force | $P_a$ | $P_b$ | Direction | $P_a$ | $P_b$ | Direction | $P_a$ | $P_b$ |
| Control (n=8) | Both | -9.5 (62.8) | | | 10.0 (19.8) | | | -312.8 (202.7) | | | 317.1 (206.6) | | | -0.2 (6.7) | | | 2.4 (4.1) | | |
| TMJR (n=5) | Contralateral | -48.8 (21.2) | 0.156 | | 9.9 (10.9) | 0.897 | | -243.9 (23.1) | 0.699 | | 249.6 (24.4) | 0.699 | | -11.2 (4.4) | 0.093 | | 2.3 (2.6) | 0.897 | |
| | Ipsilateral | -6.0 (4.1) | 0.456 | 0.048* | 4.7 (5.6) | 0.241 | 0.596 | -163.9 (62.1) | 0.070 | 0.216 | 164.2 (62.3) | 0.070 | 0.216 | -2.2 (1.1) | 0.456 | 0.048* | 1.6 (1.9) | 0.456 | 0.860 |

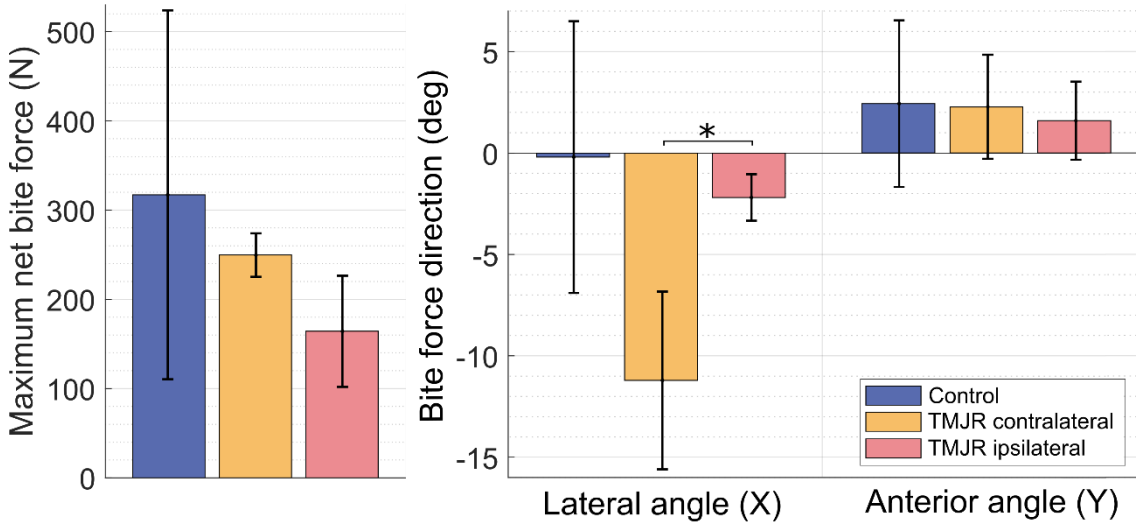



Figure 6.4: Net maximum voluntary bite force and direction for control subjects (blue) and unilateral total TMJR patients biting on their contralateral (yellow) or ipsilateral (pink) first molars. Bite force is reported as the reaction force on the mandibular teeth with respect to the mandibular anatomic coordinate system. The lateral component of bite force directed buccally is defined as positive, and that directed lingually is defined as negative. Statistically significant differences ($p < 0.05$) are identified by an asterisk.

The superficial masseter, anterior temporalis and medial pterygoid muscles were the highest contributors to bite force, a finding consistent across subject groups (Fig. 6.8). The working side muscles exhibited higher muscle forces than the non-working side muscles, with the exception of the posterior temporalis during unilateral ipsilateral molar biting (working: 2.7 ± 0.8 N, non-working: 3.6 ± 1.5 N), and the medial pterygoid during unilateral contralateral molar biting (working: 1.6 ± 2.7 N, non-working: 16.0 ± 6.0 N) (Table 6.3). Unilateral total TMJR patients, when biting on their contralateral molars had a significantly lower medial pterygoid asymmetry index than when biting on their ipsilateral molars (median difference: -1.50, $p = 0.048$) or compared to the control subjects (median difference: -1.34, $p = 0.028$) (Fig. 6.5). When biting on the contralateral molars, unilateral total TMJR patients had a significantly higher posterior temporalis asymmetry index than when biting on their ipsilateral molars (median difference: 1.10, $p = 0.048$). Unilateral total TMJR patients, when biting on the contralateral molars had significantly higher anterior temporalis asymmetry index than when biting on their ipsilateral molars (median difference: 0.24, $p = 0.048$) and when compared to control subjects (median difference: 0.31, $p = 0.028$) (Fig. 6.5).

Table 6.3: Maximum muscle force magnitude for each muscle on the working and non-working side of the mandible and the asymmetry index of each muscle for each participant group. Values are given as mean (SD). P values are given for comparisons between healthy controls and unilateral total TMJR patients, determined through Mann-Whitney U-tests ($P_a$), and for comparisons between unilateral total TMJR patients biting on their contralateral and ipsilateral molars, determined through Wilcoxon signed-rank tests ($P_b$). * represents significant differences.

| | Muscle | Control (n=8) | | TMJR (n=5) | | | | | | | | | |
|---|---|---|---|---|---|---|---|---|---|---|---|---|---|
| | | | | Contralateral biting | | | | Ipsilateral biting | | | | | |
| | | Maximum muscle force (N) | Asymmetry index | Maximum muscle force (N) | $P_a$ | Asymmetry index | $P_a$ | Maximum muscle force (N) | $P_a$ | $p_b$ | Asymmetry index | $P_a$ | $p_b$ |
| Working side | Anterior temporalis | 75.7 (73.1) | 0.16 (0.14) | 66.9 (7.5) | 0.366 | 0.58 (0.27) | 0.028* | 37.5 (14.3) | 0.241 | 0.048* | 0.22 (0.02) | 0.594 | 0.048* |
| | Posterior temporalis | 18.4 (34.0) | -0.14 (0.77) | 11.9 (1.3) | 0.519 | 0.97 (0.05) | 0.156 | 2.7 (0.8) | 0.749 | 0.048* | -0.09 (0.14) | 1.000 | 0.048* |
| | Superficial masseter | 119.6 (49.0) | 0.15 (0.08) | 107.2 (14.2) | 1.000 | 0.16 (0.01) | 0.519 | 72.5 (31.0) | 0.110 | 0.377 | 0.21 (0.01) | 0.070 | 0.048* |
| | Deep anterior masseter | 5.6 (6.5) | 0.21 (0.17) | 3.9 (0.6) | 0.699 | 0.49 (0.07) | 0.049* | 2.2 (0.8) | 0.070 | 0.112 | 0.27 (0.10) | 0.456 | 0.048* |
| | Deep posterior masseter | 4.4 (6.7) | 0.91 (0.07) | 1.9 (0.2) | 0.897 | 0.67 (0.05) | 0.028* | 1.3 (0.5) | 0.110 | 0.216 | 0.82 (0.10) | 0.166 | 0.112 |
| | Medial pterygoid | 24.5 (21.1) | 0.62 (0.43) | 1.6 (2.7) | 0.049* | -0.78 (0.38) | 0.028* | 8.1 (3.1) | 0.166 | 0.112 | 0.69 (0.23) | 0.915 | 0.048* |
| | Inferior lateral pterygoid | 16.6 (12.7) | 0.18 (0.36) | 8.6 (1.7) | 0.519 | - | - | - | - | - | - | - | - |
| | Superior lateral pterygoid | 0.2 (0.5) | 0.67 (0.26) | 0.0 (0.0) | 0.699 | - | - | - | - | - | - | - | - |
| Non-working side | Anterior temporalis | 51.0 (36.2) | | 19.1 (13.0) | 0.245 | | | 24.3 (9.5) | 0.110 | 1.000 | | | |
| | Posterior temporalis | 7.4 (6.3) | | 0.2 (0.3) | 0.093 | | | 3.6 (1.5) | 0.456 | 0.048* | | | |
| | Superficial masseter | 93.3 (55.6) | | 77.1 (11.3) | 0.897 | | | 48.0 (20.3) | 0.070 | 0.112 | | | |
| | Deep anterior masseter | 3.0 (1.9) | | 1.3 (0.1) | 0.093 | | | 1.4 (0.7) | 0.110 | 0.596 | | | |
| | Deep posterior masseter | 0.1 (0.0) | | 0.4 (0.1) | 0.028* | | | 0.1 (0.0) | 0.456 | 0.048* | | | |
| | Medial pterygoid | 9.9 (21.8) | | 16.0 (6.0) | 0.156 | | | 1.1 (0.7) | 1.000 | 0.048* | | | |
| | Inferior lateral pterygoid | 15.0 (23.3) | | - | - | | | 6.2 (3.4) | 0.749 | - | | | |
| | Superior lateral pterygoid | 0.0 (0.0) | | - | - | | | 0.0 (0.0) | 0.070 | - | | | |

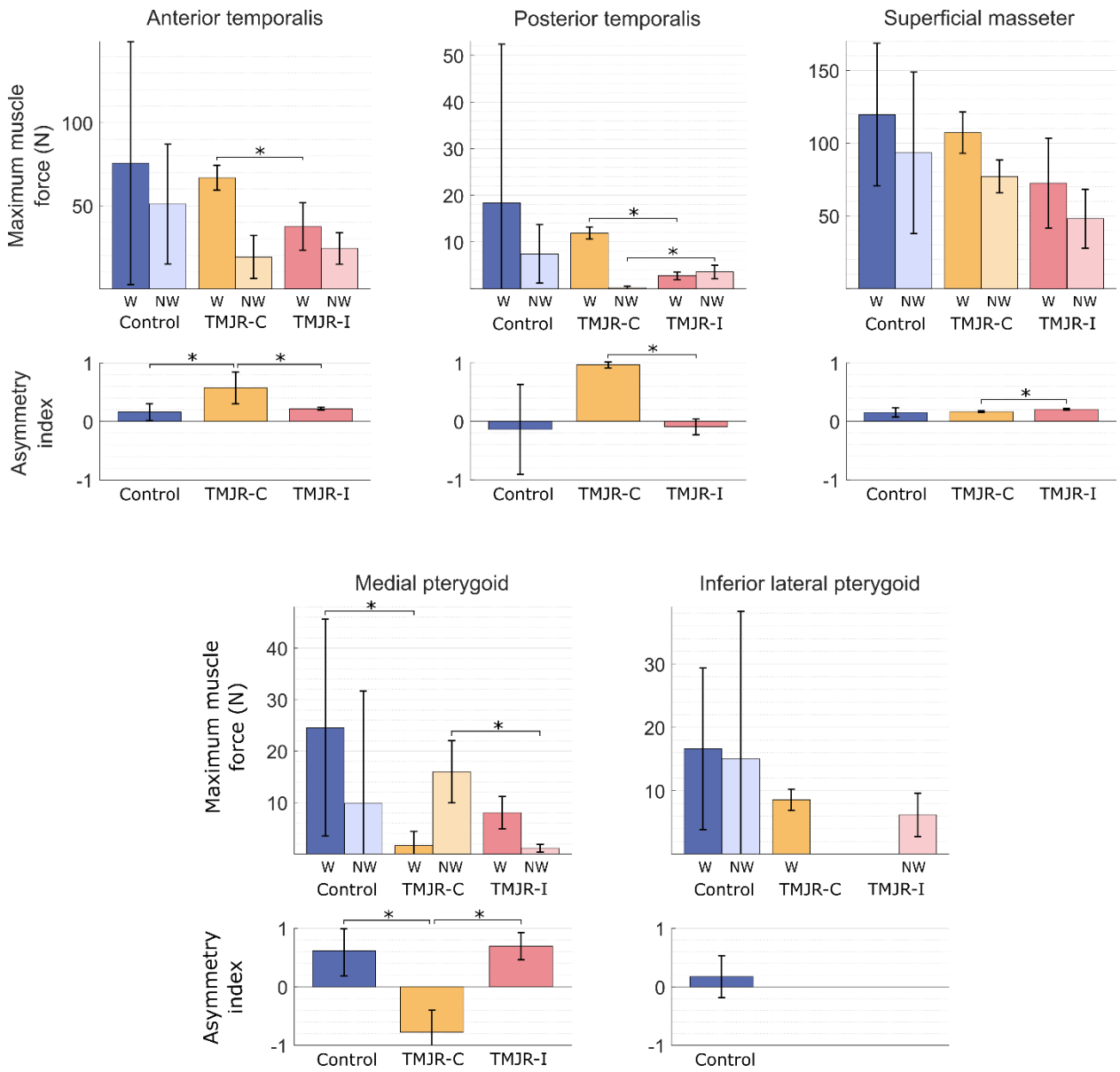



Figure 6.5: Net maximum muscle force and asymmetry index of the medial pterygoid, inferior lateral pterygoid, posterior temporalis, anterior temporalis, and superficial masseter muscles for control subjects (blue) and unilateral total TMJR patients biting on their contralateral (yellow) or ipsilateral (pink) first molars. Muscle forces are given for the working (W) and non-working (NW) sides of the jaw. Statistically significant differences ($p < 0.05$) are identified by an asterisk. TMJR-C and TMJR-I indicate unilateral total TMJR patients biting on their contralateral and ipsilateral molars, respectively.

Control subjects had similar mean net joint forces on both TMJs (working: 86.0 ± 84.1 N, non-working: 51.8 ± 44.4 N). There was a non-significant trend that unilateral total TMJR patients had higher net joint forces on their non-working condyle than their working condyle, both for biting on the contralateral molars (working: 14.2 ± 5.9 N, non-working: 48.5 ± 10.4 N) and the ipsilateral molars (working: 15.1 ± 7.9 N, non-working: 25.6 ± 10.8 N) (Fig. 6.6). All subject groups experienced compressive mean joint forces in the superior/inferior direction on the non-working condyle (control: -43.0 ± 43.1 N, unilateral contralateral: -44.3 ± 7.3 N, unilateral ipsilateral: -24.9 ± 10.9 N), and tensile forces on the working condyle (control: 33.7 ± 116.3 N, unilateral contralateral: 6.0 ± 1.8 N, unilateral ipsilateral: 13.5 ± 8.1 N) (Table 6.4). When biting on the contralateral molars, the working joint of unilateral total TMJR patients had a significantly higher lateral force direction compared to biting on their ipsilateral molars (median difference: 60.1°, p = 0.048) or that of control subjects (median difference: 63.6°, p = 0.028). Unilateral total TMJR patients when biting on the contralateral molars had a significantly lower ratio of TMJ force to bite force on the working condyle than that of control subjects (median difference: 0.17, p = 0.049) (Fig. 6.7).

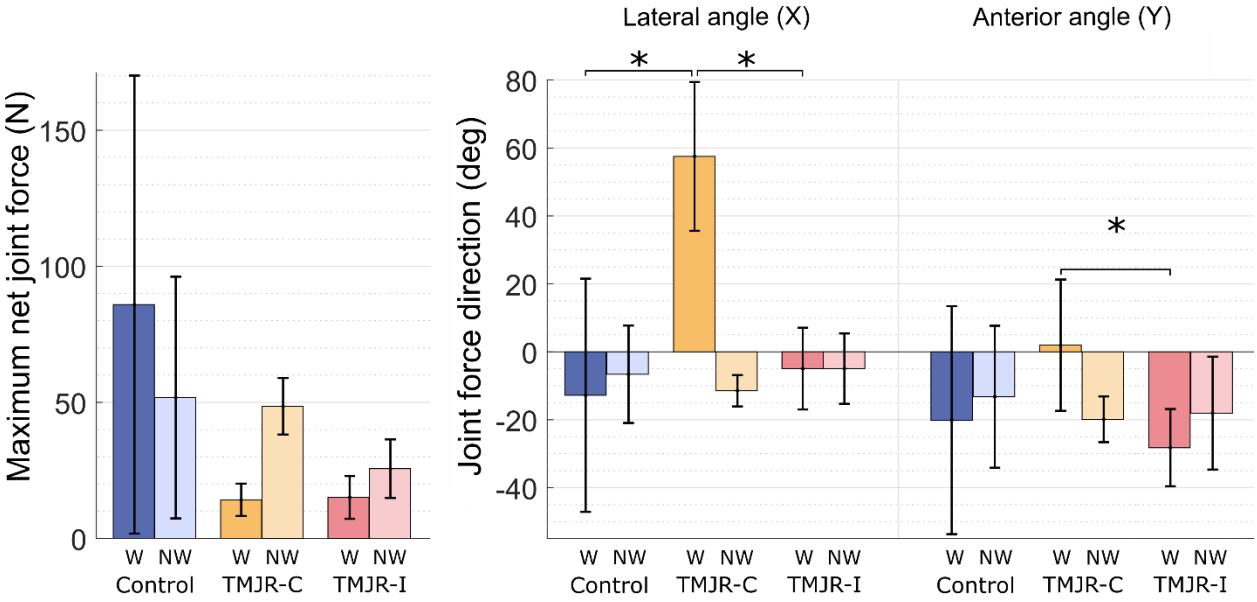



Figure 6.6: Maximum net joint force and direction for the working (W) and non-working (NW) joints of control subjects (blue) and unilateral total TMJR patients biting on their contralateral (yellow) or ipsilateral (pink) first molars. To aid comparison of the muscle and TMJ reaction loads between biting sides, the lateral component of joint force directed laterally is defined as positive, and that directed medially is defined as negative. Statistically significant differences ($p < 0.05$) are identified by an asterisk. TMJR-C and TMJR-I indicate unilateral total TMJR patients biting on their contralateral and ipsilateral molars, respectively.

Table 6.4: TMJ reaction force magnitude, direction and ratio of TMJ force to bite force for the working and non-working condyles of control subjects and unilateral total TMJR patients at the time of maximum voluntary bite force. Values are given as mean (SD). To aid comparison of the muscle and TMJ reaction loads between biting sides, the lateral component of joint force directed laterally is defined as positive, and that directed medially is defined as negative. Values are given as mean (SD). P values are given for comparisons between healthy controls and unilateral total TMJR patients, determined through Mann-Whitney U-tests ($P_a$), and for comparisons between unilateral total TMJR patients biting on their contralateral and ipsilateral molars, determined through Wilcoxon signed-rank tests ($P_b$). * represents significant differences.

| | Biting side | TMJ | TMJ force (N) | | | | | | | | | | | | TMJ force direction (°) | | | | | | TMJ to BF ratio | | |
|---|---|---|---|---|---|---|---|---|---|---|---|---|---|---|---|---|---|---|---|---|---|---|---|
| | | | X | | | Y | | | Z | | | Total | | | X | | | Y | | | | | |
| | | | Force | $P_a$ | $P_b$ | Force | $P_a$ | $P_b$ | Force | $P_a$ | $P_b$ | Force | $P_a$ | $P_b$ | Direction | $P_a$ | $P_b$ | Direction | $P_a$ | $P_b$ | Ratio | $P_a$ | $P_b$ |
| Control (n=8) | Both | Working | 2.5 (20.9) | | | 3.8 (19.0) | | | 33.7 (116.3) | | | 86.0 (84.1) | | | -12.8 (34.3) | | | -20.1 (33.6) | | | 0.24 (0.12) | | |
| | | Non-working | -5.0 (13.0) | | | -10.7 (24.4) | | | -43.0 (43.1) | | | 51.8 (44.4) | | | -6.6 (14.4) | | | -13.2 (20.9) | | | 0.17 (0.12) | | |
| TMJR (n=5) | Contralateral | Working | 12.1 (7.6) | 0.156 | | -0.1 (1.7) | 0.915 | | 6.0 (1.8) | 0.519 | | 14.2 (5.9) | 0.070 | | 57.5 (21.9) | 0.028* | | 1.9 (19.3) | 0.519 | | 0.06 (0.02) | 0.049* | |
| | | Non-working | -9.4 (5.1) | 0.156 | | -16.7 (8.4) | 0.156 | | -44.3 (7.3) | 0.245 | | 48.5 (10.4) | 0.699 | | -11.5 (4.6) | 0.156 | | -19.9 (6.7) | 0.245 | | 0.19 (0.03) | 0.156 | |
| | Ipsilateral | Working | -0.4 (1.7) | 0.456 | 0.048* | -5.6 (1.4) | 0.749 | 0.048* | 13.5 (8.1) | 0.594 | 0.216 | 15.1 (7.9) | 0.156 | 0.860 | -4.9 (12.0) | 0.915 | 0.048* | -28.2 (11.4) | 0.594 | 0.048* | 0.11 (0.07) | 0.070 | 0.216 |
| | | Non-working | 0.0 (0.8) | 0.915 | 0.048* | -4.4 (2.0) | 0.337 | 0.048* | -24.9 (10.9) | 0.749 | 0.112 | 25.6 (10.8) | 0.594 | 0.112 | -4.9 (10.4) | 0.915 | 0.377 | -18.1 (16.6) | 0.456 | 0.377 | 0.15 (0.03) | 0.749 | 0.112 |

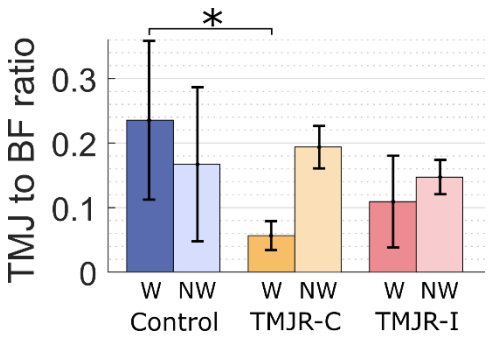



Figure 6.7: Ratio of TMJ loading to bite force for the working (W) and non-working (NW) joints of control subjects (blue) and unilateral total TMJR patients biting on their contralateral (yellow) or ipsilateral (pink) first molars. Statistically significant differences ($p < 0.05$) are identified by an asterisk. TMJR-C and TMJR-I indicate unilateral total TMJR patients biting on their contralateral and ipsilateral molars, respectively.

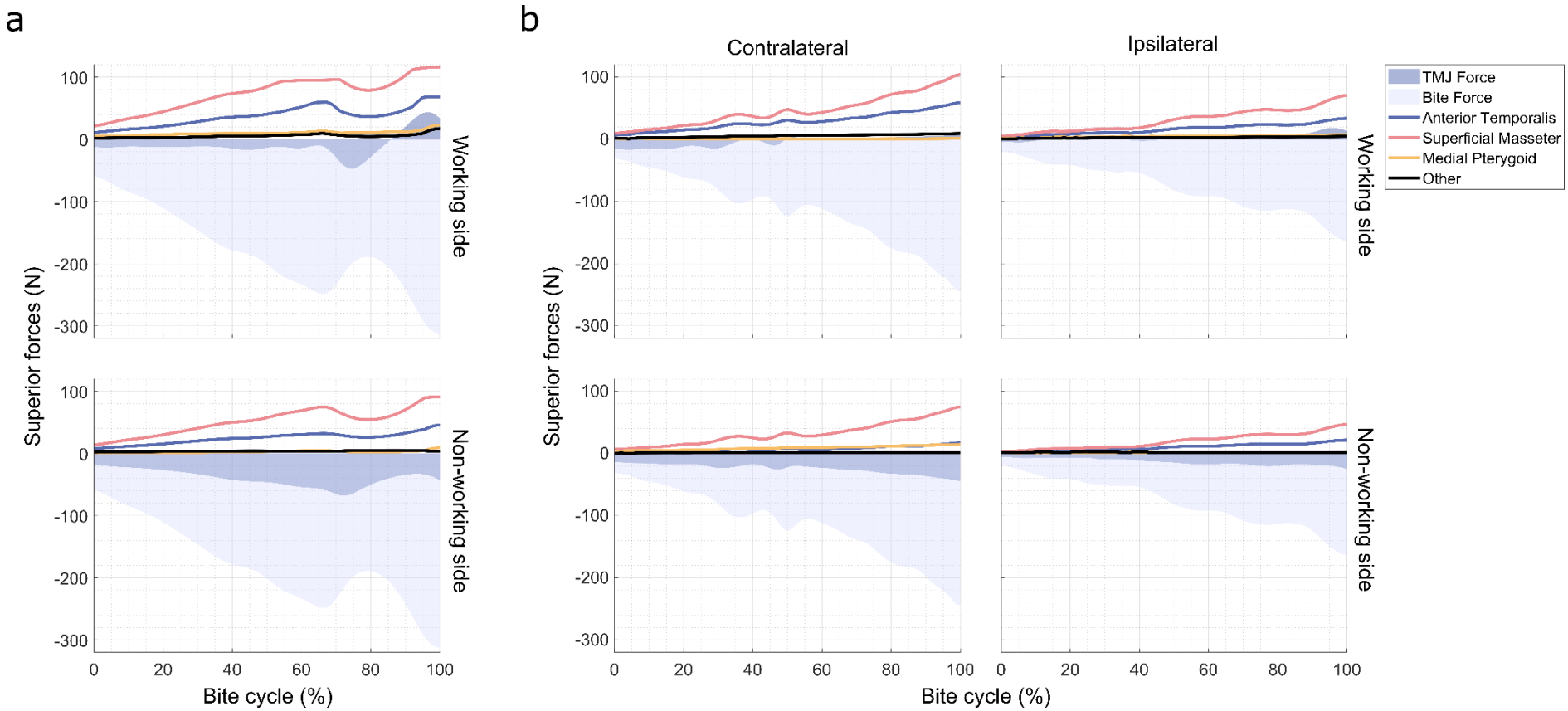



Figure 6.7: Contribution of joint force and dominant muscle forces to the superior-inferior component of bite force during a maximum force bite for control subjects (a) and unilateral total TMJR patients when biting on their contralateral and ipsilateral molars (b). Anterior temporalis (blue), superficial masseter (pink) and medial pterygoid (yellow) forces are indicated separately, contribution from remaining muscles is summed and represented as “other” (black).

## 6.6 DISCUSSION

Clinical evaluation shows that TMJR surgery increases maximum interincisal opening distance by 9mm, and reduces joint pain and dietary restrictions by 74% and 77%, respectively (Dimitroulis et al. 2018). However, 3D bite force, muscle force and joint loads in TMJR patients, which are key determinates of muscle and joint function post-operatively, remain poorly understood. The objective of this study was to use subject-specific 3D bite force measurements to evaluate the magnitude and direction of joint loading in TMJR patients and healthy controls. There was a non-significant trend that unilateral total TMJR patients had lower net joint force than healthy controls, particularly on the contralateral joint. Unilateral total TMJR patients, when biting with their contralateral molars had TMJ loading on the working condyle directed significantly more laterally than healthy controls, and significantly lower ratios of TMJ force to bite force than healthy controls, thus supporting the study hypothesis.

Comparable net maximum voluntary bite force was observed between control subjects and unilateral total TMJR patients. Control subjects had a net maximum voluntary bite force of 317.1 ± 206.6 N, which is consistent with a previously reported unidirectional maximum voluntary bite force range for healthy females of 269.6 to 424.9 N (Calderon et al. 2006; Alam and Alfawzan 2020). There were large variations in maximum voluntary bite force in the control subjects. This finding reflects variability of normal force documented in the literature, believed to be a result of variations in muscle strength, periodontal support, motor control and general physical health (Ikebe et al. 2005, Jansen van Vuuren et al. 2020). Uniaxial maximum voluntary bite force in TMJR patients, using their contralateral molars, has been reported to be 194.5 N (Linsen et al. 2021a), which is lower than the net maximum voluntary bite force measured in this study of 249.6 N; however this study did not record shear force at the occlusal surface during contralateral biting, which may underestimate the resultant occlusal load; although Linsen et al studied a mixed-gender sample (15 M, 24 F) which may increase the occlusal loading. From a clinical standpoint, all participants had mean maximum voluntary bite force sufficient to chew raw carrot (118 N) or cooked meat (124 N) (Poli et al. 2021) suggesting that unilateral total TMJR surgery does not result in a functional limitation to biting performance. This is supported by clinical studies finding high levels of satisfaction and reduction in dietary restrictions following total TMJR surgery with the ArthroJaw TMJR system (Dimitroulis et al. 2018).

Large lateral shear forces of 49 ± 21 N were measured in unilateral total TMJR patients when biting on the contralateral molars. To our knowledge, this is the first study to measure 3D maximum voluntary bite force following total TMJR surgery and therefore the first quantification of lateral shear forces in this cohort. This finding suggests that these patients rely on a grinding motion to breakdown food when biting on the contralateral molars. From a clinical standpoint, these shear forces ought to be considered when planning dental treatments for unilateral total TMJR patients, as comparable shear forces have been shown to propagate cracks in dental enamel (~100 N) (Chai et al. 2009), lead to failure of restored teeth (92 N) (Wandscher et al. 2014) and dental implants (106 N) (Forero et al. 2019).

The present study showed that in unilateral total TMJR patients, both the posterior and anterior temporalis muscles have lower forces on the operated side, leading to larger muscle asymmetry than healthy controls. This is consistent with studies finding large temporalis asymmetry following TMD surgery (Raustia et al. 1997). Contraction of the temporalis muscle elevates the mandible and produces vertical bite force when chewing; thus, this postsurgical weakness may limit the maximum voluntary bite force of TMJR patients, particularly when biting on the ipsilateral side. Unilateral total TMJR patients had high medial pterygoid forces on the operated side, regardless of biting side. This may be a compensation for the loss of the inferior lateral pterygoid function, since animal studies have shown that the absence of an individual masticatory muscle may be compensated for by ipsilateral synergistic muscle function (Rafferty et al. 2012). Despite this compensation, the loss of the lateral pterygoid muscle has been associated with decreased anterior motion of prosthetic condyles, leading to the reduced jaw movement capacity (Wojczyńska et al. 2021; Woodford et al. 2023). This study found low force generation in the deep masseter muscles, which is consistent with another musculoskeletal model of the masticatory system (Ackland et al. 2017); however, fine wire EMG studies predict larger activation of the deep masseter muscles, and this may represent a limitation in the muscle models employed and associated cost functions (Van Eijden et al. 1993).

During TMJR surgery, the insertion of the masseter muscle, the pterygomasseteric sling, is partially stripped from the mandible. After fixation of the ramal component, the pterygomasseteric sling can be reattached via sutures, which would be expected to decrease masseter forces on the operated side (Linsen et al. 2020). However, this study found similar levels of masseter asymmetry between controls and unilateral total TMJR patients, indicating healthy post-surgical masseter function in the patients studied. All TMJR patients in this study

were fitted with the ArthroJaw customised TMJR system which has a titanium (Ti-6Al-4V) condyle-ramus unit, designed to maximise exposure of mandibular bone, facilitating reattachment of the masseter muscle (Ackland et al. 2017; Dimitroulis et al. 2018). Additionally, studies of biomaterials created for orthopaedic applications have shown high proliferation and adhesion of osteoblasts and fibroblasts on titanium implants (Markhoff et al. 2017), suggesting that the masseter may ultimately reattach to the surface of the titanium implant (Singh et al. 2022). This adhesion may lead to the higher post-surgical masseter forces which have been measured for patients with custom titanium alloy prosthetics compared to stock cobalt chromium alloy prosthetics (Linsen et al. 2020).

The muscular condition of unilateral TMJR patients is similar to that measured for other unilateral maxillofacial conditions such as unilateral posterior crossbite (UPC). Patients with UPC can have mandibular asymmetry (Bell and Kiebach 2014), reverse-sequence chewing pattern (Throckmorton et al. 2001b), muscle asymmetries (Piancino et al. 2016) and reduced ipsilateral bite force capacity (Sonnesen et al. 2001; Sonnesen and Bakke 2007). If left untreated, the asymmetrical functionality of UPC patients is believed to lead to TMJ dysfunction (Thilander et al. 2002; Thilander and Bjerklin 2012) and bone remodelling at the TMJ (Bell and Kiebach 2014). Orthodontic treatment to achieve mandibular symmetry successfully returns normal function to UPC patients (Throckmorton et al. 2001b; Piancino et al. 2016); indicating that a focus on symmetric morphology and function may also be beneficial for TMJR treatments.

Unilateral total TMJR surgery is associated with degradation of the native contralateral TMJ, this changes the morphology of the native joint (Kim et al. 2021) and leads to subsequent bilateral total TMJR surgery in up to 40% of cases (Franco et al. 1997). Previous investigations have speculated that this is due to altered loading patterns resulting from hypermobility of the native joint (Leiggener et al. 2012), or joint overloading (Perez et al. 2016). However, this study found that for unilateral total TMJR patients, the native side of their jaw is more efficient at transmitting muscle force to bite force than the prosthetic side, as evidenced by the low joint loads and ratio of TMJ force to bite force for the native contralateral joint. These findings follow a similar trend to mathematical models of TMJ loading for unilateral total TMJR patients (van Loon et al. 1998) and suggest that joint problems on the native contralateral TMJ do not result from joint overloading during biting. The low joint loads may be an unconscious compensation by the neuromuscular system to protect the joint, which may have been degraded by biological mechanisms. Alternatively, as unilateral biting is the dominant loading event to the masticatory

system; this joint degradation may be due to underloading of the joint, which has been well documented to lead to joint degradation in the knee (Vanwanseele et al. 2002; Wellsandt et al. 2016) and hip (Loureiro et al. 2018) joints.

The results reported in this study are not direct biomechanical measurements, but are indirect estimates calculated using computational models. Direct in-vivo measurements of 3D bite force and TMJ loading are not possible, and this has restricted our understanding of maxillofacial biomechanics in both healthy and pathological populations. This technique of combining experimental measurements and computational modelling, referred to as in-silico modelling, has been applied widely in the field of orthopaedic biomechanics and is shown to provide accurate measures of joint loading in the hip, knee, ankle and shoulder joints (Innocenti et al. 2022). Established computational models of the TMJ are limited due to the complexity of the masticatory system. However, the present study demonstrates the potential for computational modelling to expand the understanding of TMJ biomechanics where in vivo quantification is not possible.

There are a number of limitations of this study. The small sample size may have underpowered our capacity to detect significant differences in maximum voluntary bite force considering the large variation in maximum voluntary bite force for each subject group. However, our sample size was sufficient to highlight significant differences in bite force direction, muscle forces and asymmetries, TMJ loading direction and ratio of TMJ force to bite force. Additionally, this study involved only female participants, which ought to be considered when interpreting these results. This was chosen to reflect the gender imbalance among TMJR patients of whom 86.1% are female (Granquist et al. 2020). This is believed to stem from differing behavioural, psychosocial and hormonal factors (Roda et al. 2007). Further research is required to assess jaw biomechanics in the male population. Our use of dental plates for motion tracking of the jaw may introduce kinematics measurement errors through movement or vibration of the markers, mismatch between the alignment of the rubber sample with respect to the teeth between the model and experiments, and assumptions in the modelling of rubber-clasp interactions (Appendix D). Furthermore, for unilateral total TMJR patients, all muscles were modelled as intact with full capacity, with the exception of the superior and inferior sub-regions of the lateral pterygoid muscle which were modelled as completely severed (Bhargava et al. 2019; Pinheiro 2021). Sensitivity analysis shows that this introduces minimal error to calculated muscle and joint forces (see Appendix D). However, future studies ought to explore MRI or EMG to quantify the status of the pterygoid, masseter, and temporalis muscles on a

subject-specific basis. Finally, anisotropically scaled generic rigid-body musculoskeletal models were used instead of fully subject-specific models, this may introduce small offsets in joint centre and muscle attachment points. While previous studies have shown that small differences in TMJ location have only minor influence on muscle and joint loading (van Loon et al. 1998); future studies should create fully subject-specific models using MRI and CT data to determine precise muscle insertion and joint centre locations to increase the accuracy of these results.

This study found that unilateral total TMJR patients tended to have lower maximum voluntary bite force than that of healthy controls, particularly when biting on their ipsilateral molars. This may be linked to the asymmetric force distribution between the contralateral and ipsilateral temporalis muscles. Additionally, unilateral total TMJR patients had lower net TMJ loading than controls, particularly on the contralateral joint. This abnormal loading may be a mechanism associated with degenerative changes that have been observed in the contralateral joint following unilateral total TMJR surgery. The results of this study may facilitate the biomechanical design and evaluation of maxillofacial implants, prosthetic devices and dental restorations, to improve their long-term performance. Furthermore, these results may influence physiotherapy prescription following unilateral total TMJR surgery, for example, to prioritise strengthening of the operated elevator muscles and increasing the loading of the contralateral joint.

# Chapter 7: Conclusions and future work

## 7.1 SUMMARY

This thesis assessed current techniques for evaluating jaw TMJ kinematics, developed new techniques to quantify 3D, dynamic bite force and occlusal pressure during biting and chewing, and obtained new information describing the kinematics, maximum voluntary bite force, muscle forces and joint loading of the native mandible, and those following unilateral total TMJR.

Chapter 3 aimed to systematically identify and compare and contrast the measurement modalities used to quantify *in vivo* mandibular and TMJ kinematics in six degrees-of-freedom. The techniques identified fall into four main categories, namely mechanical linkage systems, magnetic tracking systems, video motion analysis and radiographic tracking. This study highlighted the benefits and user requirements of each system and compiled accuracy data for each technique. These findings may help guide future selection and use of jaw motion tracking technology both for clinical and research applications.

In chapter 4, miniature low-profile electromagnetic field sensors were used in combination with intraoral scanning to record high precision mandibular kinematics during biting and chewing. Recorded mandibular kinematics were then used as the input to a computational modelling pipeline to evaluate subject-specific dynamic bite force and occlusal contact pressure during chewing and biting over the entire dental arch. A validation experiment was performed finding that the modelling framework presented accurately evaluates bite force, given sufficiently precise measurement of mandibular kinematics. This experimental and computational modelling pipeline presents the first technique capable of recording 3D dynamic bite forces in participants with healthy dentition. A greater understanding of 3D dynamic bite force could lead to a leap in our understanding of the mechanics of the maxillofacial system; as shear bite force is linked to the long-term survival rates of dental prosthetics and restorations and maxillofacial orthopaedic implants including TMJ prosthesis. Furthermore, a deeper understanding of 3D bite forces may be relevant to the diagnosis of TMJ disorders and will lead to improved accuracy of finite element and musculoskeletal models of the masticatory system.

In chapter 5, jaw and TMJ kinematics were evaluated during mandibular border movements and chewing in unilateral total TMJR patients and healthy controls. Unilateral total

TMJR patients has restricted anterior mobility of their prosthetic condyles which restricted border movements; however, this did not translate to significant differences in chewing kinematics compared to healthy controls. Furthermore, during chewing, unilateral total TMJR patient's prosthetic condyles were positioned significantly inferiorly to those of healthy controls, suggesting a weakness of the elevator muscles on the operated side. This is the first time that chewing kinematics has been evaluated in TMJR patients. This study highlighted the positive functional outcomes during daily activities following TMJR surgery and may provide future direction for prosthetic TMJ design to enhance postsurgical implant functionality and improve long-term clinical outcomes for patients.

Chapter 6 combined the mandibular kinematics evaluated in chapter 5 with the computational modelling pipeline developed in chapter 4 to evaluate the 3D dynamic bite force of unilateral total TMJR patients and healthy controls. These bite forces were used in musculoskeletal models to investigate muscle and joint forces during a maximum force bite. Unilateral total TMJR patients had lower TMJ loading than controls subjects, particularly on the native contralateral joint. This inadequate loading may be a mechanism associated with degenerative changes that have been observed in the contralateral joint following unilateral TMJR surgery. The results of this study may facilitate the design and evaluation of TMJ prosthesis, prosthetic devices, dental restorations and maxillofacial orthopaedic implants; furthermore, these results may influence physiotherapy prescription following unilateral total TMJR surgery to enhance long-term patient outcomes.

## 7.2 LIMITATIONS

There are overarching limitations in the experimental design and modelling that ought to be considered. First, the motion tracking experiments that underlie chapters 5 and 6 had a limited sample size. Total unilateral TMJR patients and healthy control subjects were recruited and participated in these experiments between 28/04/2021 and 27/06/2022. This study was completed in Melbourne, Australia, which was in intermittent COVID-19 lockdowns from 31/03/2020 to 21/10/2021, during which movement, occupation and healthcare were heavily restricted, thus reducing our capacity to recruit participants and run experiments. Furthermore, all elective surgeries, including total TMJR surgery, were banned during these lockdowns, further limiting our access to post-surgical total TMJR patients for participation in this study. Despite these limitations, the sample was sufficient to detect significant differences in the mandibular kinematics during border movements between total unilateral TMJR patients and healthy controls. However, due to the inherent variability in human bite force, the sample size

may have underpowered our capacity to detect significant differences in maximum voluntary bite force. Nevertheless, significant differences were detected in bite force direction, muscle forces and asymmetries, TMJ loading direction and ratio of TMJ force to bite force. Second, only women were included in the studies of chapter 5 and 6. The inclusion criteria was chosen because females represent the majority (86.1%) of all total TMJR patients (Granquist et al. 2020); however, further research is required to assess jaw biomechanics in males to generalise the study findings more broadly. Third, only custom implants were considered. Approximately 41% of total TMJR procedures currently use custom implants, with those numbers expected to grow (Zou et al. 2018); and at present, custom implants demonstrate superior postsurgical mouth opening and muscle function compared to stock implants (Kanatsios et al. 2022).

Fourth, the musculoskeletal model used in chapter 6 to evaluate muscle forces and joint loading has not been validated, and this should be considered when interpreting the results of this study. The musculoskeletal model solves for muscle forces and TMJ reaction forces by minimising the sum of squares of the muscle activations subject to force- and moment-equilibrium constrains and the upper limits of each muscles maximum isometric muscle force (Ackland et al. 2015, 2017). This objective function has been shown to effectively recruit the muscles of mastication while allowing for asymmetric recruitment patterns (May et al. 2001). However, future studies into the biomechanics of the masticatory system should focus on validating this model using either EMG data of the masticatory muscles or an instrumented implant to measure *in vivo* TMJ forces. Fifth, for the musculoskeletal model of unilateral total TMJR patients, all muscles were modelled as healthy with full capacity, with the exception of the operated lateral pterygoid muscle, which was modelled as completely severed, as has been done previously (Bhargava et al. 2019; Pinheiro 2021). Future studies should collect additional MRI data to quantify the status of the masseter, temporalis and pterygoid muscles on a subject-specific basis.

## 7.3 FUTURE DIRECTIONS

This thesis provides an investigation of the kinematics, maximum voluntary bite force, muscle force and joint loading of the native mandible and the prosthetic TMJ. The studies forming this thesis report a new approach to the measurement of occlusal loading. They evaluate the chewing kinematics of unilateral total TMJR patients and healthy controls and model the muscle and joint forces during biting to better understand the biomechanical changes following TMJR surgery. There are a number of exciting future directions in this field related to TMJ prosthesis design, evaluation of TMJ kinematics, the expansion and clinical application

of the bite force computational pipeline and advances to our current maxillofacial musculoskeletal models.

### 7.3.1 Future directions for TMJ prosthesis design

Given the restrictions in anterior movement of prosthetic condyles highlighted in chapter 5, future TMJ prosthesis designs ought to focus on returning some anterior gliding movement of the prosthetic condyle over the prosthetic fossa component. Anterior condylar mobility underpins healthy mandibular border movements; the lack of anterior mobility of prosthetic condyles limits mandibular movements and leads to asymmetric mouth opening trajectories in unilateral total TMJR patients. Total TMJR systems typically have a condyle-fossa interface resembling a ball joint. Elongation of the fossa component would allow more anterior sliding of the condyle, although an anterior stop should be included to prevent dislocation. However, to further increase anterior prosthetic condylar movement, the lateral pterygoid function needs to be considered. Previous studies suggest that even partial return of lateral pterygoid function would enhance post-surgical outcomes, including jaw and TMJ mobility (Voiner et al. 2011) and increased bite force (Osborn 1995). Some studies are investigating the possibility of suturing the enthesis of the lateral pterygoid muscle to the prosthetic condylar neck, with good initial outcomes (Mommaerts 2019). Future research ought to investigate this option further for its potential to improve mandibular mobility, reduce muscle asymmetries and alter the lateral joint reaction forces as these changes could improve functional outcomes and long-term stability of prosthetic and native contralateral joints.

Following unilateral total TMJR surgery, patients experience lower resultant joint forces particularly to the native contralateral joint, as discussed in chapter 6. This reduced loading may be a mechanism for the degradation to the native contralateral joint often seen in unilateral total TMJR patients. Post-surgical rehabilitation protocol may be harnessed to counteract this phenomenon. Increasing the loading to the native contralateral joint may slow or prevent this joint degradation. Increased loading to the native contralateral joint may be applied through physical jaw exercises or by predominantly chewing on the ipsilateral side. Further studies, measuring the effect of different rehabilitation practices on the kinematics, maximum voluntary bite force, muscle force and joint loading of patients would provide valuable information and clarify future improvements to rehabilitation practices.

### 7.3.2 Evaluation of TMJ kinematics

Increased understanding of jaw and TMJ kinematics in the healthy and pathological populations would allow us to better understand the development and mechanisms behind TMJ disorders and facilitate improved diagnosis and treatment for patients. While the kinematic measurement systems used in this thesis have given accurate and valuable results, the magnetic tracking system (DMD) of chapter 4 is inaccessible outside Europe and requires a dental clinic and clinician, and the optoelectronic tracking system developed in chapter 5 employs subject-specific equipment which is expensive and time consuming to produce. Future research into jaw and TMJ kinematics ought to consider the use of low-dose x-ray fluoroscopy to give direct measurements of jaw motion while circumventing the use of extra-oral devices or the errors associated with skin motion artefact. This is particularly promising for studies of chewing, where intra- and extra-oral measurement devices may interfere with natural jaw movements. Video motion techniques that use laser scanning of the teeth are a promising lower cost and user-friendly system for research purposes. Furthermore, deep learning based markerless motion tracking could be employed to give low fidelity measurements of jaw kinematics in a user-friendly manner. At present, there is no device appropriate for clinical measurements of jaw kinematics, therefore clinical evaluations are currently limited to measures of MIO distance. However, the development of reliable markerless jaw motion tracking technologies could lead to rapid clinical evaluations of jaw kinematics. This could quickly increase our understanding of pathological jaw kinematics, improve patient understanding of functional limitations, provide intra-operative feedback during TMJ surgery and improve diagnosis and classification of TMJ disorders.

### 7.3.3 Clinical application of the bite force computational modelling pipeline

The experimental and computational modelling pipeline presented in chapter 4 is the first non-invasive technique to measure 3D dynamic bite forces in the healthy population. At present, the procedure requires high user input and lengthy simulation times, restricting its use to research applications. However, simulation time could be reduced through the use of a Eulerian formulation, or by fine tuning the mesh and mass scaling properties of a classic Lagrangian formulation. The simulation time is heavily dependent on the compressibility of the rubber sample participants bit into. Using a rubber material with lower Poisson's ratio than that used in chapters 4 or 6 would decrease simulation time, however this would be at the cost of kinematic accuracy. These changes would decrease simulation time; however, the high user input would still restrict this methodology to research applications. For clinical applications,

given a large enough training set of jaw kinematic measurements, dental geometry and calculated bite forces, it may be possible to use AI to circumvent the need to time consuming simulations altogether. Furthermore, the process of resolving bite forces into muscle and joint loads is easily automated and computationally simple. Therefore, clinical measurements of kinematics during biting, through either magnetic sensors or simple optoelectronic approaches, combined with 3D occlusal anatomy, which is commonly acquired during clinical treatment, could lead to rapid delivery of bite forces, occlusal pressure and muscle and joint loading.

Clinical evaluations of 3D bite force, occlusal pressure and muscle and joint loading could transform maxillofacial orthopaedic practices, dental care and our understanding and diagnosis of TMJ disorders. To highlight the potential of clinical measurements of 3D bite force, consider the treatment of atrophic edentulous alveolus. Traditionally treated with reconstructive surgery including bone grafts, jaw osteotomies, alveolar ridge distraction and zygomatic implants; these complex surgeries are time consuming and have high morbidity (Dimitroulis et al. 2023). The development of additive manufacturing technologies has facilitated the development of subject-specific subperiosteal implants such as the OsseoFrame (Maxoniq, Melbourne) (Figure 7.1). These are custom 3D printed devices designed to interface with each patients remaining bony anatomy; however, the mechanical design and evaluation of the OsseoFrame is based on current literature of uniaxial worst case bite forces. When successful, subperiosteal implants significantly improve masticatory function and quality of life; however, the OsseoFrame currently has high failure rates (33.3%) due to exposure of the excessively bulky frame through the soft tissue (Dimitroulis et al. 2023). Patients with atrophic edentulous alveolus are typically elderly with severely compromised dentition. The evaluation of patient specific 3D bite forces would allow the OsseoFrame to be designed for realistic bite forces much below the worst-case value currently used during the design process, leading to less bulky designs. Less conservative design of the OsseoFrame has the immediate advantage of less failures and revision surgeries due to implant exposure; however, this also reduces stress-shielding to the surrounding bone, improving long-term bone strength and patient outcomes. Further to this, subject-specific evaluations of the mechanical loading of the jaw could optimise other maxillofacial orthopaedic devices such as reconstruction plates and partial and total TMJ replacement systems to enhance long-term patient outcomes and reduce surgical time and expense.

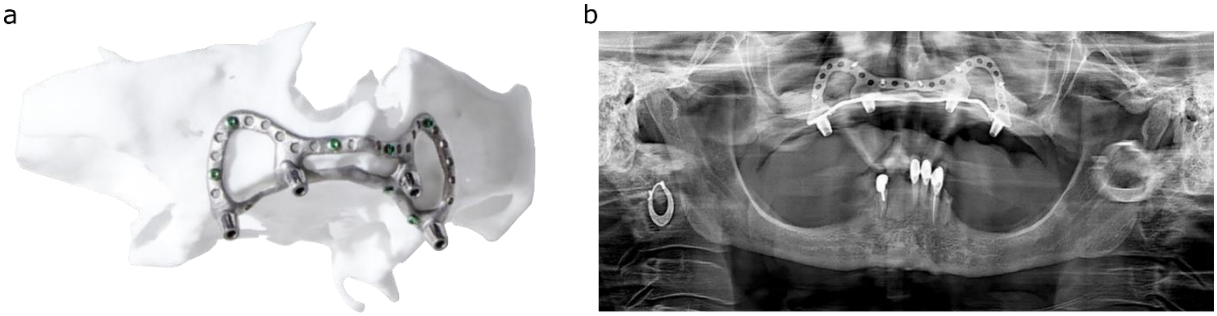



Figure 7.1: OsseoFrame (Maxoniq) subperiosteal implant design (a) and panoramic x-ray showing patient 12 months post-operatively. Figure adapted from Dimitroulis et al (2023).

Rapid clinical evaluation of bite force and occlusal pressure could also enhance dental treatments. Subject- and tooth-specific shear forces could guide the selection of dental implants and influence prescription of conservative dental approaches such as mouthguards for patients with bruxism. Pre-treatment occlusal pressure distributions could be harnessed to precisely design the cusp location and height of dental crowns to facilitate healthy occlusion and prevent long-term issues associated with malocclusion.

Finally, clinical evaluation of mandibular biomechanics could be combined with artificial neural networks to facilitate detection and classification of dental and maxillofacial pathology. Furthermore, AI could be used to predict outcomes of TMD treatments to aid the decision-making process and reinforce realistic expectations of patient outcomes. Combining such predictive modelling with biomechanical data has already proven useful in improving diagnosis, treatment selection and outcome prediction for spine and knee pathologies (Azimi et al. 2020; Tokgoz et al. 2023). Improved diagnosis and treatment would be of particular benefit for patients with TMD symptoms. TMD patients face notoriously long pathways to diagnosis and care, this has been linked to the multidisciplinary nature of TMD treatment, medical practitioners uncertainty in how to manage orofacial pain, cyclical referrals, unnecessary consultations and a lack of clarity between dental and medical approaches to TMD (Breckons et al. 2017). This has negative consequences on patients social, emotional and financial wellbeing.

### 7.3.4 Advances to maxillofacial musculoskeletal modelling

The final study of this thesis employs maxillofacial musculoskeletal modelling. Since its inception in the early 1990s the biomechanical community has collectively improved the accuracy and applicability of early models of the upper and lower extremities. However, at present, there are no open-source maxillofacial musculoskeletal models publicly available; and

therefore, our ability to accurately model the masticatory system is restricted. Future research ought to focus on creating an EMG-assisted maxillofacial model using surface and in-dwelling fine-wire EMG to capture *in vivo* muscle function during biting and mandibular border movements. Furthermore, masticatory muscle parameters are currently based on data obtained from a small sample of cadaver specimens, fine tuning these parameters based on isometric jaw tasks and medical imaging would provide valuable gains to model accuracy. The modelling of mandibular border movements is further complicated by the hyoid bone. Reliably including motion of the hyoid and its muscle attachments into musculoskeletal modelling studies requires dynamic x-ray images to quantify its position. This is impractical in many studies and instead better mathematical models of hyoid motion during mandibular border movements may improve modelling accuracy. In addition to these accuracy gains, understanding the sensitivity of the models output to offsets in muscle insertion points or to external load application method (point load or distributed loading) would aid the interpretation and comparison of maxillofacial musculoskeletal modelling results.

Improving maxillofacial musculoskeletal models will facilitate greater understanding of maxillofacial biomechanics in the healthy and pathological population. Greater confidence in model output may help healthcare providers make better informed decisions, plan surgeries and design personalised rehabilitation programs. Furthermore, increased fidelity in musculoskeletal modelling output would have knock on effects to mathematical and finite element models of the masticatory system which are commonly developed from data derived from musculoskeletal models. Finally, as musculoskeletal, mathematical and finite element models are fundamental for the design and evaluation of prosthetic devices, advances to maxillofacial musculoskeletal models will inherently improve the performance of these devices delivering long-term benefits for patients.

# Bibliography

Aaron LA, Burke MM, Buchwald D (2000) Overlapping Conditions Among Patients With Chronic Fatigue Syndrome, Fibromyalgia, and Temporomandibular Disorder. Arch Intern Med 160:221–227

Abbink JH, Van Der Bilt A, Bosman F, Van Der Glas HW (1999) Speed-dependent Control of Cyclic Open-Close Movements of the Human Jaw with an External Force Counteracting Closing. J Dent Res 78:878–886

Ackland D, Robinson D, Lee PVS, Dimitroulis G (2018) Design and clinical outcome of a novel 3D-printed prosthetic joint replacement for the human temporomandibular joint. Clin Biomech 56:52–60

Ackland DC, Moskaljuk A, Hart C, et al (2015) Prosthesis Loading after Temporomandibular Joint Replacement Surgery: A Musculoskeletal Modeling Study. J Biomech Eng 137:41001

Ackland DC, Robinson D, Redhead M, et al (2017) A personalized 3D-printed prosthetic joint replacement for the human temporomandibular joint: From implant design to implantation. J Mech Behav Biomed Mater 69:404–411

Aggarwal VR, Main CJ (2019) The effectiveness of self-management interventions in adults with chronic orofacial pain: A systematic review, meta-analysis and meta-regression. Eur J Pain 23:849–865. https://doi.org/10.1002/ejp.1358

Ahlers MO, Petersen T, Katzer L, et al (2023) Condylar motion analysis: a controlled, blinded clinical study on the interindividual reproducibility of standardized evaluation of computer-recorded condylar movements. Sci Rep 13:11721. https://doi.org/https://dx.doi.org/10.1038/s41598-023-37139-4

Airoldi RL, Gallo LM, Palla S (1994) Precision of the Jaw Tracking System JAWS-3D. J Orofac Pain 8:155–164

Akashi M, Hasegawa T, Takahashi S, Komori T (2018) Four-Dimensional Computed Tomography Evaluation of Condylar Movement in a Patient With Temporomandibular Joint Osteoarthritis. J Oral Maxillofac Surg 76:304–313

Akashi M, Shibuya Y, Takahashi S, et al (2016) Four-dimensional computed tomography

evaluation of jaw movement following mandibular reconstruction : A pilot study. J Cranio-Maxillofacial Surg 44:637–641

Al-ani Z (2021) Temporomandibular Joint Osteoarthrosis: a review of clinical aspects and management. Prim Dent J 10:132–140. https://doi.org/10.1177/2050168420980977

Al-Omiri MK, Sghaireen MG, Alhijawi MM, et al (2014) Maximum bite force following unilateral implant-supported prosthetic treatment: within-subject comparison to opposite dentate side. J Oral Rehabil 41:624–629

Albano MG, François J, Andrade V De, Levy G (2019) Patient education in dental medicine: A review of the literature. Eur J Dent Educ 23:110–118. https://doi.org/10.1111/eje.12409

Alexander TA, Gibbs CH, Thompson WJ (1984) Investigation of chewing patterns in deep-bite malocclusions before and after orthodontic treatment. Am J Orthod 85:21–27

Allison KM, Nip ISB, Rong P (2022) Use of Automated Kinematic Diadochokinesis Analysis to Identify Potential Indicators of Speech Motor Involvement in Children With Cerebral Palsy. Am J speech-language Pathol 31:2835–2846. https://doi.org/https://dx.doi.org/10.1044/2022_AJSLP-21-00241

Alsawaf MM, Missert W, Janecka IP (1993) Effect of lateral cranial base surgery on temporomandibular joint function. J Prosthet Dent 69:200–208

Alstergren P, Davidson T (2017) Oral Rehabilitation Pharmacological treatment of oro-facial pain – health technology assessment including a systematic review with network meta-analysis. J Oral Rehabil 44:800–826. https://doi.org/10.1111/joor.12539

Amhamed M, Whittle T, Maulina T, et al (2016) Effect of experimental anterior temporalis muscle pain on jaw movements. J Oral Rehabil 43:889–899

Anderson K, Throckmorton GS, Buschang PH, Hayasaki H (2002) The effects of bolus hardness on masticatory kinematics. J Oral Rehabil 29:689–696. https://doi.org/10.1046/j.1365-2842.2002.00862.x

Atwood DA (1968) A critique of research of the posterior limit of the mandibular position. J Prosthet Dent 20:21–36

Auerbach SM, Laskin DM, Frantsve LME, Orr T (2001) Depression, Pain, Exposure to Stressful Life Events, and Long-Term Outcomes in Temporomandibular Disorder

Patients. J oral Maxillofac Surg 59:628–633. https://doi.org/10.1053/joms.2001.23371

Auvenshine RC, Pettit NJ (2020) The hyoid bone: an overview. CRANIO 38:6–14. https://doi.org/10.1080/08869634.2018.1487501

Ayn DY, Hakim MA, August M, et al (2022) Hypomobility and Hypermobility Disorders of the Temporomandibular Joint. In: Peterson's Principles of Oral and Maxillofacial Surgery

Azimi P, Yazdanian T, Benzel EC, et al (2020) A Review on the Use of Artificial Intelligence in Spinal Diseases. Asian Spine J 14:543

Baeyens JP, Gilomen H, Erdmann B, et al (2013) In vivo measurement of the 3D kinematics of the temporomandibular joint using miniaturized electromagnetic trackers: Technical report. Med Biol Eng Comput 51:479–484

Bakke M (2006) Bite Force and Occlusion. Semin Orthod 12:120–126

Baltali E, Zhao KD, Koff MF, et al (2008a) Kinematic Assessment of the Temporomandibular Joint Before and After Partial Metal Fossa Eminence Replacement Surgery: A Prospective Study. J Oral Maxillofac Surg 66:1383–1389

Baltali E, Zhao KD, Koff MF, et al (2008b) A Method for Quantifying Condylar Motion in Patients With Osteoarthritis Using an Electromagnetic Tracking Device and Computed Tomography Imaging. J Oral Maxillofac Surg 66:848–857

Bando E, Nishigawa K, Nakano M, et al (2009) Current status of researches on jaw movement and occlusion for clinical application. Jpn Dent Sci Rev 45:83–97

Baqaien MA, Al-Salti FM, Muessig D (2007) Changes in condylar path inclination during maximum protrusion between the ages of 6 and 12 years. J Oral Rehabil 34:27–33

Barbier L, Vander Sloten J, Krzesinski G, et al (1998) Finite element analysis of non-axial versus axial loading of oral implants in the mandible of the dog. J Oral Rehabil 25:847–858

Bekcioglu B, Bulut E, Bas B (2017) The Effects of Unilateral Alloplastic Temporomandibular Joint Replacement on the Opposite-Side Natural Joint: A Finite-Element Analysis. J Oral Maxillofac Surg 75:2316–2322

Bell RA, Kiebach TJ (2014) Posterior crossbites in children: Developmental-based diagnosis and implications to normative growth patterns. Semin Orthod 20:77–113.

https://doi.org/10.1053/j.sodo.2014.04.002

Bernhardt O, Küppers N, Rosin M, Meyer G (2003) Comparative tests of arbitrary and kinematic transverse horizontal axis recordings of mandibular movements. J Prosthet Dent 89:175–179

Bescond G, Gales M, Glineur R, et al (2023) Complete 3D Kinematics Parameters of the Temporo-Mandibular Joints Using in Vivo Data Fusion. IRBM 44:. https://doi.org/10.1016/j.irbm.2023.100804

Bhargava D, Neelakandan RS, Dalsingh V, et al (2019) A three dimensional (3D) musculoskeletal finite element analysis of DARSN temporomandibular joint (TMJ) prosthesis for total unilateral alloplastic joint replacement. J Stomatol Oral Maxillofac Surg 120:517–522

Bhaskaracharya M, Memon SM, Whittle T, Murray GM (2015) Jaw movements in patients with a history of pain: An exploratory study. J Oral Rehabil 42:18–26

Bhatka R, Throckmorton GS, Wintergerst AM, et al (2004) Bolus size and unilateral chewing cycle kinematics. Arch Oral Biol 49:559–566. https://doi.org/10.1016/j.archoralbio.2004.01.014

Bonjardim LR, Gaviao MBD, Pereira LJ, Castelo PM (2005) Bite force determination in adolescents with and without temporomandibular dysfunction. J Oral Rehabil 32:577–583

Breckons M, Bissett SM, Exley C, Durham J (2017) Care Pathways in Persistent Orofacial Pain: Qualitative Evidence from the DEEP Study. JDR Clin Transl Res 2:48–57. https://doi.org/10.1177/2380084416679648

Brierly G, Thomas A, Dimitroulis G (2022) A five-year review of the OMX temporomandibular prosthetic total joint replacement system. Oral Maxillofac Surg

Buschang PH, Hayasaki H, Throckmorton GS (2000) Quantification of human chewing-cycle kinematics. Arch Oral Biol 45:461–474. https://doi.org/http://dx.doi.org/10.1016/S0003-9969%2800%2900015-7

Buschang PH, Throckmorton GS, Travers KH, Hayasaki H (2001) Incisor and mandibular condylar movements of young adult females during maximum protrusion and lateratrusion of the jaw. Arch Oral Biol 46:39–48. https://doi.org/10.1016/S0003-9969(00)00096-0

C. S, A. U, D. S, et al (2011) Three-dimensional mandibular motion after closed and open reduction of unilateral mandibular condylar process fractures. J Cranio-Maxillofacial Surg 39:249–255. https://doi.org/http://dx.doi.org/10.1016/j.jcms.2010.06.005

Caldas R, Mundt M, Potthast W, et al (2017) A systematic review of gait analysis methods based on inertial sensors and adaptive algorithms. 57:204–210

Calixtre LB, Nakagawa TH, Alburquerque-Sendin F, et al (2017) Inter- and intra-rater reliability of 3D kinematics during maximum mouth opening of asymptomatic subjects. J Biomech 64:245–252

Carla A, Carvalho B De, Practice P, et al (2017) Acupuncture in Temporomandibular Disorder Myofascial Pain Treatment: A Systematic Review. J Oral Facial Pain Headache 225–232. https://doi.org/10.11607/ofph.1719

Carlsson GE (1999) Epidemiology and Treatment Need for Temporomandibular Disorders. J Orofac Pain 13:232–237

Ćatić A, Naeije M (1999) Location of the hinge axis and the kinematic centre in asymptomatic and clicking temporomandibular joints. J Oral Rehabil 26:661–665

Celebi N, Rohner EC, Gateno J, et al (2011) Development of a mandibular motion simulator for total joint replacement. J Oral Maxillofac Surg 69:66–79

Chang AR, Han JJ, Kim D-S, et al (2015) Evaluation of intra-articular distance narrowing during temporomandibular joint movement in patients with facial asymmetry using 3-dimensional computed tomography image and tracking camera system. J Cranio-Maxillofacial Surg 43:342–348

Chen C-C, Chen Y-J, Chen S-C, et al (2011) Evaluation of soft-tissue artifacts when using anatomical and technical markers to measure mandibular motion. J Dent Sci 6:95–101

Chen C-C, Lin C-C, Chen Y-J, et al (2013a) A method for measuring three-dimensional mandibular kinematics in vivo using single-plane fluoroscopy. Dentomaxillofacial Radiol 42:

Chen C-C, Lin C-C, Hsieh H-P, et al (2021) In vivo three-dimensional mandibular kinematics and functional point trajectories during temporomandibular activities using 3d fluoroscopy. Dentomaxillofac Radiol 50:20190464. https://doi.org/https://dx.doi.org/10.1259/dmfr.20190464

Chen C-C, Lin C-C, Lu T-W, et al (2013b) Feasibility of differential quantification of 3D temporomandibular kinematics during various oral activities using a cone-beam computed tomography-based 3D fluoroscopic method. J Dent Sci 8:151–159

Choi B-T, Hwang D-Y, Lee G-H, et al (2019) Computerized ultrasonic axiographic evaluation of condylar movement in patients with internal derangement of the temporomandibular joint. Angle Orthod 89:924–929. https://doi.org/10.2319/110618-792.1

Coffey JP, Mahan PE, Gibbis CH, Welsch BB (1989) A Preliminary Study of the Effects of Tooth Guidance on Working-Side Condylar Movement. J Prosthet Dent 62:157–162

Connelly ST, Silva R, Gupta R, Hare MO (2019) Temporomandibular Joint Discectomy Followed by Disc Replacement Using Viable Osteochondral and Umbilical Cord Allografts Results in Improved Patient Outcomes. J Oral Maxillofac Surg 78:63–74. https://doi.org/10.1016/j.joms.2019.05.024

Cooper BC, Kleinberg I (2007) Examination of a large patient population for the presence of symptoms and signs of temporomandibular disorders. Cranio - J Craniomandib Pract 25:114–126

Cordeiro C da C, Pozza DH, Tamaki T, Guimarães AS (2018) The importance of the posterior joint space for functional mandibular movements: A laboratory cross-sectional study. J Clin Exp Dent 10:e61–e65. https://doi.org/10.4317/jced.54168

Coutant J-C, Ella Nguema B, Mesnard M, et al (2011) Temporo Mandibular Joint Kinematic: The Specificity of the Rotatory Component Involved in Disc-Condyle Displacements along the Temporal Bone Surface. In: Jobbagy A (ed) IFMBE Proceedings. p 799+

Coutant J-C, Mesnard M, Morlier J, et al (2008) Discrimination of objective kinematic characters in temporomandibular joint displacements. Arch Oral Biol 53:453–461

Crane EA, Cassidy RB, Rothman ED, Gerstner GE (2010) Effect of registration on cyclical kinematic data. J Biomech 43:2444–2447

Crane EA, Rothman ED, Childers D, Gerstner GE (2013) Analysis of temporal variation in human masticatory cycles during gum chewing. Arch Oral Biol 58:1464–1474

Crowe M, Sheppard L (2011) A review of critical appraisal tools show they lack rigor: Alternative tool structure is proposed. J Clin Epidemiol 64:79–89

De Felicio CM, Mapelli A, Sidequersky FV, et al (2013) Mandibular kinematics and masticatory muscles EMG in patients with short lasting TMD of mild-moderate severity. J Electromyogr Kinesiol 23:627–633

De Meurechy N, Mommaerts MY (2018) Alloplastic temporomandibular joint replacement systems: a systematic review of their history. Int J Oral Maxillofac Surg 47:743–754. https://doi.org/10.1016/j.ijom.2018.01.014

Dijkstra PA, de Bont LGM, Stegenga B, Boering G (1995) Temporomandibular joint mobility assessment: a comparison between four methods. J Oral Rehabil 439–444

Dimitroulis G (2011) Temporomandibular joint surgery: what does it mean to the dental practitioner? Aust Dent J 56:257–264. https://doi.org/10.1111/j.1834-7819.2011.01351.x

Dimitroulis G (2018) Management of temporomandibular joint disorders: A surgeon's perspective. Aust Dent J 63:79–90. https://doi.org/10.1111/adj.12593

Dimitroulis G, Austin S, Lee PVS, Ackland D (2018) A new three-dimensional, print-on-demand temporomandibular prosthetic total joint replacement system: Preliminary outcomes. J Cranio-Maxillofacial Surg 46:1192–1198

Dimitroulis G, Gupta B, Wilson I, Hart C (2023) The atrophic edentulous alveolus . A preliminary study on a new generation of subperiosteal implants. Oral Maxillofac Surg 69–78. https://doi.org/10.1007/s10006-022-01044-3

Dionne RA (1997) Pharmacologic treatments for temporomandibular disorders. Oral Surgery, Oral Med Oral Pathol Oral Radiol Endodontology 83:134–142

Downs SH, Black N (1998) Feasibility of creating checklist for assessment of method quality both of randomised and non randomised studies of health care innovations. J Epidemiol Community Health 52:377–384

Driemel O, Ach T, Muller-Richter UDA, et al (2009a) Historical development of alloplastic temporomandibular joint replacement before 1945. Int J Oral Maxillofac Surg 38:301–307. https://doi.org/10.1016/j.ijom.2008.12.014

Driemel O, Braun S, Muller-Richter UDA, et al (2009b) Historical development of alloplastic temporomandibular joint replacement after 1945 and state of the art. Int J Oral Maxillofac Surg 38:909–920. https://doi.org/10.1016/j.ijom.2009.01.022

Drummond JL (2008) Degradation, Fatigue, and Failure of Resin Dental Composite

Materials. J Dent Res 87:710–719

Durham J, Arrarwal V, Davies SJ, et al (2013) Temporomandibular Disorders (TMDs): an update and management guidance for primary care from the UK Specialist Interest Group in Orofacial Pain and TMDs (USOT). Royal College of Surgeons of England

Durham J, Breckons M (2016) Self-management programmes in temporomandibular disorders: results from an international Delphi process. J Oral Rehabil 43:929–936. https://doi.org/10.1111/joor.12448

Eerikainen E, Kononen M (1987) Forces required by complete dentures for penetrating food in simulated function. J Oral Rehabil 14:607–613

Eggers GWN (1946) Arthroplasty of the temporomandibular joint in children with interposition of tantalum foil. JBJS 28:603–606

Elledge R, Mercuri LG, Attard A, et al (2019) Review of emerging temporomandibular joint total joint replacement systems. Br J Oral Maxillofac Surg 57:722–728. https://doi.org/10.1016/j.bjoms.2019.08.009

Elm E Von, Altman DG, Egger M, et al (2007) The Strengthening the Reporting of Observational Studies in Epidemiology ( STROBE ) Statement Guidelines for Reporting Observational Studies. Epidemiology 18:800–804

Eriksson L, Westesson P (2001) Discectomy as an Effective Treatment for Painful Temporomandibular Joint Internal Derangement: A 5-Year Clinical and Radiographic Follow-Up. J Oral Maxillofac Surg 59:750–758. https://doi.org/10.1053/joms.2001.24288

Ermolin VI, Chkadua TZ, Staricov NA, et al (2023) The effects of a total TMJ endoprosthesis on the contralateral condyle. Vliyanie dvukhkomponentnogo endoproteza visochno-nizhnechelyustnogo sustava na kontralateral'nyi myshchelkovyi otrostok 102:9–15. https://doi.org/https://dx.doi.org/10.17116/stomat20231020619

Ettlin DA, Mang H, Colombo V, et al (2008) Stereometric assessment of TMJ space variation by occlusal splints. J Dent Res 87:877–881. https://doi.org/http://dx.doi.org/10.1177/154405910808700903

Ewers R, Schicho K, Undt G, et al (2005) Basic research and 12 years of clinical experience in computer-assisted navigation technology: A review. Int J Oral Maxillofac Surg 34:1–8

Fang J-J, Kuo T-H (2008) Modelling of mandibular movement. Comput Biol Med 38:1152–1162

Farella M, Palla S, Erni S, et al (2008) Masticatory muscle activity during deliberately performed oral tasks. Physiol Meas 29:1397–1410. https://doi.org/10.1088/0967-3334/29/12/004

Farronato M, Tartaglia GM, Maspero C, et al (2021) In vitro and in vivo assessment of a new workflow for the acquisition of mandibular kinematics based on portable tracking system with passive optical reflective markers. Appl Sci 11:. https://doi.org/10.3390/app11093947

Feng Y, Shu J, Liu Y, et al (2021) Biomechanical analysis of temporomandibular joints during mandibular protrusion and retraction motions: A 3d finite element simulation. Comput Methods Programs Biomed 208:106299. https://doi.org/https://dx.doi.org/10.1016/j.cmpb.2021.106299

Feng Y, Zhan L, Sun X, et al (2023) A fully digital workflow to register maxillomandibular relation using a jaw motion tracer for fixed prosthetic rehabilitation: A technical report. J Esthet Restor Dent 35:1068–1076. https://doi.org/https://dx.doi.org/10.1111/jerd.13058

Ferrario VF, Sforza C (1994) Biomechanical model of the human mandible in unilateral clench: Distribution of temporomandibular joint reaction forces between working and balancing sides. J Prosthet Dent 72:169–176

Ferrario VF, Sforza C, Lovecchio N, Mian F (2005) Quantification of translational and gliding components in human temporomandibular joint during mouth opening. Arch Oral Biol 50:507–515. https://doi.org/http://dx.doi.org/10.1016/j.archoralbio.2004.10.002

Ferrario VF, Sforza C, Serrao G, et al (2004a) Single tooth bite forces in healthy young adults. J Oral Rehabil 31:18–22

Ferrario VF, Sforza C, Zanotti G, Tartaglia GM (2004b) Maximal bite forces in healthy young adults as predicted by surface electromyography. J Dent 32:451–457

Flanagan D, Ilies H, O'Brien B, et al (2012) Jaw Bite Force Measurement Device. J Oral Implantol 38:361–364

Flot F, Stricker M, Chassagne JF (1984) Role of the intermediate prosthesis with a noncemented cupula in the reconstructive surgery of the temporomandibular joint. Ann

Chir Plast Esthet 29:253–255

Franco PF, Talwar RM, Wolford LM (1997) Unilateral TMJ total joint reconstruction and the effects on the contralateral joint. AAOMS 79th Annual Meeting and Scientific Sessions. J Oral Maxillofac Surg 55:113

Fushima K, Gallo LM, Krebs M, Palla S (2003) Analysis of the TMJ intraarticular space variation: A non-invasive insight during mastication. Med Eng Phys 25:181–190

Gallo LM, Airoldi GB, Airoldi RL, Palla S (1997) Description of mandibular finite helical axis pathways in asymptomatic subjects. J Dent Res 76:704–713

Gallo LM, Brasi M, Ernst B, Palla S (2006) Relevance of mandibular helical axis analysis in functional and dysfunctional TMJs. J Biomech 39:1716–1725

Gallo LM, Fushima K, Palla S (2000) Mandibular helical axis pathways during mastication. J Dent Res 79:1566–1572

Gallo LM, Gössi DB, Colombo V, Palla S (2008) Relationship between kinematic center and TMJ anatomy and function. J Dent Res 87:726–730

Gatchel RJ, Stowell AW, Wildenstein L, et al (2006) Efficacy of an early intervention for patients with acute temporomandibular disorder–related pain. J Am Dent Assoc 137:339–347

Gauer R, Semidey MJ (2015) Diagnosis and treatment of temporomandibular disorders. Am Fam Physician 91:378–386

Genovesi W, Comenale IC, Genovesi Filho W, Veloso Fernandes M (2022) Biomechanical comparative analysis of temporomandibular joint, glenoid fossa and head of the condyle of conventional models prothesis with new PEEK design. J Oral Biol Craniofacial Res 12:529–541

Gerbino G, Zavattero E, Berrone S, Ramieri G (2016) One stage treatment of temporomandibular joint complete bony ankylosis using total joint replacement. J Cranio-Maxillofacial Surg 44:487–492

Gerbino G, Zavattero E, Bosco G, et al (2017) Temporomandibular joint reconstruction with stock and custom-made devices: Indications and results of a 14-year experience. J Cranio-Maxillofacial Surg 45:1710–1715. https://doi.org/10.1016/j.jcms.2017.07.011

Gerstner GE, Lafia C, Lin D (2005) Predicting masticatory jaw movements from chin

movements using multivariate linear methods. J Biomech 38:1991–1999

Ghodsi S, Rasaeipour S (2018) Revising Average Condylar Inclinations Using Electronic Pantograph Assessment: A Cross-Sectional Study. Dent Hypotheses 9:84–89

Giannakopoulos HE, Sinn DP (2012) Biomet Microfixation Temporomandibular Joint Replacement System: A 3-Year Follow-Up Study of Patients Treated During 1995 to 2005. J Oral Maxillofac Surg 70:787–794. https://doi.org/10.1016/j.joms.2011.09.031

Giannakopoulos HE, Sinn DP, Quinn PD (2012) Biomet microfixation temporomandibular joint replacement system: A 3-year follow-up study of patients treated during 1995 to 2005. J Oral Maxillofac Surg 70:787–794. https://doi.org/10.1016/j.joms.2011.09.031

Gibbs CH, Messerman T, Reswick JB, Derda HJ (1971) Functional Movements of the Mandible. J Prosthet Dent 26:604–620

Gibbs CH, Suit SR, Benz ST (1973) Masticatory movements of the jaw measured at angles of approach to the occlusal plane. J Prosthet Dent 30:283–288

Gibbs CH, Wickwire NA, Jacobson AP, et al (1982) Comparison of typical chewing patterns in normal children and adults. J Am Dent Assoc 105:33–42

Godoi DA De, Alvares J, Bonini D, et al (2010) Symptoms of Temporomandibular Disorders in the Population: An Epidemiological Study. J Orofac Pain 24:270–278

Goob J, Erdelt K, Schweiger J, et al (2020) Reproducibility of a magnet-based jaw motion analysis system. Int J Comput Dent 23:39–48

Gosen AJ (1974) Mandibular leverage and occlusion. J Prosthet Dent 31:369–376. https://doi.org/10.1016/0022-3913(74)90144-9

Goto TK, Langenbach GEJ, Hannam AG (2001) Length changes in the human masseter muscle after jaw movement. Anat Rec 262:293–300

Granquist EJ, Bouloux G, Dattilo D, et al (2020) Outcomes and Survivorship of Biomet Microfixation Total Joint Replacement System: Results From an FDA Postmarket Study. J Oral Maxillofac Surg 78:1499–1508

Gray RJ, Quayle AA, Hall CA, Schofield MA (1994) Physiotherapy in the treatment of temporomandibular joint disorders: a comparative study of four treatment methods. Br Dent J 176:257–261. https://doi.org/10.1038/sj.bdj.4808429

Greene CS (2010) Managing the Care of Patients With Temporomandibular Disorders. J Am

Dent Assoc 141:1086–1088. https://doi.org/10.14219/jada.archive.2010.0337

Grochala J, Grochala D, Kajor M, et al (2021) A Novel Method of Temporomandibular Joint Hypermobility Diagnosis Based on Signal Analysis. J Clin Med 10:5145

Guo J, Chen J, Wang J, et al (2022) EMG-assisted forward dynamics simulation of subject-specific mandible musculoskeletal system. J Biomech 139:111143. https://doi.org/https://dx.doi.org/10.1016/j.jbiomech.2022.111143

Gutman Y, Keller J (2018) Jaw Tracking Device and Methods of Analysis of Patient's Specific TMJ Kinematics. ACTA Sci Dent Sci 2:73–79

Hahn GW (1964) Vitallium mesh mandibular prosthesis. J Prosthet Dent 14:777–784

Hamrick KS, Andrews M, Guthrie J, et al (2011) How Much Time Do Americans Spend on Food?

Hanley B, Tucker CB (2018) Differences between motion capture and video analysis systems in calculating knee angles in elite-standard race walking. J Sports Sci 36:1250–1255

Hart HF, Culvenor AG, Collins NJ, et al (2016) Knee kinematics and joint moments during gait following anterior cruciate ligament econstruction: A systematic review and meta-analysis. Br J Sports Med 50:597–612

Hasan I, Madarlis C, Keilig L, et al (2016) Changes in biting forces with implant-supported overdenture in the lower jaw: A comparison between conventional and mini implants in a pilot study. Ann Anat 208:116–122

Hattori Y, Satoh C, Kunieda T, et al (2009) Bite forces and their resultants during forceful intercuspal clenching in humans. J Biomech 42:1533–1538. https://doi.org/10.1016/j.jbiomech.2009.03.040

Hattori Y, Satoh C, Seki S, et al (2003) Occlusal and TMJ Loads in Subjects with Experimentally Shortened Dental Arches. J Dent Res 82:532–536

Hayasaki H, Saitoh I, Iwase Y, et al (2008) Movement of the instantaneous center of rotation and the position of the lateral excursion center during lateral excursion. Cranio - J Craniomandib Pract 26:253–262

Hayashi K, Hayashi M, Reich B, et al (2012) Functional data analysis of mandibular movement using third-degree b-spline basis functions and self-modeling regression. Orthod Waves 71:17–25

Hayashi K, Reich B, Delong R, et al (2009) A novel statistical model for mandibular helical axis analysis. J Oral Rehabil 36:102–109

Hellsing G (1980) On the regulation of interincisor bite force in man. J Oral Rehabil 7:403–411

Hill AM, Bull AMJ, Dallalana RJ, et al (2007) Glenohumeral motion : review of measurement techniques. Knee Surgery, Sport Traumatol Arthrosc 15:1137–1143

Hirai S, Ogawa T, Shigeta Y, et al (2009) Characteristics of mandibular movements in patients with square mandible. Oral Surgery, Oral Med Oral Pathol Oral Radiol Endodontology 108:e75–e81

Hoffmann RG, Kotchen M, Kotchen TA, et al (2011) Temporomandibular Disorders and Associated Clinical Comorbidities. Clin J Pain 27:268–274

Hosogai A, Hayashi T, Kohno S, et al (2008) A precise and useful method for coordinating computed tomography and jaw movement frames of reference. Nihon Hotetsu Shika Gakkai Zasshi 52:529–536

Huang W, Akashi M, Nishio T, et al (2020) Can four-dimensional computed tomography support diagnosis and treatment planning?: a case report before and after coronoidectomy. Oral Maxillofac Surg 24:515–520. https://doi.org/https://dx.doi.org/10.1007/s10006-020-00876-1

Hüe O (2011) Condylar Paths during Protrusion in Edentulous Patients: Analysis with Electronic Axiography. J Prosthodont 20:294–298

Hugger A, Boloni E, Berntien U, Stuttgen U (2001) Accuracy of an ultrasonic measurement system for jaw movement recording. J Dent Res 80:1226

Hujoel PP (1994) A meta-analysis of normal ranges for root surface areas of the permanent dentition. J Clin Periodontol 21:225–229

Ingawale S, Goswami T (2009) Temporomandibular Joint: Disorders, Treatments, and Biomechanics. Ann Biomed Eng 37:976–996. https://doi.org/10.1007/s10439-009-9659-4

Israel HA (2016) Internal Derangement of the Temporomandibular Joint: New Perspectives on an Old Problem. Oral Maxillofac Surg Clin North Am 28:313–333. https://doi.org/10.1016/j.coms.2016.03.009

Iwasaki LR, Crosby MJ, Gonzalez Y, et al (2009) Temporomandibular joint loads in subjects with and without disc displacement. Orthop Rev (Pavia) 1:. https://doi.org/10.4081/or.2009.e29

Iwasaki LR, Gonzalez YM, Liu Y, et al (2017) TMJ energy densities in healthy men and women. Osteoarthr Cartil 25:846–849. https://doi.org/10.1016/j.joca.2016.12.027

Iwasaki LR, Petsche PE, McCall WD, et al (2003) Neuromuscular objectives of the human masticatory apparatus during static biting. Arch Oral Biol 48:767–777. https://doi.org/10.1016/S0003-9969(03)00171-7

Iwase Y, Saitoh I, Okamoto A, et al (2019) Comparison of dynamic occlusal contacts during chewing between children with primary dentition and normal adult females. Pediatr Dent J 29:116–122. https://doi.org/10.1016/j.pdj.2019.07.004

Johnson GM, Coe H, Wirawan R, et al (2007) Objective Discrimination Between Mandibular Open/Close Excursion Patterns: A Clinical Case Report. J Craniomandib Sleep Pract 25:218–224

Johnson GR, Anderson JM (1990) Measurement of three-dimensional shoulder movement by an electromagnetic sensor. Clin Biomech 5:131–136

Johnson J, Johansson M, Ryd A (2015) Impact of trismus on health-related quality of life and mental health. Head Neck 1672–1680

Johnson NR, Roberts MJ, Doi SA, Batstone MD (2017) Total temporomandibular joint replacement prostheses: a systematic review and bias- adjusted meta-analysis. Int J Oral Maxillofac Surg 46:86–92

Jurt A, Lee J-YJ-Y, Gallo LM, Colombo V (2020) Influence of bolus size and chewing side on temporomandibular joint intra-articular space during mastication. Med Eng Phys 86:41–46. https://doi.org/https://dx.doi.org/10.1016/j.medengphy.2020.10.006

Kalaykova S, Lobbezoo F, Naeije M (2011) Effect of chewing upon disc reduction in the temporomandibular joint. J Oral Facial Pain Headache 25:49–55

Kalladka M, Quek S, Heir G, et al (2014) Temporomandibular joint osteoarthritis: Diagnosis and long-term Conservative management: A topic review. J Indian Prosthodont Soc 14:6–15

Kanatsios S, Thomas AM, Tocaciu S (2022) Comparative clinical outcomes between stock vs

custom temporomandibular total joint replacement systems. J Cranio-Maxillofacial Surg 50:322–327. https://doi.org/10.1016/j.jcms.2022.02.003

Kapos FP, Exposito FG, Oyarzo JF, Durham J (2020) Temporomandibular disorders: a review of current concepts in aetiology, diagnosis and management. Oral Surg 13:321–334. https://doi.org/10.1111/ors.12473

Kawaguchi T, Kawata T, Kuriyagawa T, Sasaki K (2007) In vivo 3-dimensional measurement of the force exerted on a tooth during clenching. J Biomech 40:244–251. https://doi.org/10.1016/j.jbiomech.2006.01.004

Kawashima Bori F, Fukuhara M, Masaki C, et al (2020) The relationship between masticatory performance and intakes of foods and nutrients in Japanese male workers: A cross-sectional study. J Oral Rehabil 47:1142–1149

Keeling SD, Gibbs CH, Lupkiewicz SM, et al (1991) Analysis of repeated-measure multicycle unilateral mastication in children. Am J Orthod Dentofac Orthop 99:402–408

Keller EE, Baltali E, Liang X, et al (2012) Temporomandibular custom hemijoint replacement prosthesis: Prospective clinical and kinematic study. J Oral Maxillofac Surg 70:276–288

Kenworthy CR, Morrish RB, Mohn C, et al (1997) Bilateral condylar movement patterns in adult subjects. J Orofac Pain 11:328–36

Kim D-S, Choi S-C, Lee S-S, et al (2013) Principal direction of inertia for 3D trajectories from patient-specific TMJ movement. Comput Biol Med 43:169–175

Kim JH, Park BH, Yoo MS, Lee BK (2021) Stability of the natural joint side in unilateral alloplastic total temporomandibular joint replacement using a ready-made system. Appl Sci 11:

Kim K, Wojczyńska A, Lee J (2016) The incidence of osteoarthritic change on computed tomography of Korean temporomandibular disorder patients diagnosed by RDC/TMD; a retrospective study. Acta Odontol Scand 74:337–342. https://doi.org/10.3109/00016357.2015.1136678

Kim S-G, Kim D-S, Choi S-C, et al (2010) The relationship between three-dimensional principal rotations and mandibular deviation. Oral Surgery, Oral Med Oral Pathol Oral Radiol Endodontology 110:52–60

Kimoto A, Yamashita J, Ohori H, et al (2023) A Novel Imaging Technique for Analyzing

Condylar Movement During Mastication in Patients With Jaw Deformities: Four-Dimensional Computed Tomography. J Craniofac Surg 34:1880–1883. https://doi.org/https://dx.doi.org/10.1097/SCS.0000000000009509

Kiseri B, Dayan Ç, Yildiz M, Sülün T (2018) The correlation between direction and amount of retrusive movement and condyle position and joint space. Cranio 36:250–256

Ko EW-C, Alazizi AI, Lin C-H (2015) Three-dimensional surgical changes of mandibular proximal segments affect outcome of jaw motion analysis. J Oral Maxillofac Surg 73:971–984

Ko EW-C, Huang CS, Lo L-J, Chen Y-R (2012) Longitudinal observation of mandibular motion pattern in patients with skeletal class III malocclusion subsequent to orthognathic surgery. J Oral Maxillofac Surg 70:e158–e168

Koc D, Dogan A, Bek B (2010) Bite Force and Influential Factors on Bite Force Measurements: A Literature Review. Eur J Dent 4:223–232

Kogawa EM, Calderon PS, Lauris JRP, et al (2006) Evaluation of maximal bite force in temporomandibular disorders patients. J Oral Rehabil 33:559–565

Koolstra JH, Van Eijden TMGJ (2005) Combined finite-element and rigid-body analysis of human jaw joint dynamics. J Biomech 38:2431–2439

Kordaß B, Bernhardt O, Ratzmann A, et al (2014) Standard and limit values of mandibular condylar and incisal movement capacity. Int J Comput Dent 17:9–20

Krebs M, Gallo LM, Airoldi RL, et al (1994) Three-dimensional animation of the temporomandibular joint. Technol Heal Care 2:193–207

Krebs M, Gallo LM, Airoldi RL, Palla S (1995) A new method for three-dimensional reconstruction and animation of the temporomandibular joint. Ann Acad Med Singapore 24:11–16

Kshirsagar R, Jaggi N, Halli R (2011) Bite Force Measurement in Mandibular Parasymphyseal Fractures: A Preliminary Clinical Study. Craniomaxillofac Trauma Reconstr 4:241–244

Kubota N, Hayasaki H, Saitoh I, et al (2010) Jaw Motion During Gum-Chewing in Children with Primary Dentition. CRANIO-THE J Craniomandib Pract 28:19–29

Kucukkeles N, Ozkan H, Ari-Demirkaya A, Cilingirturk AM (2005) Compatibility of

mechanical and computerized axiographs: A pilot study. J Prosthet Dent 94:190–194

Kumagai H, Suzuki T, Hamada T, et al (1999) Occlusal force distribution on the dental arch during various levels of clenching. J Oral Rehabil 26:932–935

Kummoona R (1978) Functional rehabilitation of ankylosed temporomandibular joints. Oral Surgery, Oral Med Oral Pathol 46:495–505. https://doi.org/10.1016/0030-4220(78)90379-1

Kwon JH, Im S, Chang M, et al (2019) A digital approach to dynamic jaw tracking using a target tracking system and a structured-light three-dimensional scanner. J Prosthodont Res 63:115–119

Laird MF, Ross CF, O'Higgins P (2020) Jaw kinematics and mandibular morphology in humans. J Hum Evol 139:102639. https://doi.org/10.1016/j.jhevol.2019.102639

Landes CA, Sterz M (2003) Evaluation of Condylar Translation by Sonography Versus Axiography in Orthognathic Surgery Patients. J Oral Maxillofac Surg 61:1410–1417

Lassauzay C, Peyron M-A, Albuisson E, et al (2000) Variability of the masticatory process during chewing of elastic model foods. Eur J Oral Sci 108:484–492

Leader JK, Boston JR, Rudy TE, et al (1997) Use of sound and jaw movement patterns to characterize patients with temporomandibular disorders. Annu Int Conf IEEE Eng Med Biol - Proc 4:1729–1732

Leader JK, Boston JR, Rudy TE, et al (2003) Relation of jaw sounds and kinematics visualized and quantified using 3-D computer animation. Med Eng Phys 25:191–200

Leiggener CS, Erni S, Gallo LM (2012) Novel approach to the study of jaw kinematics in an alloplastic TMJ reconstruction. Int J Oral Maxillofac Surg 41:1041–1045

Lemoine JJ, Xia JJ, Gateno J, Liebschner MAK (2005) Radiographic analysis for jaw motion normalization. J Oral Maxillofac Surg 63:961–967

Leng S, Zhao K, Qu M, et al (2011) Dynamic CT technique for assessment of wrist joint instabilities. Med Phys 38:50–57

Lepidi L, Grande F, Baldassarre G, et al (2023) Preliminary clinical study of the accuracy of a digital axiographic recording system for the assessment of sagittal condylar inclination. J Dent 135:104583. https://doi.org/https://dx.doi.org/10.1016/j.jdent.2023.104583

Lepley CR, Throckmorton GS, Ceen RF, Buschang PH (2011) Relative contributions of

occlusion, maximum bite force, and chewing cycle kinematics to masticatory performance. Am J Orthod Dentofac Orthop 139:606–613

Lewis RP, Buschang PH, Throckmorton GS (2001) Sex differences in mandibular movements during opening and closing. Am J Orthod Dentofac Orthop 120:294–303. https://doi.org/10.1067/mod.2001.115612

Lin H, Pan Y, Wei X, et al (2023) Comparison of the performance of various virtual articulator mounting procedures: a self-controlled clinical study. Clin Oral Investig 27:4017-4028. https://doi.org/10.1007/s00784-023-05028-9

Linsen SS, Oikonomou A, Martini M, Teschke M (2018) Mandibular kinematics and maximum voluntary bite force following segmental resection of the mandible without or with reconstruction. Clin Oral Investig 22:1707–1716. https://doi.org/10.1007/s00784-017-2263-3

Linsen SS, Reich RH, Teschke M (2012) Mandibular kinematics in patients with alloplastic total temporomandibular joint replacement a prospective study. J Oral Maxillofac Surg 70:2057–2064

Linsen SS, Schön A, Mercuri LG, Teschke M (2021) Unilateral, Alloplastic Temporomandibular Joint Reconstruction, Biomechanically What Happens to the Contralateral Temporomandibular Joint?— A Prospective Cohort Study. J Oral Maxillofac Surg 79:2016–2029

Linsen SS, Schön A, Mercuri LG, Teschke M (2020) How Does a Unilateral Temporomandibular Joint Replacement Affect Bilateral Masseter and Temporalis Muscle Activity?— A Prospective Study. J Oral Maxillofac Surg 79:314–323

Linsen SS, Wolf M, Mussig D (2016) Long-term outcomes of mandibular kinematics following class II malocclusion therapy with removable functional appliance therapy. Cranio 34:363–370

List T, Jensen RH (2017) Temporomandibular disorders: Old ideas and new concepts. Cephalagia 37:692–704. https://doi.org/10.1177/0333102416686302

Litin S (2009) Mayo Clinic Family Health Book

Lobbezoo F, Zwijnenburg AJ, Naeije M (2000) Functional subdivision of the human masseter and temporalis muscles as shown by the condylar movement response to electrical muscle stimulation. J Oral Rehabil 27:887–892

Lobo Leandro LF, Ono HY, de Souza Loureiro CC, et al (2013) A ten-year experience and follow-up of three hundred patients fitted with the Biomet/Lorenz Microfixation TMJ replacement system. Int J Oral Maxillofac Surg 42:1007–1013

M.A. B, F.M. A-S (2007) Changes in condylar path inclination during maximum protrusion between the ages of 6 and 12 years. J Oral Rehabil 34:27–33. https://doi.org/http://dx.doi.org/10.1111/j.1365-2842.2006.01690.x

Ma H, Shu J, Zheng T, et al (2022) The effect of mandibular movement on temporomandibular joint morphology while eating French fries. Ann Anat 244:151992. https://doi.org/https://dx.doi.org/10.1016/j.aanat.2022.151992

Machoň V, Vir J, Levorová J, et al (2020) Discectomy with Subsequent Free Fat Flap Insertion in Disc Perforation Therapy of Temporomandibular Joint. Assessment of Results 24 Months after Operation. Prague Med Rep 121:96–106

Mackerle J (2004) Finite Element Modelling and Simulations in Dentistry : A Bibliography 1990 – 2003. Comput Methods Biomech Biomed Engin 7:277–303

Maimaiti Y, Wu J, Tu'erdi M (2017) Gap arthroplasty versus interpositional arthroplasty for temporomandibular joint ankylosis: A meta-analysis. Chinese J Tissue Eng Res 21:3216–3223. https://doi.org/10.3969/j.issn.2095-4344.2017.20.017

Maixner W, Fillingim RB, Williams DA, et al (2016) Overlapping Chronic Pain Conditions: Implications for Diagnosis and Classification. J Pain 17:T93–T107. https://doi.org/10.1016/j.jpain.2016.06.002.Overlapping

Manfredini D, Cantini E, Romagnoli M, Bosco M (2003) Prevalence of Bruxism in Patients with Different Research Diagnostic Criteria for Temporomandibular Disorders (RDC/TMD) Diagnoses. Cranio - J Craniomandib Sleep Pract 21:279–285. https://doi.org/10.1080/08869634.2003.11746263

Manfredini D, Guarda-Nardini L, Winocur E, et al (2011) Research diagnostic criteria for temporomandibular disorders: A systematic review of axis I epidemiologic findings. Oral Surgery, Oral Med Oral Pathol Oral Radiol Endodontology 112:453–462

Manfredini D, Piccotti F, Ferronato G, Guarda-nardini L (2010) Age peaks of different RDC/TMD diagnoses in a patient population. J Dent 38:392–399. https://doi.org/10.1016/j.jdent.2010.01.006

Mapelli A, Galante D, Lovecchio N, et al (2009) Translation and rotation movements of the

mandible during mouth opening and closing. Clin Anat 22:311–318. https://doi.org/10.1002/ca.20756

Mapelli A, Machado BCZ, Garcia DM, et al (2016) Three-dimensional analysis of jaw kinematic alterations in patients with chronic TMD - disc displacement with reduction. J Oral Rehabil 43:824–832

Martin C, Alarcon JA, Palma JC (2000) Kinesiographic study of the mandible in young patients with unilateral posterior crossbite. Am J Orthod Dentofac Orthop 118:541–548

Matheson EM, Fermo JD, Blackwelder RS (2023) Temporomandibular Disorders: Rapid Evidence Review. Am Fam Physician 107:52

May B, Saha S, Saltzman M (2001) A three-dimensional mathematical model of temporomandibular joint loading. Clin Biomech 16:489–495

McKay GS, Yemm R, Cadden SW (1992) The structure and function of the temporomandibular joint. Br Dent J 173:127–132. https://doi.org/10.1038/sj.bdj.4807966

Melchior M de O, Mazzetto MO, Magri LV (2019) Relation of painful TMD with the speech function: What are the possible characteristics of mandibular movements and the main symptoms reported? CODAS 31:. https://doi.org/10.1590/2317-1782/20182018161

Melo RA, Maria C, Machado B, Almeida EO De (2020) Conservative therapies to treat pain and anxiety associated with temporomandibular disorders: a randomized clinical trial. Int Dent J 70:245–253. https://doi.org/10.1111/idj.12546

Mercuri LG (2016) Temporomandibular joint replacement: past, present and future material considerations. In: TMS 2014: 143rd Annual Meeting & Exhibition: Annual Meeting Supplemental Proceedings. Springer International Publishing, pp 183–190

Mercuri LG (2019) Temporomandibular joint replacement devices - dark past to challenging future. Stomatol Dis Sci 3:. https://doi.org/10.20517/2573-0002.2018.25

Mercuri LG (1998) Alloplastic temporomandibular joint reconstruction. Oral Surgery, Oral Med Oral Pathol Oral Radiol Endodontology 85:631–637

Mercuri LG (2013) The role of custom-made prosthesis for temporomandibular joint replacement. Rev Española Cirugía Oral y Maxilofac 35:1–10. https://doi.org/10.1016/j.maxilo.2012.02.003

Mercuri LG, Anspatch WE (2003) Principles for the revision of total alloplastic TMJ

prostheses. Int J Oral Maxillofac Surg 353–359

Mercuri LG, Edibam NR, Giobbie-Hurder A (2007) Fourteen-Year Follow-Up of a Patient-Fitted Total Temporomandibular Joint Reconstruction System. J Oral Maxillofac Surg 1140–1148

Mericske-stern R (1998) Three-Dimensional Force Measurements With Mandibular Overdentures Connected to Implants by Ball-Shaped Retentive Anchors . A Clinical Study. Int J Oral Maxillofac Implant 13:36–43

Mesin L (2020) Crosstalk in surface electromyogram: literature review and some insights. Phys Eng Sci Med 43:481–492. https://doi.org/10.1007/s13246-020-00868-1

Messerman T (1967) A means for studying mandibular movements. J Prosthet Dent 17:36–43

Miloro M, Mcknight M, Han MD, Markiewicz MR (2017) Discectomy without replacement improves function in patients with internal derangement of the temporomandibular joint *. J Cranio-Maxillofacial Surg 45:1425–1431. https://doi.org/10.1016/j.jcms.2017.07.003

Minami I, Wirianski A, Harakawa R, et al (2018) The three-axial gyroscope sensor detects the turning point between opening and closing phases of chewing. Clin Exp Dent Res 4:249–254

Minami I, Zhao N, Oogai K, et al (2011) A comparison between jerk-cost derived from a jaw-tracking system with that from an accelerometer. J Oral Rehabil 38:661–667

Mioche L, Bourdiol P, Peyron M-A (2004) Influence of age on mastication: effects on eating behaviour. Nutr Res Rev 17:43–54. https://doi.org/10.1079/nrr200375

Miura H, Araki Y, Umenai T (1997) Chewing activity and activities of daily living in the elderly. J Oral Rehabil 24:457–460

Miura H, Miura K, Mizugai H, et al (2000) Chewing ability and quality of life among the elderly residing in a rural community in Japan. J Oral Rehabil 27:731–734

Miyowaki S, Tanimoto Y, Kawakami T, et al (2001) Motion of the human mandibular condyle during mastication. J Dent Res 80:437–442. https://doi.org/10.1177/00220345010800020701

Moher D, Liberati A, Tetzlaff J, Altman DG (2009) Preferred reporting items for systematic reviews and meta-analyses: The PRISMA statement. BMJ Br Med J 339:332–336

Mommaerts MY (2019) On the reinsertion of the lateral pterygoid tendon in total temporomandibular joint replacement surgery. J Cranio-Maxillofacial Surg 47:1913–1917. https://doi.org/10.1016/j.jcms.2019.11.018

Morikawa K, Isogai R, Nonaka J, et al (2022) A New Intraoral Six-Degrees-of-Freedom Jaw Movement Tracking Method Using Magnetic Fingerprints. Sensors 22:. https://doi.org/10.3390/s22228923

Morneburg T, Pröschel PA (1998) Differences between traces of adjacent condylar points and their impact on clinical evaluation of condyle motion. Int J Prosthodont 11:317–324

Mountziaris PM, Kramer PR, Mikos AG (2009) Emerging intra-articular drug delivery systems for the temporomandibular joint. Methods 47:134–140. https://doi.org/10.1016/j.ymeth.2008.09.001

Murphy MA, Sunnerhagen KS, Johnels B, Willén C (2006) Three-dimensional kinematic motion analysis of a daily activity drinking from a glass : a pilot study. Jounral NeoroEngineering Rehabil 3:

Murphy MK, MacBarb RF, Wong ME, Athanasiou KA (2013) Temporomandibular Disorders: A Review of Etiology, Clinical Management, and Tissue Engineering Strategies. Int J Oral Maxillofac Implants 28:393. https://doi.org/10.11607/jomi.te20

Naeije M (2002) Local kinematic and anthropometric factors related to the maximum mouth opening in healthy individuals. J Oral Rehabil 29:534–539

Naeije M, Hofman N (2003) Biomechanics of the human temporomandibular joint during chewing. J Dent Res 82:528–531

National Academies of Sciences Engineering and Medicine (2020) Temporomandibular Disorders: Priorities for Research and Care. Washington (DC)

Nitzan DW, Price A (2001) The Use of Arthrocentesis for the Treatment of Osteoarthritic Temporomandibular Joints. J Oral Maxillofac Surg 59:1154–1159. https://doi.org/10.1053/joms.2001.26716

Nowak Z, Checinski M, Nitecka-buchta A, et al (2021) Intramuscular Injections and Dry Needling within Masticatory Muscles in Management of Myofascial Pain. Systematic Review of Clinical Trials. Int J Environ Res Public Health 18:9552

Ogawa T, Koyano K, Umemoto G (1998) Inclination of the occlusal plane and occlusal

guidance as contributing factors in mastication. J Dent 26:641–647

Ogawa T, Ogawa M, Koyano K (2001) Different responses of masticatory movements after alteration of occlusal guidance related to individual movement pattern. J Oral Rehabil 28:830–841

Okeson JP (2019) Management of temporomandibular disorders and occlusion. Elsiver Health Sciences

Ombregt L (2013) A System of Orthopaedic Medicine, Third. Elsiver

Orlow LW (1903) Ankylosis mandibulae vera. Dtsch Zeitschrift fur Chir 66:399–508

Osborn JW (1995) Biomechanical implications of lateral pterygoid contribution to biting and jaw opening in humans. Arch Oral Biol 40:1099–1108

Ostry DJ, Vatikiotis-Bateson E, Gribble PL (1997) An examination of the degrees of freedom of human jaw motion in speech and mastication. J Speech, Lang Hear Res 40:1341–1351

Otake Y, Suzuki N, Hattori A, et al (2006) Real-time mandibular movement analysis system using four-dimensional cranial bone model. Syst Comput Japan 37:1–12

Owens S, Buschang PH, Throckmorton GS, et al (2002) Masticatory performance and areas of occlusal contact and near contact in subjects with normal occlusion and malocclusion. Am J Orthod Dentofac Orthop 121:602–609

Palinkas M, Nassar MSP, Cecílio FA, et al (2010) Age and gender influence on maximal bite force and masticatory muscles thickness. Arch Oral Biol 55:797–802. https://doi.org/10.1016/j.archoralbio.2010.06.016

Pantoja LLQ, de Toledo IP, Pupo YM, et al (2019) Prevalence of degenerative joint disease of the temporomandibular joint: a systematic review. Clin Oral Investig 23:2475–2488

Partsch C, Bruhn C, Kantorowicz A (1932) Die chirurgischen Erkrankungen der Mundhöhle, der Zähne und Kiefere. In: Handbuch der Zahnheilkunde. Bergmann, Munchen, pp 359–361

Peck CC, Murray GM, Johnson CWL, Klineberg IJ (1999) Trajectories of condylar points during working-side excursive movements of the mandible. J Prosthet Dent 81:444–452

Peck CC, Murray GM, Johnson CWL, Klineberg IJ (1997) The variability of condylar point pathways in open-close jaw movements. J Prosthet Dent 77:394–404

Perez DE, Wolford LM, Schneiderman E, et al (2016) Does Unilateral Temporomandibular

Total Joint Reconstruction Result in Contralateral Joint Pain and Dysfunction? J Oral Maxillofac Surg 74:1539–1547

Peters A, Galna B, Sangeux M, et al (2010) Quantification of soft tissue artifact in lower limb human motion analysis: A systematic review. Gait Posture 31:1–8

Piancino MG, Falla D, Merlo A, et al (2016) Effects of therapy on masseter activity and chewing kinematics in patients with unilateral posterior crossbite. Arch Oral Biol 67:61–67. https://doi.org/http://dx.doi.org/10.1016/j.archoralbio.2016.03.013

Piancino MG, Kyrkanides S (2016) Understanding Masticatory Function in Unilateral Crossbites. Wiley

Pinheiro M (2021) Biomechanical evaluation of the human mandible after temporomandibular joint replacement under different biting conditions. Sci Rep 11:1–12

Pinto-Borges H, Pinto J, Carvalho O, et al (2023) Stresses, friction, and wear on different materials and design for temporomandibular joint total joint replacement (TMJ TJR). Tribol Int 178:. https://doi.org/10.1016/j.triboint.2022.108051

Poli O, Manzon L, Niglio T, et al (2021) Masticatory Force in Relation with Age in Subjects with Full Permanent Dentition: A Cross-Sectional Study. Healthcare 9:700

Pourahmadi MR, Takamjani IE, Jaberzadeh S, et al (2019) Kinematics of the Spine During Sit-to-Stand Movement Using Motion Analysis Systems: A Systematic Review of Literature. J Sport Rehabil 28:77–93

Proffit WR, Fields HW, Nixon WL (1983) Occlusal Forces in Normal- and Long-face Adults. J Dent Res 62:566–570

Pruim GJ, de Jongh HJ, ten Bosch JJ (1980) Forces acting on the mandible during bilateral static bite at different bite force levels. J Biomech 13:755–763. https://doi.org/10.1016/0021-9290(80)90237-7

Raadsheer MC, van Eijden TMGJ, van Ginkell FC, Prahl-Andersen B (1999) Contribution of Jaw Muscle Size and Craniofacial Morphology to Human Bite Force Magnitude. Jouranl Dent Res 78:31–42

Radin EL, Martin RB, Burr DB, et al (1984) Effects of Mechanical Loading on the Tissues of the Rabbit Knee. J Orthop Res 2:221–234

Ratzmann A, Mundt T, Schwahn C, et al (2007) Comparative clinical investigation of

horizontal condylar inclination using the JMA® electronic recording system and a protrusive wax record for setting articulators . Int J Comput Dent 10:265–284

Raustia AM, Oikarinen KS, Pernu H (1997) Changes in electrical activity of masseter and temporal muscles after temporomandibular joint surgery: A one-year follow up. Int J Oral Maxillofac Surg 26:253–257

Reicheneder C, Kardari Z, Proff P, et al (2013) Correlation of condylar kinematics in children with gender, facial type and weight. Ann Anat 195:243–247

Reisine ST, Weber J (1989) The effects of temporomandibular joint disorders on patients' quality of life. Community Dent Health 6:257–270

Remijn L, Groen BE, Speyer R, et al (2017) Can mastication in children with cerebral palsy be analyzed by clinical observation, dynamic ultrasound and 3D kinematics? J Electromyogr Kinesiol 32:22–29

Rismanchian M, Bajoghli F, Mostajeran Z, et al (2009) Effect of implants on maximum bite force in edentulous patients. J Oral Implantol 35:196–200

Robinson D, Aguilar L, Gatti A, et al (2019) Load response of the natural tooth and dental implant: A comparative biomechanics study. J Adv Prosthodont 11:169–178

Roda RP, Bagán J V, María J, et al (2007) Review of temporomandibular joint pathology. Part I: Classification, epidemiology and risk factors. Med Oral Patol Oral Cir Bucal 292–298

Roehrle O, Saini H, Ackland DC (2018) Occlusal loading during biting from an experimental and simulation point of view. Dent Mater 34:58–68

Rohrle O, Pullan AJ (2007) Three-dimensional finite element modelling of muscle forces during mastication. J Biomech 40:3363–3372

Röhrle O, Saini H, Ackland DC (2018a) Occlusal loading during biting from an experimental and simulation point of view. Dent Mater 34:58–68

Röhrle O, Saini H, Lee PVS, Ackland DC (2018b) A novel computational method to determine subject-specific bite force and occlusal loading during mastication. Comput Methods Biomech Biomed Engin 21:453–460. https://doi.org/http://dx.doi.org/10.1080/10255842.2018.1479744

Röhrle O, Waddell JN, Foster KD, et al (2009) Using a Motion-Capture System to Record

Dynamic Articulation for Application in CAD/CAM Software. J Prosthodont 18:703–710

Romeed SA, Malik R, Dunne SM (2012) Stress Analysis of Occlusal Forces in Canine Teeth and Their Role in the Development of Non-Carious Cervical Lesions: Abfraction. Int J Dentisry 153–159. https://doi.org/10.1155/2012/234845

Rossi SS De, Stern I, Sollecito TP (2023) Disorders of the Masticatory Muscles. Dent Clin 57:449–464. https://doi.org/10.1016/j.cden.2013.04.007

Rudisch A (2003) Magnetic resonance imaging predictors of temporomandibular joint pain. J Am Dent Assoc 134:705–714. https://doi.org/10.14219/jada.archive.2003.0256

Rues S, Schindler H, Turp J, et al (2008) Motor behavior of the jaw muscles during different clenching levels. Eur J Oral Sci 116:223–228. https://doi.org/10.1111/j.1600-0722.2008.00537.x

Russell P, Pearcy MJ, Unsworth A (1993) Measurement of the range and coupled movements observed in the lumbar spine. Br J Rheumatol 32:490–497

Ryan J, Akhter R, Hassan N, et al (2019) Epidemiology of Temporomandibular Disorder in the General Population: a Systematic Review. Adv Dent Oral Heal 10:555787. https://doi.org/10.19080/ADOH.2019.10.555787

Sadat-Khonsari R, Fenske C, Kahl-Nieke B, et al (2003a) Mandibular instantaneous centers of rotation in patients with and without temporomandibular dysfunction. J Orofac Orthop 64:256–264

Sadat-Khonsari R, Fenske C, Kahl-Nieke B, et al (2003b) The helical axis of the mandible during the opening and closing movement of the mouth. J Orofac Orthop 64:178–185

Sagl B, Schmid-Schwap M, Piehslinger E, et al (2021) An in silico investigation of the effect of bolus properties on TMJ loading during mastication. J Mech Behav Biomed Mater 124:104836. https://doi.org/10.1016/j.jmbbm.2021.104836

Sagl B, Schmid-Schwap M, Piehslinger E, et al (2019) A Dynamic Jaw Model With a Finite-Element Temporomandibular Joint. Front Physiol 10:1–12

Saitoh I, Hayasaki H, Iwase Y, Nakata M (2002) Improvement in Jaw Motion Following Treatment of Unilateral Crossbite in a Child with Primary Dentition: A Case Report. Cranio 20:129–134

Sánchez-Ayala A, Farias-Neto A, Campanha NH, Garcia RCMR (2013) Relationship Between Chewing Rate and Masticatory Performance. Cranio - J Craniomandib Sleep Pract 31:118–122

Schierz O, Klinger N, Schon G, Reissmann DR (2014) The reliability of computerized condylar path angle assessment. Int J Comput Dent 17:35–51

Schiffman E, Ohrbach R, Truelove E, et al (2015) Diagnostic Criteria for Temporomandibular Disorders (DC/TMD) for Clinical and Research Applications: Recommendations of the International RDC/TMD Consortium Network and Orofacial Pain Specialist Group. J Oral Facial Pain Headache 28:6–27

Schiffman EL, Velly AM, Look JO, et al (2014) Effects of four treatment strategies for temporomandibular joint closed lock. Int J Oral Maxillofac Surg 43:217–226. https://doi.org/10.1016/j.ijom.2013.07.744

Schindler HJ, Rues S, Türp JC, et al (2007) Jaw clenching: muscle and joint forces, optimization strategies. J Dent Res 86:843–847

Schwestka-Polly R, Kubein-Meesenburg D, Nagerl H, et al (1999) Alteration of the functional condition of the mandible during clinical treatment. Ann Anat 181:45–50

Scott B, Butterworth C, Lowe D, Rogers SN (2008) Factors associated with restricted mouth opening and its relationship to health-related quality of life in patients attending a Maxillofacial Oncology clinic. Oral Oncol 430–438

Sella-Tunis T, Pokhojaev A, Sarig R, et al (2018) Human mandibular shape is associated with masticatory muscle force. Sci Rep 8:1–10. https://doi.org/10.1038/s41598-018-24293-3

Sforza C, Tartaglia GM, Lovecchio N, et al (2009) Mandibular movements at maximum mouth opening and EMG activity of masticatory and neck muscles in patients rehabilitated after a mandibular condyle fracture. J Cranio-Maxillofacial Surg 37:327–333. https://doi.org/10.1016/j.jcms.2009.01.002

Sforza C, Ugolini A, Rocchetta D, et al (2010) Mandibular kinematics after orthognathic surgical treatment. A pilot study. Br J Oral Maxillofac Surg 48:110–114

Shiga H, Stohler CS, Kobayashi Y (2001) The effect of bolus size on the chewing cycle in humans. Odontology 89:49–53. https://doi.org/10.1007/s10266-001-8185-0

Shiller DM, Ostry DJ, Gribble PL (1999) Effects of gravitational load on jaw movements in

speech. J Neurosci 19:9073–9080

Shiller DM, Ostry DJ, Gribble PL, Laboissière R (2001) Compensation for the effects of head acceleration on jaw movement in speech. J Neurosci 21:6447–6456

Shimada A, Yamabe Y, Torisu T, et al (2012) Measurement of dynamic bite force during mastication. J Oral Rehabil 39:349–356. https://doi.org/10.1111/j.1365-2842.2011.02278.x

Shinogaya T, Bakke M, Thomsen CE, et al (2001) Effects of ethnicity, gender and age on clenching force and load distribution. Clin Oral Investig 5:63–68

Shu J, Feng Y, Zheng T, et al (2021a) Temporomandibular condylar articulation and finite helical axis determination using a motion tracking system. Med Eng Phys 94:80–86. https://doi.org/https://dx.doi.org/10.1016/j.medengphy.2021.06.007

Shu J, Li A, Ma H, et al (2023) The effects of the size and strength of food on jaw motion and temporomandibular joints. Med Eng Phys 116:103989. https://doi.org/https://dx.doi.org/10.1016/j.medengphy.2023.103989

Shu J, Li A, Shao B, et al (2022a) Descriptions of the dynamic joint space of the temporomandibular joint. Comput Methods Programs Biomed 226:107149. https://doi.org/https://dx.doi.org/10.1016/j.cmpb.2022.107149

Shu J, Ma H, Liu Y, et al (2022b) In vivo biomechanical effects of maximal mouth opening on the temporomandibular joints and their relationship to morphology and kinematics. J Biomech 141:111175. https://doi.org/https://dx.doi.org/10.1016/j.jbiomech.2022.111175

Shu J, Ma H, Xiong X, et al (2021b) Mathematical analysis of the condylar trajectories in asymptomatic subjects during mandibular motions. Med Biol Eng Comput 59:901–911. https://doi.org/https://dx.doi.org/10.1007/s11517-021-02346-6

Siegler S, Hayes R, Nicolella D, Fielding A (1991) A technique to investigate the three-dimensional kinesiology of the human temporomandibular joint. J Prosthet Dent 65:833–839

Siu W-S, Shih Y-F, Lee S-Y, et al (2022) Alterations in kinematics of temporomandibular joint associated with chronic neck pain. J Oral Rehabil 49:860–871. https://doi.org/https://dx.doi.org/10.1111/joor.13347

Slade G, Durham J (2020) Prevalence, Impact and Costs of Treatment for

Temporomandibular Disorders. In: Temporomandibular Disorders: Priorities for Research and Care

Slade GD, Fillingim RB, Sanders AE, et al (2013) Summary of Findings From the OPPERA Prospective Cohort Study of Incidence of First-Onset Temporomandibular Disorder: Implications and Future Directions. J Pain 14:T116–T124. https://doi.org/https://doi.org/10.1016/j.jpain.2013.09.010

Slater J, Visscher CM, Lobbezoo F, Naeije M (1999) The intra-articular distance within the TMJ during free and loaded closing movements. J Dent Res 78:1815–1820

Small CF, Bryant JT, Dwosh IL, et al (1996) Validation of a 3D optoelectronic motion analysis system for the wrist joint. Clin Biomech 11:481–483

Smith AE, Sc D, Robinson M (1957) A New Surgical Procedure for the Creation of a False Temporomandibular Joint in Cases of Ankylosis by Means of Non-electrolytic Metal. Am J Surg 94:837–845

Smith DM, Mclachlan KR, Mccall WD (1986) A Numerical Model of Temporomandibular Joint Loading. J Dent Res 65:1046–1052

Soboļeva U, Lauriņa L, Slaidiņa A (2005) Jaw tracking devices--historical review of methods development. Part II. Stomatologija 7:72–6

Sonnesen L, Bakke M (2007) Bite force in children with unilateral crossbite before and after orthodontic treatment. A prospective longitudinal study. Eur J Orthod 29:310–313. https://doi.org/10.1093/ejo/cjl082

Sonnesen L, Bakke M, Solow B (2001) Bite force in pre-orthodontic children with unilateral crossbite. Eur J Orthod 23:741–749

Speksnijder CM, Mutsaers NEA, Walji S (2022) Functioning of the Masticatory System in Patients with an Alloplastic Total Temporomandibular Joint Prostheses Compared with Healthy Individuals: A Pilot Study. Life 12:2073

Stiesch-Scholz M, Demling A, Rossbach A (2006) Reproducibility of jaw movements in patients with craniomandibular disorders. J Oral Rehabil 33:807–812

Stohler CS (1999) Muscle-Related Temporomandibular Disorders. J Orofac Pain 13:273–284

Sugihara D, Kawara M, Suzuki H, et al (2020) Mandibular Jaw Movement and Masticatory Muscle Activity during Dynamic Trunk Exercise. Dent J 8:.

https://doi.org/10.3390/dj8040132

Takada K, Miyawaki S, Tatsuta M (1994) The effects of food consistency on jaw movement and posterior temporalis and inferior orbicularis oris muscle activities during chewing in children. Arch Oral Biol 39:793–805

Tamaki K, Celar AG, Beyrer S, Aoki H (1997) Reproduction of excursive tooth contact in an articulator with computerized axiography data. J Prosthet Dent 78:373–378

Tamura K, Shiga H (2014) Gender differences in masticatory movement path and rhythm in dentate adults. J Prosthodont Res 58:237–242. https://doi.org/10.1016/j.jpor.2014.06.001

Tatli U, Machon V (2017) Internal Derangements of the Temporomandibular Joint: Diagnosis and Management. In: Emes Y, Aybar B, Dergin G (eds) Temporomandibular Joint Pathology. IntechOpen, Rijeka, p Ch. 3

Teng TT-Y, Ko EW-C, Huang CS, Chen Y-R (2015) The Effect of early physiotherapy on the recovery of mandibular function after orthognathic surgery for Class III correction: Part i - Jaw-motion analysis. J Cranio-Maxillofacial Surg 43:131–137

Terajima M, Endo M, Aoki Y, et al (2008) Four-dimensional analysis of stomatognathic function. Am J Orthod Dentofac Orthop 134:276–287

Tersi L, Barre A, Fantozzi S, Stagni R (2013) In vitro quantification of the performance of model-based mono-planar and bi-planar fluoroscopy for 3D joint kinematics estimation. Med Biol Eng Comput 51:257–265

Theusner J, Plesh O, Curtis DA, Hutton JE (1993) Axiographic tracings of temporomandibular joint movements. J Prosthet Dent 69:209–215

Thilander B, Bjerklin K (2012) Posterior crossbite and temporomandibular disorders (TMDs): Need for orthodontic treatment? Eur J Orthod 34:667–673. https://doi.org/10.1093/ejo/cjr095

Thilander B, Rubio G, Pena L, de Mayorga C (2002) Prevalence of temporomandibular dysfunction and its association with malocclusion in children: An epidemiologic study. Angle Orthod 72:146–154. https://doi.org/10.17796/1053-4628-41.2.161

Thompson RC, Oegema TR, Lewis JL, Wallace L (1991) Osteoarthrotic changes after acute transarticular load. An animal model. J Bone Jt Surg - Ser A 73:990–1001. https://doi.org/10.2106/00004623-199173070-00005

Throckmorton GS, Buschang BH, Hayasaki H, Phelan T (2001a) The effects of chewing rates on mandibular kinematics. J Oral Rehabil 28:328–334. https://doi.org/10.1046/j.1365-2842.2001.00679.x

Throckmorton GS, Buschang PH, Hayasaki H, Pinto AS (2001b) Changes in the masticatory cycle following treatment of posterior unilateral crossbite in children. Am J Orthod Dentofac Orthop 120:521–529. https://doi.org/10.1067/mod.2001.118626

Throckmorton GS, Ellis E, Hayasaki H, et al (2003) Jaw kinematics during mastication after unilateral fractures of the mandibular condylar process. Am J Orthod Dentofac Orthop 124:695–707

Tokgoz E, Levitt S, Sosa D (2023) Total Knee ArthroplastyAdvancing Engineering of Total Knee Arthroplasty. In: Total Knee Arthroplasty

Tomonari H, Kwon S, Kuninori T, Miyawaki S (2017) Differences between the chewing and non-chewing sides of the mandibular first molars and condyles in the closing phase during chewing in normal subjects. Arch Oral Biol 81:198–205

Tortopidis D, Lyons MF, Baxendale RH, Gilmour WH (1998) The variability of bite force measurement between sessions, in different positions within the dental arch. J Oral Rehabil 25:681–686

Travers KH, Buschang PH, Hayasaki H, Throckmorton GS (2000) Associations between incisor and mandibular condylar movements during maximum mouth opening in humans. Arch Oral Biol 45:267–275

Treacy K (1999) Awareness/relaxation training and transcutaneous electrical neural stimulation in the treatment of bruxism. J Oral Rehabil 26:280–287

Trize DDM, Calabria MP, Oliveira S De, Franzolin B (2018) Is quality of life affected by temporomandibular disorders? Einstein 16:1–6. https://doi.org/10.31744/einstein

Ugolini A, Mapelli A, Segu M, et al (2017) Kinematic analysis of mandibular motion before and after orthognathic surgery for skeletal Class III malocclusion: A pilot study. Cranio 35:94–100

Ugolini A, Mapelli A, Segu M, et al (2018) Three-dimensional mandibular motion in skeletal Class III patients. CRANIO-THE J Craniomandib Pract 36:113–120

Umesh S, Padma S, Asokan S, Srinivas T (2016) Fiber Bragg Grating based bite force

measurement. J Biomech 49:2877–2881

van Eijden TMGJ (1991) Three-Dimensional Analysis of Human Bite-Force Magnitude and Moment. Arch Oral Biol 36:535–539

van Loon J, Otten E, Bont LGM De, Verkerke GJ (1998) Loading of a unilateral temporomandibular joint prosthesis: A three-dimensional mathematical study. J Dent Res 77:1939–1947

van Loon JP, de Bont LGM, Boering G (1995) Evaluation of temporomandibular joint prostheses. Review of the literature from 1946 to 1994 and implications for future prosthesis designs. J Oral Maxillofac Surg 53:984–996. https://doi.org/10.1016/0278-2391(95)90110-8

Van Loon JP, Falkenström CH, De Bont LGM, et al (1999) The theoretical optimal center of rotation for a temporomandibular joint prosthesis: A three-dimensional kinematic study. J Dent Res 78:43–48

Varga S, Spalj S, Varga ML, et al (2011) Maximum voluntary molar bite force in subjects with normal occlusion. Eur J Orthod 33:427–433

Vilanova LSR, Gonçalves TMSV, Pimentel MJ, et al (2014) Mastication movements and sleep quality of patients with myofascial pain: Occlusal device therapy improvements. J Prosthet Dent 112:1330–1336

Visscher CM, Huddleston Slater JJR, Lobbezoo F, Naeije M (2000) Kinematics of the human mandible for different head postures. J Oral Rehabil 27:299–305

Vitti M, Basmajian J V (1977) Integrated Actions of Masticatory Muscles: Simultaneous EMG from Eight Intramuscular Electrodes. Anat Rec 187:173–189

Voiner J, Yu J, Deitrich P, et al (2011) Analysis of mandibular motion following unilateral and bilateral alloplastic TMJ reconstruction. Int J Oral Maxillofac Surg 40:569–571

Wagner A, Seemann R, Schicho K, et al (2003) A comparative analysis of optical and conventional axiography for the analysis of temporomandibular joint movements. J Prosthet Dent 90:503–509

Waltimo A, Kononen M (1993) A novel bite force recorder and maximal isometric bite force values for healthy young adults. Scandanavian J Dent Res 101:171–175

Wang D, Fu H, Zeng R, Yang X (2009) Changes of Mandibular Movement Tracings After the

Correction of Mandibular Protrusion by Bilateral Sagittal Split Ramus Osteotomy. J Oral Maxillofac Surg 67:2238–2244

Wang J-L, Wang J, Chen K-N, et al (2023) Designing customized temporomandibular fossa prosthesis based on envelope surface of condyle movement: validation via in silico musculoskeletal simulation. Front Bioeng Biotechnol 11:. https://doi.org/10.3389/fbioe.2023.1273263

Warbuton G (2021) Internal derangements of the temporomandibular joint. In: Oral and Maxillofacial Surgery for the Clinician. pp 1361–1380

Werkman DF, Mercuri LG, Troost JP, et al (2022) An international Survey on TMJ Surgeon's Implementation and Management of Discectomy in Treating TMJ Internal Derangement. J Oral Maxillofac Surg 79:1423–1433. https://doi.org/10.1016/j.joms.2021.01.002.An

Widmalm SE, Lillie JH, Ash MM (1981) Anatomical and electromyographic studies of the lateral pterygoid muscle. J Oral Rehabil 14:429–446

Wieckiewicz M, Zietek M, Nowakowska D, Wieckiewicz W (2014) Comparison of selected kinematic facebows applied to mandibular tracing. Biomed Res Int 2014:

Wilding RJC (1993) The Association Between Chewing Efficiency and Occlusal Contact Area in Man. Arch Oral Biol 38:589–596

Wilkes CH (1989) Internal Derangements of the Temporomandibular Joint - Pathological Variations. Arch Otolaryngol - Head Neck Surg 115:469–477

Winocur-Arias O, Friedman-Rubin P, Ras KA, et al (2022) Local myalgia compared to myofascial pain with referral according to the DC/TMD: Axis I and II results. BMC Oral Health 22:1–10. https://doi.org/10.1186/s12903-022-02048-x

Winter A, Schurig A, Rasche E, et al (2020) The flexural strength of CAD/CAM polymer crowns and the effect of artificial ageing on the fracture resistance of CAD/CAM polymer and ceramic single crowns. J Mater Sci Mater Med 31:. https://doi.org/10.1007/s10856-019-6347-2

Wojczynska A, Gallo LM, Bredell M, Leiggener CS (2019) Alterations of mandibular movement patterns after total joint replacement: a case series of long-term outcomes in patients with total alloplastic temporomandibular joint reconstructions. Int J Oral Maxillofac Surg 48:225–232. https://doi.org/10.1016/j.ijom.2018.06.005

Wojczynska A, Leiggener CS, Bredell M, et al (2016) Alloplastic total temporomandibular joint replacements: do they perform like natural joints? Prospective cohort study with a historical control. Int J Oral Maxillofac Surg 45:1213–1221

Wojczyńska AZ, Markova M, Ettlin DA, et al (2021) In-vivo kinematic assessment of alloplastic temporomandibular joint replacements by means of helical axis: A cohort study with historical control. J Biomech 122:

Wolford LM, Dingwerth DJ, Talwar RM, Pitta MC (2003) Comparison of 2 temporomandibular joint total joint prosthesis systems. J Oral Maxillofac Surg 61:685–690. https://doi.org/10.1053/joms.2003.50112

Woodburn J, Turner DE, Helliwell PS, Barker S (1999) A preliminary study determining the feasibility of electromagnetic tracking for kinematics at the ankle joint complex. Rheumatology 38:1260–1268

Woodford SC, Robinson DL, Abduo J, et al (2023) Kinematics of the jaw following total temporomandibular joint replacement surgery. J Biomech 159:111741. https://doi.org/10.1016/j.jbiomech.2023.111741

Woodford SC, Robinson DL, Mehl A, et al (2020) Measurement of normal and pathological mandibular and temporomandibular joint kinematics: A systematic review. J Biomech 111:109994

Woodford SC, Robinson DR, Edelmann C, et al (2021) Low-Profile Electromagnetic Field Sensors in the Measurement and Modelling of Three-Dimensional Jaw Kinematics and Occlusal Loading. Ann Biomed Eng 1–11

Yamamoto T, Nishigawa K, Bando E, Hosoki M (2009) Effect of different head positions on the jaw closing point during tapping movements. J Oral Rehabil 36:32–38

Yamazaki T, Matsumoto A, Sugamoto K, et al (2014) Accurate 3D kinematic measurement of temporomandibular joint using X-ray fluoroscopic images. In: Medical Imaging 2014: Biomedical Applications in Molecular, Structural, and Functional Imaging. International Society for Optics and Photonics

Yashiro K, Iwata A, Takada K, et al (2015a) Temporomandibular joint articulations on working side during chewing in adult females with cross-bite and mandibular asymmetry. J Oral Rehabil 42:163–172

Yashiro K, Yamamoto K, Takada K, et al (2015b) Influence of balancing-side occlusal

interference on smoothness of working-side condylar movement and intra-articular space in chewing efforts. J Oral Rehabil 42:10–17

Yatabe M, Zwijnenburg A, Megens CCEJ, Naeije M (1997) Movements of the mandibular condyle kinematic center during jaw opening and closing. J Dent Res 76:714–719

Yatabe M, Zwijnenburg A, Megens CCEJ, Naeije M (1995) The Kinematic Center: A Reference for Condylar Movements. J Dent Res 74:1644–1648

Yen C-I, Chou P-Y, Chen C-H, et al (2017) Kinematic, Kinetic and Surface Electromyography Analysis Following Zygomatic Fracture Reconstruction. J Med Biol Eng 37:468–473

Yu JH, Lin CC, Chen YH (2017) Changes in mandibular border movements in adult patients after correction of functional anterior crossbite. J Dent Sci 12:139–144. https://doi.org/10.1016/j.jds.2016.10.005

Yuan Q, Wang P, Liu L, et al (2016) Acupuncture for musculoskeletal pain: A meta-analysis and meta-regression of sham-controlled randomized clinical trials. Sci Rep 6:30675. https://doi.org/10.1038/srep30675

Zaugg B, Hämmerle CHF, Palla S, Gallo LM (2012) Implant-supported mandibular splinting affects temporomandibular joint biomechanics. Clin Oral Implants Res 23:897–901

Zhang L, Shen L, Zhang L, et al (2022) Dynamic 3D images fusion of the temporomandibular joints: A novel technique. J Dent 126:104286. https://doi.org/https://dx.doi.org/10.1016/j.jdent.2022.104286

Zhang S, He K, Lin C, et al (2020) Efficacy of occlusal splints in the treatment of temporomandibular disorders: a systematic review of randomized controlled trials. Acta Odontol Scand 78:580–589. https://doi.org/10.1080/00016357.2020.1759818

Zhang X, Ashton-Miller JA, Stohler CS (1995) Three-dimensional unilateral method for the bilateral measurement of condylar movements. J Biomech 28:1007–1011

Zhao K, Breighner R, Holmes III D, et al (2015) A Technique for Quantifying Wrist Motion Using Four-Dimensional Computed Tomography : Approach and Validation. J Biomech Eng 137:

Zhao NN, Whittle T, Murray GM, Peck CC (2012) The effects of capsaicin-induced intraoral mucosal pain on jaw movements in humans. J Oral Facial Pain Headache 26:277–287

Zou L, He D, Ellis E (2018) A Comparison of Clinical Follow-Up of Different Total Temporomandibular Joint Replacement Prostheses: A Systematic Review and Meta-Analysis. J Oral Maxillofac Surg 76:294–303

# Appendices

## APPENDIX A

Table A.A.1: Results of methodological quality assessment on each study that employs video motion analysis. The quality question numbers refer to those outlined in Table 3.1. Each question was attributed a score of 2, 1 or 0 based on whether the question was clearly addressed, partially addressed or not addressed respectively. For each study quality scores were collated to give that paper an overall quality rating ranging from 0 to 22.

| Authors | Quality Question | | | | | | | | | | | Overall Quality Rating |
|---|---|---|---|---|---|---|---|---|---|---|---|---|
| | 1 | 2 | 3 | 4 | 5 | 6 | 7 | 8 | 9 | 10 | 11 | |
| Optoelectronic Tracking | | | | | | | | | | | | |
| Abbink et al., 1999 | 2 | 2 | 1 | 2 | 1 | 2 | 1 | 2 | 2 | 0 | 2 | 17 |
| Amhamed et al., 2016 | 2 | 2 | 1 | 2 | 1 | 2 | 2 | 2 | 2 | 0 | 2 | 18 |
| Bhaskaracharya et al., 2015 | 2 | 2 | 1 | 2 | 2 | 2 | 0 | 2 | 2 | 1 | 2 | 18 |
| Buschang et al., 2000 | 2 | 2 | 2 | 2 | 2 | 2 | 2 | 2 | 2 | 1 | 2 | 21 |
| Buschang et al., 2001 | 2 | 2 | 2 | 2 | 2 | 2 | 2 | 2 | 2 | 0 | 2 | 20 |
| Calixtre et al., 2017 | 2 | 2 | 2 | 1 | 1 | 2 | 2 | 2 | 0 | 1 | 2 | 17 |
| Ćatić & Naeije, 1999 | 2 | 2 | 1 | 1 | 1 | 2 | 0 | 2 | 1 | 0 | 2 | 14 |
| Chang et al., 2015 | 2 | 2 | 2 | 2 | 1 | 0 | 1 | 2 | 2 | 2 | 2 | 18 |
| Coutant et al., 2008 | 1 | 2 | 1 | 1 | 1 | 1 | 1 | 2 | 1 | 1 | 2 | 14 |
| Coutant et al., 2011 | 1 | 2 | 1 | 2 | 1 | 1 | 1 | 2 | 1 | 0 | 2 | 14 |
| Crane et al., 2010 | 2 | 2 | 1 | 2 | 1 | 2 | 2 | 2 | 2 | 0 | 2 | 18 |
| Crane et al., 2013 | 2 | 1 | 1 | 2 | 1 | 2 | 2 | 2 | 2 | 0 | 2 | 17 |
| De Felicio et al., 2013 | 2 | 2 | 2 | 2 | 2 | 2 | 2 | 2 | 2 | 1 | 2 | 21 |
| Ettlin et al., 2008 | 2 | 2 | 1 | 2 | 1 | 2 | 2 | 0 | 2 | 0 | 2 | 16 |
| Fang & Kuo, 2008 | 2 | 2 | 1 | 2 | 0 | 0 | 1 | 2 | 2 | 1 | 2 | 15 |
| Ferrario et al., 2005 | 2 | 2 | 2 | 2 | 1 | 2 | 2 | 2 | 2 | 2 | 2 | 21 |
| Fushima et al., 2003 | 2 | 2 | 2 | 2 | 2 | 2 | 1 | 2 | 2 | 2 | 2 | 21 |
| Gallo et al., 1997 | 2 | 2 | 2 | 2 | 2 | 2 | 1 | 2 | 2 | 2 | 2 | 21 |
| Gallo et al., 2000 | 2 | 2 | 1 | 2 | 2 | 2 | 2 | 2 | 2 | 0 | 2 | 19 |
| Gallo et al., 2006 | 2 | 2 | 1 | 2 | 2 | 2 | 2 | 2 | 2 | 2 | 2 | 21 |
| Gallo et al., 2008 | 2 | 2 | 1 | 2 | 1 | 2 | 1 | 2 | 1 | 0 | 2 | 16 |
| Gerstner et al., 2005 | 2 | 2 | 2 | 2 | 1 | 1 | 2 | 2 | 2 | 1 | 2 | 19 |
| Goto et al., 2001 | 2 | 2 | 2 | 1 | 1 | 1 | 2 | 2 | 2 | 1 | 2 | 18 |
| Hayasaki et al., 2008 | 1 | 2 | 1 | 2 | 2 | 2 | 0 | 2 | 2 | 1 | 2 | 17 |
| Hayashi et al., 2009 | 2 | 2 | 1 | 2 | 1 | 1 | 0 | 2 | 2 | 1 | 2 | 16 |
| Hayashi et al., 2012 | 2 | 2 | 1 | 2 | 1 | 2 | 0 | 2 | 2 | 2 | 2 | 18 |
| Hosogai et al., 2008 | 2 | 2 | 1 | 2 | 1 | 2 | 1 | 2 | 0 | 2 | 1 | 16 |
| Johmson et al., 2007 | 1 | 2 | 1 | 1 | 1 | 1 | 1 | 2 | 1 | 2 | 2 | 15 |
| Kalaykova et al., 2011 | 2 | 2 | 1 | 2 | 2 | 2 | 0 | 2 | 2 | 0 | 2 | 17 |
| Kim et al., 2010 | 2 | 1 | 1 | 2 | 1 | 0 | 1 | 2 | 1 | 1 | 2 | 14 |
| Kim et al., 2013 | 2 | 2 | 1 | 1 | 1 | 1 | 1 | 2 | 1 | 1 | 2 | 15 |
| Krebs et al., 1994 | 2 | 2 | 2 | 2 | 2 | 2 | 2 | 2 | 2 | 2 | 2 | 22 |
| Krebs et al., 1995 | 2 | 2 | 2 | 2 | 1 | 2 | 2 | 2 | 1 | 2 | 2 | 20 |
| Kubota et al., 2010 | 2 | 2 | 2 | 2 | 1 | 2 | 0 | 2 | 2 | 0 | 2 | 17 |
| Leader et al., 1997 | 2 | 2 | 2 | 2 | 1 | 2 | 1 | 2 | 2 | 0 | 2 | 18 |
| Leader et al., 2003 | 2 | 2 | 2 | 2 | 1 | 0 | 1 | 2 | 2 | 2 | 2 | 18 |
| Leiggener et al., 2012 | 2 | 2 | 1 | 2 | 1 | 0 | 2 | 1 | 1 | 1 | 2 | 15 |
| Lemoine et al., 2005 | 2 | 2 | 1 | 2 | 1 | 1 | 1 | 2 | 1 | 2 | 2 | 17 |
| Lewis et al., 2001 | 2 | 2 | 2 | 2 | 2 | 2 | 2 | 2 | 1 | 1 | 2 | 20 |

| | | | | | | | | | | | | |
|---|---|---|---|---|---|---|---|---|---|---|---|---|
| Lobbezoo et al., 2000 | 2 | 2 | 1 | 2 | 1 | 1 | 0 | 2 | 2 | 0 | 2 | 15 |
| Mapelli et al., 2009 | 2 | 2 | 2 | 1 | 2 | 2 | 2 | 2 | 1 | 1 | 2 | 19 |
| Mapelli et al., 2016 | 2 | 2 | 2 | 1 | 2 | 2 | 2 | 2 | 1 | 0 | 2 | 18 |
| Minami et al., 2011 | 2 | 2 | 1 | 2 | 1 | 2 | 1 | 2 | 2 | 1 | 2 | 18 |
| Naeije and Hofman, 2003 | 1 | 1 | 1 | 2 | 1 | 1 | 0 | 2 | 2 | 1 | 2 | 14 |
| Naeije, 2002 | 2 | 1 | 1 | 2 | 1 | 1 | 2 | 2 | 2 | 0 | 2 | 16 |
| Ostry et al., 1997 | 2 | 1 | 2 | 2 | 1 | 0 | 2 | 2 | 0 | 1 | 2 | 15 |
| Otake et al., 2006 | 1 | 2 | 1 | 1 | 0 | 1 | 2 | 2 | 1 | 2 | 2 | 15 |
| Ogawa et al., 1998 | 2 | 2 | 2 | 2 | 2 | 2 | 2 | 2 | 2 | 1 | 2 | 21 |
| Ogawa et al., 2001 | 2 | 2 | 2 | 2 | 2 | 2 | 2 | 2 | 2 | 1 | 2 | 21 |
| Remign et al., 2017 | 2 | 2 | 1 | 1 | 2 | 2 | 0 | 2 | 2 | 1 | 2 | 17 |
| Röhrle et al., 2009 | 2 | 2 | 2 | 2 | 1 | 1 | 2 | 2 | 2 | 1 | 2 | 19 |
| Saitoh et al., 2002 | 2 | 2 | 1 | 2 | 1 | 2 | 0 | 2 | 2 | 0 | 2 | 16 |
| Sforza et al., 2009 | 2 | 2 | 2 | 2 | 1 | 1 | 2 | 2 | 2 | 1 | 2 | 19 |
| Sforza et al., 2010 | 1 | 2 | 1 | 2 | 1 | 1 | 1 | 1 | 2 | 1 | 2 | 15 |
| Sforza et al., 2011 | 2 | 2 | 2 | 2 | 1 | 2 | 2 | 2 | 2 | 1 | 2 | 20 |
| Shiller et al., 1999 | 2 | 2 | 2 | 2 | 1 | 1 | 2 | 2 | 2 | 0 | 2 | 18 |
| Shiller et al., 2001 | 2 | 2 | 2 | 2 | 0 | 1 | 2 | 2 | 2 | 1 | 2 | 18 |
| Siegler et al., 1991 | 1 | 2 | 2 | 2 | 1 | 0 | 2 | 2 | 2 | 1 | 2 | 17 |
| Slater et al., 1999 | 2 | 2 | 2 | 2 | 1 | 1 | 2 | 2 | 2 | 1 | 2 | 19 |
| Terajima et al., 2008 | 1 | 2 | 2 | 2 | 1 | 1 | 2 | 2 | 0 | 2 | 2 | 17 |
| Tomonari et al., 2017 | 2 | 2 | 1 | 2 | 1 | 2 | 1 | 2 | 1 | 2 | 2 | 18 |
| Travers et al., 2000 | 2 | 2 | 2 | 2 | 2 | 2 | 2 | 2 | 2 | 1 | 2 | 21 |
| Ugolini et al., 2017 | 2 | 2 | 2 | 1 | 2 | 2 | 2 | 2 | 1 | 1 | 2 | 19 |
| Ugolini et al., 2018 | 2 | 2 | 1 | 2 | 2 | 2 | 2 | 2 | 2 | 1 | 2 | 20 |
| Visscher et al., 2000 | 2 | 2 | 1 | 2 | 1 | 1 | 2 | 2 | 2 | 1 | 2 | 18 |
| Wojczynska et al., 2019 | 2 | 2 | 0 | 2 | 2 | 0 | 0 | 0 | 0 | 2 | 2 | 12 |
| Yashiro et al., 2015a | 2 | 2 | 1 | 2 | 2 | 1 | 1 | 1 | 2 | 0 | 2 | 16 |
| Yashiro et al., 2015b | 2 | 2 | 1 | 2 | 1 | 1 | 0 | 1 | 2 | 0 | 2 | 14 |
| Yatabe et al., 1995 | 2 | 2 | 2 | 2 | 1 | 1 | 2 | 2 | 2 | 1 | 2 | 19 |
| Yatabe et al., 1997 | 2 | 2 | 2 | 2 | 1 | 1 | 2 | 2 | 2 | 1 | 2 | 19 |
| Zaugg et al., 2012 | 2 | 2 | 2 | 2 | 1 | 2 | 2 | 2 | 2 | 2 | 2 | 21 |
| Zhang et al., 1995 | 2 | 2 | 2 | 2 | 1 | 1 | 2 | 2 | 2 | 2 | 2 | 20 |
| Zhao et al., 2012 | 2 | 2 | 2 | 2 | 1 | 1 | 2 | 2 | 2 | 0 | 2 | 18 |
| 3D Scanning | | | | | | | | | | | | |
| Kwon et al., 2019 | 1 | 2 | 2 | 0 | 0 | 1 | 1 | 2 | 2 | 2 | 2 | 15 |

Table A.A.2: Results of methodological quality assessment on each study that employs mechanical linkage systems, magnetic tracking systems and radiographic tracking. The quality question numbers refer to those outlined in Table 3.1. Each question was attributed a score of 2, 1 or 0 based on whether the question was clearly addressed, partially addressed or not addressed respectively. For each study quality scores were collated to give that paper an overall quality rating ranging from 0 to 22.

| **Authors** | **Quality Question** | | | | | | | | | | | **Overall Quality Rating** |
|---|---|---|---|---|---|---|---|---|---|---|---|---|
| | **1** | **2** | **3** | **4** | **5** | **6** | **7** | **8** | **9** | **10** | **11** | |
| Case Gnathic Replicator | | | | | | | | | | | | |
| Coffey et al., 1989 | 2 | 1 | 2 | 2 | 1 | 2 | 2 | 2 | 2 | 2 | 2 | 20 |
| Gibbs et al., 1971 | 0 | 2 | 1 | 2 | 1 | 2 | 2 | 2 | 2 | 1 | 2 | 17 |
| Axiography | | | | | | | | | | | | |
| Alsawaf et al., 1993 | 2 | 2 | 2 | 1 | 1 | 2 | 2 | 2 | 1 | 0 | 2 | 17 |
| Bernhardt et al., 2003 | 2 | 2 | 2 | 1 | 1 | 2 | 1 | 2 | 1 | 2 | 2 | 18 |
| Ghodsi & Rasaeipour, 2008 | 2 | 2 | 1 | 2 | 2 | 2 | 0 | 2 | 2 | 0 | 2 | 17 |
| Hirari et al., 2009 | 1 | 2 | 0 | 1 | 1 | 2 | 0 | 1 | 1 | 0 | 2 | 11 |
| Hüe, 2011 | 1 | 2 | 2 | 2 | 1 | 2 | 1 | 2 | 2 | 1 | 2 | 18 |
| Sadat-Khonsari et al., 2003a | 1 | 2 | 1 | 2 | 1 | 1 | 0 | 2 | 2 | 2 | 2 | 16 |
| Sadat-Khonsari et al., 2003b | 1 | 2 | 1 | 2 | 1 | 0 | 1 | 2 | 2 | 2 | 1 | 15 |
| Tamaki et al., 1997 | 1 | 2 | 1 | 2 | 2 | 1 | 2 | 2 | 2 | 0 | 2 | 17 |
| Theusner et al., 1993 | 2 | 2 | 1 | 2 | 1 | 1 | 0 | 2 | 2 | 0 | 2 | 15 |
| Wieckiewicz et al., 2014 | 2 | 1 | 1 | 2 | 2 | 2 | 1 | 2 | 2 | 1 | 2 | 18 |
| Ultrasonic Analysis | | | | | | | | | | | | |
| Baqaien et al., 2007 | 2 | 2 | 2 | 1 | 2 | 2 | 1 | 2 | 1 | 1 | 2 | 18 |
| Kiseri et al., 2018 | 2 | 2 | 2 | 2 | 1 | 2 | 2 | 2 | 1 | 0 | 2 | 18 |
| Ko et al., 2012 | 2 | 2 | 2 | 2 | 2 | 2 | 2 | 2 | 2 | 1 | 2 | 21 |
| Ko et al., 2015 | 2 | 2 | 0 | 2 | 1 | 2 | 0 | 2 | 1 | 0 | 2 | 14 |
| Kordaß et al., 2014 | 2 | 1 | 0 | 2 | 1 | 1 | 0 | 2 | 2 | 1 | 2 | 14 |
| Linsen et al., 2016 | 2 | 2 | 2 | 1 | 2 | 2 | 1 | 2 | 2 | 1 | 2 | 19 |
| Morneburg et al., 1998 | 2 | 2 | 1 | 2 | 1 | 1 | 0 | 2 | 2 | 1 | 2 | 16 |
| Ratzmann et al., 2007 | 2 | 2 | 0 | 1 | 1 | 0 | 0 | 2 | 1 | 1 | 2 | 12 |
| Reicheneder et al., 2013 | 1 | 2 | 2 | 2 | 2 | 1 | 2 | 2 | 2 | 1 | 2 | 19 |
| Schwestka-Polly et al., 1999 | 1 | 2 | 2 | 2 | 1 | 1 | 2 | 2 | 1 | 0 | 2 | 16 |
| Stiesch-Scholz et al., 2006 | 2 | 2 | 1 | 2 | 1 | 2 | 2 | 2 | 2 | 1 | 2 | 19 |
| Teng et al., 2015 | 2 | 2 | 2 | 1 | 2 | 2 | 1 | 2 | 2 | 0 | 2 | 18 |
| Wang et al., 2009 | 1 | 2 | 0 | 2 | 2 | 2 | 0 | 2 | 1 | 0 | 2 | 14 |
| Yen et al., 2017 | 1 | 2 | 1 | 2 | 2 | 2 | 0 | 2 | 2 | 0 | 2 | 16 |
| Magnetic Tracking | | | | | | | | | | | | |
| Baeyens et al., 2013 | 2 | 2 | 2 | 0 | 0 | 1 | 2 | 2 | 1 | 1 | 2 | 15 |
| Baltali et al., 2008a | 2 | 2 | 2 | 1 | 2 | 2 | 2 | 2 | 1 | 1 | 2 | 19 |
| Baltali et al., 2008b | 2 | 2 | 2 | 2 | 1 | 2 | 2 | 2 | 1 | 2 | 2 | 20 |
| Keller et al., 2012 | 2 | 2 | 0 | 2 | 2 | 2 | 0 | 0 | 0 | 1 | 2 | 13 |
| Minami et al., 2018 | 2 | 2 | 2 | 2 | 1 | 2 | 1 | 2 | 2 | 2 | 2 | 20 |
| Yamamoto et al., 2009 | 2 | 2 | 2 | 2 | 2 | 2 | 2 | 2 | 2 | 2 | 2 | 22 |
| Video X-ray Fluoroscopy | | | | | | | | | | | | |
| Chen et al., 2013a | 2 | 2 | 2 | 0 | 0 | 1 | 2 | 2 | 1 | 2 | 2 | 16 |
| Chen et al., 2013b | 2 | 2 | 2 | 2 | 1 | 1 | 2 | 2 | 2 | 0 | 2 | 18 |
| Yamazaki et al., 2014 | 1 | 1 | 2 | 2 | 0 | 0 | 1 | 2 | 1 | 1 | 2 | 13 |

## APPENDIX B

### Electromagnetic sensor accuracy

The precision of the DMD sensor position tracking was verified by calculating the distance between two sensors set on a custom-designed 3D-printed plate that rigidly cradled the sensors, separating them with a distance of 50.00 mm. The plate with the sensors attached was moved through the entire capture volume of the DMD system over approximately 30 seconds, and the difference between the calculated and actual sensor spacing was computed and used as a measure of the system precision (Figure A4.1).

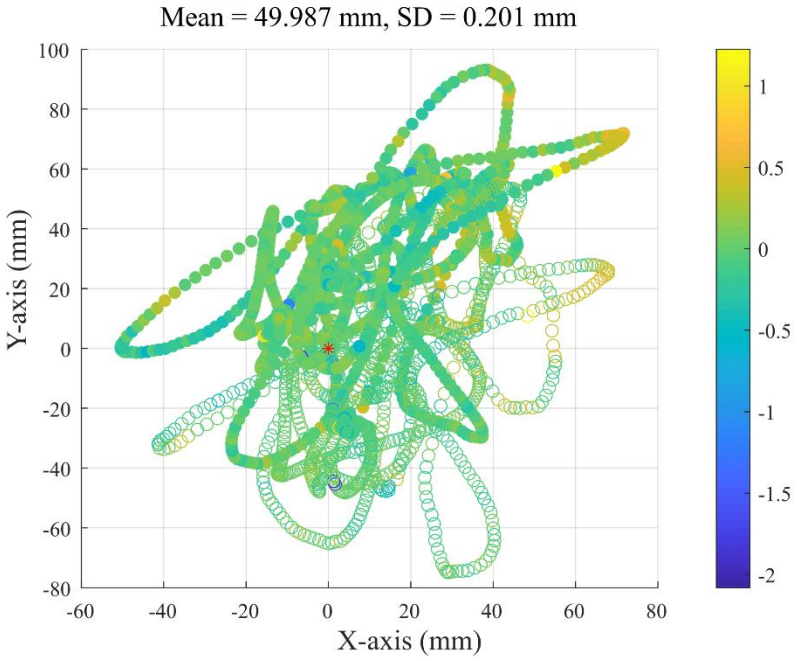



Figure A.B.1: DMD precision, evaluated from differences between calculated and actual sensor spacing as two sensors glued to a plate were moved through the magnetic field capture volume. The colour bar indicates the range of position measurement error in millimetres. The actual sensor spacing was 50.00 mm. Displayed are a sample of the complete trajectories used in the calculation.

**Mesh convergence**

A mesh convergence analysis was then conducted to evaluate the effect of different virtual rubber sample element sizes on the calculated load cell response. A reduction in element size from 0.35 mm to 0.3 mm was found to decrease the errors introduced both through solving the contact formulation and mesh discretisation by 0.7%; however, this was at the expense of increased computational time.

**Mass scaling**

Mass scaling was applied to the simulations to reduce the computation time. To assess whether this addition still lead to a meaningful solution the maximum ratio of kinetic energy to internal energy was calculated as a percentage for all simulations to ensure that inertial forces remained insignificant throughout the simulations. All values remain below the accepted 2% (Table A4.1).

Table A.B.1: Maximum ratio of kinetic energy to internal energy for each simulation.

| | Tooth | Chewing | Maximal-force biting |
|---|---|---|---|
| Left | Second molar | 0.11 % | 0.03 % |
| | First molar | 0.04 % | 0.01 % |
| | Premolar | 0.97 % | 0.08 % |
| Central | Incisor | 0.29 % | 0.04 % |
| Right | Premolar | 0.10 % | 0.03 % |
| | First molar | 0.06 % | 0.01 % |
| | Second molar | 0.09 % | 0.01 % |

**Error propagation**

The effect of the propagated errors from the kinematic measurement system on the calculated bite force values was analysed by running 4 separate simulations of mean chewing on the right 1st molar with the mandible offset by the mean measurement error of ±0.01 mm, as well as mean plus standard deviation of ±0.21 mm. These offsets resulted in approximately ± 2 N (mean) and ± 42 N (mean ± SD) of worst-case bite force calculation error at the maximum bite location (Figure A4.2 and Table A4.2).

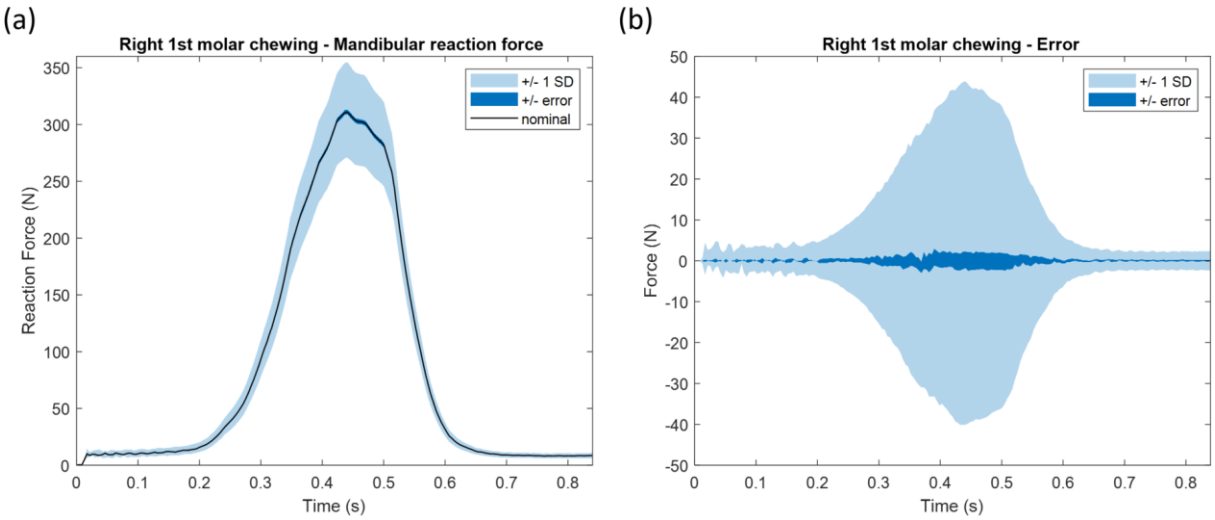



Figure A.B.2: (a) Effect of propagated kinematic measurement errors on the calculated bite force of the right 1st molar across the chewing cycle. (b) Resulting mean error in bite force calculation (dark blue) and error from ± 1 SD of the kinematic measurement error (light blue).

| Cycle progression | Bite force magnitude (N) | | | | |
|---|---|---|---|---|---|
| | Nominal | Nominal + 0.01 mm | Nominal - 0.01 mm | Nominal + 0.21 mm | Nominal - 0.21 mm |
| 25% | 50.61 | 51.23 | 50.14 | 61.56 | 44.11 |
| 50% | 102.21 | 102.54 | 100.79 | 119.81 | 91.14 |
| 75% | 178.19 | 179.29 | 176.29 | 204.62 | 163.29 |
| 100% | 310.74 | 312.93 | 308.92 | 354.60 | 270.66 |

Table A.B.2: Results of the four propagated measurement error simulations at 25%, 50%, 75% and 100% of the chewing cycle. Results are given for the nominal mandibular z-translation, and that offset by the mean kinematic measurement error (±0.01 mm), and offset by the mean kinematic measurement error plus one standard deviation (±0.21 mm).

## APPENDIX C

### Motion tracking plate validation

Accuracy of the subject-specific jaw motion tracking was assessed in one male participant (age: 41 years) with healthy dentition and no history of mandibular disorders or dental pain. Dental impressions were taken of the maxillary and mandibular dental arches and subject-specific motion tracking plates were manufactured. The participant had a lip and check retractor inserted to expose the teeth and was instructed to insert the two motion tracking plates. Six 4mm hemispherical retroreflective markers were then fixed to the incisors and premolars using dental adhesive, three on the maxillary teeth and three on the mandibular teeth (Fig. S1). Jaw motion tracking using these teeth mounted markers represented the reference "gold standard". Three 4mm hemispherical retroreflective markers were attached to each plate (Fig S1) to allow simultaneous motion tracking of the six tooth mounted markers and the six plate mounted markers. The participant was instructed to perform maximum border movements and chewing on a rubber sample as per the study protocol (see manuscript "Motion tracking experiments") whilst the positions of the 12 retroreflective markers were recoded using an optoelectronic tracking system sampling at 100Hz and filtered using a low-pass filter with a cut-off frequency of 10Hz. For each motion capture frame, the distance between the centrode of the tooth-mounted markers and the centroid of the plate-mounted markers were calculated. The resulting standard deviation of this distance (0.13 mm) was used as a measure of motion measurement accuracy of the tracking plates employed in the present study.

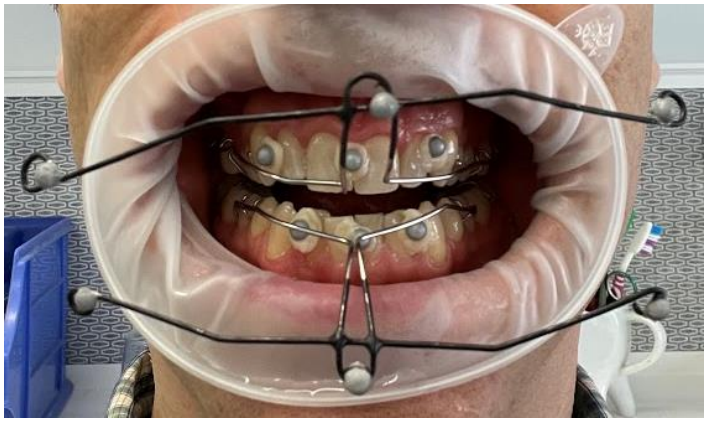


Figure A.C.1: Subject wearing motion tracking plates and 4mm hemispherical retroreflective markers attached to the mandibular and maxillary incisors and premolars.

**Case study - Bilateral total TMJ replacement**

Pilot kinematics data was collected for one adult female bilateral total TMJ replacement patient (age: 58.8 yrs, measurement time post op: 1.1 yrs). Bilateral total TMJ replacement resulted in decreased inferior incisal displacements at maximum mouth gape (33.1 mm) relative to controls (41.8 mm), this may be due to the small anterior translations of the prosthetic condyles (0.2 mm) compared to those of healthy controls (13.8 mm) (Fig. A.C.1 & Table A.C.1). Maximum lateral incisal translations were limited for the bilateral total TMJ replacement patient (2.3 mm) relative to controls (11.7 mm) (Fig. A.C.2 & Table A.C.1). During chewing the bilateral total TMJ replacement patient had a small mandibular rotation in the sagittal plane at the chewing start point (2.0°), which is comparable to that of controls (3.6°) and lower than that of unilateral total TMJ replacement patients chewing on the ipsilateral and contralateral molars (7.5° and 7.2°, respectively) (Table A.C.2). During chewing cycles, the bilateral total TMJ replacement patient's mandible moved in a hinge like motion about the condylar axis, characterised by negligible movement of both condyles and large posterior incisal movements during mouth opening (2.7 mm) compared to healthy controls (0.3 mm) (Fig. A.C.3).

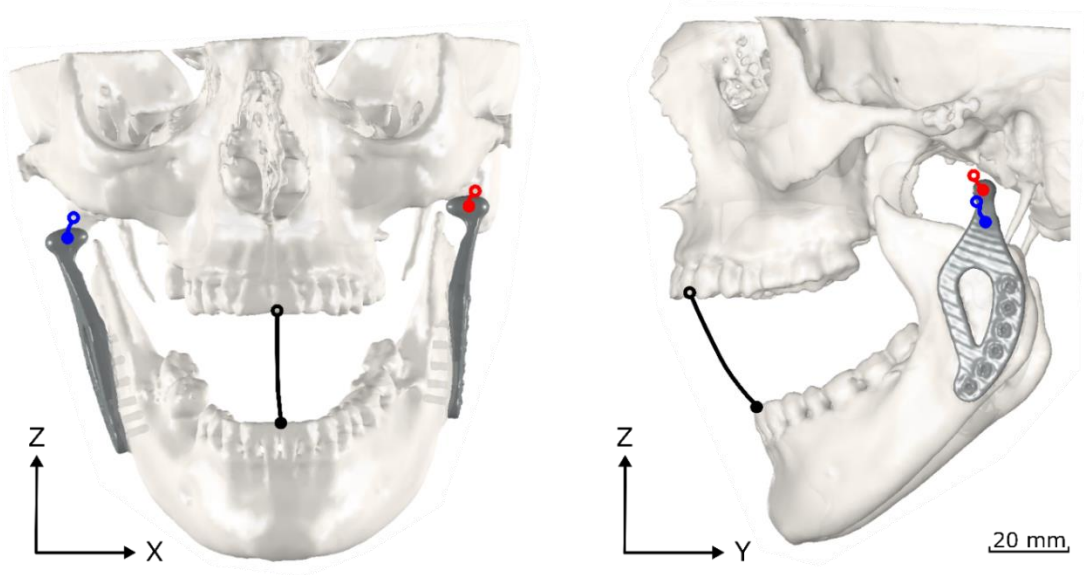



Figure A.C.1: Example of maximum mouth opening trajectory for the bilateral total TMJ replacement patient, viewed from the frontal and sagittal plane. Open circles represent landmarks at the maximum occlusion position, closed circles represent landmarks at the maximum mouth open position. Black, red, and blue lines indicate incisal, left condyle and right condyle trajectories respectively.

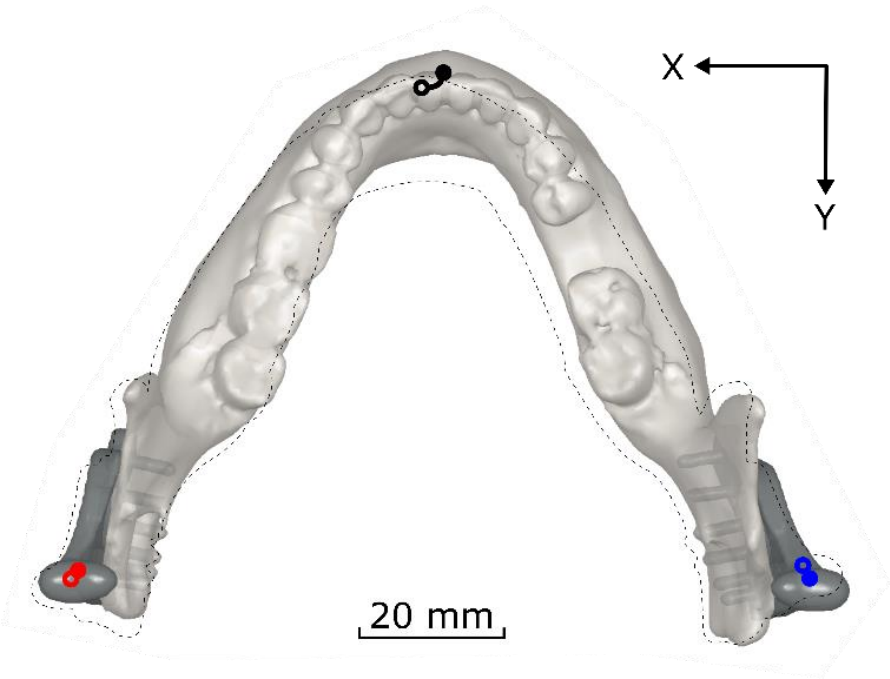



Figure A.C.2: Example of maximum lateral excursion towards the right projected onto the transverse plane for a bilateral total TMJ replacement patient. Dashed line represents mandible position at maximum occlusion position, rendered mandible represents mandible position at maximum lateral excursion position. Open circles represent landmarks at the mouth closed position, closed circles represent landmarks at the maximum lateral position. Black, red, and blue lines indicate incisal, left condyle and right condyle trajectories respectively.

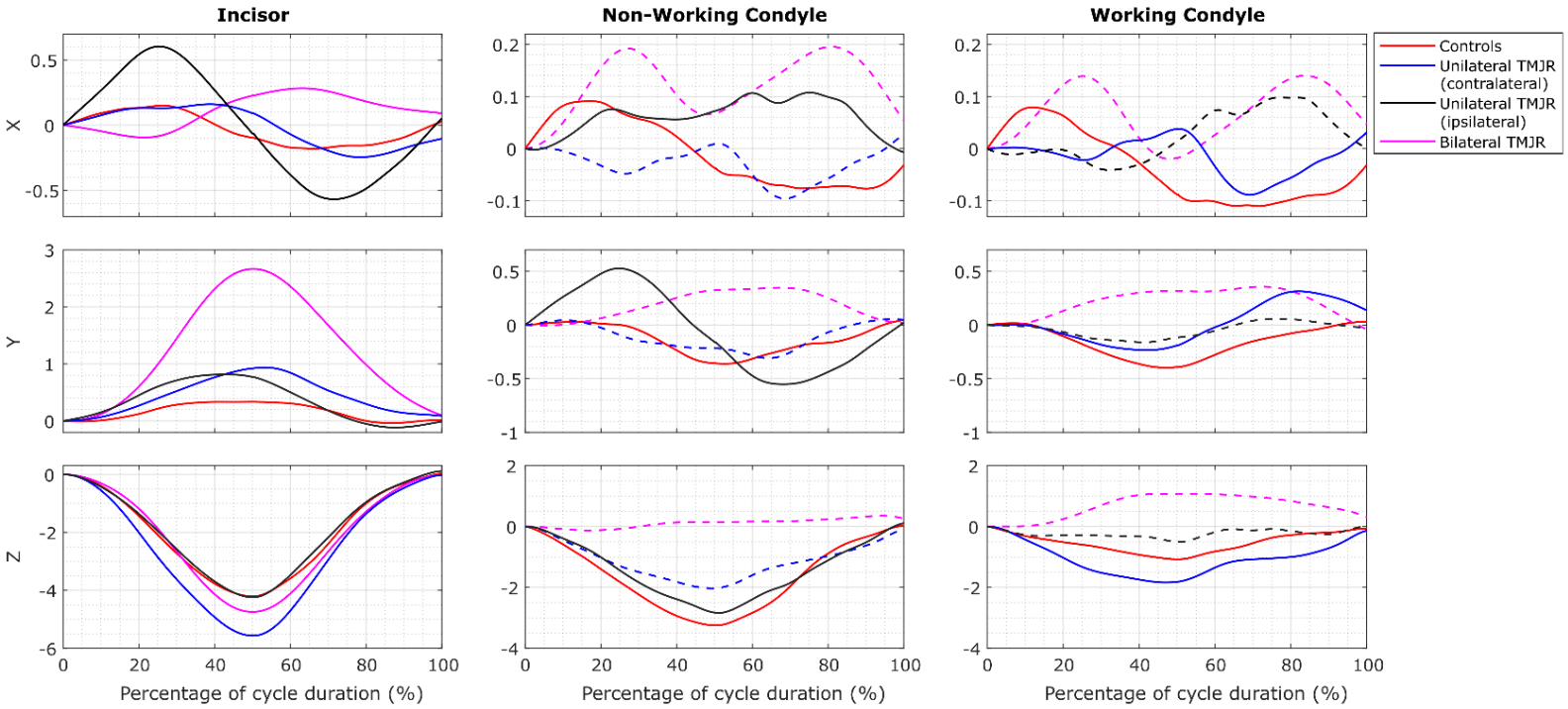



Figure A.C.3: Mean movements of the mandibular incisor point, non-working condyle and working condyle during one normalised cycle of molar chewing. Movements are shown for control subjects chewing on either side of their mouth (red), unilateral total TMJ replacement patients chewing on their contralateral molars (blue) and their ipsilateral molars (black), and the bilateral total TMJ replacement patient chewing on either side of the mouth (magenta). The start and end point of each cycle is from a mouth partially open position, compressing the rubber sample between the molars. Dashed lines represent movement of a prosthetic condyle. Positive X, Y and Z represent lateral (left), posterior and superior directions respectively.

Table A.C.1: Mean kinematic values at the maximum mouth opening, maximum lateral translation, and maximum protrusive positions for the bilateral total TMJ replacement patient. Displacement values are measured as the position of each landmark with respect to its position with the mandible in the maximum occlusion position.

| Movement | Condyle | Incisor displacement (mm) | | | | Condyle displacement (mm) | | | | Mandibular angle (degrees) | | |
|---|---|---|---|---|---|---|---|---|---|---|---|---|
| | | X | Y | Z | Linear distance | X | Y | Z | Linear distance | Sagittal (X=0) | Coronal (Y=0) | Transverse (Z=0) |
| Maximum mouth opening | both | 0.9 | 18.8 | -33.1 | 38.0 | -1.8 | -0.2 | -6.7 | 7.0 | 24.3 | 1.8 | 3.4 |
| Maximum lateral excursion | non-working | 2.3 | 0.6 | -4.6 | 5.3 | -0.9 | -1.7 | -1.5 | 2.8 | 7.9 | 1.5 | 1.3 |
| | working | | | | | -0.9 | 0.1 | -1.8 | 2.6 | | | |
| Maximum protrusion | both | -1.0 | -0.7 | -2.6 | 3.3 | -1.1 | -1.9 | -0.2 | 2.2 | 9.3 | 1.8 | 1.6 |

Table A.C.2: Mean kinematic values at the start point and turning point of molar chewing cycles for the bilateral total TMJ replacement patient. Displacement values are measured as the position of each landmark with respect to its position with the mandible in the maximum occlusion position.

| Cycle position | Incisor displacement (mm) | | | | Condylar displacement (mm) | | | | | | | | Mandibular angle (degrees) | | |
|---|---|---|---|---|---|---|---|---|---|---|---|---|---|---|---|
| | | | | | Non-Working side | | | | Working side | | | | | | |
| | X | Y | Z | Linear distance | X | Y | Z | Linear distance | X | Y | Z | Linear distance | Sagittal (X=0) | Coronal (Y=0) | Transverse (Z=0) |
| Start point | 1.3 | -1.2 | -7.8 | 8.2 | 0.7 | 2.3 | -9.0 | 9.4 | 0.8 | 2.9 | -9.2 | 9.8 | 2.0 | 1.0 | 0.5 |
| Turning point | 0.9 | 1.7 | -13.0 | 13.2 | 0.7 | 2.6 | -8.4 | 8.9 | 0.8 | 3.3 | -8.4 | 9.1 | 2.7 | 1.0 | 0.4 |

## APPENDIX D

### Bite force calculation

*Motion tracking plate validation*

The motion tracking error was evaluated in one male participant (age: 41 years) with healthy dentition and no history of dental pain or mandibular disorders. Subject-specific motion tracking plates were constructed for this subject as per the study protocol (see Materials and Methods). The participant had a lip and cheek retractor inserted to expose the teeth and was instructed to insert the two motion tracking plates. Following this, six 4 mm hemispherical retroreflective markers were fixed to the incisors and premolars using dental adhesive, three on the maxillary teeth and three on the mandibular teeth (Figure A.C.1). Three 4mm hemispherical retroreflective markers were attached to each plate (Figure A.C.1) to allow simultaneous motion tracking of the tooth mounted and plate mounted markers. The participant was instructed to chew on a rubber sample whilst the positions of the 12 retroreflective markers were recorded using an optoelectronic tracking system sampling at 100Hz and filtered using a low-pass filter with a cut-off frequency of 10Hz. Motion tracking using the teeth mounted markers represented the "gold standard" measurement of jaw motion. For each motion capture frame, the distance between the centrode of the tooth-mounted markers and the centroid of the plate-mounted markers was calculated. The resulting standard deviation of this distance (0.13 mm) was used as a measure of motion measurement accuracy of the tracking plates in the present study.

*Material characterisation*

The rubber material was modelled as a visco-hyperelastic material with a near incompressible material response. The material properties of the rubber sample were derived experimentally following the authors previously published protocol. The hyperelastic response was modelled using the phenomenological Ogden model, with the strain energy density function defined as:

$$W(\lambda_1, \lambda_2, \lambda_3) = \sum_{i=1}^{N} \frac{\mu_i}{\alpha_i} (\lambda_1^{\alpha_i} + \lambda_2^{\alpha_i} + \lambda_3^{\alpha_i} - 3) \quad (1)$$

Where N = 1, $\lambda_i$ are the principal stretch ratios and $\mu_i$ and $\alpha_i$ are the phenomenological material constants ($4.60 \times 10^5$ and 2.09 Pa, respectively) obtained using least squares optimisation on experimentally measured stress-strain curves ($R^2$ = 0.9985) (Figure A.D.1a).

The viscoelastic material response was modelled as a second order Prony series, with relaxation modulus given by:

$$g_R(t) = 1 - \sum_{i=1}^{N} g_i\left(1 - \exp\left(\frac{-t}{\tau_i}\right)\right) \quad (2)$$

Where N = 2, $t$ is time, and $g_i$ and $\tau_i$ are the phenomenological material constants (first order: $6.30 \times 10^{-2}$ and 0.99 s, second order: $5.58 \times 10^{-2}$ and 0.19 s, respectively) obtained using least squares optimisation on experimentally measured stress-relaxation curves ($R^2 = 0.9994$) (A.D.1b).

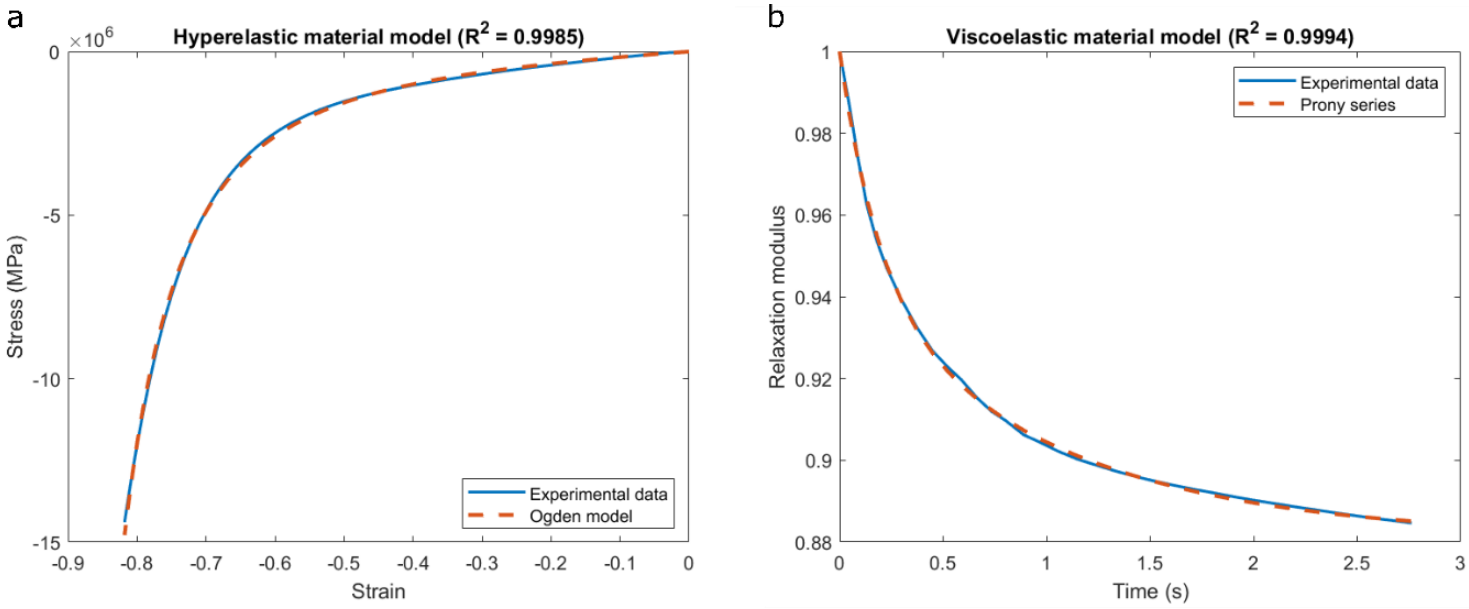
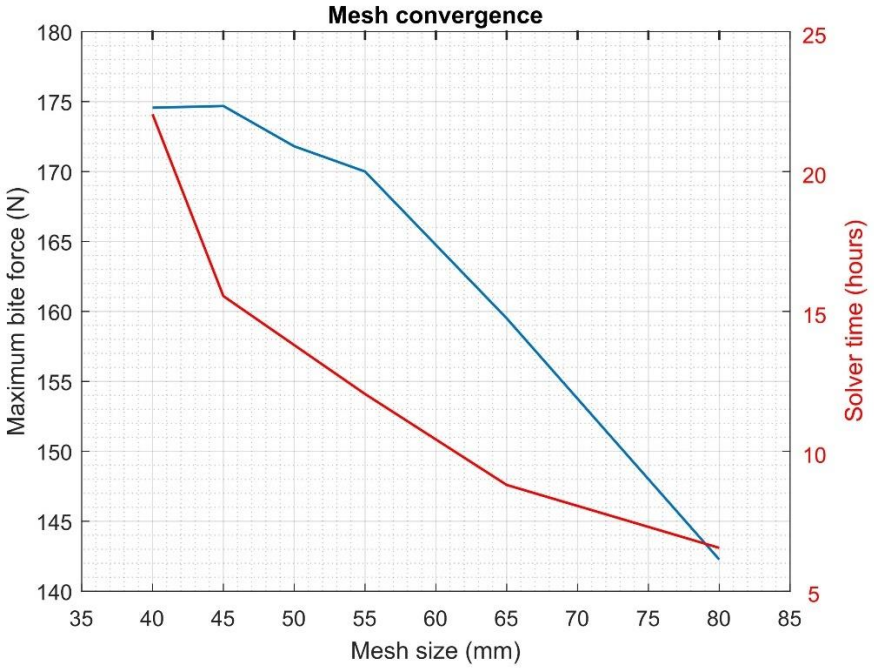



Figure A.D.1: Material model fit to experimental data. (a) Hyperelastic material response, Ogden model (N=1) fit to average experimentally measured stress-strain data. (b) Viscoelastic material response, Prony series (N=2) fit to average experimentally measured stress-relaxation data.

*Mesh convergence*

The rubber material used in Chapter 6 had different material properties to that used in Chapter 4, therefore a mesh convergence analysis was run to confirm an appropriate rubber mesh size. Maximum bite force was identified to converge at a localised mesh size of 0.4 mm (Fig. A.D.2).




FigureA.D.2: Mesh convergence analysis results showing the maximum bite force (blue) and solver time (red) variation with mesh size.

*Mass scaling*

Mass scaling was applied to the simulations to reduce the computation time. To assess whether this addition still led to a meaningful solution the maximum ratio of kinetic energy to internal energy was calculated as a percentage for all simulations to ensure that inertial forces remained insignificant throughout the simulations. The mean ratio of kinetic energy to internal energy is $7.79 \times 10^{-5} \pm 1.60 \times 10^{-4}$ %. All values remained below the accepted 2%.

*Wire interference*

Finite element simulations contained only the rigid geometry of the teeth and the deformable geometry of the rubber. The wire clasps of the mouthpieces were not included in the model. To assess the effect of this simplification, one model was created with 0.7 mm wires added around the first molars, and between the mandibular premolars (FigureA.D.3b), to represent the mouthpiece attachment points (FigureA.D.3a).

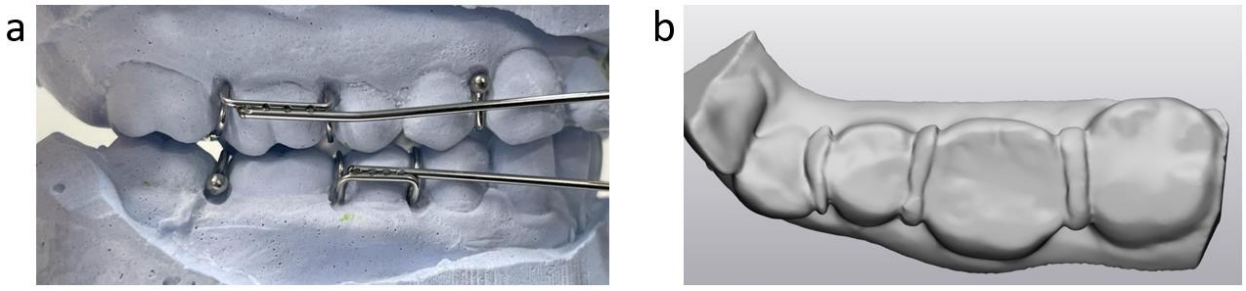



Figure A.D.3: Dental stone casts with mouthpieces attached showing maximum occlusion position (a), model of mandibular teeth with 0.7 mm wires between the teeth (b).

Modelling the wires increased the net bite force by 36.5 N, which corresponded to an error of 11.8 % (Figure A.D.4).

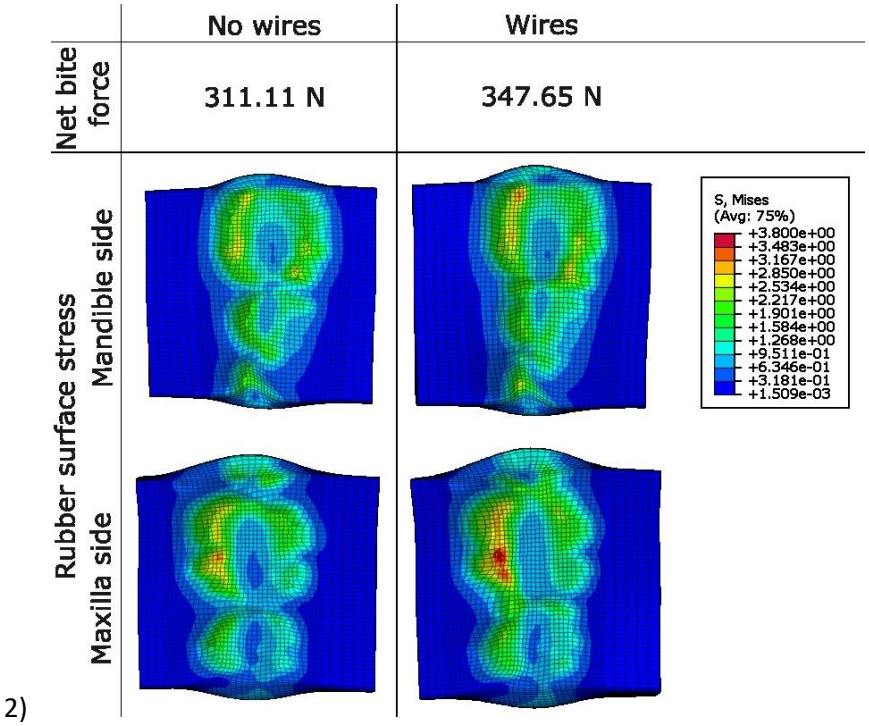



Figure A.D.4: Results of sensitivity analysis studying the effects of the mouthpiece wires on bite force results.

## Musculoskeletal modelling

Each participant's musculoskeletal model was based on a previously published generic, unscaled rigid body model with musculotendon properties defined in **Error! Reference source not found.** (Ackland et al. 2017). For each participant the muscle attachment points were anisotropically scaled based on their intercondylar distance and the distance between the mid-condyle point and the mandibular incisors. For each muscle a constant ratio of optimum fibre length and tendon slack length was maintained during scaling.

Table A.D.19:Musculotendon properties of the generic, unscaled rigid body musculoskeletal model.

| Muscle | | Volume ($cm^3$) | PCSA ($cm^2$) | Pennation angle (°) | Optimum fibre length (mm) | Tendon slack length (mm) | Max isometric force (N) |
|---|---|---|---|---|---|---|---|
| Left | Anterior temporalis | 32.2 | 6.4 | 15.3 | 50.4 | 39.7 | 231.0 |
| | Posterior temporalis | 20.7 | 4.5 | 11.6 | 45.6 | 42.0 | 166.5 |
| | Superficial masseter | 25.2 | 5.7 | 16.5 | 44.2 | 50.5 | 204.6 |
| | Deep anterior masseter | 5.0 | 1.5 | 6.7 | 33.5 | 26.3 | 55.4 |
| | Deep posterior masseter | 3.2 | 1.3 | 6.7 | 24.0 | 21.3 | 49.4 |
| | Medial pterygoid | 16.9 | 4.9 | 12.0 | 34.5 | 67.6 | 180.0 |
| | Inferior lateral pterygoid | 10.8 | 2.3 | 1.3 | 47.9 | 19.3 | 84.6 |
| | Superior lateral pterygoid | 3.6 | 0.8 | 0.0 | 47.1 | 20.6 | 28.5 |
| Right | Anterior temporalis | 33.4 | 6.4 | 15.3 | 52.3 | 41.3 | 231.0 |
| | Posterior temporalis | 21.7 | 4.5 | 11.6 | 47.9 | 44.0 | 166.5 |
| | Superficial masseter | 25.8 | 5.7 | 16.5 | 45.4 | 51.8 | 204.6 |
| | Deep anterior masseter | 5.2 | 1.5 | 6.7 | 34.9 | 27.3 | 55.4 |
| | Deep posterior masseter | 3.2 | 1.3 | 6.7 | 24.4 | 21.6 | 49.4 |
| | Medial pterygoid | 17.5 | 4.9 | 12.0 | 35.6 | 69.7 | 180.0 |
| | Inferior lateral pterygoid | 10.0 | 2.3 | 1.3 | 44.2 | 17.9 | 84.6 |
| | Superior lateral pterygoid | 3.7 | 0.8 | 0.0 | 48.4 | 21.1 | 28.5 |

The effect of modelling the masseter and temporalis muscles with full capacity was investigated through a sensitivity analysis. For one total unilateral TMJR patient musculoskeletal models were setup with the maximum isometric forces of the ipsilateral anterior temporalis, posterior temporalis, superficial masseter, deep anterior masseter and deep posterior masseter muscles modelled as 50%, 60%, 70%, 80%, 90% and 100% of their full capacity. The ipsilateral inferior lateral pterygoid and superior lateral pterygoid remained removed from the model, and the applied bite force remained the same. As the ipsilateral masseter and temporalis strength is decreased there is higher influence from the contralateral superficial masseter and the ipsilateral medial pterygoid muscles (Figure A.D.5). This resulted in higher compressive and tensile TMJ loading during ipsilateral molar biting for weakened masseter and temporalis muscles (Figure A.D.6). There is no available literature directly compares EMG activity of the temporalis and masseter muscles of TMJR patients to healthy controls. However, studies comparing contralateral to ipsilateral muscle function of unilateral total TMJR patients found operated to non-operated muscle force ratios of 0.97 and 0.89 for the masseter and temporalis, respectively, 12 months after surgery (Raustia et al. 1997). Therefore, it is reasonable to assume that the temporalis and masseter muscles of the unilateral total TMJ replacement patients in this study were operating between 90% to 100% of their full capacity.

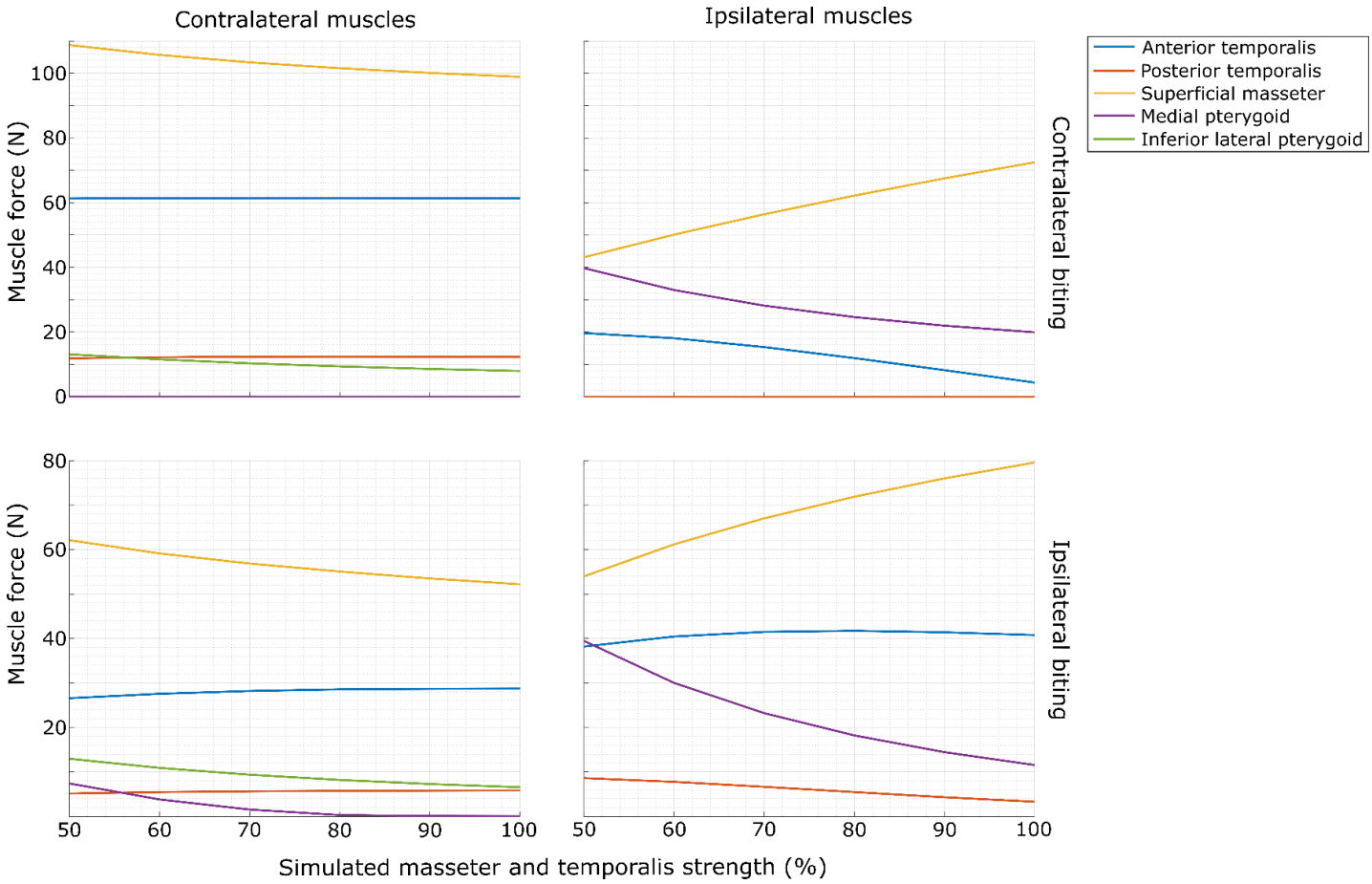



Figure A.D.5: Resultant muscle forces for the anterior temporalis, posterior temporalis, superficial masseter, medial pterygoid and inferior lateral pterygoid muscles when the maximum isometric force of the temporalis and masseter sub-regions are modelled as 50%, 60%, 70%, 80%, 90% and 100% of their full capacity.

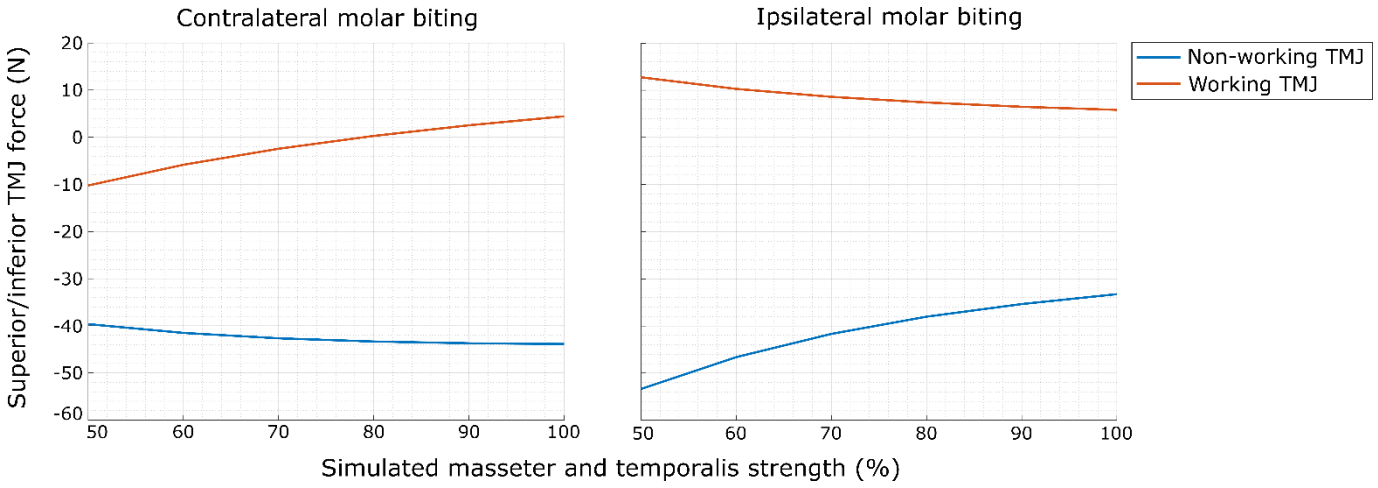



Figure A.D.6: TMJ loading when the maximum isometric force of the temporalis and masseter sub-regions are modelled as 50%, 60%, 70%, 80%, 90% and 100% of their full capacity.

# APPENDIX E

25 March 2019

Dr D Robinson
Biomedical Engineering
The University of Melbourne

Dear Dr Robinson

I am pleased to advise that the Psychology Health and Applied Sciences Human Ethics Sub-Committee approved the following Project:

Project title: **Measurement of chewing kinematics following temporomandibular joint replacement**
Researchers: **Dr G Dimitroulis, Prof V P Lee, Dr D C Ackland, Dr D Robinson**
Ethics ID: **1853328**

The Project has been approved for the period: **25-Mar-2019 to 31-Dec-2019**

It is your responsibility to ensure that all people associated with the Project are made aware of what has actually been approved.

Research projects are normally approved to 31 December of the year of approval. Projects may be renewed yearly for up to a total of five years upon receipt of a satisfactory annual report. If a project is to continue beyond five years a new application will normally need to be submitted.

Please note that the following conditions apply to your approval. Failure to abide by these conditions may result in suspension or discontinuation of approval and/or disciplinary action.

(a) **Limit of Approval:** Approval is limited strictly to the research as submitted in your Project application.

(b) **Variation to Project:** Any subsequent variations or modifications you might wish to make to the Project must be notified formally to the Human Ethics Sub-Committee for further consideration and approval. If the Sub-Committee considers that the proposed changes are significant, you may be required to submit a new application for approval of the revised Project.

(c) **Incidents or adverse effects:** Researchers must report immediately to the Sub-Committee anything which might affect the ethical acceptance of the protocol including adverse effects on participants or unforeseen events that might affect continued ethical acceptability of the Project. Failure to do so may result in suspension or cancellation of approval.

(d) **Monitoring:** All projects are subject to monitoring at any time by the Human Research Ethics Committee.

(e) **Annual Report:** Please be aware that the Human Research Ethics Committee requires that researchers submit an annual report on each of their projects at the end of the year, or at the conclusion of a project if it continues for less than this time. Failure to submit an annual report will mean that ethics approval will lapse.

(f) **Auditing:** All projects may be subject to audit by members of the Sub-Committee.

If you have any queries on these matters, or require additional information, please contact me using the details below. Please quote the ethics ID number and the title of the Project in any future correspondence. On behalf of the Sub-Committee I wish you well in your research.

Yours sincerely

Mr Tony Callahan
Secretary, Psychology Health & Applied Sciences HESC
Phone: 8344 2017, Email: t.callahan@unimelb.edu.au

THE UNIVERSITY OF MELBOURNE

HUMAN RESEARCH ETHICS

# PROJECT APPLICATION FORM

## How To Use This Form

1. **Consider and refer to relevant guidelines and regulations.**
   References to specific guidelines are provided, with hyperlinks, throughout this form. The primary guide for human research ethics in Australia is the ***National Statement on Ethical Conduct in Human Research (2007) - Updated May 2015***. Human research ethics applications at the University of Melbourne are reviewed and approved under the warrant of the *National Statement*. References to the *National Statement* are abbreviated (e.g. ***NS* §2.1**.)
2. **Use plain English.**
   Use clear, non-technical language in your application. Be concise. Spell out the first instances of acronyms and abbreviations. Avoid jargon. Do not repeat information. Following these directions ensures effective review of your application. It will avoid unnecessary delays which result if applications are not clear and concise.
3. **Consider ethical principles.**
   Your application will be reviewed according to the principles of ethical research outlined in the *National Statement*, namely:
   - **Research Merit and Integrity** (***NS* §1.1 - §1.3**)
   - **Justice** (***NS* §1.4 - §1.5**)
   - **Beneficence** (***NS* §1.6 - §1.9**)
   - **Respect** (***NS* §1.10 - §1.13**)
4. **Use the current version of the application form.**
   Ensure that you are using the current version by downloading **this form** each time you prepare a new application.
5. **Detailed instructions for specific questions are available online.**
   If you are unsure about how best to answer a particular question, consult the Human Research Ethics **Guidance Document**. That document provides detailed guidance on how to answer specific questions in this form.
6. **Where possible, avoid printing this form.**
   Consult your HEAG to find out if they still require hard copies of your application. If you must print this form, consider printing double-sided and in grayscale (black and white).
7. **Save your completed application as a PDF and upload it to Themis.**
   Refer to your local Human Ethics Advisory Group (**HEAG**) for detailed instructions on how and when to submit your application.

## ANSWER ALL OF THE QUESTIONS IN THIS FORM

| | | |
|---|---|---|
| **Ethics ID number:** *(assigned by Themis)* | 1853328.1 | |
| **Project Title:** *(as recorded in Themis)* | Measurement of chewing kinematics following temporomandibular joint replacement | |
| **Responsible Researcher:** *(as recorded in Themis)* | Dr. Dale Robinson | |
| **Application Type:** *(mark with an "X")* | x | **Minimal Risk** |
| | | **Standard Project** |

# 1. Project Details

| 1.1 Project Summary | Summarise your research project in plain language.<br>**[Limit: 300 words]** |
|---|---|

**A) Aims and Objectives**

The temporomandibular joint (TMJ) connects the jaw and skull and is essential for speech, chewing and expressions of emotion. Disorders of the TMJ detrimentally impact an individual's quality of life, and can result in severe pain and dysfunction during normal daily tasks. TMJ replacement surgery may restore pain-free joint function, however, a critical limitation of current TMJ prostheses is the ball-and-socket design, which produces unnatural mandible motion. There is a clear need to improve the design of current TMJ prostheses to allow greater joint translation to achieve more natural prosthetic condyle movement.

The aim of this project is to measure the jaw motion and bite forces of patients following a total joint replacement of the temporal mandibular joint, and to compare these data to normal controls. These data will be used to create a computational model of normal and prosthetic TMJ, which will be used to improve the design of current TMJ prostheses to achieve more natural prosthetic condyle movement.

**B) Key Question(s)**

What is the jaw motion and bite force of a patient following TMJ replacement surgery and how does this vary from a natural joint?

How can the design of the current TMJ prostheses be redesigned to achieve jaw movement that better resembles that of a natural joint?

**C) Research Design**

Five subjects that have received a TMJ replacement from greater than one year previously, along with five age-matched controls with healthy TMJs, will be recruited for chewing kinematics and force measurement experiments. In these experiments, subjects will bite on a rubber strip whilst wearing a customised dental plate. The plate will allow the motion of the mandible to be tracked relative to the maxilla. This motion will be used in a computational model to determine the experimental bite force and joint loads. These data will be compared between the TMJ patients and the controls.

| Specific Guidelines Checklist | | |
|---|---|---|
| **Type an "X" in the left-hand column beside all items that apply to your research project.** Linked sections of the National Statement contain relevant guidelines and requirements that you need to address when completing your application. | | |
| | **Children and/or young people (< 18 years old)** will be recruited as participants. | → **Refer to *NS* §4.2.** |
| x | **People in dependent or unequal relationships** will be recruited as participants.<br>(There are pre-existing relationships between participants and researchers, or between participants and others involved in facilitating or implementing the research. E.g. student/teacher, patient/doctor, employee/employer.) | → **Refer to *NS* §4.3.** |
| | **People in countries other than Australia** will be recruited as participants. | → **Refer to *NS* §4.8.** |
| | One or more of the following describes the research project:<br>• it will be about **Aboriginal and/or Torres Strait Islander individuals or peoples**, their health, or their culture(s), language(s) or histories;<br>• it will be about the impact(s) or effect(s) of some phenomenon or phenomena on **Aboriginal and/or Torres Strait Islander individuals or peoples;**<br>• it will *specifically target* **Aboriginal and/or Torres Strait Islander people** to be recruited as participants;<br>• it will be conducted in a geographic location where a significant number of the population are likely to be **Aboriginal and/or Torres Strait Islander.** | → **Refer to *NS* §4.7.**<br>→ **Refer to *Values and Ethics*.**<br>→ **Refer to *GERAIS*.**<br>→ **This application is ineligible for minimal risk review.** |
| | One or both of the following describes the research project:<br>• it will *specifically target* **women who are pregnant** to be recruited as participants;<br>• it will be focused on **women who are pregnant and/or the human foetus** (including human foetal tissue or human embryos). | → **Refer to *NS* §4.1.**<br>→ **This application is ineligible for minimal risk review.** |
| | **People who may be involved in illegal activities** will be recruited as participants, ***and the research project could potentially expose such activities.*** | → **Refer to *NS* §4.6.**<br>→ **This application is *likely* ineligible for minimal risk review.** |
| | **People with cognitive impairment, intellectual disability, or mental illness** will be recruited as participants. | → **Refer to *NS* §4.5.**<br>→ **This application is ineligible for minimal risk review.** |
| | **People who are highly dependent on medical care** will be recruited as participants. | → **Refer to *NS* §4.4.**<br>→ **This application is ineligible for minimal risk review.** |
| | **None of the above** applies to this research project. | |

## Additional Modules Checklist

**Type an "X" in the left-hand column beside all items that apply to your research project.** This checklist will help you determine if you need to complete any other modules in addition to this application form. Linked sections of the *National Statement* contain relevant guidelines and requirements that you need to address when completing this form and any applicable additional modules.

| | | |
|---|---|---|
| | This research project will involve the **creation of a databank** (i.e. your stored data will be made available to other parties for secondary use in future research projects). | → **Refer to *NS* §3.2.**<br>→ **Complete and attach the *Privacy and Databanks Module*.** |
| | This research project will involve the **collection of information for a databank** (i.e. your stored data will be made available to other parties for secondary use in future research projects). | → **Refer to *NS* §3.2.**<br>→ **Complete and attach the *Privacy and Databanks Module*.** |
| | This research project will involve **accessing information from an existing databank** (i.e. you will be accessing and making use of stored data that was previously collected – not for this specific project – by other parties). | → **Refer to *NS* §3.2.**<br>→ **Complete and attach the *Privacy and Databanks Module*.** |
| | This research project will involve obtaining identifiable (or potentially identifiable) **personal information (including health information)** about individuals ***without their consent.*** | → **Complete and attach the *Privacy and Databanks Module*.** |
| | This research project will involve the collection and/or use of **human tissue/biological samples or materials** (e.g. blood, saliva, cheek swabs, hair, human embryonic or foetal tissue). | →**Refer to *NS* §3.4.**<br>→ **Complete and attach the *Body Tissue and Genetic Research Module*.** |
| | This research project will involve **human genetics.** | → **Refer to *NS* §3.5.**<br>→ **This application is ineligible for minimal risk review.**<br>→ **Complete and attach the *Body Tissue and Genetic Research Module*.** |
| | This research project will involve **medical interventions, therapies or trials.** | → **Refer to *NS* §3.3.**<br>→ **This application is ineligible for minimal risk review.**<br>→ **Complete and attach the *Interventions, Therapies and Trials Module*.** |
| **X** | This research project will involve **administration of ionising radiation.** | → **Complete and attach the *Ionising Radiation Module*.** |
| | **None of the above** applies to this research project. | |

# 2. Background and Method

| 2.1 Background and Significance | Provide a summary of background information. Explain the significance of the proposed research in the context of this background. **Refer to *NS* §5.2.5.**<br>**[Limit: 500 words]** |
|---|---|

**A) Background:**

The temporomandibular joint (TMJ) is a synovial joint that allows movement of the jaw (i.e., mandible) relative to the skull, and is essential for daily activities such as speech, chewing and expression of emotion. TMJ disorders are the most frequent cause of chronic orofacial pain and manifest in a number of diseases including osteoarthritis, ankyloses, severe condylar resorption, trauma and cancer, which often lead to pain and joint dysfunction. For the most severe conditions, TMJ replacement surgery with prosthetic components (i.e., TMJ alloplasty) is an end-stage treatment to restore pain-free joint function when more conservative approaches have proven unsuccessful.

The design of all current regulatory-approved TMJ prostheses are similarly configured, where the natural TMJ is replaced with a metallic condyle articulating within a hemispherical polyethylene fossa. Whilst this ball-and-socket joint is inherently stable, it only permits rotational joint motion, which differs from the natural TMJ where the concave slot of the glenoid fossa allows up to 16 mm of mandibular condyle translation [1]. Mandible translation is essential for normal masticatory performance, as it allows the molars to generate large shear forces, hence, the restricted mandible motion following TMJ alloplasty has been attributed to reduced chewing function [2]. This is particularly problematic where both joints are replaced in bilateral TMJ alloplasty and, as a result, significantly altered jaw movements compared to controls or uni-lateral TMJ replacements have been reported [2,3]. There is a clear need to improve the design of current TMJ prostheses to allow greater joint translation to achieve more natural prosthetic condyle movement.

Typically, TMJ prostheses are designed using FE analysis, which requires a 3D model of the jaw anatomy and, ideally, measurements of the 3D position of the mandible (i.e., kinematics) and the corresponding bite force. Whilst jaw and maxilla kinematics have been obtained for both natural and prosthetic TMJs [2,3], very few studies have coupled these measurements with bite force [4]. Furthermore, most bite force measurement devices only provide the vertical component of load, which neglects the significant shear forces known to occur during mastication [5].

**References**


[1] Van Loon, J. P., Falkenström, C. H., De Bont, L. G. M., Verkerke, G. J., and Stegenga, B., 1999, “The Theoretical Optimal Center of Rotation for a Temporomandibular Joint Prosthesis: A Three-Dimensional Kinematic Study,” J. Dent. Res., 78(1), pp. 43–48.

[2] Wojczyńska, A., Leiggener, C. S., Bredell, M., Ettlin, D. A., Erni, S., Gallo, L. M., and Colombo, V., 2016, “Alloplastic Total Temporomandibular Joint Replacements: Do They Perform like Natural Joints? Prospective Cohort Study with a Historical Control,” Int. J. Oral Maxillofac. Surg., 45(10), pp. 1213–1221.

[3] Voiner, J., Yu, J., Deitrich, P., Chafin, C., and Giannakopoulos, H., 2011, “Analysis of Mandibular Motion Following Unilateral and Bilateral Alloplastic TMJ Reconstruction,” Int. J. Oral Maxillofac. Surg., 40(6), pp. 569

[4] Lepley, C. R., Throckmorton, G. S., Ceen, R. F., and Buschang, P. H., 2011, "Relative Contributions of Occlusion, Maximum Bite Force, and Chewing Cycle Kinematics to Masticatory Performance," Am. J. Orthod. Dentofac. Orthop., 139(5), pp. 606–613.

[5] Röhrle, O., Saini, H., Lee, P. V. S., and Ackland, D. C., 2018, "A Novel Computational Method to Determine Subject-Specific Bite Force and Occlusal Loading during Mastication," Comput. Methods Biomech. Biomed. Eng., pp. 1–8.

**B) Significance of This Research:**

This study will obtain novel measurements of 3D kinematics and bite force for patients following TMJ joint replacement and for patients with normal asymptomatic TMJs. These novel data will provide a more detailed understanding of the implications of TMJ replacement and by applying these data in subject-specific FE models of the jaw and skull [1]), it will be possible to develop a TMJ prosthesis that provides for greater translation to facilitate a more natural form of joint motion.

## 2.2 Research Design and Method

Provide details of your research design and your proposed method. **Refer to *NS* §5.2.5 - §5.2.6.**

**Attach a copy of any measures, scales, questionnaires, survey instruments (including online surveys), interview questions/themes, and/or focus group topics/questions to be used.**

**A) Participants (or Recruitment Targets, such as medical records):**

Ten subjects will be recruited for testing; Five TMJ patients who have undergone TMJ replacement and five controls with asymptomatic TMJs. The subjects will be chosen to achieve an age-match between the group of TMJ patients and the controls. The control subjects will be excluded if they have a prior history of TMJ surgery, pain or congenital abnormalities. TMJ replacement patients will be recruited that have received their joint replacement surgery of more than 1 year previously.

This sample size follows from the limited number of patients available for recruitment who live locally (i.e., in Melbourne) and have recently received a TMJ replacement. A similar study to our proposed research examined mandible motion for TMJ replacement subjects incorporated 4 patients and still yielded significant findings (Wojczyńska, et al., 2018, Int. J. Oral Maxillofac. Surg). Furthermore, the proposed experimental technique has only been previously validated for a single subject (see Röhrle et al., 2018, Comput. Methods Biomech. Biomed. Eng), hence, it is logical to only develop this new technique for a slightly larger sample size.

**B) Recruitment:**

Control subjects will be recruited by the responsible researcher by paper-based advertisements placed on notice boards around the University of Melbourne, and through colleagues and personal contacts of the research group. Recruitment of TMJ patients will be administered by Dr George Dimitroulis through his specialist practice in Melbourne CBD.

**C) Participant Incentives:**

Ability to see and understand first-hand the use of modern biomechanics research technology, and ultimately, to gain knowledge of how the human temporal mandibular joint moves prior and following TMJ replacement surgery (via the final peer-reviewed publications of the findings).

**D) Participant Task(s):**

Subjects will be asked to perform a series of movements to evaluate their range of jaw movement (i.e., opening, protrusion/retraction, lateral translation), followed by compressive occlusal movements (i.e., chewing) on a soft strip of rubber that is 20x10x5 mm in size, whilst wearing a customised dental plate attached to the mandibular dental arch. The chewing cycle will be repeated 5 times at different positions on the left and right side of the maxillary and mandibular teeth, including the first molar and pre-molar. Each customised dental plate is designed such that the subject may clench and completely close their jaw and lips without obstruction. Prior to use, the dental plates and rubber strip will be sterilised using a denture cleaning tablet dissolved in water overnight. Attached to each dental plate are three retro-reflective markers that are tracked to measure the 3D kinematics of the mandible. Three additional markers will be placed on the subject's forehead and the bridge of the nose to track their maxilla kinematics.

Control subjects will be instructed to perform a maximal bite on the piece of rubber, whereas TMJ replacement patients will perform a bite within the range they would comfortably perform during eating. Each subject will be given the opportunity to stretch their jaw and warm up by chewing on a piece of fruit or soft lolly and will be given rest periods on request. The subjects will be instructed to maintain care against swallowing the piece of rubber. It is estimated that all testing will take approximately one hour per subject, including rests.

**E) Data/Material Collection Technique(s):**

All subjects will have dental impressions taken by Dr. George Dimitroulis at his specialist practice in Melbourne CBD. The 5 control patients will receive a CT scan at the Melbourne Brain Centre (University of Melbourne), whilst pre-operative CT scans of the TMJ patients that were previously obtained for their treatment will be provided by Epworth Hospital. These scans will be used to construct 3D computational models of each patient's jaw anatomy. In order to measure the post-operative anatomy and prosthesis position of the TMJ patients, CT scans will be taken at the Melbourne Brain Centre.

All ten subjects will be invited to the CAREN laboratory for testing, which is located in the Melbourne School of Engineering. Each subject will be requested to wear their hair tied back and not to wear clothing or reflective jewellery that may interfere with the measurement system. Each subject will be seated in a chair and, assisted by the researcher, will have their customised dental plate positioned on their mandibular teeth. To maintain hygiene and avoid infection whilst fitting the plate, the researcher will wear sterilised examination gloves. A thin wire on the dental plate extends between the patients lips and outside the mouth and has three retroreflective markers attached. An additional three markers will be placed on the subject's forehead and the bridge of the nose. These markers will be used to measure the motions of the mandible and maxilla during the jaw range-of-motion and chewing tasks.

Each subject will be asked to close their jaw in order to establish a reference position of the mandible relative to the maxilla. The subject will then be asked to perform a set of jaw movements (opening and closing, protrusion and retraction and lateral translation), repeating each task five times. The researcher will then position the rubber sample at the desired position in the subject's mouth who will then perform a compressive occlusal movement. This movement cycle will be repeated 5 times for the left and right first molar and pre-molars. The entire chewing cycle will be recorded by a motion analysis system comprising four calibrated infra-red cameras.

**F) Data Analysis:**

The motion data will be employed to calculate the kinematics and bite force using a previously published computer model (see reference [5] for details). These data will be applied in a musculoskeletal model generated for the patient to determine the corresponding muscle forces and joint loads. Significant differences between the controls and the TMJ patients will be determined via standard statistical analysis. A second detailed computational model will be constructed of each subjects TMJ to evaluate joint loading, bone and implant stresses. These data will be used to redesign the TMJ prosthesis to facilitate more natural joint movement.

# 3. Risks, Benefits and Monitoring

| | |
|---|---|
| **3.1 Potential Risks to Participants** | Does your research project pose any potential risks to participants? What are those risks? How will they be negated, minimised or managed?<br>**Refer to *NS* §2.1.**<br>**Note that the risks you identify here should also be described in your Plain Language Statement (PLS). Attach a copy of any distress protocol or adverse event protocol (if applicable).** |

**A) Potential Risks**

1. This is a risk of the patient swallowing the rubber strip and potentially choking.
2. There is an infection risk presented by the objects being placed in the patient's mouth, and from the researcher's hands when positioning these objects. The containers used to hold the objects also present an infection risk.
3. There is risk of a soft tissue injury (i.e., muscle strain) when any of the subjects bite the rubber strip.
4. For the TMJ patients, there is a risk of prosthesis failure if they bite too excessively on the rubber strip.
5. There is a risk of the dental plate having a surface that causes a cut in the mouth or on the tongue.
6. Side effects associated with a CT scan which uses ionising radiation.
7. Dependent relationships.

**B) Risk Management Strategy**

1. To minimise the choking risk, only a small rubber strip (20x10x5 mm) is used that is of a similar softness to an eraser, as consistent with previous experiments (see reference [5] for details). Whilst this object is unlikely to choke an adult, it still presents a swallowing risk. This will be managed by careful demonstration of how to safely position the rubber strip. For instance, the patient will be instructed to always maintain pressure of the rubber specimen with their teeth and to never move the specimen towards the rear of their mouth with their tongue. If the patient needs to release the rubber strip, they will be instructed to spit the specimen into a provided container.
2. To minimise infection risks, the dental plate and rubber samples will be soaked overnight in water with a denture cleaning tablet, which kills 99.9% of bacteria on the objects. All containers used in the experiments will be cleaned in an autoclave in the University of Melbourne Department of Dentistry. Benches and surfaces will be disinfected with a commercial surface cleaner prior and following experimentation. Whilst adjusting objects in the patients mouths, researchers will wear sterilised examination gloves.
3. To prevent soft tissue injuries, each subject will be given the opportunity to stretch their jaw and warm up by chewing on a piece of fruit or soft lolly. To prevent fatigue, the subjects will be given rest periods during the experiment an on request.
4. To prevent any potential failure of the prosthesis when biting on the rubber strip, these TMJ patients will be instructed to only bite down to a pain-free amount, comparable to what they would comfortably perform when eating. These patients will be recruited more than 1 year following surgery, a period that would be sufficient to allow the bone and prosthesis to osseointegrate into a solid structure and by this time the patients would have already used their jaw to bite down on food of a similar consistency to the rubber.
5. The dental plate will be machined so there are no sharp features that present a cut risk.
6. The radiation dosage for imaging the mandible and maxilla using a cone-beam CT is very low, which poses a minimal risk of harmful effects from radiation (see Ionising Radiation Module).
7. Participants may be students and staff members at the University of Melbourne who have dependent relationships with the Principal Researchers (e.g. student/professor, colleague/colleague). The TMJ patients also have a dependent relationship with the surgeon who is collaborating on this project. The participants will be provided with a Plain Language Statement in which the voluntary nature of participation is strongly emphasized. It will also be specified to the participants that they may withdraw from the study at any time without fear of prejudice.

| **3.2 Potential Risks to Non-Participants** | Does your research project pose any potential risks to non-participants? (This could possibly include risks to researchers or independent contractors.) If so, how will these risks be minimised? **Refer to *NS* §2.1.** |
|---|---|

Only subjects are receiving CT scans, so there is no risk to researchers.

## 3.3 Risks, Benefits and Justification

In light of the risks and expected benefits of the research project, explain how the expected benefits of the research justify any risks it may pose. **Refer to *NS* §1.6 - §1.7 and *NS* §2.1.**

### A) Expected Benefits

This study will provide novel experimental data describing the bite force and kinematics of patients following TMJ replacement surgery and controls. These data will provide the most detailed information to date demonstrating the effects of TMJ replacement surgery. It will be possible to use this data to construct computational models by which the prosthetic TMJ device may be redesigned to behave more similarly to a natural joint.

### B) Justification of Risks by Expected Benefits

Whilst the injury and infection risks are low, the potential benefits of improving the shortcomings of TMJ surgery are high. This project will provide new insights into the implications following joint replacement surgery since no previous study has coupled bite force measurements with 3D kinematics following this procedure. This research will provide data by which the prosthetic TMJ may be redesigned to behave more naturally, which would improve post-operative outcomes for the patient by better allowing them chew food.

Obtaining the CT scans of the subjects is essential for all aspects of this project, including the data collection and building the computational models. Whilst MRI would offer an alternative, these are less accurate at reproducing the bone geometry compared to CT and more susceptible to metal artefact effects from the implant. Further, MRI does not provide information regarding bone quality, an important consideration when evaluating the integrity of an implanted device. It was shown that for imaging the mandible and maxilla, the radiation dosage presented a very low risk of harm to the patient (see Ionising Radiation Module). Considering the importance and value added to the experimental and computational analyses, the research benefits of this project (i.e., better understanding the effects of TMJ replacement, and an improved prosthesis design) justify the use of this imaging modality.

## 3.4 Management and Monitoring

How will researchers manage and monitor conduct of the research project? **Refer to *NS* §5.5.**

### A) Management

*[Provide details of how and by whom the research project will be managed, throughout the life of the project, to ensure that it complies with the protocols set out in this application, and with all relevant legislation and regulations. Address cases where several people are or may be involved in recruiting, interviewing, obtaining data or data analysis.]*

The responsible researcher (Dr Robinson) will manage this project, ensuring that it complies with the protocols set out in this application, and with all relevant legislation and regulations. Ethics management will follow the guidelines in the National Statement on Ethical Conduct in Human Research (updated 2018).

Management and oversight of this project will primarily be achieved by Dr Robinson.

Data will ultimately be disposed of by the Principal Researcher, not more than five years after publication. Paper records will be shredded, whilst electronic records will be deleted.

### B) Monitoring

*[If the research will be carried out at some distance from the responsible researcher (i.e. interstate or in countries other than Australia), describe the systems in place to ensure compliance with the research protocols you have outlined in this application. If the research will be undertaken by a student, describe how the student will be supervised to ensure compliance with the protocols, including details of any local supervision to be organised for research conducted overseas or interstate.*

The Principal Researcher (Dr Dale Robinson) will not be absent for any substantial part of this project. This researcher has extensive experience with similar research protocols and the collection of biomechanics data. He will comply with the protocols and guidelines as required. The Co-Researcher, Dr Dave Ackland will assist in performing these experiments and in maintaining the procedures outlined in this application.

The collection of dental impressions will be performed by the Co-Researcher, Dr George Dimitroulis. This will be performed according to standard procedures required for specialist registration by the Dental Board of Australia, which meet the protocols regarding risk management and patient confidentiality outlined in this application.

### C) Independent Contractors

N/A

## 4. Consent

| 4.1 Obtaining Informed Consent | | **Type an "X" in the left-hand column beside as many of the following options as apply** to your research project. **Use the space provided below** to explain how you will obtain informed consent from participants. If you seek a waiver of consent, or the use of opt-out consent, use the space provided to justify your request. **Refer to *NS* §2.2, *NS* §2.3.** |
|---|---|---|
| x | **Written consent** will be sought from (or on behalf of) participants. | → **Refer to *NS* §2.2.6.**<br>→ **Attach a copy of your consent form(s).** |
| | **Verbal consent** will be sought from (or on behalf of) participants. | → **Refer to *NS* §2.2.5 - §2.2.6.**<br>→ **Explain why you have chosen this form of consent, and how an individual's consent to participate will be recorded.**<br>→ **Attach a copy of your consent script(s).** |
| | **Consent will be implied,** rather than explicitly obtained. | → **Refer to *NS* §2.2.5 - §2.2.6.**<br>→ **Explain why you have chosen this form of consent.** |
| | **Third parties (e.g. parents/guardians of minors) will provide consent** on behalf of participants. | → **Refer to *NS* §2.2.12.**<br>→ **Explain who will be providing consent on behalf of participants and why.** |
| | **Third parties (e.g. community elders, school boards) will be involved** in whole of community participation decisions. | → **Refer to *NS* §2.2.13.**<br>→ **Provide details of which third parties will be involved, why they will be involved, and how this will be accomplished.** |
| | This application seeks a **waiver of consent.** | → **Explain why you are seeking this option. Justify your request by referring to the conditions described in *NS* §2.3.10 - §2.3.11.** |
| | This application proposes to use **opt-out consent.** | → **Explain why you are seeking this option. Justify your request by referring to the conditions described in *NS* §2.3.6.** |
| The consent forms will be obtained by the students who perform the experiments. Written consent forms will be obtained and the researcher will read the consent form again before the experiment starts. The potential subjects will be first asked if they are willing to participate in the experiment, and they will only participate if they are willing to do so. | | |

| 4.2 Limited Disclosure | Do you propose to use limited disclosure, concealment or deception for this research project? (Answer Yes or No. If Yes, use the space below to explain.) **Refer to *NS* §2.3.** | |
|---|---|---|
| | **YES or NO:** | **NO** |
| *[If NO, you may leave this space blank. If YES, provide a justification for the limited disclosure, concealment or deception. Comment on the special considerations discussed in **NS §2.3**. Indicate whether you intend to debrief participants, and justify that position. If you are seeking a waiver of consent for all participants, select NO.]* | | |

| 4.3 Future Use of Data, Materials, or Tissues | Do you intend for the data and/or materials and/or tissues collected for this research project to be reused in future research? **Type an "X" in the left-hand column beside as many of the following options as apply** to your research. **Use the space provided** to specify which data/materials/tissues will be reused, if any. **Refer to *NS* §2.2.14.** |
|---|---|

| | | |
|---|---|---|
| | Consent (or waiver of consent) will be **specific.** | → Data/materials/tissues will be used *only* for this research project (i.e. **no future use**). |
| **x** | Consent (or waiver of consent) will be **extended.** | → Data/materials/tissues used in this research project may also be used in future projects that are *closely related* to this project, *or in the same general area* of research as this project. |
| | Consent (or waiver of consent) will be **unspecified.** | → Data/materials/tissues used in this project may also be used in *any* future research. |
| The computation models and TMJ kinematics and bite force may be used in ongoing research aimed at improving the design of TMJ prostheses. | | |

| **4.4 Conflict of Interest** | Does your research present or involve any conflict of interest, whether potential, real, or perceived; or will the researcher(s) have dual roles in relation to the participants? (Answer Yes or No. If Yes, use the space below to explain.) **Refer to *NS* §5.4, University of Melbourne Research Integrity and Misconduct Policy (MPF1318), and *Australian Code for the Responsible Conduct of Research* §7.2.** | |
|---|---|---|
| | **YES or NO:** | NO |
| *[If YES, explain what the potential conflict of interest is and how it will be managed. If applicable, you may also need to include a comment on the Plain Language Statement and Consent form declaring that potential conflict of interest. If NO, you may leave this space blank.]* | | |

| **4.5 Information for Participants** | How will relevant information about the research project be provided to potential participants? **Attach a copy of any advertisement (print or online), Plain Language Statement (PLS), consent form, letter, email, telephone script, and/or debriefing statement** to be used. **Refer to *NS* §5.2.23.** |
|---|---|
| The written consent form and plain language statement will be sent to subjects before experiments. The subjects will read and sign both documents. On the day of the experiment, the researcher will collect the consent form, and before the experiment, the researcher will read the consent form again and explain the experiment in plain language. The subject will have an opportunity to answer any questions about the research project and experiments before commencement. | |

***Plain Language Statement (PLS):*** Your PLS must satisfy the requirements set out in the *National Statement* (*NS* §2.2.1 - §2.2.3, §2.2.6). The Research Ethics and Integrity's website has **guidance on composing your plain language statement**, as well as an **example PLS template**. A list of PLS requirements is also provided at the end of this form. ***Ensure that your PLS is written in plain language. Ensure that the information contained in your PLS is consistent with the information in your application.***

***Consent Form:*** Your consent form must satisfy the requirements set out in the *National Statement* (*NS* §2.2). The Research Ethics and Integrity's website has **guidance on composing your consent form**, as well as an **example consent form**. A list of consent form requirements is also provided at the end of this form. ***Ensure that your consent form is written in plain language. Ensure that the information contained in your consent form is consistent with the information in your application.***

# 5. Dissemination and Data Management

| **5.1 Providing Results to Participants** | How will the results of the research project be provided to participants in an accessible format? **Refer to *NS* §1.5.** |
|---|---|
| *[Describe how participants will be given access to the results of the research. If you will only be using pre-collected data and/or tissue, state "N/A". If you are seeking a waiver of consent, state "N/A".]* | |

Peer-review publications will be made available on request.

| 5.2 Reporting Project Outcomes | How will outcomes of the research project be made public? **Refer to *NS* §1.3.** |
|---|---|

Conference presentations and peer-review papers.

| 5.3 Data Management | How do you propose to manage the data collected in this research project? Specify what types of data will be collected, how they will be stored and in what format. How will access to the data be controlled and by whom? Discuss retention, security, and data sharing plans. What measures will be taken to protect participants' privacy, and their data?<br>**Refer to *NS* §1.11, the *Australian Code for Responsible Conduct of Research* §2, and the University of Melbourne Research Integrity and Misconduct Policy (MPF1318).** |
|---|---|

**A) Privacy and Confidentiality**

Subjects will be de-identified.

**B) Security and Storage of Data**

Data will be stored securely on the University of Melbourne IT network. The data will be stored on a shared drive that is only accessible by the researchers listed on this project. Any hard copy information will be locked in a cupboard and only accessible by the Principal Researcher.

**C) Retention**

Data will ultimately be disposed of by the Principal Researcher, not more than five years after publication. Paper records will be shredded, whilst electronic records will be deleted.

# 6. Other Issues

| 6.1 Other Ethical Issues | Are there any other issues, not addressed above or in additional modules, which are relevant to the ethical review of your research project? **Refer to the relevant sections of the *National Statement* identified in the Specific Guidelines Checklist, if applicable.** |
|---|---|

N/A

| Attachments Checklist | |
|---|---|
| Review your answers above to determine which attachments (if any) are required for your application. **Type an "X" in the left-hand column beside all items that apply to your research project.** Attach a copy of the items you have selected. | |
| **x** | **Plain Language Statement (PLS) for Participants** |
| **x** | **Consent Form for Participants** |
| | **Additional PLS(s)** (e.g. for parents, teachers, schools) |
| | **Additional Consent Form(s)** (e.g. for parents, teachers, schools; or assent forms for children) |
| | **Recruitment Materials** (e.g. advertisement(s), posters, letter(s) or email(s) of invitation) |
| | **Questionnaire(s) and/or Survey Instrument(s)** |
| | **Measure(s) and/or Scale(s)** |
| | **List of Interview Questions and/or Themes** |
| | **List of Focus Group Questions and/or Themes** |
| | **Participant Distress Protocol** |
| | **Adverse Event Protocol** |
| | **Debriefing Statement** |
| | **Approval(s) of research by an HREC external to the University of Melbourne** |
| | **Other External Approval(s)** (e.g. schools, communities) |
| | **Full Protocol** (for Medical Research) |
| | **Translations and/or Back-Translations** (where languages other than English used) |
| | **Privacy and Databanks Module** |
| | **Body Tissue and Genetic Research Module** |
| **x** | **Ionising Radiation Module** |
| | **Interventions, Therapies and Trials Module** |
| | **Other Documents** (e.g. contracts, agreements) – specify which: |
| | |

**Plain Language Statement (PLS) Requirements:**

1. Clearly identify the University of Melbourne (i.e. by prominent placement of the University's logo) and the department(s)/ school(s)/faculty(-ies) involved. If printed, the PLS should be on University of Melbourne letterhead.
2. Clearly identify the title of the project, and the name(s) and contact details of the Principal Researcher and Other Researchers. For student projects, specify the student's level of study.
3. Clearly explain the purpose of the research project.
4. Clearly explain what participants will be asked to do, and provide an estimated time commitment.
5. If participants will be photographed, audio- or video-recorded, clearly state as much.
6. Clearly explain any risks arising from participation, as well as any procedures or measures in place to minimise such risks.
7. Describe any expected benefits to the wider community. If applicable, also describe any expected benefits to participants.
8. List any payments, incentives or reimbursements to be made to participants.
9. State that involvement in the project is voluntary and that participants are free to withdraw from participation at any time. Explain any implications of withdrawal, including whether it will be possible for participants to withdraw any data already collected from or about them.
10. Describe the likelihood and form of dissemination of the research results, including publication.
11. Describe the arrangements in place to protect the confidentiality of participants' data, and advise participants of any legal limitations to such confidentiality. If the sample size for the project is small, advise participants that this may make them identifiable.
12. The project HREC number (which is the ethics ID number assigned by Themis) and the date and version number of the PLS must appear on the PLS. If the PLS is printed, put this information in the footer.
13. Explain what will happen to participants' data after the research project ends (i.e. how long it will be retained, whether it might be used again for future research and if so who would have access.)
14. Include the following statement: "This research project has been approved by the Human Research Ethics Committee of The University of Melbourne. If you have any concerns or complaints about the conduct of this research project, which you do not wish to discuss with the research team, you should contact the Manager, Human Research Ethics, Research Ethics and Integrity, University of Melbourne, VIC 3010. Tel: +61 3 8344 2073 or Email: humanethics-complaints@unimelb.edu.au All complaints will be treated confidentially. In any correspondence please provide the name of the research team or the name or ethics ID number of the research project."
15. If the research is externally funded, state the amount(s) and source(s) of funding for the research.
16. If there are any potential conflicts of interest for any of the researchers, sponsors (if applicable) or institutions, disclose these potential conflicts of interest.
17. If any participants will be in a dependent relationship with any of the researchers, state that decisions about participation will not affect the dependent relationship. (E.g. students' grades will not be affected if they decline to participate or withdraw from the project at any stage).

**Consent Form Requirements:**

1. Clearly identify the University of Melbourne (i.e. by prominent placement of the University's logo) and the department(s)/ school(s)/faculty(-ies) involved. If printed, the consent form should be on University of Melbourne letterhead.
2. Clearly identify the title of the project, the name(s) and contact details of the Principal Researcher and Other Researchers. For student projects, specify the student's level of study.
3. If participants will be photographed, audio- or video-recorded, clearly state as much.
4. State that involvement in the project is voluntary and that participants are free to withdraw consent at any time, and to withdraw any unprocessed data previously supplied. Also state that the purpose of the project is research.
5. Describe the arrangements in place to protect the confidentiality of participants' data, and advise participants of any legal limitations to such confidentiality. If the sample size for the project is small, advise participants that this may make them identifiable.

# Declaration by the Responsible Researcher

The information contained in this application is, to the best of my knowledge and belief, accurate.

I have read the University's current human ethics guidelines. I accept responsibility for the conduct of the procedures set out in the attached application in accordance with: those guidelines, with the ***University's Research Integrity and Misconduct Policy (MPF1318)***, and with any other condition laid down by the University of Melbourne's Central Human Research Ethics Committee (CHREC), its Human Ethics Sub-Committees (HESCs), or by the Human Ethics Advisory Group (HEAG) which will review this application. I have attempted to identify all risks related to the research that may arise in conducting this research. I acknowledge our obligations as researchers and the rights of the participants stipulated in the ***National Statement on Ethical Conduct in Human Research (2007) - Updated May 2015***. I certify that the research team has the appropriate qualifications, experience and facilities to conduct the research described in the attached application, and to deal with any emergencies and contingencies related to research that may arise throughout the life of the project.

If approval is granted, the project will be undertaken in strict accordance with the approved protocol and relevant laws, regulations and guidelines.

I, the Responsible Researcher, agree to:

- start this research project only after obtaining final approval from the HESC (if this is a standard project), or the HEAG (if this is a minimal risk project);
- carry out this research only where adequate funding is available to enable the research to be carried out according to good research practice and in an ethical manner;
- provide additional information as requested by the CHREC, HESC, or HEAG;
- provide progress reports to the CHREC, HESC, or HEAG as requested, including annual and final reports;
- maintain the confidentiality of all data collected from, or about, research participants and maintain security procedures for the protection of their privacy;
- submit an amendment if any modification to the research design or protocol is proposed (including any change of researchers) and to proceed with the research only after the amendment has been approved by the HESC (if this is a standard project) or by the HEAG (if this is a minimal risk project);
- notify the HESC (if this is a standard project) or the HEAG (if this is a minimal risk project) in writing immediately if any adverse event occurs during the course of the research;
- notify the HESC (if this is a standard project) or the HEAG (if this is a minimal risk project) in writing immediately if any complaints are received about the research;
- comply with an audit of the research undertaken, if requested by the CHREC, HESC, or HEAG;
- use only the data/tissue samples collected for this research, and for which HESC/HEAG approval has been given.

I certify that all members of the research team have read this application and the ***National Statement on Ethical Conduct in Human Research (2007) - Updated May 2015*** and that they have agreed to comply with the provisions of the latter.

| Responsible Researcher Name | Signature | Date |
|---|---|---|
| Dale Robinson | | 15/11/18 |

# Declaration by Human Ethics Advisory Group (HEAG)

| For HEAG use only.<br>Enter the date the application was received, then type an "X" in the left-hand column beside each item as applicable. | | |
|---|---|---|
| **Date Application Received:** | | |
| | **Technical review** has been completed by the HEAG. | The merit of the proposed research project set out in this application has been reviewed on technical grounds.<br>**Refer to *NS* §1.1.** |
| | **Ethical review** has been completed by the HEAG. | The HEAG has reviewed the proposed research project set out in this application for compliance with the principles of Human Research Ethics. |
| | The **Minimal Risk** review process is appropriate for the proposed research project set out in this application. | **→ Complete Declaration A (below)** |
| | The **Standard Project** review process is appropriate for the proposed research project set out in this application | **→ Complete Declaration B (below)** |

| **Declaration A (Minimal Risk):** | The HEAG has reviewed this project. The HEAG considers the methodological/technical and ethical aspects of the proposal to be appropriate to the tasks proposed. **The HEAG grants approval for this research project to commence.** The HEAG considers that the researcher(s) has/have the necessary qualifications, experience and facilities to conduct the research described in the attached application in a manner that complies with the University's policy on the management of research data and records, and to deal with any emergencies and contingencies that may arise. *[Note: If the HEAG Chair is also a researcher in this project, the declaration should be signed by another authorised member of the HEAG.]* | |
|---|---|---|
| **Name of HEAG Chair/Authorised Member** | **Signature** | **Date** |
| | | |

| **Declaration B (Standard Project):** | The HEAG has reviewed this project and considers the methodological/technical and ethical aspects of the proposal to be appropriate to the tasks proposed. **The HEAG regards this project as ready to submit to the HESC.** The HEAG considers that the researcher(s) has/have the necessary qualifications, experience and facilities to conduct the research described in the attached application in a manner that complies with the University's policy on the management of research data and records, and to deal with any emergencies and contingencies that may arise. *[Note: If the HEAG Chair is also a researcher in this project, the declaration should be signed by another authorised member of the HEAG.]* | |
|---|---|---|
| **Name of HEAG Chair/Authorised Member** | **Signature** | **Date** |
| | | |